

On the Flavor Problem in Strongly Coupled Theories

Dissertation

zur Erlangung des Grades “Doktor der Naturwissenschaften”
am Fachbereich Physik, Mathematik und Informatik
der Johannes Gutenberg-Universität in Mainz

Martin Bauer

geboren in Mainz

Mainz, September 2012

Datum der mündlichen Prüfung: 28.11.2012

D77 (Dissertation Universität Mainz)

UNIVERSITY OF MAINZ

ABSTRACT

THEORETICAL HIGH ENERGY PHYSICS (THEP)
INSTITUT FÜR PHYSIK

Doctor rerum naturalium

by **Martin Bauer**

This thesis is on the flavor problem of Randall Sundrum models and their strongly coupled dual theories. These models are particularly well motivated extensions of the Standard Model, because they simultaneously address the gauge hierarchy problem and the hierarchies in the quark masses and mixings. In order to put this into context, special attention is given to concepts underlying the theories which can explain the hierarchy problem and the flavor structure of the Standard Model (SM). The AdS/CFT duality is introduced and its implications for the Randall Sundrum model with fermions in the bulk and general bulk gauge groups is investigated. It will be shown that the different terms in the general 5D propagator of a bulk gauge field can be related to the corresponding diagrams of the strongly coupled dual, which allows for a deeper understanding of the origin of flavor changing neutral currents generated by the exchange of the Kaluza Klein excitations of these bulk fields.

In the numerical analysis, different observables which are sensitive to corrections from the tree-level exchange of these resonances will be presented on the basis of updated experimental data from the Tevatron and LHC experiments. This includes electroweak precision observables, namely corrections to the S and T parameters followed by corrections to the $Zb\bar{b}$ vertex, flavor changing observables with flavor changes at one vertex, viz. $\mathcal{B}(B_d \rightarrow \mu^+ \mu^-)$ and $\mathcal{B}(B_s \rightarrow \mu^+ \mu^-)$, and two vertices, viz. $S_{\psi\phi}$ and $|\epsilon_K|$, as well as bounds from direct detection experiments.

The analysis will show that all of these bounds can be brought in agreement with a new physics scale Λ_{NP} in the TeV range, except for the CP violating quantity $|\epsilon_K|$, which requires $\Lambda_{\text{NP}} = \mathcal{O}(10)$ TeV in the absence of fine-tuning. The numerous modifications of the Randall Sundrum model in the literature, which try to attenuate this bound are reviewed and categorized.

Subsequently, a novel solution to this flavor problem, based on an extended color gauge group in the bulk and its thorough implementation in the RS model, will be presented, as well as an analysis of the observables mentioned above in the extended model. This solution is especially motivated from the point of view of the strongly coupled dual theory and the implications for strongly coupled models of new physics, which do not possess a holographic dual, are examined.

Finally, the top quark plays a special role in models with a geometric explanation of flavor hierarchies and the predictions in the Randall-Sundrum model with and without the proposed extension for the forward-backward asymmetry A_{FB}^t in top pair production are computed.

ZUSAMMENFASSUNG

Gegenstand dieser Arbeit ist das Flavor Problem in Randall Sundrum Modellen und stark gekoppelten Theorien, welche dieselbe Physik beschreiben und mit Hilfe der AdS/CFT Korrespondenz miteinander identifiziert werden können. Diese Theorien sind besonders attraktive Erweiterungen des Standardmodells, weil sie im Stande sind das Hierarchie Problem zu lösen und gleichzeitig eine Erklärung für die Hierarchien im Flavor Sektor liefern. Beide Seiten der AdS/CFT Korrespondenz werden ausführlich vorgestellt und ein tieferes Verständnis von Flavor ändernden Kopplungen welche von extradimensionalen Eichfeldern im Randall Sundrum Modell induziert werden, anhand der Diagramme der dualen Theorie ermöglicht.

Eine Diskussion verschiedener Flavor ändernder Ströme, erzeugt durch den Austausch dieser Felder auf Born niveau wird präsentiert und mit den aktuellsten Werten der Experimente an Tevatron und LHC verglichen. Diskutiert werden flavor diagonale Kopplungen, unter anderem Korrekturen zu elektroschwachen Präzessionsmessungen, den S und T Parametern, und zur Kopplung des Z an bottom quarks, flavor wechselnde Kopplungen an einem Vertex, in Form der Zerfallsbreiten $\mathcal{B}(B_d \rightarrow \mu^+ \mu^-)$ und $\mathcal{B}(B_s \rightarrow \mu^+ \mu^-)$, sowie flavor ändernde Kopplungen an zwei Vertices, insbesondere die Observablen $S_{\psi\phi}$ und $|\epsilon_K|$. Ausserdem wird auf Limits auf den direkten Nachweis solcher neuer Resonanzen eingegangen.

Alle diese Messungen stehen im Einklang mit einer Skala für neue Physik von $\Lambda_{\text{NP}} = \mathcal{O}(\text{TeV})$, abgesehen von Korrekturen zur CP verletzenden Observable $|\epsilon_K|$, welche nur mit den Daten in Einklang gebracht werden kann, falls die Skala der neuen Physik um eine Größenordnung angehoben ist.

Viele Lösungen für dieses Problem existieren in der Literatur und werden vorgestellt und kategorisiert, um anschließend eine neue Lösung in Form einer Erweiterung der starken Symmetriegruppe zu präsentieren. Diese Lösung ist besonders motiviert durch ihre Implikationen für die duale Theorie und die Konsequenzen die der damit verbundene Mechanismus für Theorien ohne holographische Äquivalenz induziert. Im dementsprechend erweiterten Modell werden daraufhin die oben zusammengefassten Observablen berechnet, und die Verträglichkeit aller Observablen im Flavor Sektor mit einer neuen Physik Skala im TeV-Bereich festgestellt.

Abschließend wird auf die Vorhersagen für die Asymmetrie in der top antitop Produktion eingegangen, und die Resultate sowohl für das Randall Sundrum Modell, als auch für das erweiterte Modell gezeigt.

Contents

Acknowledgements	vii
Preface	ix
1 Introduction: Problems beyond the Standard Model	1
1.1 Solutions to the Gauge Hierarchy Problem	3
Supersymmetry	4
Technicolor and Composite Higgs Models	7
Technicolor	7
Partial Compositeness	14
Composite Higgs	17
Collective Symmetry Breaking	18
Extra Dimensions	21
Flat Extra Dimensions	21
Warped Extra Dimensions	25
1.2 Solutions to the Flavor Problem	27
Abelian Flavor Symmetries	29
Non Abelian Flavor Symmetry	32
2 The Randall Sundrum Model and its Holographic Interpretation	35
2.1 Why this and not that?	35
2.2 AdS/CFT	40
The Holographic Dual of the Minimal RS Model	49
The Holographic Dual of Higgsless, Custodially Protected, Composite Higgs and Little Higgs Theories	51
2.3 Profiles of Gauge Bosons	54
The Electroweak Gauge Sector of the SM	65
2.4 Profiles of Fermions	69
Bulk Profiles	76
2.5 Hierarchies in Quark Masses and Mixings and the RS GIM Mechanism	78
Hierarchic Quark Masses and Mixings from Anarchic Fundamental Parameters	78
The RS-GIM Mechanism	83
2.6 Four Fermion Interactions	88
3 Solving the Flavor Problem in Strongly Coupled Theories	91
3.1 Electroweak Precision Observables	92
Oblique Parameters	93
Corrections to $Z \rightarrow b\bar{b}$	96

3.2	RS GIM Working	100
	$B_s - \bar{B}_s$ Mixing	101
	B Meson Decays to Muons	105
3.3	Limitations of the RS GIM Mechanism	108
	The Flavor Problem of the RS Model	109
	A List of Solutions to the Flavor Problem	111
	ParametricSuppressions	111
	Global Symmetries and MFV	112
	Alternative Solutions	114
3.4	A Solution in the Gauge Sector	115
	Extension of the Color Gauge Group	115
3.5	Implications for Other Theories	123
3.6	The Extension of the Scalar Sector	127
	A Realistic Higgs Sector	129
	Adjusting the Fermion Profiles	134
3.7	Flavor Observables and LHC Bounds	137
	Electroweak Precision Observables	137
	Flavor Violating Observables	137
	Bounds from Direct Detection	139
4	The Asymmetry in Top Pair Production	145
4.1	Top-Antitop Pair Production and Observables at Tevatron and the LHC	145
4.2	The Forward-Backward Asymmetry in the SM	148
4.3	New Physics and the Forward-Backward Asymmetry	152
	New Physics in the s Channel	153
	New Physics in the t and u Channel	155
4.4	Cross Section and Asymmetry in the Minimal RS Model	157
	Leading Order Contributions of the RS Model with and without Custodial Protection	157
	The Asymmetry in the RS Model at NLO in QCD	163
4.5	Numerical Analysis	165
4.6	Axigluon Contributions to the Cross Section and the Asymmetry	170
5	Conclusions	175
A	Generating Parameter Points	177
	Reference Points	178
B	Neutral Meson Mixing	181
C	Input Parameters	187
D	Higgs Potential for the Extended Scalar Sector	191
	Bibliography	193

Acknowledgements

Preface

Before the advent of the Standard Model, physicists had become used to experiments producing unexpected new particles or other signposts to a new theory almost before the chalk dust had settled on the old one. They have been waiting 30 years for that to happen with the Standard Model.

Gordon Kane

When Gordon Kane wrote this statement seven years ago, despite its success, one crucial ingredient of the Standard Model (SM) was still missing, the Higgs boson. In the meantime, the Large Hadron Collider (LHC) has started running, and essentially rediscovered every known particle in the SM and nothing else, but one scalar resonance at roughly 126 GeV. If this scalar is the Higgs, one can conclude from vacuum stability bounds, that its mass nicely agrees with the SM as a complete theory of non-gravitational forces up to almost the Planck scale. At this point, its couplings are not measured with an accuracy that would allow it to identify the SM Higgs with all its predicted characteristics. However, one can already say that electroweak symmetry breaking (EWSB), as it is described by the SM, is the correct low energy theory. The desert of scales above the electroweak scale that the LHC begins to explore, lets one wonder how many orders of magnitude this “low” energy description actually covers. Thus, from an experimental point of view, the SM is a success. Theoretically, the LHC measurements have made the questions left open by the SM only more pressing. This thesis will address two of the most puzzling ones: What sets the electroweak scale, and what is the reason for the hierarchies in the masses and mixings of the quarks? The first question has been the driving force for building models of physics beyond the SM for decades. In the SM, the electroweak scale is a free parameter and unstable against radiative corrections. It must therefore be fine-tuned to a large degree in order to agree with the experiment, unless some symmetry or mechanism protects it from these radiative corrections.

In the first part of the Chapter 1, a survey of ideas that can solve this problem will be presented. The emphasis will be put on theories which assume the Higgs to be a strongly coupled bound state by some new force. If the LHC continues to set better and better exclusion limits on new resonances, this explanation becomes attractive, because the Goldstone bosons of QCD are roughly an order of magnitude lighter than its characteristic scale and the difference between the Higgs mass and the mass of possible new resonances could be explained in a similar way. As will be explained there, these theories are generically in conflict with bounds from flavor observables, because they allow for flavor changing neutral currents (FCNCs) at tree level. It will be shown that, if fermions are partially composite fields, one can avoid most of these bounds, and also finds an explanation for the hierarchies in the quark sector. Quark masses and mixings are also unmotivated in the SM, and models which can explain them are the subject of the second part of the first chapter.

One of the most fascinating insights of the last fifteen years regarding new physics is that, due to a conjecture by Maldacena, one can describe concepts in strongly coupled theories by a five dimensional (5D) model, based on a compact extra dimension with an unfactorizable Anti-de Sitter metric, the Randall Sundrum (RS) model. It adds to the fascination, that the concept of partial compositeness is automatically implemented in these models by making the quarks 5D fields.

In the first half of Chapter 2, this duality will be motivated, and the two different ways of describing the same physics will be used for a deeper understanding of the analyses in the latter parts of the thesis. As a new result, a dual interpretation of the small momentum expansion of the 5D propagator for gauge bosons will be presented there. The rest of Chapter 2 will be devoted to the technical formulation of the fundamentals of the RS model. Important in this context is the geometrical explanation of how the suppression of FCNCs is realized by the RS-GIM mechanism.

Chapter 3 includes an update on the RS contributions to electroweak precision measurements, including the consequences of a new global fit for the oblique parameters S and T and the impact of new theoretical results on the conclusions drawn from the $Z\bar{b}b$ for the RS parameter space. The effectiveness of the RS-GIM mechanism will be demonstrated on the basis of observables connected to the decay of B_s and B_d mesons to muons and $B_s - \bar{B}_s$ mixing. The heavy b quark makes them well suited to test the limits of the RS-GIM mechanism, because the suppression of FCNCs becomes less effective the heavier the involved flavors are. While it turns out that these observables generically agree even with the small errors from recent LHCb measurements, one finds that the CP violating quantity in $K - \bar{K}$ mixing, ϵ_K will induce a fine-tuning of the order of one percent if no additional suppression of the RS contributions is implemented.

This is rooted in a chiral enhancement and large renormalization group effects, and therefore it is a largely model independent problem for any new physics with vector couplings to quarks. In RS models it is the only observable which needs fine-tuning and this issue has therefore been termed the “RS flavor problem”. After the explanations proposed in the literature are collected and interpreted in the dual theory, a novel solution based on an extension of the color gauge group will be presented and discussed in detail. This solution is especially attractive, because it preserves the anarchical flavor structure of the Yukawa matrices, which is essential in order to explain the hierarchies in quark masses and mixings. In the extended model the aforementioned observables will be computed, as well as the cross section for direct detection of the involved new resonances at the LHC.

The fact that the size of the couplings of RS gauge fields to quarks depends on the the quark mass, makes top observables an ideal candidate to look for effects of the RS model. Possible contributions to the forward-backward asymmetry measured by CDF and DØ, as well as the agreement with the total cross section in top antitop pairs will therefore be studied in Chapter 4. In a model-independent analyses, the impact of general new physics in the s and t channel will be computed and in particular the effects in the RS model as well as in the RS model with the proposed extension will be shown.

Concluding remarks and an outlook on future work in Chapter 5 will complete the thesis.

1 Introduction: Problems beyond the Standard Model

The Standard Model of elementary particles (SM) is arguably the most successful theory in physics today. It has passed a myriad of tests, and with the discovery of the Higgs boson this year, every particle necessary to describe electroweak symmetry breaking (EWSB) within the SM has been observed. The data from colliders is so convincing, that most of the evidence for physics beyond the SM only becomes apparent at astronomical scales, *e.g.* Dark Matter, or quantum gravity effects. Other hints are found at mass scales which are orders of magnitude smaller than the electroweak breaking scale, as in the indirect detection of neutrino masses. Physics at the electroweak breaking scale, however, seems to be completely described by the SM. Nevertheless, there are good theoretical arguments for why the SM should be extended at a scale much closer to the electroweak breaking scale than one would expect from these experiments. One can see this by regarding the SM Lagrangian as a part of a more general effective field theory (EFT),

$$\mathcal{L}_{\text{eff}} = c_0 \Lambda_{\text{UV}}^4 + c_2 \Lambda_{\text{UV}}^2 H^\dagger H - \lambda (H^\dagger H)^2 + \mathcal{L}_{\text{Gauge}}^{(4)} + \mathcal{L}_{\text{Yukawa}}^{(4)} + \frac{\mathcal{L}^{(5)}}{\Lambda_{\text{UV}}} + \frac{\mathcal{L}^{(6)}}{\Lambda_{\text{UV}}^2} + \dots, \quad (1.1)$$

in which $\mathcal{L}_{\text{Gauge}}^{(4)}$ comprises the familiar $SU(3)_C \times SU(2)_L \times U(1)_Y$ gauge interactions and $\mathcal{L}_{\text{Yukawa}}^{(4)}$ the Yukawa couplings, and Λ_{UV} denotes the for now unspecified scale at which this EFT has to be completed by an underlying theory. The mass dimension of the operators in $\mathcal{L}^{(i)}$ is denoted by the superscript (i) ,¹ and the ellipsis stands for higher order operators. Therefore, prior to EWSB all operators are of mass dimension four or higher, aside from a constant term and the Higgs mass operator, which carry mass dimension zero, and two respectively and as a consequence have coefficients of positive mass dimension. In the language of renormalization group flow, these operators are the only relevant operators which can be constructed from the SM field content.

Although not in this context, it was realized very early that a scalar mass term will lead to a radiative sensitivity on the cut-off scale [1].² The constant term is even sensitive to the fourth power of the cut off scale. In other words, there is no reason to expect the coefficients of these operators to be connected to any scale other than Λ_{UV} . Likewise, the irrelevant operators in (1.1) with mass dimension larger than four are expected to be suppressed by this scale. However in order for EWSB to work

¹Throughout the thesis, we will use natural units $c = \hbar = 1$.

²A more careful statement would be: Such an operator leads to a quadratic sensitivity on masses of particles interacting with the Higgs up to the cut-off scale, as the dependence on the cut-off scale itself is an artifact of cut-off regularization, which does not show up in dimensional regularization. We will however adopt this slight abuse of language.

as described by the SM, the coefficient of the Higgs mass operator has to be of the order of the electroweak scale, *i.e.* $\Lambda_{\text{EW}} \approx 1 \text{ TeV}$. This introduces a large unexplained hierarchy in scales, unless there is new physics at Λ_{EW} or the dimensionless coefficient c_2 is tuned to be of the order $c_2 \approx \Lambda_{\text{EW}}^2 / \Lambda_{\text{UV}}^2$. Even more severe is the problem of the cosmological constant, which is indirectly measured at $c_0 \approx (10^{-12} \text{ GeV})^4 / \Lambda_{\text{UV}}^4$ [2], and either calls for a UV completion at the millielectronvolt scale or a fine-tuning of hundreds of orders of magnitude if one assumes that Λ_{UV} is of the order of the Planck scale $M_{\text{Pl}} = 10^{19} \text{ GeV}$.

Both hierarchies become a problem if one expects the theory to be *natural*, for which we will adopt the definition of 't Hooft,

The naturalness criterion states that one such [dimensionless and measured in units of the cut-off] parameter is allowed to be much smaller than unity only if setting it to zero increases the symmetry of the theory. If this does not happen, the theory is unnatural.[3]

A good measure to judge the attractiveness of a physical theory is therefore the absence of these small parameters, or equivalently the absence of large hierarchies between scales. However, since the cosmological constant is not directly relevant for the physics of the SM, we will ignore this problem and concentrate on the hierarchy problem of the SM in Part 1.1 of this chapter.

This hierarchy problem becomes even more puzzling if one considers higher dimensional operators. If it can be explained by new physics at the electroweak scale, one would expect from the EFT ansatz (1.1), that also the suppression scale of the irrelevant operators are of the order $\Lambda_{\text{UV}} = \Lambda_{\text{EW}}$. However, if not prevented by some mechanism in the new physics sector, bounds from measurements on flavor changing processes involving quarks will enforce at least

$$\Lambda_{\text{UV}} \gtrsim 10^3 \text{ TeV}. \quad (1.2)$$

A UV completion of the SM should therefore not only be able to explain why the electroweak scale is stabilized against radiative corrections, but also why higher dimensional operators are absent or suppressed by orders of magnitude compared to Λ_{EW} .

The question of how both of these requirements can be brought in agreement is one of the most pressing issues for models of physics beyond the SM. Further, while the marginal operators in $\mathcal{L}_{\text{Gauge}}$ all have natural coefficients,³ the Yukawa couplings in $\mathcal{L}_{\text{Yukawa}}$ exhibit hierarchical structures which are not explained by SM physics either, and although these parameters are not radiatively unstable, the question what sets the masses and mixings of quarks and leptons is also to be answered by physics beyond the SM. Part 1.2 of this chapter will describe models which aim to explain the hierarchies of the Yukawa sector and mechanisms which generate a hierarchy between the coefficients of higher dimensional operators relevant for flavor changing processes

³With the exception of operators allowing for strong CP violation.

and the electroweak scale.

While the questions behind the hierarchies of the SM are an important guideline for new physics models, one should keep in mind, that hierarchies are not completely absent in EFTs. An example can be found in the effective theory of nucleon-nucleon interactions below the pion threshold, which is basically a collection of contact terms between nucleons. The coefficients of these contact terms are suppressed by the pion mass scale $m_\pi \approx 140$ MeV or in some cases by the QCD scale $\Lambda_{\text{QCD}} \approx 1$ GeV. However, the inverse s -channel scattering length of protons and neutrons is measured to $1/a_s \approx 10$ MeV, which implies fundamental coefficients in the Lagrangian which are tuned by at least 1%. In this case, one knows the UV completion and as of now no explanation for this hierarchy of scales has been found, apart from the theory being fine-tuned, see [4] for details. Besides all the models and ideas introduced in this chapter, the possibility that finetuning might appear elsewhere in nature should therefore not be ignored.

1.1 Solutions to the Gauge Hierarchy Problem

The need for fundamental scalar fields in the theory of weak and electromagnetic forces is a serious flaw. Aside from the subjective aesthetic argument, there exists a real difficulty connected with the quadratic mass divergences which always accompany scalar fields.

————— Leonard Susskind

There are two aspects to the gauge hierarchy problem: One is the huge hierarchy between the electroweak scale and the Planck scale. The other is the problem that the Higgs boson mass is radiatively unstable. Therefore, even if some new physics fixes the electroweak scale at tree level, it would still be unstable against radiative corrections, in contrast to the hierarchies in the flavor sector. As a consequence, a solution for the hierarchy problem can have different meanings. It can describe a mechanism which protects the Higgs boson mass parameter from quadratic corrections, which sets in at an acceptable scale (*e.g.* Supersymmetry, Technicolor, gauge-Higgs unification with nonlocal loop potential). Or, it may leave the theory radiatively unstable up to the Planck scale, but explains why this scale is considerably lower than what we expect (*e.g.* Large Extra Dimensions). The first type of models does not explain why the ratio of the scales of electroweak symmetry breaking and gravity appears to be so tremendously large, but rather makes it a natural thing to have such a disparity, because all relevant operators are eliminated from the theory or protected from renormalization effects through a symmetry. The other class of models argues that this ratio is actually not a ratio of fundamental masses and the weakness of gravity is an illusion, generated by another big scale, *e.g.* the volume of additional compact dimensions.

Another key observation is, that only scalar fields suffer from quadratic radiative

corrections. One can therefore also distinguish between theories which allow for fundamental scalars, but protect their mass terms through a symmetry, in line with t'Hooft's original definition of naturalness, and models which simply ban all fundamental scalars from the theory. Naively, one might expect mass terms for vector bosons to be quadratically and fermion masses to be linearly divergent as well. In the SM however, they are only logarithmically divergent, because all vector bosons are gauge bosons and their masses are protected by gauge symmetries, while the fermion masses are protected by chiral symmetry, which is rooted in the different representations of left- and right-handed Weyl fermions under the $SU(2)_L$ gauge group, and can therefore also be interpreted as a protection connected to the gauge sector. It is hence remarkable, that all mechanisms which protect the mass of a fundamental scalar are related to extensions of the spacetime symmetry!

It is important to carve out such similarities and differences of the various approaches in order to explore the essential mechanisms of an answer to the hierarchy problem. If a number of models show similar problems or results, this might be a hint at some underlying structure, or lead to the realization that some sector of the SM behaves different than the rest, once the hierarchy problem is taken care of. An example for this is the top quark mass. Based solely on mass ratios to the electroweak scale, one can argue that it is perfectly compatible with the electroweak scale, but a number of models which stabilize the electroweak scale turn out to have a problem implementing such a heavy quark. That might be due to all of these models being wrong, but it can also mean that nature tries to tell us that the top quark differs in more than just the mass from the other five known flavors.

The following sections will give an overview of the various solutions to the gauge hierarchy problem, pointing out their theoretical and phenomenological implications. With regard to the subject of the thesis and also in anticipation of Section 1.2, an emphasis will be put on (Quark) Flavor when it comes to discussing bounds from observables. Also, the section about strongly interacting theories will be more detailed, since many of the introduced concepts will turn out to be mirrored in models with warped geometry due to the AdS/CFT duality presented in the next chapter.

Supersymmetry

In a nutshell, supersymmetric transformations relate scalar with fermionic degrees of freedom and as a consequence, if fermions are protected from radiative corrections which are not proportional to their masses (or the vev), by chiral symmetry, their scalar *superpartners* must inherit this protection via the *supersymmetry* (SUSY). Since it changes the spin of the states it acts on, SUSY is an extension of the spacetime symmetry.

It was generally believed, that this part (the space-time symmetry) of the SM was a settled matter after Coleman and Mandula published a paper in 1967, which states that the most general symmetry of a relativistic QFT which fulfills some fundamental assumptions, like analyticity of scattering amplitudes and the occurrence of a mass

gap, is locally⁴ a direct product of the Poincaré group and an internal symmetry group [8].⁵ Only in 1974 the first supersymmetric Lagrangian (in four dimensions) was constructed by Wess and Zumino [11]. They already note (footnote 5), that supergroups build a loophole in the Coleman-Mandula theorem, which was subsequently generalized by Haag, Lopuszanski and Sohnius [12]. They also point out, that quadratic divergences of the mass renormalization for scalar fields cancel.

How does this work? In the most simple supersymmetric extension of the SM, the *minimal supersymmetric Standard Model* (MSSM) [13], every SM fermion has two scalar superpartners, the s(uper)fermions, the Higgs boson has neutral and charged Weyl fermions as superpartners, the *higgsinos*, and superpartners of the Gauge fields, called *gauginos*, are Majorana fermions. The solution to the hierarchy problem can therefore be understood in a diagrammatic way, where only the leading corrections to the Higgs boson mass from the top and its superpartners, the *stops* (denoted by \tilde{t}) are considered, just to show the principle. In a cutoff regularisation, the one-loop correction of the Higgs mass⁶ from the top quark with mass m_t and Yukawa coupling λ_t reads

$$\begin{array}{c} t \\ \circlearrowleft \\ \text{---} H \text{---} \end{array} \rightarrow \Delta m_H^2|_{\text{top}} = \frac{3\lambda_t^2}{8\pi^2} \left[-\Lambda^2 + 6m_t^2 \log\left(\frac{\Lambda}{m_t}\right) - 2m_t^2 \right]. \quad (1.3)$$

Whereas the contribution from the stops with mass $M_{\tilde{t}}$ and Yukawa coupling $\lambda_{\tilde{t}}$ gives

$$\begin{array}{c} \tilde{t} \\ \text{---} H \text{---} \end{array} + \begin{array}{c} \tilde{t} \\ \text{---} H \text{---} \end{array} \rightarrow \Delta m_H^2|_{\text{stops}} = \frac{3\lambda_{\tilde{t}}}{8\pi^2} \left[-\Lambda^2 + 2M_{\tilde{t}}^2 \log\left(\frac{\Lambda}{M_{\tilde{t}}}\right) \right] - \frac{3\lambda_{\tilde{t}}^2 v^2}{8\pi^2} \left[-1 + 2 \log\left(\frac{\Lambda}{M_{\tilde{t}}}\right) \right]. \quad (1.4)$$

Both contributions by themselves are quadratically divergent, but if the Lagrangian is supersymmetric, the couplings of stop and top must be related, $\lambda_{\tilde{t}}^2 = -\lambda_t^2$, so that

$$\Delta m_H^2|_{\text{top}} + \Delta m_H^2|_{\text{stops}} = 3 \frac{\lambda_{\tilde{t}}^2}{4\pi^2} \left[(m_t^2 - M_{\tilde{t}}^2) \log\left(\frac{\Lambda}{M_{\tilde{t}}}\right) + 3m_t^2 \log\left(\frac{M_{\tilde{t}}}{m_t}\right) \right]. \quad (1.5)$$

⁴It is stated on the level of Lie algebras. As a consequence, a discrete symmetry transformation which does not commute with spacetime transformations is not excluded by the theorem.

⁵The paper was motivated by the then fashionable effort to organize quarks in so-called *supermultiplets* of a unified spin-flavor $SU(6)$, see [9]. At the same time an alternative model which groups hadrons and mesons in a multiplet was proposed, but went generally unnoticed, although it includes the first notion of a *supergroup*, *i.e.* a group generated from anticommuting algebra elements [10].

⁶To be precise, the one which couples to the up sector. The MSSM needs two Higgs doublets with opposite hypercharge in order to cancel the anomalies from the Higgsinos.

Quadratic divergences cancel and, as expected for a chirally protected mass, all remaining divergences are logarithmic and vanish in the limit where the Higgs vev goes to zero. In the limit of exact supersymmetry, $m_t = M_{\tilde{t}}$, all corrections vanish. Moreover, since SUSY is a symmetry of the quantum theory, no divergences will occur at any loop order, in fact, the masses are not renormalized at all, see [14, Sec. 4]. However, the MSSM does not only—in conflict with experiment—predict degenerate masses of superpartners, but it necessarily gives the Higgs boson a positive mass squared.⁷ As a consequence, in order to have nondegenerate masses in the MSSM (or massive particles at all), supersymmetry needs to be broken. There is no phenomenologically viable way to incorporate SUSY breaking with only the MSSM field content and a breaking communicated at tree level (a direct couplings to the SUSY-breaking field) will also lead to inconsistencies⁸, see *e.g.* [5, Sec. 7].

One therefore assumes a *hidden sector*, in which SUSY is broken and some kind of messenger fields communicate the breaking to the MSSM. In the spirit of effective field theory one writes down the relevant terms of the most general Lagrangian parametrizing the breaking. This introduces 124 new parameters to the MSSM, which are in general unrelated, and will lead to a breaking of the chiral protection of the scalar masses, because $M_{\tilde{t}} = m_t + m_{\text{SUSY}}$ in (1.5) is now sensitive to the size of the breaking terms. They are usually given by

$$m_{\text{SUSY}} \sim \frac{\langle \mathcal{F} \rangle}{\Lambda}, \quad (1.6)$$

where $\langle \mathcal{F} \rangle$ denotes the vev of the SUSY breaking field and Λ is the SUSY breaking scale (the mass of the messenger field). These masses should clearly not exceed the TeV scale by much $m_{\text{SUSY}} \lesssim \text{TeV}$ in a natural model. However, since the SUSY breaking sfermion masses induce radiative corrections relative to their Yukawa couplings, one can relax this bound depending on flavor. For example a 200 GeV stop contributes roughly as much to Δm_H^2 as a sbottom at 3.5 TeV. Natural supersymmetric models may therefore allow for a large splitting in the superpartner mass spectrum [7]. It should be noted, that such an ansatz requires the SUSY breaking sector to generate this hierarchy in superpartner masses.

The modeling of the SUSY breaking sector may accommodate further attractive features. For a large enough SUSY breaking scale, renormalization group running may eventually turn one of the scalar mass parameters negative, triggering condensation of the corresponding field. It would be a disaster, if this would be any sfermion mass, because it would induce a color- or electromagnetic breaking vacuum. However, the Higgs boson mass parameter will get the largest negative corrections by the top Yukawa and thus generically turns negative first, ultimately triggering EWSB. This is known as *radiative symmetry breaking* [6] and although it depends on the values m_{SUSY} at the SUSY breaking scale, it is a step beyond the ignorance of the EWSB

⁷In order to achieve EWSB in a (unbroken) supersymmetric extension of the SM, one therefore has to include additional fields, which do not have superpartners in the SM, see for example the discussion in [15, Sec.5.4].

⁸There is for example no scalar-gaugino-gaugino term allowed by SUSY, therefore the gauginos remain massless in such a scenario.

mechanism in the SM. Another interesting property of SUSY models is, that the running of the gauge couplings will lead to gauge coupling unification at a scale of about $\Lambda \sim 10^{16}$ GeV, which can be understood as a strong hint at a *grand unified theory* (GUT), in which all MSSM gauge interactions are low energy remnants of a single large gauge symmetry (this assumes a *desert* of energy scales up to the GUT scale with no new physics besides the MSSM).

But there are further additional concepts necessary in order to bring a supersymmetric field theory in agreement with experiment. In contrast to the SM, there are renormalizable couplings involving the new scalar superpartners, which allow for Lepton and Baryon number violation. These couplings lead to rapid proton decay and must either be forbidden or extremely small. The most established solution for this problem is called *R parity*, a discrete symmetry which allows only vertices with two superpartners attached, and thus eliminates the dangerous couplings, first introduced in [16]. Some interesting consequences of such an additional symmetry is that superpartners will only be pair produced at colliders and that there is a stable lightest supersymmetric particle (LSP) with a mass around the electroweak scale, which makes for an ideal dark matter candidate. Less restrictive solutions are possible, *e.g.* imposing Lepton-, Baryon number conservation as a global symmetry [17] or minimal flavor violation [18, 19].

The MSSM allows also for one parameter carrying mass dimension, which is not from the SUSY-breaking sector and as a consequence should be sensitive to the scale where the UV-completion of the MSSM sets in, the GUT or the Planck scale. Yet, this so called μ -parameter is related to the weak scale, since it plays a fundamental role in EWSB. This is the MSSM fine-tuning problem, and although the situation is better than in the SM (because the μ -parameter does not renormalize), the scale disparity remains.

Technicolor and Composite Higgs Models

Technicolor

In essence, the idea of Technicolor (TC) solves the gauge hierarchy problem by replacing the scalar Goldstone degrees of freedom necessary to give masses to the electroweak gauge bosons by composite bound states. It is based on the observation, that even in the absence of a Higgs boson the electroweak symmetry is broken by the quark condensate $\langle \bar{q}q \rangle = \langle \bar{q}_L q_R \rangle + \langle \bar{q}_R q_L \rangle$ formed at the scale at which QCD becomes strongly coupled, Λ_{QCD} .

In such a scenario, fermions are massless and the SM with N_F quark flavors exhibits a global $SU(N_F)_L \times SU(N_F)_R \times U(1)_B$ chiral (and Baryon number) symmetry⁹, which is broken down to $SU(N_F)_V \times U(1)_B$ by the quark condensate. Due to Goldstones theorem this symmetry breaking generates $N_F^2 - 1$ massless Goldstone bosons, in the

⁹The axial $U(1)$ is broken by quantum effects and therefore the η' is massive even in the chiral limit.

case of one generation ($N_F = 2$), three pions. The electroweak gauge group gauges a subgroup of the full global symmetry and since q_L and q_R transform differently under this subgroup the electroweak symmetry is broken by the formation of the quark condensate as well. It even breaks the electroweak symmetry in the correct pattern, since the quark condensate has the same quantum numbers as a fundamental Higgs scalar. As a consequence, the coupling of the W^\pm to the conserved weak currents $J_\mu^\pm = q_L \gamma_\mu T^\pm q_L$ results in a correction to the W propagator below Λ_{QCD} [21],

$$\text{pions} = \frac{-i}{q^2 - g^2 \Pi(q^2)/2} \left(\eta_{\mu\nu} - \frac{q_\mu q_\nu}{q^2} \right) \quad (1.7)$$

$$\text{where} \quad \Pi_{\mu\nu}(q) = i \int d^4x e^{-iq \cdot x} \langle 0 | T \{ J_\mu^+(x) J_\nu^-(0) \} | 0 \rangle = \left(\eta_{\mu\nu} - \frac{q_\mu q_\nu}{q^2} \right) \Pi(q^2).$$

One ends up with a mass for the W^\pm proportional to the residue of the pole of the vacuum polarization function $\Pi(q^2)$, which follows from pion exchange,

$$\langle 0 | J_\mu^+ | \pi(p) \rangle = i \frac{f_\pi}{\sqrt{2}} p_\mu \quad \Rightarrow \quad M_W = \sqrt{\frac{N_F}{2}} \frac{g f_\pi}{2}, \quad (1.8)$$

where f_π denotes the pion decay constant. The thereby generated masses for the electroweak gauge bosons

$$M_W \approx 28 \sqrt{\frac{N_F}{2}} \text{ MeV}, \quad M_Z \approx 32 \sqrt{\frac{N_F}{2}} \text{ MeV}, \quad (1.9)$$

are however too small by a factor of roughly $4000/\sqrt{N_F}$ in order to explain the measured values. It is interesting to explore the implications of such a world without a Higgs,¹⁰ but the important statement here is, that the confining phase of QCD would describe a viable mechanism of electroweak symmetry breaking if f_π was replaced by the electroweak scale v .

In the late seventies, this observation led Weinberg [23] and Susskind [24] to propose a theory in which electroweak symmetry breaking is arranged by an upscaled version of QCD, for which the name *technicolor* (TC) became most established. The simplest model includes two flavors of *techniquarks*,¹¹ transforming in the fundamental representation of the TC gauge group $G_{\text{TC}} = SU(N_{\text{TC}})$ where the right-handed components transform as singlets and the left-handed components as doublet under the SM $SU(2)_L$ in order to form a *techniquark condensate* with the right quantum numbers. The new gauge group has a β function just like QCD, only that the coupling g_{TC} becomes strong at the scale

$$\Lambda_{\text{TC}} = \sqrt{\frac{3}{N_{\text{TC}}}} \frac{f_\pi^{\text{TC}}}{f_\pi} \Lambda_{\text{QCD}} \sim 4\pi f_\pi^{\text{TC}}, \quad (1.10)$$

¹⁰The Fermi constant for example would be larger by a factor $2v^2/N_F f_\pi^2$ and processes driven by the weak force like β -decay would occur much more rapidly. A comprehensive discussion of such a Gedankenworld can be found in [22].

¹¹In the case $N_F > 2$, additional, for now massless, *technipions* appear (the analog of QCD Kaons and η s).

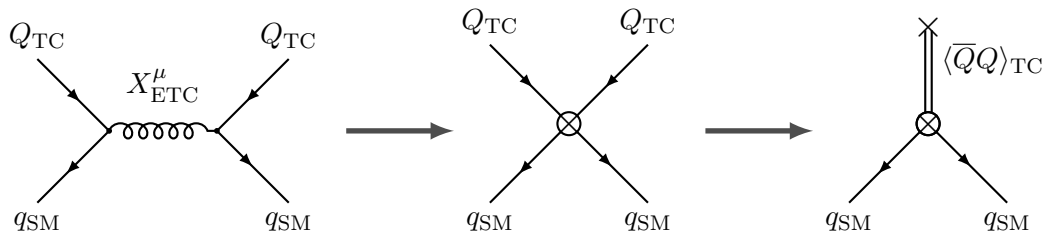


Figure 1.1: Diagrammatic representation of the generation of effective Yukawa couplings for the SM fermions in extended Technicolor theories. In a first step, the heavy *ETC* gauge bosons are integrated out and in a second step the technicolor condensate forms.

where f_{π}^{TC} is the analog of the pion decay constant and has a value around the electroweak scale. Thus, there is no hierarchy problem in TC theories, because the electroweak scale is dynamically generated by the confining phase of a non-abelian gauge theory.

While technicolor solves the hierarchy problem and gives masses to the electroweak gauge bosons, it does not provide masses for fermions. In order to implement a Yukawa coupling, one must communicate the EWSB to the SM quarks and leptons. The solution to this problem was developed soon after the original papers, based on an enlarged technicolor gauge group $G_{\text{ETC}} \supset G_{\text{TC}}$, in which SM and TC fermions transform under the same representation, so that the corresponding ETC gauge bosons couple the TC fermions to the SM fermions [25, 26]. These models are called *extended technicolor* (ETC), and after integrating out the heavy ETC gauge bosons at some scale $\Lambda_{\text{ETC}} > \Lambda_{\text{TC}}$, and after Fierz transformations, there appear three different types of dimension six operators,

$$\mathcal{L}_{d=6} = a_{ij} \frac{\bar{Q}T^i Q \bar{Q}T^j Q}{\Lambda_{\text{ETC}}^2} + b_{ij} \frac{\bar{Q}T^i Q \bar{q}T^j q}{\Lambda_{\text{ETC}}^2} + c_{ij} \frac{\bar{q}T^i q \bar{q}T^j q}{\Lambda_{\text{ETC}}^2}. \quad (1.11)$$

where T^i denote the G_{ETC} generators. The a -terms, connect TC fermions, which are denoted by Q , with each other, the b -terms couple TC fermions to SM fermions, which will from now on be denoted by q (we concentrate on the quark sector), and the c -terms couple SM fermions among each other. For the current discussion the a -terms are unimportant.¹² The b -terms generate the effective Yukawa couplings after formation of the techniquark condensate at the ETC scale, as illustrated in Figure 1.1,

$$\mathcal{L}_{\text{Yukawa}} \ni \frac{b}{\Lambda_{\text{ETC}}^2} \bar{q}_L \langle \bar{Q}Q \rangle_{\text{ETC}} q_R. \quad (1.12)$$

¹²They will give masses to additional technipions in the $N_F > 1$ case, in the same way as the pion mass difference is generated by photon exchange, see [27, p.61] for further details.

Here the subscript at the vertical bar reads “evaluated at the respective scale”. Therefore, the quark masses are given by

$$m_q \sim b \frac{\langle \bar{Q}Q \rangle|_{\text{ETC}}}{\Lambda_{\text{ETC}}^2} = b \frac{N_{\text{TC}} \Lambda_{\text{TC}}^3}{\Lambda_{\text{ETC}}^2}, \quad (1.13)$$

where we have assumed that $\langle \bar{Q}Q \rangle|_{\text{ETC}} = \langle \bar{Q}Q \rangle|_{\text{TC}} = N_{\text{TC}} \Lambda_{\text{TC}}^3$. Since Λ_{TC} is set by the electroweak breaking scale, for fixed N_{TC} , the scale Λ_{ETC} can be extracted from (1.13) if the physical quark masses are used as an input. Allowing for a step-wise breaking of the extended symmetry at different scales $\Lambda_1 > \Lambda_2 > \Lambda_3$ would make it even possible to dynamically generate the hierarchy between the three generations which will therefore obtain masses $m_{q_3} > m_{q_2} > m_{q_1}$.

However, Λ_{ETC} is severely constrained from the third type of contributions to (1.11), the c -terms, which generate FCNC processes suppressed by the same scale that enters the effective Yukawas. From Table 1.1 we know that even in more optimistic scenarios (assuming no additional CP violation), this bound amounts to at least $\Lambda_{\text{ETC}} > 10^3$ TeV, which translates in a maximal quark mass of ($N_{\text{TC}} < 10, \Lambda_{\text{TC}} \sim 1\text{TeV}$)

$$m_q < b \times 10 \text{ MeV}. \quad (1.14)$$

Especially the large mass of the top quark poses therefore a problem for theories where the Higgs is described by a bound state.

This problem can be attenuated by considering theories that are *not* like QCD [20]. In a QCD-like theory, the running of the coupling is fast because asymptotic freedom sets in quickly above Λ_{QCD} , as illustrated on the upper left panel of Figure 1.2. The techniquark condensate will therefore stay roughly the same between the ETC scale and the TC scale and the assumption going into (1.13) is justified. More precisely, the running is given by

$$\langle \bar{Q}Q \rangle|_{\text{ETC}} = \exp \left(\int_{\Lambda_{\text{TC}}}^{\Lambda_{\text{ETC}}} \frac{d\mu}{\mu} \gamma_m(\alpha(\mu)) \right) \langle \bar{Q}Q \rangle|_{\text{TC}}, \quad (1.15)$$

and QCD-like running corresponds to an anomalous dimension $\gamma_m(\alpha(\mu)) \approx \gamma\alpha(\mu) \approx \gamma/\ln(\mu)$, which results in a power-logarithmic enhancement factor proportional to $\ln(\Lambda_{\text{ETC}})^\gamma/\ln(\Lambda_{\text{TC}})^\gamma$, similar to QCD radiative corrections to semileptonic electroweak processes.

For general strongly coupled theories, such a behaviour is not mandatory. It may well be, that the coupling evolves slowly for a large range of scales, before asymptotic freedom sets in, as depicted on the lower left panel of Figure 1.2. In such a case, the coupling stays close to a constant, so that $\gamma_m(\alpha(\mu)) \approx \gamma\alpha(\mu) \approx \gamma\alpha^*$ and the radiative corrections give a power-law enhancement factor $(\Lambda_{\text{ETC}}/\Lambda_{\text{TC}})^\gamma$. In terms of the beta function, this behaviour corresponds to the convergence to a *conformal fixed point*, but not quite reaching it, as illustrated in the lower right panel of Figure 1.2. Yang-Mills theories with this behaviour are called *walking* and the corresponding *walking technicolor* (WTC) theories allow for a significant amplification of the a - and b -terms in (1.11), while the FCNC inducing c -terms, which do not couple to the technicolor sector, still feel the full ETC scale suppression. In the WTC scenario, we can thus

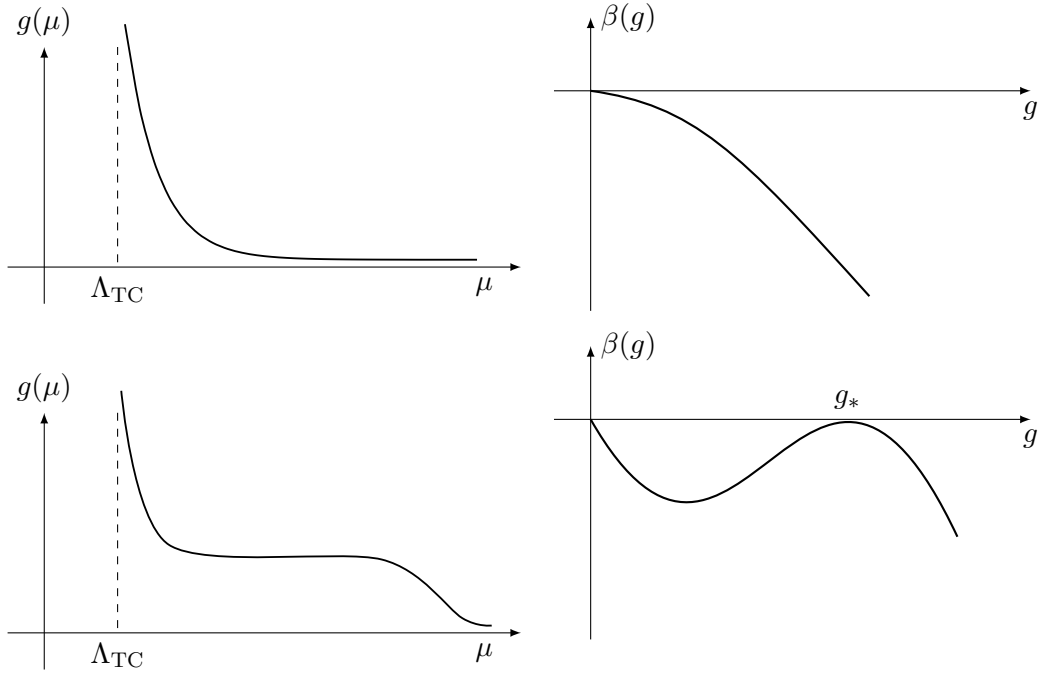


Figure 1.2: Couplings and beta functions of strongly coupled theories.

rewrite the operators in (1.11) at the TC scale symbolically as (symbolically in the sense that a Lagrangian itself should be independent of the energy scale)

$$\mathcal{L}_{d=6} = a_{ij} \frac{\overline{Q}T^i Q \overline{Q}T^j Q}{\Lambda_{\text{ETC}}^{2-2\gamma}} + b_{ij} \frac{\overline{Q}T^i Q \overline{q}T^j q}{\Lambda_{\text{ETC}}^{2-\gamma}} + c_{ij} \frac{\overline{q}T^i q \overline{q}T^j q}{\Lambda_{\text{ETC}}^2}. \quad (1.16)$$

For walking technicolor theories, analyses based on the Schwinger-Dyson equation show that the anomalous dimension has an upper bound of $\gamma \sim 1$, see *e.g.* [27, p.75]. Equivalently, one can say that the scaling dimension of the techniquark condensate $\Delta_{\overline{Q}Q} \equiv \dim\langle \overline{Q}Q \rangle = 3 - \gamma$, is bound from below by $\Delta_{\overline{Q}Q} = 2$. This generates an upper bound

$$m_q \lesssim b N_{\text{TC}} \frac{\Lambda_{\text{TC}}^{3-\gamma}}{\Lambda_{\text{ETC}}^{2-\gamma}}, \quad (1.17)$$

which allows for quark masses as large as ($N_{\text{TC}} < 10$, $\Lambda_{\text{TC}} \sim 1\text{TeV}$)

$$m_q < b \times 10 \text{ GeV}, \quad (1.18)$$

which would still need fine-tuned parameters in order to explain the large top mass. Equation (1.17) suggests, that this bound can be loosened further by choosing a larger number of colors N_{TC} , or increasing the number of flavors N_F of technifermions which take part in the condensation. However, the β -function of an $SU(N_C)$ gauge theory

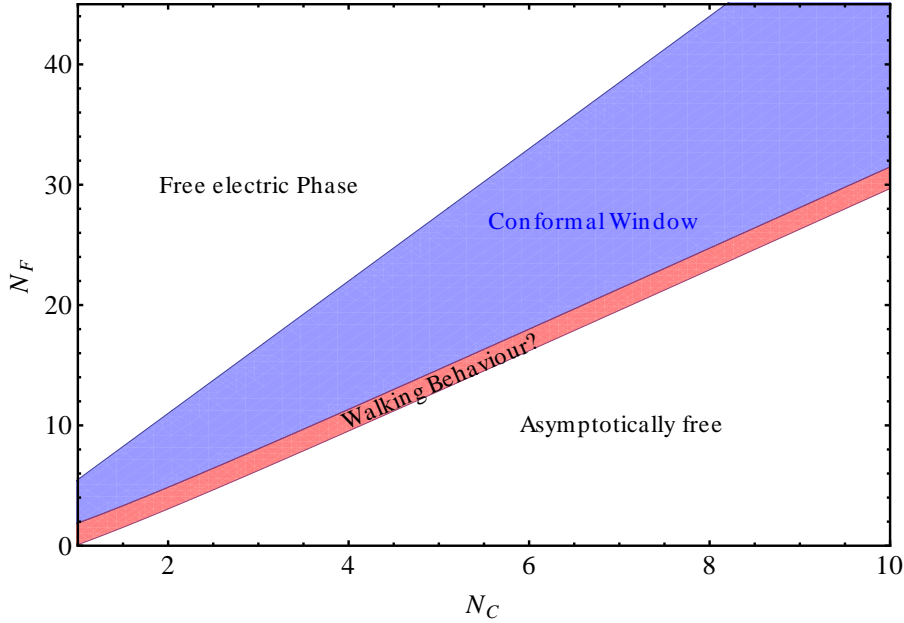


Figure 1.3: Phase diagram of an $SU(N_C)$ Yang-Mills theory with N_C numbers of color and N_F copies of fermions in the fundamental representation.

is a function of the number of flavors and colors,

$$\beta(g) = -\frac{g^3}{(4\pi)^2} (11N_C - 2N_F) + \frac{g^5}{(4\pi)^4} \left(\frac{34}{3}N_C^2 - \frac{1}{2}N_F \left[\frac{16}{3} - \frac{20}{3}N_C \right] \right) + \mathcal{O}(g^7), \quad (1.19)$$

and those must be chosen in a certain ratio in order to end up just below the lower boundary of the conformal window (the region where the theory may evolve to an infrared fixed point),

$$\frac{11}{2}N_C > N_F > \frac{17N_C^2}{4 + 5N_C} \quad (1.20)$$

which allows for walking gauge theories, see Figure 1.3. A technicolor theory is therefore constrained in the possible values of N_F and N_{TC} . Also, a larger number of flavors will give rise to additional technipions which have not been seen at colliders. It is however possible to allow for theories, which are not $SU(N_C)$, but $SO(N)$ or $Sp(N)$ and also the technifermions must not be in the fundamental representation, but may be in the adjoint or even higher representations of the gauge group, which changes the conformal window and therefore the possible N_F, N_C configurations (a

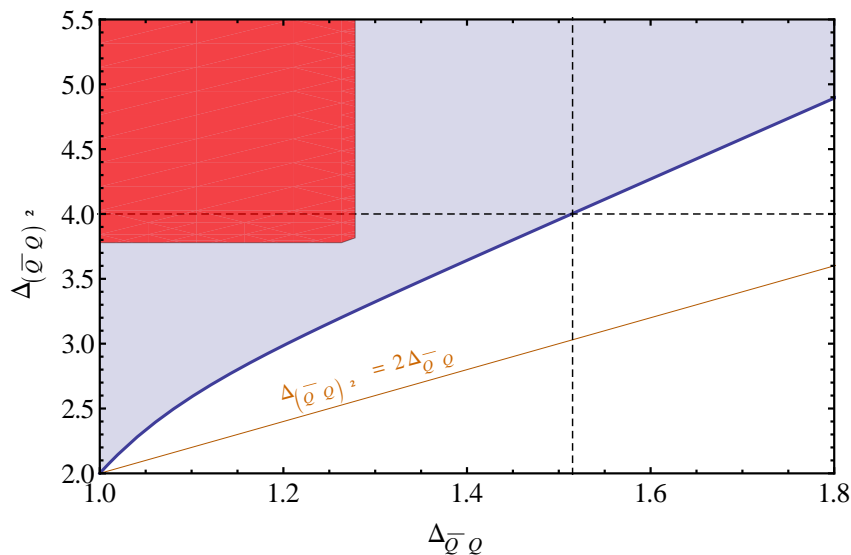


Figure 1.4: Region in the $\Delta_{\bar{Q}Q} - \Delta_{(\bar{Q}Q)^2}$ plane which is excluded using numerical methods, shown in blue. These bounds depend on the global symmetry of the technicolor condensate (and become weaker for a larger symmetry group), which is assumed to be $SU(2)$ in this plot. The red region in the upper left corner is the preferred region by flavor bounds on the ETC scale and a natural top mass. The dashed cross indicates the lowest possible value of $\Delta_{\bar{Q}Q}$, while $\Delta_{(\bar{Q}Q)^2} = 4$, and the orange line depicts the large N limit $\Delta_{(\bar{Q}Q)^2} = 2\Delta_{\bar{Q}Q}$.

good review is [28]).

Alternatively one can avoid the bound on the technicolor condensate scaling dimension $\Delta_{\bar{Q}Q} \geq 2$ and ask for even larger anomalous dimensions $\gamma > 1$, considering the confining gauge theory is *at* a strongly interacting fixed point, which means *in* the conformal window in Figure 1.3 or actually reaching g^* in the lower right panel of Figure 1.2. These theories are called *conformal technicolor* (CTC) and, in contrast to WTC, such a Yang-Mills theory requires an *external* source which breaks the conformal symmetry in order to create a mass gap and force the techniquark condensate to form. In this respect CTC is very similar to supersymmetry, where also an external breaking ultimately triggers EWSB. Ideally, one would aim for a theory, in which the scaling dimension of the technicolor condensate is as close to $\Delta_{\bar{Q}Q} = 1$ as possible, and the top mass is as natural as in the SM, while the ‘‘Higgs mass’’ operator still is at $\Delta_{(\bar{Q}Q)^2} \equiv \dim\langle\bar{Q}Q\bar{Q}Q\rangle = 4$ so that the hierarchy problem can be avoided [29]. However, the limit $\Delta_{\bar{Q}Q} = 1$ corresponds to the free noninteracting theory, in which always $\Delta_{(\bar{Q}Q)^2} = 2$. Yet for slightly different values $\Delta_{\bar{Q}Q} = 1 + \epsilon$, with $\epsilon = 1/\text{few}$, the relation $\Delta_{(\bar{Q}Q)^2} = 2\Delta_{\bar{Q}Q}$ does not hold, except in the large N_C limit, in which matrix elements factorize. The question is, how small can ϵ be, while $\Delta_{(\bar{Q}Q)^2} \geq 4$? Although there is very limited knowledge about strongly interacting theories, the

large amount of symmetry of a conformal theory allows to extract information on the bounds on the scaling dimension $\Delta_{\bar{Q}Q}$ in dependence of $\Delta_{(\bar{Q}Q)^2}$ numerically. The progress made over the last years in these studies leads to the blue curve plotted in Figure 1.4, corresponding to a fit function from [30, Sec. 3.2]. The blue shaded region corresponds to the numerically excluded region. The result is, that there exists no conformal field theory in the phenomenologically preferred region, indicated by the red shaded rectangle. Additional assumptions, like minimal flavor violation, are thus necessary to find a viable CTC theory. Nevertheless, CTC may be the only way to implement strongly coupled EWSB without introducing composite fermions.

Partial Compositeness

The concept of partial compositeness was introduced in 1991 by Kaplan [31]. It is based on the fact that there may be a fourth kind of dimension six operators not included in (1.11), if the strongly coupled sector allows for fermionic bound states with the same quantum numbers as the SM fermions, build from three technifermions,

$$d_{ij} \frac{\bar{q}T^i Q \bar{Q}T^j Q}{\Lambda_{\text{ETC}}^2}. \quad (1.21)$$

This bound state will appear as a composite Dirac-fermion and leads to a novel mechanism to generate fermion masses. The basic idea is, that the elementary SM fermions are massless and do not couple directly to the technicolor condensate, *i.e.* the TC condensate has a small or even a *negative* anomalous dimension, so that the b -terms are irrelevant. The composite fermions however may have a marginal Yukawa coupling with the TC condensate (suggestively called H in this section), because the Yukawa operator does now only contain composites and its scaling dimension is therefore not the sum of the scaling dimensions of its constituents.¹³ Only through the linear mixing generated by the operator (1.21) will EWSB be communicated to the SM fermions.

Kaplan first developed his idea in upscaled QCD TC and therefore he considered the techniquarks to form technibaryons $Q\bar{Q}Q \rightarrow |\psi(0)|^2 B$, with $|\psi(0)|^2$ the wavefunctions overlap of the techniquarks in the technibaryon, measuring the coupling strength. Naive dimensional analysis tells us $|\psi(0)|^2 \sim \Lambda_{\text{TC}}^3$, which can be supported by comparison with the QCD analogue, see [32, eq. (2.12) and (2.13)].

Denoting the left/right-handed Lorentz-chirality of the $SU(2)_L$ -doublet composite by B_L and B_R and the $SU(2)_L$ -singlet with components B_L^c and B_R^c , one can write down an effective Lagrangian,

$$\mathcal{L} \ni \frac{\Lambda_{\text{TC}}^3}{\Lambda_{\text{ETC}}^2} (\tilde{d} \bar{q}_R B_L^c + d \bar{q}_L B_R) - m_B \bar{B} B - \tilde{m}_B \bar{B}^c B^c + \bar{B}_L (\lambda H B_R^c) + h.c.. \quad (1.22)$$

Here, d and \tilde{d} denote the mixing parameters from (1.21) and its analogue involving a right-handed SM-quark, λ is an $\mathcal{O}(1)$ Yukawa coupling in the composite sector, and

¹³In the original paper, a coupling to a composite Higgs was not considered and only explicit mass terms for the composite fermions were introduced.

m_B, \tilde{m}_B are the vector masses of the technibaryons. In walking TC, it is assumed that the technibaryons B and B^c have large anomalous dimensions, bound from below only by the unitarity constraint for fermionic operators $\dim B \geq 3/2$. We can therefore again symbolically put in the effect of the walking in the above Lagrangian at the TC scale, so that

$$\tilde{d} \frac{\Lambda_{\text{TC}}^3}{\Lambda_{\text{ETC}}^2} \bar{q}_R B_L^c + d \frac{\Lambda_{\text{TC}}^3}{\Lambda_{\text{ETC}}^2} \bar{q}_L B_R \quad \rightarrow \quad \tilde{d} \frac{\Lambda_{\text{TC}}^{3-\tilde{\gamma}}}{\Lambda_{\text{ETC}}^{2-\tilde{\gamma}}} \bar{q}_R B_L^c + d \frac{\Lambda_{\text{TC}}^{3-\gamma}}{\Lambda_{\text{ETC}}^{2-\gamma}} \bar{q}_L B_R, \quad (1.23)$$

if we denote the anomalous dimension for B by γ and for B^c by $\tilde{\gamma}$. We will further employ the redefinition $\gamma \rightarrow 3 - \gamma$, in order to make contact with the more recent, holographically inspired literature [61]. The Lagrangian now reads

$$\begin{aligned} \mathcal{L} \ni & \tilde{d} \Lambda_{\text{ETC}} \left(\frac{\Lambda_{\text{TC}}}{\Lambda_{\text{ETC}}} \right)^{\tilde{\gamma}} \bar{q}_R B_L^c + d \Lambda_{\text{ETC}} \left(\frac{\Lambda_{\text{TC}}}{\Lambda_{\text{ETC}}} \right)^{\gamma} \bar{q}_L B_R, \\ & -m_B \bar{B} B - \tilde{m}_B \bar{B}^c B^c + \bar{B}_L (\lambda H B_R^c) + h.c.. \end{aligned} \quad (1.24)$$

Note, that in this notation the unitarity bound requires $3 > \gamma > 0$ and unintuitively smaller γ means stronger coupling. Upon diagonalization of the mass mixing terms, with mass eigenstates denoted by ψ and χ respectively,

$$\begin{pmatrix} q_L \\ B_L \end{pmatrix} = \begin{pmatrix} \cos \varphi_L & -\sin \varphi_L \\ \sin \varphi_L & \cos \varphi_L \end{pmatrix} \begin{pmatrix} \psi_L \\ \chi_L \end{pmatrix}, \quad \tan \varphi_L = \frac{d \Lambda_{\text{TC}}^{\gamma}}{m_B \Lambda_{\text{ETC}}^{\gamma-1}}, \quad (1.25)$$

$$\begin{pmatrix} q_R \\ B_R^c \end{pmatrix} = \begin{pmatrix} \cos \varphi_R & -\sin \varphi_R \\ \sin \varphi_R & \cos \varphi_R \end{pmatrix} \begin{pmatrix} \psi_R \\ \chi_R^c \end{pmatrix}, \quad \tan \varphi_R = \frac{\tilde{d} \Lambda_{\text{TC}}^{\tilde{\gamma}}}{\tilde{m}_B \Lambda_{\text{ETC}}^{\tilde{\gamma}-1}}, \quad (1.26)$$

the Lagrangian reads

$$\mathcal{L} \ni -m_\chi \bar{\chi} \chi - \tilde{m}_\chi \bar{\chi}^c \chi^c + (\bar{\psi}_L \sin \varphi_L + \bar{\chi}_L \cos \varphi_L) \lambda H (\psi_R \sin \varphi_R + \chi_R^c \cos \varphi_R) + h.c.. \quad (1.27)$$

Note that the right-handed component of the $SU(2)_L$ doublet vector quark does not mix, so that $B_R = \chi_R$ and analogously $B_L^c = \chi_L^c$. Before EWSB, the field ψ remains massless and we identify it with the SM fermions. The fields χ, χ^c are the New Physics mass eigenstates with masses

$$m_\chi = \Lambda_{\text{ETC}}^{1-\gamma} \sqrt{m_B^2 \Lambda_{\text{ETC}}^{2\gamma-2} + d^2 \Lambda_{\text{TC}}^{2\gamma}}, \quad m_{\tilde{\chi}} = \Lambda_{\text{ETC}}^{1-\tilde{\gamma}} \sqrt{\tilde{m}_B^2 \Lambda_{\text{ETC}}^{2\tilde{\gamma}-2} + \tilde{d}^2 \Lambda_{\text{TC}}^{2\tilde{\gamma}}}. \quad (1.28)$$

The fact that the SM fermions are admixtures of elementary and composite fermions with a composite component proportional to $\sin \varphi_L$ or $\sin \varphi_R$ motivates the name *partial compositeness*. After EWSB, the SM fermions gain masses through effective Yukawa couplings to the TC condensate H , whose size is also controlled by the mixing angles, and thus by the anomalous dimension of the composite technibaryons,

$$Y_\psi = \sin \varphi_L \lambda \sin \varphi_R. \quad (1.29)$$

Any Yukawa coupling can thus be generated with a fundamental parameter $\lambda = \mathcal{O}(1)$, based on the choice of the mixing angles

$$\sin \varphi_L = d \frac{\Lambda_{\text{TC}}^\gamma}{m_\chi} \Lambda_{\text{ETC}}^{1-\gamma} \quad \text{and} \quad \sin \varphi_R = \tilde{d} \frac{\Lambda_{\text{TC}}^{\tilde{\gamma}}}{m_{\tilde{\chi}}} \Lambda_{\text{ETC}}^{1-\tilde{\gamma}}, \quad (1.30)$$

and therefore, ultimately on the anomalous dimensions of B and B^c . Here, in contrast to WTC, even for very large values of $\Lambda_{\text{ETC}} \sim M_{\text{Planck}}$, also the top mass can be explained, given that the corresponding anomalous dimension is $\gamma < 2$.

Another virtue of partial compositeness becomes evident if one generalizes to 3 generations of SM quarks. In that case each SM quark has a set of composite partners B_i, B_i^c , $i = 1 \dots 3$. The composites have different anomalous dimensions, so that the corresponding effective Yukawa matrices (shown here for the up-type quarks) read

$$\mathbf{Y} = \begin{pmatrix} \sin \varphi_{u_L} & 0 & 0 \\ 0 & \sin \varphi_{c_L} & 0 \\ 0 & 0 & \sin \varphi_{t_L} \end{pmatrix} \boldsymbol{\lambda} \begin{pmatrix} \sin \varphi_{u_R} & 0 & 0 \\ 0 & \sin \varphi_{c_R} & 0 \\ 0 & 0 & \sin \varphi_{t_R} \end{pmatrix}, \quad (1.31)$$

where $\boldsymbol{\lambda}$ is assumed to be an anarchic order one matrix in straight generalization of λ in (1.29). In analogy to the Yukawa couplings in (1.27), there might be further bosonic technicolor resonances, which couple to the composite fermions, for example

$$\mathcal{L} \ni g (\bar{B}_i \gamma_\mu \rho^\mu B_i + \bar{B}_i^c \gamma_\mu \rho^\mu B_i^c), \quad (1.32)$$

which, after diagonalization of the mass mixings, leads to the couplings of the SM fermions

$$\mathcal{L} \ni (\mathbf{g}_L)_{ij} \bar{\psi}_L^i \gamma_\mu \rho^\mu \psi_L^j + (\mathbf{g}_R)_{ij} \bar{\psi}_R^i \gamma_\mu \rho^\mu \psi_R^j, \quad (1.33)$$

with

$$\mathbf{g}_L = g \begin{pmatrix} \sin \varphi_{u_L}^2 & 0 & 0 \\ 0 & \sin \varphi_{c_L}^2 & 0 \\ 0 & 0 & \sin \varphi_{t_L}^2 \end{pmatrix}, \quad \mathbf{g}_R = g \begin{pmatrix} \sin \varphi_{u_R}^2 & 0 & 0 \\ 0 & \sin \varphi_{c_R}^2 & 0 \\ 0 & 0 & \sin \varphi_{t_R}^2 \end{pmatrix}. \quad (1.34)$$

and although these couplings are flavor diagonal, they will have off-diagonal entries in the basis in which the Yukawas are diagonal, because only matrices proportional to the identity commute with the unitary change of basis matrices. This leads to FCNCs. However, the corresponding FCNCs are always suppressed by the same small mixing angles which generate the Yukawa couplings. Therefore, as long as the top does not participate, FCNCs are generically small in models with partial compositeness. Since Randall-Sundrum models with bulk fermions do have this feature, we will examine it in more detail in Section 2.5.

Composite Higgs

TC models are *higgsless* theories, because they do not have a scalar Higgs doublet. QCD-like theories do not predict a sharp scalar resonance at all.¹⁴ There are candidates, for example the TC analogue of the $\sigma/f_0(550)$, but as in QCD it is very broad. In WTC, it may be narrow and even lighter than assumed from scaled up QCD [33], but still heavier than preferred by the LHC measurements.¹⁵ Also, in walking TC theories, there is a Pseudo Nambu-Goldstone boson (PNGB) connected to the breaking of approximate scale invariance, if one is close enough to the conformal window, the so called *dilaton*, which shares the quantum numbers with the neutral SM scalar Higgs component, but has different self-couplings [34].

Composite Higgs models were first proposed and worked out by Kaplan and Georgi in the early eighties [36]. They are philosophically different from TC, because they implement electroweak symmetry breaking in two steps. A global symmetry breaks at some scale $f > v$, which leaves the electroweak symmetry intact but generates four composite Pseudo Nambu-Goldstone bosons. These PNGBs correspond to the degrees of freedom of the Higgs doublet. One can imagine them as being a set of technikaons, if one wants to push further the analogy with QCD. In practice, models without additional Goldstone bosons are preferable, and so the minimal composite Higgs model proposes a global symmetry breaking $SO(5)/SO(4)$, which gives exactly four GBs [37].

The problem of fermion mass generation persists, and is usually solved by introducing partially composite fermions. After integrating out the heavy composite states, one ends up with an effective Yukawa coupling as in (1.31). A potential for the Higgs is then generated at loop level by Yukawa and gauge boson couplings which induce a negative mass squared and force the composite Higgs to take on its vev. However, it is not self-evident, that this loop-induced potential results in a vacuum which breaks the electroweak symmetry. This can be illustrated in terms of the ratio between the EWSB component of the vev, v , and the scale at which the global symmetry is broken, f , given by the angle $\sin \theta = v/f$, see Figure 1.5. Gauge boson loops “like” to preserve the gauge symmetry, *i.e.* they tend to induce a potential with a symmetry preserving minimum, $\theta = 0$. On the other hand, Yukawa couplings generate contributions to the Higgs potential which point in the direction of EWSB and prefer $\theta = \pi/2$.¹⁶ Although very challenging for TC models, the heavy top is therefore a blessing for composite Higgs models, since it allows for a symmetry breaking minimum of the potential. Thus, in an interesting analogy, composite Higgs models and SUSY share a fondness for the large top Yukawa, which is crucial in both scenarios to achieve EWSB. It is however a matter of fine-tuning to get an angle which is still in agreement with electroweak and flavor bounds, which prefer a large scale f , *i.e.* $\sin^2 \theta \sim 0.1$. Thus, even though it does not pose a problem to write down the top Yukawa itself, its large

¹⁴Unitarization of WW scattering is achieved by the exchange of heavier TC vector composites.

¹⁵It should be noted that this might not be true for theories with technifermions in higher representations [35]

¹⁶This was known at the time when Georgi and Kaplan proposed their model, but the top quark was assumed to be lighter than ~ 50 GeV and its contributions negligible. Therefore, new dynamics were necessary and they introduced an additional axial $U(1)_A$.

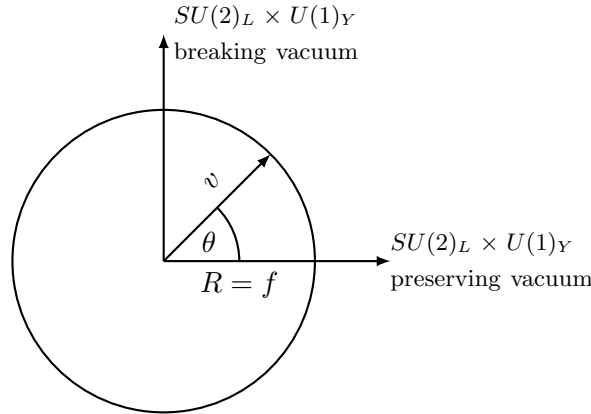


Figure 1.5: Circle of a priori degenerate minima in Composite Higgs models with radius $R = f$, the scale at which the global theory is broken and the Higgs emerges as a pseudo Nambu-Goldstone boson. The angle θ measures the (mis-)alignment with the EWSB vacuum.

contribution to the potential reintroduces a tension comparable to the situation of higgsless TC models, consult [61, Sec.3.4] for details.

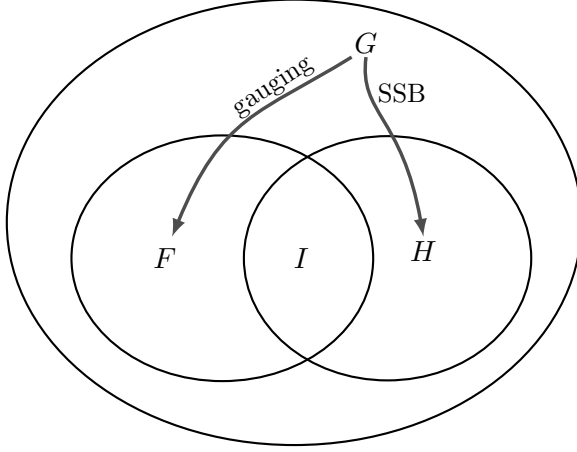
In terms of the angle $\sin \theta$, it also becomes clear how composite Higgs models can be seen as a link between the SM with an elementary Higgs scalar and TC theories. If $f \rightarrow \infty$, $\sin \theta \rightarrow 0$ and all composite states besides the Higgs decouple, so that the theory effectively has an elementary Higgs. For $v \rightarrow f$ however, $\sin \theta \rightarrow 1$ and the model predicts only a single characteristic scale, at which the composites form and EWSB occurs, just like TC.

Collective Symmetry Breaking

In composite Higgs models one can achieve a natural separation of scales $v < f$, but the Higgs mass does still encounter quadratically divergent corrections up to the compositeness scale, because gauge and Yukawa interactions explicitly break the shift symmetry which protects it. Therefore, a large separation $v \ll f$ is unnatural. Loosely speaking, one could say that the Higgs does not profit from being a Nambu Goldstone boson.

This was the inspiration for the mechanism of *collective symmetry breaking*, which is realized in a class of models called *little Higgs* [38].¹⁷ The idea is, that the global symmetry, which breaks dynamically in the composite Higgs model is larger than necessary in order to accommodate the four Goldstone bosons which are identified with the degrees of freedom of the Higgs, and the electroweak gauge group is enlarged as well, so that there is at least another copy of W^\pm s and the Z , which becomes heavy by eating the additional GBs.

¹⁷The name is motivated, because the Higgs in these models is naturally light = little. See Section 1.3 in [38].



Simplest Little Higgs:

$$\begin{aligned}
 G &= SU(3) \times SU(3) \times U(1) \\
 H &= SU(2) \times SU(2) \times U(1) \\
 F &= SU(3) \times U(1) \\
 I &= SU(2) \times U(1)
 \end{aligned}$$

Figure 1.6: Diagram illustrating the relations between the different symmetry groups in a Little Higgs theory. Ignoring gauge interactions and spontaneous symmetry breaking (SSB), G is the global symmetry of the Lagrangian. A subgroup F – larger than the SM gauge group I – is gauged, which breaks the global symmetry. Another global subgroup H is left after SSB. A number of GBs make some of the F gauge bosons heavy, while the ones from I remain massless. The remaining GBs form the Higgs.

If either the SM electroweak gauge bosons *or* the new gauge bosons couple to the Higgs, there will still be a leftover global symmetry, which makes the Higgs a Goldstone boson, *i.e.* massless, but if *both* gauge degrees of freedom couple to the Higgs a mass term is generated, which will then only be logarithmically divergent.

This is illustrated best on the basis of a model introduced by Schmaltz, which he called the *Simplest Little Higgs* [39]. It will be even more simplified here, because we will ignore the $U(1)$ gauge groups. Consider a Lagrangian with two scalar fields, invariant under the global symmetry $G = SU(3)_1 \times SU(3)_2$ (ignoring additional $U(1)$ factors),

$$\mathcal{L} = (\partial_\mu \phi_1)^\dagger (\partial^\mu \phi_1) + (\partial_\mu \phi_2)^\dagger (\partial^\mu \phi_2) + V(|\phi_1|^2, |\phi_2|^2). \quad (1.35)$$

Both scalar fields will take on a vev f , so that the symmetry breaks down to $H = SU(2)_1 \times SU(2)_2$ at that scale. A scheme of the symmetry breaking is provided in Figure 1.6. We adopt the parametrization

$$\begin{aligned}
 \phi_1 &= \exp \left[\frac{i}{f} \begin{pmatrix} \mathbf{0}_{2 \times 2} & \kappa \\ \kappa^\dagger & 0 \end{pmatrix} + \frac{\tilde{\kappa}}{\sqrt{2}f} \mathbb{1}_{3 \times 3} \right] \exp \left[\frac{i}{f} \begin{pmatrix} \mathbf{0}_{2 \times 2} & h \\ h^\dagger & 0 \end{pmatrix} + \frac{\eta}{\sqrt{2}f} \mathbb{1}_{3 \times 3} \right] \begin{pmatrix} 0 \\ 0 \\ f \end{pmatrix}, \\
 \phi_2 &= \exp \left[\frac{i}{f} \begin{pmatrix} \mathbf{0}_{2 \times 2} & \kappa \\ \kappa^\dagger & 0 \end{pmatrix} + \frac{\tilde{\kappa}}{\sqrt{2}f} \mathbb{1}_{3 \times 3} \right] \exp \left[-\frac{i}{f} \begin{pmatrix} \mathbf{0}_{2 \times 2} & h \\ h^\dagger & 0 \end{pmatrix} - \frac{\eta}{\sqrt{2}f} \mathbb{1}_{3 \times 3} \right] \begin{pmatrix} 0 \\ 0 \\ f \end{pmatrix}.
 \end{aligned} \quad (1.36)$$

Here $\{\kappa = (\kappa^-, \kappa^0), \tilde{\kappa}\}$ and $\{h = (h^-, h^0), \eta\}$ denote each five Goldstone bosons from the breaking G/H . Now assume that the diagonal subgroup $F = SU(3)_{\text{diag}}$ of G is gauged, so that the kinetic part of (1.35) becomes

$$\mathcal{L}_{\text{kin}} = (D_\mu \phi_1)^\dagger (D^\mu \phi_1) + (D_\mu \phi_2)^\dagger (D^\mu \phi_2) \quad (1.37)$$

with $D_\mu = \partial_\mu - ig T^a A_\mu^a$, $a = 1, \dots, 8$. This is an explicit breaking of the subgroup H , so that only $I = H \cap F = SU(2)_{\text{diag}}$ (generated by the T^a s with the Pauli matrices in the upper left corner) remains unbroken. The interaction terms from (1.37) can be written as

$$\sum_i |D_\mu \phi_i|^2 \ni \text{Tr} \left\{ g^2 (A_\mu^a T^a)^2 (\phi_1 \phi_1^\dagger + \phi_2 \phi_2^\dagger) \right\}, \quad (1.38)$$

where g is the weak coupling constant in this model and (ignoring the singlet η)

$$\phi_1 \phi_1^\dagger + \phi_2 \phi_2^\dagger = \begin{pmatrix} h^\dagger h & 0 \\ 0 & f^2 - h^\dagger h \end{pmatrix}. \quad (1.39)$$

And, if we denote the new gauge bosons by X and the SM ones as usual, we find in the mass eigenbasis

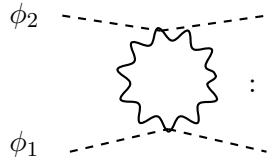
$$A_\mu^a T^a = \frac{1}{\sqrt{2}} \begin{pmatrix} B_\mu^0 + \frac{X_\mu^8}{\sqrt{3}} & W_\mu^+ & X_\mu^0 \\ W_\mu^- & \frac{X_\mu^8}{\sqrt{3}} - B_\mu^0 & X_\mu^- \\ \bar{X}_\mu^0 & X_\mu^+ & \frac{-2}{\sqrt{3}} X_\mu^8 \end{pmatrix}, \quad (1.40)$$

so that

$$\begin{aligned} \text{Tr} \left\{ g^2 (A_\mu^a T^a)^2 (\phi_1 \phi_1^\dagger + \phi_2 \phi_2^\dagger) \right\} &= \frac{g^2}{2} f^2 \left(\frac{8}{3} X_\mu^8 X^{\mu 8} + \bar{X}_\mu^0 X^{\mu 0} + X_\mu^+ X^{\mu -} \right) \\ &+ \frac{g^2}{2} h^2 (W_\mu^+ W^{\mu -} + 2B_\mu^0 B^{\mu 0} - X_\mu^+ X^{\mu -} - 2X_\mu^8 X^{\mu 8}) \\ &+ \frac{2g^2}{\sqrt{3}} h^2 X_\mu^8 B^{\mu 0}. \end{aligned} \quad (1.41)$$

Two things become evident from this result. First, the five gauge bosons corresponding to the broken T^a s, $a = 1, \dots, 5$ have *eaten* the κ fields from (1.36) and gain masses proportional to the scale f , while the remaining three gauge bosons will become massive if the Higgs field h acquires a vev. Second, the couplings to the Higgs in the second line of (1.41) are of the same magnitude but of opposite sign between the new gauge fields and the weak gauge fields. This leads to a cancellation (between equal spin fields), which will assure that no quadratic divergent loop diagrams appear in the theory. The reason is, that if one covariant derivative in (1.37) was replaced by $D_\mu \rightarrow \partial_\mu$, all GBs of the corresponding scalar would be exact. Thus, only gauge interactions including both scalars ϕ_1 and ϕ_2 break the shift symmetry and can give

a contribution to the Higgs mass. A corresponding diagram is given by



$$\frac{g^4}{16\pi^2} \log\left(\frac{\Lambda^2}{\mu^2}\right) |\phi_1^\dagger \phi_2|^2 = \frac{g^4}{16\pi^2} \log\left(\frac{\Lambda^2}{\mu^2}\right) (f^2 - 2h^\dagger h)^2,$$

(1.42)

and a similar mass is generated for the real singlet η . Such a cancellation must also be installed in the fermion sector, so that these models at least have an additional top-partner. Light fermions may give quadratic corrections up to a larger scale because their Yukawa couplings are small (the same reason which allows for a splitting in the MSSM sfermion mass spectrum).

Thus, the hierarchy between the scale of compositeness and the electroweak scale is explained and one naturally achieves the desired $\sin^2\theta \sim 1/(16\pi^2) \ll 1$. For completeness, it should be mentioned that it is also possible to construct little Higgs models with one symmetry breaking scalar, but two different gauge groups with a common factor group. In these scenarios, collective symmetry breaking is achieved by multiple gauged subgroups of the global symmetry (if only one gauge group is active, the residue global symmetry protects the Higgs mass). In the minimal model, one can get along with exactly four gauge partners for the four electroweak SM gauge bosons [40].

Extra Dimensions

Flat Extra Dimensions

Additional compact spatial dimensions may provide an explanation for the extreme weakness of gravity, if it is the only force which feels the extra volume and is thus diluted by propagating in the extra dimension.

Historically, additional compact dimensions were first proposed by Nordström [43] and subsequently by Kaluza and Klein [45, 44] almost 100 years ago, originally introduced with the purpose to find a unified theory of gravity and electrodynamics. In the context of the hierarchy problem however, the significance of extra dimensions was only realized by Arkani-Hamed, Dvali and Dimopoulos (ADD) in 1998 [48]. Their idea was motivated by the observation, that gravity, in contrast to the SM, is only tested at distances of order 0.1 mm, corresponding to an energy scale of 10^3 eV [46].¹⁸ At these energies, for small masses, Newtons law is a good approximation of general relativity. A modification of the inverse square law might therefore have gone undetected if it only comes to the fore at distances smaller than a tenth of a millimeter. To be

¹⁸This bound is so weak, that there are serious attempts to explain the cosmological fine-tuning problem –the question why the cosmological constant is so small despite quartic radiative corrections– by a modification of gravity close to this scale [47].

more precise, consider an extension of Minkowski spacetime M^4 by n compact extra dimensions S^n ,

$$M = M^4 \times S^n. \quad (1.43)$$

These extra dimensions are assumed to be only accessible by gravity, while the SM is confined to a *domain wall* or *brane* with a thickness δ – in contrast to the volume of the extra dimensions, which is called *bulk*. The radii of these extra dimensions are considered small enough to have escaped detection so far, but still large compared to the Planck length. In spherical coordinates it follows for the spatial infinitesimal line element (assuming all radii R equal for simplicity)

$$ds^2 = g_{ij}dx^i dx^j = dr^2 + r^2 d\Omega_2^2 + R^2 d\Omega_n^2, \quad (1.44)$$

so that $\sqrt{|g|} \sim R^n r^2$, with $g \equiv \det g_{MN}$ and $M, N = 0, 1, \dots, n+4$. The Poisson equation for the gravitational potential of a point-like source, measured at $r \gg R$ then reads

$$\partial_i \left(\sqrt{|g|} g_{ij} \partial_j \right) V(r) = R^n \partial_r (r^2 \partial_r) V(r) = \delta(r) \quad (1.45)$$

which is solved by

$$V(r) \sim -\frac{G_{4+n}}{R^n r} = -\frac{G_4}{r}, \quad (1.46)$$

where G_{4+n} denotes the gravitational constant in $4+n$ dimensions and $G_4 = G_{4+n}/R^n$ the effective four-dimensional gravitational constant. The weakness of gravity, or equivalently the size of the effective 4D Planck mass

$$M_{\text{Pl}}^2 \sim 1/G_4 = R^n M_{\text{Pl}(4+n)}^{n+2}, \quad (1.47)$$

is attributed to the number and size of additional compact extra dimensions, so that the fundamental constant $M_{\text{Pl}(4+n)}$ might be of the order of the weak scale. For experiments at macroscopic distances, $r \gg R$, the existence of compact extra dimensions manifests itself as a seemingly extreme weakness of gravity, while at a more fundamental level it can be explained by the field lines of gravity escaping in new spatial directions. At distances $r < R$ however, the radial coordinate of the compact dimensions in (1.45) is treated on the same footing as the one corresponding to the infinite dimensions. As a consequence one would expect a radical modification to the inverse square law once experiments are able to resolve the compact dimensions. This of course depends on their size, which on the other hand is roughly fixed by the requirement to solve the hierarchy problem. The hierarchy between the weak and the Planck scale is explained for the following arrangements of number and radii of extra dimensions (assuming $M_{\text{Pl}(4+n)} = 1 \text{ TeV}$)

Number n	1	2	3	...
Radius R	$\sim 10^{13} \text{ m}$	$\sim 10^{-9} \text{ m}$	$\sim 10^{-11} \text{ m}$...

Physically, the size of the radius is fixed by the vacuum expectation value of the purely extra-dimensional components of the metric tensor, g_{nn} , the *radion* or *modulus* fields. It can thus be argued, that the hierarchy problem in the ADD model is only reformulated in a geometric language. The large ratio between the Planck and the weak scale is replaced by the ratio between brane thickness and radii of the extra dimensions δ/R . In addition, phenomenological problems arise if the fundamental Planck scale is small. If gravity becomes strong at energy scales $E \sim M_{\text{PL}(4+n)} = 1 - 10 \text{ TeV}$, processes like graviton mediated proton decay are only suppressed by that scale and therefore vastly increased over the experimentally acceptable limit. As in SUSY, such a process must be forbidden by additional gauged symmetries (Baryon- or Lepton number) or by a properly adjusted localization of matter fields along the extended brane, the so called *fat brane* or *split fermion* scenario, in which the couplings between different matter fields may be small due to a small overlap of the localization functions inside the brane [41].

A signature of extra dimensional models is the existence of an infinite tower of excited states (think higher harmonics of a particle in a box) of every field which may propagate into the bulk. In the ADD scenario, this would imply new massive resonances with the same quantum numbers as a graviton. The masses of these modes are set by the radius, $m_n \sim n/R$ for the n th mode, which represents an interesting signature, because depending on the number of extra dimensions, an almost continuous spectrum of graviton states is predicted ($M_{\text{PL}(4+n)} = 1 \text{ TeV}$),

$$\delta m_n \sim \frac{1}{R} = M_{\text{PL}(4+n)} \left(\frac{M_{\text{PL}(4+n)}}{M_{\text{PL}}} \right)^{\frac{2}{n}}, \quad \text{e.g. } \delta m = 10^3 \text{ eV}, \quad \text{for } n = 2. \quad (1.48)$$

On the basis of these ideas, models which allow for all SM fields to propagate in the extra dimensions, the *Universal Extra Dimension* (UED) scenarios were explored [42]. Generically, they do not add anything to the understanding of the hierarchy problem as the difference between brane gauge theory and bulk gravity is removed. They can clearly not be large extra dimensions, based on the equation above, so that the radius is usually a free variable and a solution to the hierarchy problem is generically not provided.

UED however set the stage for extra-dimensional higgsless models, in which the additional compact dimension is not a manifold, but an orbifold, for example a circle with opposing points glued together by factoring out a \mathbb{Z}_2 , technically an interval S_1/\mathbb{Z}_2 , as shown in Figure 1.7. This process leaves two fixed points, $\phi = 0$ and $\phi = \pi$. Depending on whether they have negative or positive parity under \mathbb{Z}_2 , $\chi(\phi) \rightarrow \pm\chi(-\phi)$, fields propagating in the bulk must now get assigned either Neumann or Dirichlet boundary conditions (BCs) at the fixed points and consequentially fields with negative parity have no zero mode. This technique is known as Scherk-Schwarz mechanism and was already found in the seventies [49]. Orbifolding is also necessary in each UED scenario with an odd number of extra dimensions, because fermions are Dirac fermions in the fundamental representation for such a setup and chiral zero modes can only be achieved by projecting out the unwanted degrees of freedom, which will be discussed in detail in Section 2.1. Choosing negative parity for the appropriate linear combination of electroweak gauge fields makes it possible to implement EWSB via BCs. However,

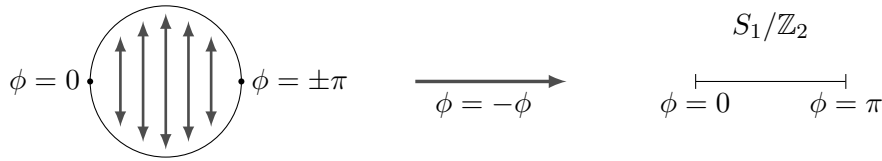


Figure 1.7: Sketch of the orbifolding procedure.

if the BCs are set by orbifolding, the theory mimics a nonlinear sigma model with a bunch of vector resonances (the KK modes of the SM fields), who ensure tree-level unitarity of the WW scattering amplitude. A breaking via mixed BCs (with a finite vev) can be modeled with a scalar living on a 4D brane at one of the fixed points, but will inevitably bring back the hierarchy problem again. See [50], especially Section 6, for a clear discussion.

Also related to the UED idea are *gauge-Higgs unification* models, in which the Higgs is made of the extra dimensional components of a bulk gauge field. This idea was well born in the seventies [51], but only realized as a solution to the hierarchy problem some 20 years later [52]. As the scalar component of a bulk gauge field A_M , the gauge symmetry $A_M \rightarrow A_M + \partial_M \alpha$ will prevent the Higgs from getting a mass term. The mechanism is very similar to SUSY, in which the chiral symmetry is inherited by putting scalars and fermions in a supermultiplet, while in gauge-Higgs unification scalars share the gauge symmetry with a gauge boson by forming a higher dimensional gauge field together. Clearly, since the Higgs is an electroweak doublet and a bulk gauge boson transforms under the adjoint representation, even the simplest implementation requires an enlarged gauge group $SU(3) \supset SU(2)_L \times U(1)_Y$ [53, Sec. 3.2]. Its adjoint representation decomposes into the representations of the $SU(2)_L$ subgroup according to $\mathbf{8} \rightarrow \mathbf{3} + \mathbf{2} + \mathbf{2} + \mathbf{1}$. More precisely, considering again S_1/\mathbb{Z}_2 as the extra dimension, the bulk gauge field can be decomposed just like the 5D generalization of (1.40), so that the scalar components of the generalized $(X_M^0, X_M^-) = H$ are identified with the degrees of freedom of the Higgs boson and likewise the vector components of the W_M, X_M^8, B_M^0 fields should give the electroweak gauge bosons. Therefore, the BCs of these fields must be Neumann, in order to acquire a zero mode, while the zero mode of their respective vector or scalar components vanish. Although the $SU(3)$ gauge symmetry is broken at the boundaries, the remnant protection allows only for a radiatively generated Higgs potential which is non-local in the extra-dimension (generated by Wilson lines). As a consequence it is finite to all orders (another similarity with SUSY), but leads generically to a small Higgs quartic coupling and thus to a too light Higgs. Another characteristic of these models is, that 5D Yukawa interactions are automatically provided by the fifth component of the kinetic term for the fermions, but this means also that without additional assumptions, all fermion masses are equal and proportional to the gauge coupling (for details see [54] and references therein).

Warped Extra Dimensions

A qualitatively different implementation of compact extra dimensions was found by Randall and Sundrum in 1998, who assumed a non-flat extension of 4D Minkowski spacetime [55]. The idea is, that the compactification radius may be of the Planck length $r_c \sim \ell_{\text{Pl}}$, so that the hierarchy between scales is not due to the volume of the extra dimension, but results from a specific choice of large negative bulk cosmological constant (see Section 2.1 for details). As a consequence, the fifth dimension is subject to a strong curvature k , so that $kr_c \approx 12$, leading to an unfactorizable metric

$$ds^2 = e^{-2\sigma(\phi)} \eta_{\mu\nu} dx^\mu dx^\nu - r_c^2 d\phi^2, \quad (1.49)$$

where the fifth dimension can be represented by an S_1/\mathbb{Z}_2 orbifold with the coordinate ϕ running from $0 \leq \phi \leq \pi$ and $\sigma(\phi) \equiv kr_c|\phi|$. At the fixed points are two branes, the Planck brane at $\phi = 0$ and the TeV brane at $\phi = \pi$. The names result from the fact that the metric is rescaled at each four dimensional slice of the bulk according to the *warp factor* $e^{-2\sigma(\phi)}$.

This translates into a rescaling of dimensionful parameters in the effective 4D Lagrangian. In order to see this, consider the case where all SM fields are localized on the TeV brane (as in the original paper). With $G \equiv \det(G_{MN})$, the determinant of the 5D metric tensor, and η its 4D counterpart, the Higgs potential part of the action reads

$$\begin{aligned} S \ni & \int d^4x \int_{-\pi}^{\pi} d\phi \sqrt{|G|} \left(\mu^2 H^\dagger H - \lambda (H^\dagger H)^2 \right) \frac{\delta(|\phi| - \pi)}{r_c} \\ & = \int d^4x \sqrt{|\eta|} e^{-4kr_c\pi} \left(\mu^2 H^\dagger H - \lambda (H^\dagger H)^2 \right) \\ & = \int d^4x \sqrt{|\eta|} \left(\mu_{\text{eff}}^2 \tilde{H}^\dagger \tilde{H} - \lambda (\tilde{H}^\dagger \tilde{H})^2 \right). \end{aligned} \quad (1.50)$$

Here, $\tilde{H} = e^{-kr_c\pi} H$ is just a field redefinition, but the effective 4D Higgs mass parameter

$$\mu_{\text{eff}} = e^{-kr_c\pi} \mu = \frac{\Lambda_{\text{IR}}}{\Lambda_{\text{UV}}} \mu, \quad (1.51)$$

in which Λ_{IR} should be identified with the weak scale, is the product of the fundamental mass scale $\mu \approx M_{\text{Pl}}$ and the warp factor. The size of a dimensionful variable therefore changes depending on the position along the extra dimension from the Planck scale at the Planck brane to the weak scale at the TeV brane. One can further deduce from the curvature part of the 5D Einstein-Hilbert action, that

$$\begin{aligned} S \ni & -M_{\text{Pl}(5)}^3 \int d^4x \int_{-\pi}^{\pi} d\phi \sqrt{|G|} R_5 \\ & = -M_{\text{Pl}(5)}^3 \int d^4x \int_{-\pi}^{\pi} d\phi \sqrt{|\eta|} r_c e^{-2\sigma(\phi)} R_4 \\ & = -\frac{M_{\text{Pl}(5)}^3}{k} \left[1 - e^{-2kr_c\pi} \right] \int d^4x \sqrt{|\eta|} R_4, \end{aligned} \quad (1.52)$$

where the 5D curvature, derived from G_{MN} , and the 4D curvature, derived from the 4D block of G_{MN} , $g_{\mu\nu} = e^{-2\sigma}\eta_{\mu\nu}$, are related by $R_5(G) = e^{2\sigma(\phi)}R_4(g) + \dots$ up to terms which vanish upon ϕ -integration or cancel with cosmological constant terms. Matching with the 4D Einstein-Hilbert action implies that

$$M_{\text{Pl}}^2 = \frac{M_{\text{Pl}(5)}^3}{k} \left[1 - e^{-2kr_c\pi} \right], \quad (1.53)$$

which, as a consequence of the strong curvature, is largely independent of the radius r_c , in contrast to (1.47). Likewise, the masses of the KK excitations are not tied to the radius of the extra dimension, but depend on the curvature scale $m_n \sim nM_{\text{KK}}$, where

$$M_{\text{KK}} \equiv ke^{kr_c\pi} = k \frac{\Lambda_{\text{IR}}}{\Lambda_{\text{UV}}}. \quad (1.54)$$

The observation, that (1.53) is not sensitive to the limit $r_c \rightarrow \infty$ led to a subsequent paper of Randall and Sundrum, in which they proposed a model with an infinite warped extra dimension as an alternative to compactification [56].

Equation (1.50) suggests, that solving the hierarchy problem only require the Higgs to stay at the IR brane. The conclusions are not altered if all other SM fields are promoted to bulk fields, which was explored soon after the original paper for bulk gauge bosons in [57], and bulk fermions in [58, 59]. Similar to the split fermion idea in UED, a localization in the bulk will lead to a suppression of dangerous higher dimensional operators, because the overlaps of the extra dimensional wavefunctions determine the size of the couplings. Due to the warping it can also accommodate hierarchical fermion masses and mixings coming from anarchic 5D Yukawa couplings, as well as a suppression of tree-level flavor violating effects. These features will be elaborated on in Section 2.4 and 2.5.

In the context of the AdS/CFT duality, it can be motivated, that the RS model is dual to a strong interacting four dimensional theory, see Section 2.2. Therefore, many concepts introduced in Section 1.1 have an alternative, so called *holographic* 5D description, which may at first glance look like an entirely different theory. So is for example the warped higgsless model dual to a walking TC theory [63]. The warped version of a gauge-Higgs unification model is a dual description of a composite pseudo-Nambu Goldstone Higgs¹⁹ [62, Sec.4] and the mechanism of collective symmetry breaking can be implemented by an enlarged bulk gauge group [60].

It is interesting to note, that this dual description for the RS scenario, where gravity is in the bulk and the graviton can therefore be understood as a composite of the brane Yang-Mills theory seemingly contradicts a no-go theorem, the Weinberg-Witten theorem [79]. It states among other things, that a massless graviton cannot be a composite state. Very reminiscent of the Coleman-Mandula theorem and SUSY, the AdS/CFT correspondence makes use of a loophole, because the 5D graviton can be described by a composite state on the four dimensional boundary, see [80] for details.

¹⁹An indication of this relation may be that the extra-dimensional components of the gauge fields transforms under the 5D gauge symmetry like under a shift symmetry.

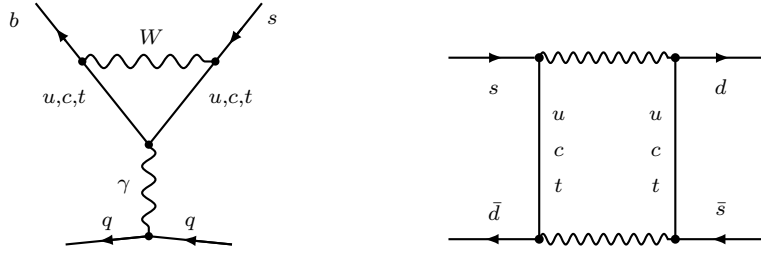


Figure 1.8: Diagrams contributing to FCNCs in the SM.

1.2 Solutions to the Flavor Problem

The famous question of “Who ordered the muon?” has now been escalated to “Why does Nature repeat herself?”

————— *Frank Wilczek & Anthony Zee*

Hierarchies in the flavor sector are not radiatively unstable and might therefore be considered a less severe problem than the gauge hierarchy problem. However, if the hierarchy problem is solved by new physics at the electroweak scale, one immediately runs into trouble with flavor observables. The reason is, that in the SM, the Z boson, the gluon and the photon couple flavor universal and as a consequence, flavor changing neutral currents (FCNCs) are loop-suppressed. Furthermore, these loop processes are additionally suppressed due to the so called *GIM mechanism* [67]. It is based on the fact, that flavor-violating diagrams, like the ones shown in Figure 1.8 can be described by an effective Hamiltonian

$$\mathcal{H} = \sum_i \frac{C_i}{\Lambda^2} \mathcal{O}_i \quad (1.55)$$

with four quark operators \mathcal{O}_i and Wilson coefficients

$$C_{\text{Penguin}} \sim \sum_{i=u,c,t} \lambda_i F(m_i), \quad C_{\text{Box}} \sim \sum_{i,j=u,c,t} \lambda_i \lambda_j \tilde{F}(m_i, m_j), \quad (1.56)$$

for the Penguin and Box diagram respectively. In this notation, the CKM factors are

$$\lambda_i = \begin{cases} V_{is}^* V_{id} & \text{for } K \text{ decays and } K^0 - \bar{K}^0 \text{ mixing,} \\ V_{ib}^* V_{id} & \text{for } B_d \text{ decays and } B_d^0 - \bar{B}_d^0 \text{ mixing,} \\ V_{ib}^* V_{is} & \text{for } B_s \text{ decays and } B_s^0 - \bar{B}_s^0 \text{ mixing,} \end{cases} \quad (1.57)$$

so that in all cases unitarity of the CKM matrix enforces

$$\lambda_u + \lambda_c + \lambda_t = 0. \quad (1.58)$$

In the limit of equal quark masses, these processes would never occur through SM physics alone. This is rooted in the fact that the SM gauge interactions respect the

Observable	Operator	Bound on Λ in TeV
ϵ_K	$(ds^c)(ds^c)$	$10^4 - 10^5$
Δm_K	$(ds^c)(ds^c)$	$10^3 - 10^4$
Δm_D	$(cu^c)(cu^c)$	$10^2 - 10^3$
Δm_{B_d}	$(bd^c)(bd^c)$	$10^2 - 10^3$

Table 1.1: Rough bounds from Flavor observables on the suppression scale of the corresponding four fermion operators.

full $U(3)^5$ flavor symmetry, which is only broken by the Yukawa interactions.

The functions $F(m_i)$ and $\tilde{F}(m_i, m_j)$ however depend on the quark masses and break the GIM protection. This dependence still leads in many cases to a powerful quadratic suppression, *e.g.* $\sim (m_u^2 - m_c^2)/M_W^2$, but can be weaker in processes where it is only logarithmic, *e.g.* $\sim \log(m_u/m_c)$.²⁰ New Physics at the TeV scale will generically introduce new particles with TeV masses, leading to large flavor changing neutral currents (FCNCs) already at tree level, which are excluded by the good agreement of various flavor observables with the SM. One might therefore find a viable solution for the hierarchy problem, but the flavor sector will push the scale at which it is realized orders of magnitude above the TeV scale.

In the following, the emphasis will be put on the quark sector again, even though flavor violation is even more phenomenologically constrained in the lepton sector [157]. A solution to the flavor problem must then at least provide an explanation to the question why the Wilson coefficients of the operators cited in Table 1.1 should be small. Ideally, it would also explain the structure of the Yukawa matrices, which is put in by hand in the SM. The exact structure of the Yukawa matrices cannot be measured, because many parameters are not physical, but it can be approximated under some assumptions [66]. Using the Wolfenstein parametrization [68], one can write the CKM matrix and the Yukawa matrices in the form

$$Y_d^{\text{diag}} = \begin{pmatrix} d\lambda^4 & 0 & 0 \\ 0 & s\lambda^2 & 0 \\ 0 & 0 & 1 \end{pmatrix} \frac{\sqrt{2}m_b}{v}, \quad Y_u^{\text{diag}} = \begin{pmatrix} u\lambda_u^4 & 0 & 0 \\ 0 & c\lambda_u^2 & 0 \\ 0 & 0 & 1 \end{pmatrix} \frac{\sqrt{2}m_t}{v} \quad (1.59)$$

$$V_{\text{CKM}} = \begin{pmatrix} 1 - \lambda^2/2 & \lambda & A\lambda^3(\rho - i\eta) \\ -\lambda & 1 - \lambda^2/2 & A\lambda^2 \\ A\lambda^3(\rho - i\eta) & -A\lambda^2 & 1 \end{pmatrix}, \quad (1.60)$$

with $\lambda \simeq 0.2$ denoting the Cabibbo angle, $\lambda_u \simeq 0.06$, and all other coefficients of $\mathcal{O}(1)$. The CKM matrix is given by $V_{\text{CKM}} = (U_L^u)^\dagger U_L^d$, where U_L^u and U_L^d denote the unitary rotation matrices which rotate the left-handed up- and down-type quarks from the mass to the interaction eigenbasis. One can choose the rotation matrices such that U_L^d and U_R^d depend only on λ and U_L^u and U_R^u only on λ_u . Since the Cabibbo angle is roughly equal to the parameter $\lambda \simeq \sqrt{m_d/m_s}$, which determines Y_d^{diag} , and $\lambda_u < \lambda$,

²⁰One might argue, that the top mass leads to a considerable breaking of the GIM, but it will come with a very small CKM element, canceling this effect.

it is then a good approximation to consider $V_{\text{CKM}} \sim U_L^d$ to first order. If one further assumes the Yukawa matrices to be symmetric, which implies $(U_R^d)^* = U_L^d$, one finds

$$Y_d = U_R^d Y_d^{\text{diag}} (U_L^d)^\dagger \simeq V_{\text{CKM}}^* Y_d^{\text{diag}} V_{\text{CKM}}^\dagger \simeq \begin{pmatrix} (d+s)\lambda^4 & s\lambda^3 & A(\rho-i\eta)\lambda^3 \\ s\lambda^3 & s\lambda^2 & A\lambda^2 \\ A(\rho-i\eta)\lambda^3 & A\lambda^2 & 1 \end{pmatrix} \frac{\sqrt{2}m_b}{v}. \quad (1.61)$$

In the less restrictive case that Y_d is not symmetric, but $(U_R^d)_{ij}^* \sim (U_L^d)_{ij}$, the coefficients in front of the λ^n s are undetermined, but the hierarchical structure remains. From this analysis, no statement can be made about the structure of the Yukawa in the up-sector Y_u . However, as we will see, flavor symmetries that act in the same way in the up- and down sector will relate the structures of Y_u and Y_d and also theories with Yukawa unification at some GUT scale suggest such a relation.

It is safe to say that the approaches which try to explain this flavor structure are not as inventive as the different solutions to the hierarchy problem. It basically comes down to the question of what represents the source of the small parameter λ in (1.61).

Most of these models rely on abelian flavor symmetries, which have problems with FCNCs from the irrelevant operators 1.1. On the other hand, non-abelian symmetry groups, which lead to a successful suppression of these operators abandon an explanation for the structure of the Yukawa matrices. The following sections will give a short overview over the different models and highlight the role of partial compositeness as a solution to the flavor problem.

Abelian Flavor Symmetries

Motivated by the fact, that the Yukawa matrices with the structure (1.61) ($\lambda \leftrightarrow \lambda_u$ for the up-sector) can reproduce the correct quark masses and a hierarchical CKM matrix, Froggatt and Nielsen realized [70], that one can write down a simple ansatz that parametrizes the small parameter λ , in writing the Yukawa couplings as

$$\left(\frac{\phi}{\Lambda_{\text{FI}}}\right)^n \bar{q}_L H q_R^c. \quad (1.62)$$

Here, one assumes a local continuous $U(1)$ flavor symmetry with different charges for left- and right-handed quarks depending on their family. The SM Higgs is assumed to be uncharged, but n insertions of a flavor charged scalar ϕ , the *flavon*, are necessary in order to end up with an invariant operator, which in turn leads to a corresponding power suppression by the flavor scale Λ_{FI} . This scalar will take on a vev, so that

$$\frac{\langle \phi \rangle}{\Lambda_{\text{FI}}} \sim \lambda, \quad (1.63)$$

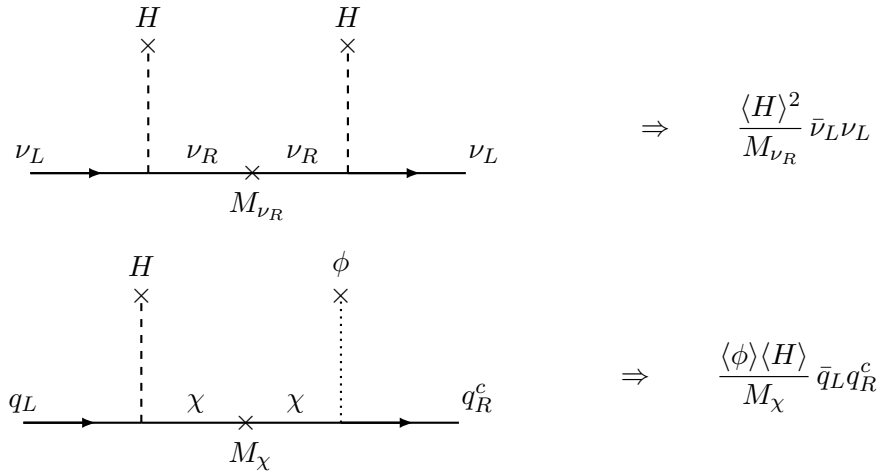


Figure 1.9: The upper diagram leads to a Majorana mass term for the left-handed neutrino upon integrating out the right-handed neutrino in the context of a seesaw mechanism. The lower diagram is the generalization in the Froggatt-Nielsen model, where new heavy fermions are integrated out, that on a fundamental level couple to SM quarks through the Higgs or the Flavor symmetry breaking flavon ϕ .

and the charge assignments for the SM quarks will lead to the structure (1.61). More precisely, if the left-handed quark q_i carries the flavor charge $a_i > 0$ and the right-handed quark q_j^c carries the flavor charge $b_j \leq 0$, the Yukawa matrix is given by

$$Y_{ij} = g_{ij} \lambda^{a_i - b_j}, \quad (1.64)$$

with g_{ij} non-hierarchic $\mathcal{O}(1)$ factors.²¹ On a fundamental level, the Froggatt-Nielsen mechanism can be considered a generalization of the seesaw mechanism, which may explain the smallness of the neutrino masses by integrating out a heavy right-handed neutrino, which is a singlet under the SM gauge group. In the same way new heavy fermions χ only charged under the flavor $U(1)$ are integrated out, so that the flavor scale is connected to their mass $\Lambda_{\text{Fl}} \sim M_\chi$. Figure 1.9 shows a diagram which generates the entries of the Yukawa matrix in (1.64). There must be several new fermions with different flavor charges in order to arrange for diagrams with additional insertions of ϕ tadpoles for the further suppressed Yukawa elements. The rotation matrices U_R^q and U_L^q and from those the CKM matrix can be derived from (1.64) and the corresponding formulas are collected in Section 2.5.

The Froggatt Nielsen mechanism can serve as a model for a variety of theories which generate the same hierarchic structure, but have different sources for the parameter λ . For example, models featuring partial compositeness or more generally models in which the Yukawa couplings run slow due to strong interactions (Nelson Strassler type

²¹For equation (1.64), and for the following equivalent formulas, no sum over indices that appear twice is implied.

models [71]),²² lead to

$$Y_{ij}(\mu) = Y_{ij}(\Lambda_{\text{Fl}}) \left(\frac{\mu}{\Lambda_{\text{Fl}}} \right)^{\gamma_{L_i} + \gamma_{R_j}}, \quad (1.65)$$

where now the respective anomalous dimension of the quarks plays the role of the flavor charges, and the ratio between the flavor scale and the electroweak scale provide the small expansion parameter λ . Another ansatz is the idea of radiative flavor breaking. In these type of models, the masses of the second and first generation quarks can only be generated at one or two loop-level respectively (for a good review see Section 6 of [72]). Therefore, $\lambda^2 \sim$ a loop factor, and

$$Y_{ij} = g_{ij} \left(\frac{1}{16\pi^2} \right)^n, \quad (1.66)$$

with $n = 1, 2$ and further structure in g_{ij} is put in by hand or by different mediators and couplings. In warped extra dimensions, the warp factor allows for large hierarchies,

$$Y_{ij} = g_{ij} e^{-kr_c\pi(c_i - c_j)}, \quad (1.67)$$

where c_i, c_j parametrize the localization of the 5D quark wavefunction along the extra dimension and g_{ij} are the fundamental 5D Yukawa couplings. This mechanism as well as its relation to the Froggatt-Nielsen model will be discussed in more detail in Section 2.5. Note, that $e^{-kr_c\pi} = \Lambda_{\text{IR}}/\Lambda_{\text{UV}}$, which is another hint at a deeper relation between strongly coupled and warped extra dimensional models considering (1.65).

All these models can be thought of as applications of the Froggatt Nielsen mechanism and yet, there are important distinctive features which for example Nelson Strassler models do have and the original Froggatt Nielsen model does not. They are related to the other aspect of the flavor problem, the question whether the experimental bounds on higher dimensional operators, which induce FCNCs can be brought in agreement with a low new physics scale. Since flavor non-diagonal operators are suppressed, the most dangerous effects in abelian flavor models come from flavor-diagonal operators, for example in the down quark sector

$$\sum_{i,j=1}^3 \frac{C_{ij}^d}{\Lambda_{\text{Fl}}^2} (\bar{Q}_i d_i^c) (\bar{Q}_j \bar{d}_j^c), \quad (1.68)$$

with Q denoting an electroweak doublet and d^c a down-type singlet. Because the abelian symmetry will enforce that the C_{ij} make up a diagonal, but not a universal matrix, after rotation to the mass eigenbasis one will have an operator (up to higher

²²It is remarkable to note, that this idea, as well as the relationship between renormalization group effects and the Froggatt Nielsen model was already envisioned in their original paper, see [70, sec.4].

orders in λ)

$$\frac{(C_{11}^d + C_{22}^d)\lambda^2}{\Lambda_{\text{FI}}^2}(\bar{Q}_2 d_1^c)(\bar{Q}_2 d_1^c), \quad (1.69)$$

and there is no reason why, considering an abelian symmetry, the diagonal coefficients C_{ii}^d should be related. In Nelson Strassler type models (or in warped extra dimensions) there is also no reason to assume this, but the coefficients are individually small, because they are proportional to the localizations of the involved light flavors or the corresponding mixing angles (compare the discussion at the end of 1.1). Further, models with Yukawa hierarchies induced from strong renormalization group running do not actually have an underlying flavor symmetry. At the flavor scale, the Yukawa coupling is an anarchic order one matrix, which does not increase the global symmetry group of the Lagrangian compared to the low energy theory. This is an advantage, because in the Froggatt Nielsen model the Yukawa couplings emerge as effective operators from a fundamental flavor symmetric theory. The breaking of this continuous symmetry by the vev of ϕ results in massless Goldstone bosons. As a consequence, it can not be realized exactly and even then, light Would-be Nambu Goldstone bosons are bound to appear. This is the reason why, after it became known that a rich flavor sector is realized in nature (basically after the discovery of the charm quark), most of the proposals for a underlying symmetry were based on discrete groups, most of them non-abelian ones (see [73, Ref.5]).

Non Abelian Flavor Symmetry

Another way to avoid the FCNC problem of abelian flavor theories is to assume non-abelian flavor symmetries, which can ensure the coefficient matrix of (1.68) to be universal. In these approaches, the maximal $U(3)^3 = U(3)_Q \times U(3)_u \times U(3)_d$ quark flavor symmetry, or a non-abelian subgroup, is considered to be broken by flavon fields which transform in a $\chi \sim (\bar{\mathbf{3}}, \mathbf{3})$ under the respective $U(3)$ s (or a corresponding equivalent for smaller flavor groups) in order to make the Yukawa couplings

$$\frac{1}{\Lambda_{\text{FI}}} \chi_u \bar{Q} \tilde{H} u^c + \frac{1}{\Lambda_{\text{FI}}} \chi_d \bar{Q} H d^c \quad (1.70)$$

invariant. The problems regarding continuous groups mentioned at the end of the last section have lost nothing of their validity and it is therefore preferable to consider a discrete flavor symmetry, in this case a discrete subgroup of $U(3)^3$. In principle, another solution would be to gauge the flavor group in order to get rid of the massless Goldstone modes. However, the small breaking in the light flavor sector will generate very light flavor gauge bosons, as was already pointed out in the very first papers considering gauged flavor groups [73]. But also if a discrete non-abelian subgroup is realized, it should emerge from a gauged group via spontaneous breaking, because fundamental global symmetries are not respected by quantum gravity (*e.g.* a black hole may eat a proton and Hawking radiate a positron). Assuming such an explanation is found, renormalizable terms in the flavon potential might still be invariant under an accidental continuous symmetry, leading to Goldstone bosons. Higher dimensional

operators will give masses to these Goldstone bosons, but they are again expected to be light, because the breaking must be proportional to powers of λ . It is anyway a challenge even for a gauged flavor symmetry to realize a potential which is able to generate the Yukawa structures [75].²³ This is already an impressive list of reasons, why non-abelian models with low flavor scales are problematic. Since FCNCs at a low scale are unavoidable if new physics (with no additional structure in the flavor sector) is assumed to solve the hierarchy problem, such a flavor structure is often simply imposed without further motivation. The practice to assume new physics to respect the flavor symmetries of the SM gauge sector, *i.e.* it is *flavor blind*, is called *Minimal Flavor Violation* (MFV). It was first implemented in [76], in the context of composite models and thoroughly defined as an effective field theory in [77]. In practice, that means that any flavored structure may be constructed only by insertions of SM Yukawa matrices, pretending they are fields transforming in the same representation as an actual $U(3)^3$ flavon. Afterwards these *spurion* fields are replaced by the constant Yukawa matrix again. For example the Wilson coefficient in (1.68) is in MFV given by

$$\begin{aligned} C^d &= \frac{1}{\Lambda_{\text{Fl}}^2} \chi_d \chi_d \left(\mathbb{1} + \frac{1}{\Lambda_{\text{Fl}}^2} \chi_d \chi_d^\dagger + \frac{1}{\Lambda_{\text{Fl}}^2} \chi_u \chi_u^\dagger + \frac{1}{\Lambda_{\text{Fl}}^4} \chi_u \chi_u^\dagger \chi_d \chi_d^\dagger + \dots \right) \\ &= Y_d Y_d \left(\mathbb{1} + Y_d Y_d^\dagger + Y_u Y_u^\dagger + Y_u Y_u^\dagger Y_d Y_d^\dagger + \dots \right), \end{aligned} \quad (1.71)$$

which is to a good approximation diagonal in the mass eigenbasis. Deviations are due to insertions of flavor invariant terms formed from the Yukawas, which are however further suppressed by the flavor scale. The concept of MFV is very popular and an ingredient of many BSM models which do not address the flavor sector inherently. Very similar at first sight, however a qualitatively different approach can be realized in models with extra dimensions. Here, it is possible to separate the source of flavor breaking from the SM by confining it to a distant brane. In the simplest setup one has n flat extra dimensions, with the SM assumed to reside on one brane and the flavor breaking fields χ on another brane [69]. Flavor breaking is then only communicated to the SM by a bulk field ϕ which couples to both branes. Because there is no direct contact between the SM fields and the flavor breaking fields, one says the flavor violation is *shined* to the IR brane. The relevant terms in the Lagrangian read

$$\mathcal{L} \ni \int d^4 x dz^n \frac{\phi^{kl}}{\Lambda_{\text{Fl}}^{n/2-2}} \chi_{kl} \delta^n(z - z_0) + \int d^4 x dz^n \frac{\phi^{kl}}{\Lambda_{\text{Fl}}^{n/2+1}} \bar{Q}_k H d_l^c \delta^n(z). \quad (1.72)$$

After solving the equations of motion, the mediator will inherit the flavor structure from the source (its boundary condition), so that $\phi_{kl} = \chi_{kl} f(z)$ and the effective Yukawa coupling from the Lagrangian above will therefore be

$$(Y_d)_{kl} \sim \frac{\chi_{kl}(z=0)}{\Lambda_{\text{Fl}}^{n/2+1}}, \quad (1.73)$$

This is exactly what one would expect from a spurion analysis. However, a plethora of phenomena can appear if one considers multiple sources sitting at different branes

²³For the full flavor group it is not even possible to find a renormalizable potential, see [74, Sec 2.2].

at different distances from the SM brane. Even interactions between different bulk flavons can have a sizable effect and lead to hierarchies in the effective Yukawas. In the worst case, shining is an alternative description of MFV for a non-abelian scenario or directly related to a Froggatt Nielsen model (with λ now given by the distance between branes). In the best case, it can be a new tool to generate hierarchies dynamically (from bulk interactions).

2 The Randall Sundrum Model and its Holographic Interpretation

The model considered in this thesis is a variation of the Randall-Sundrum (RS) model presented in Section 1.1. This model is enormously rich what concepts of model building is concerned. Following the original motivation [55], it can be understood as an extra dimensional theory with an Anti de Sitter metric in continuation of the idea of large extra dimensions. This point of view will be introduced in Section 2.1. It is also a model of strongly coupled composite fields, which becomes apparent in the light of the AdS/CFT correspondence, which will be comprehensively presented in Section 2.2. In the specific realization of the RS model that forms the basis of this thesis, all standard model fermions and gauge bosons are five dimensional fields, or in the language of the strongly coupled description, have composite admixtures (in a generalization of ρ photon mixing). The technical aspects of this field content will be the subject of Sections 2.3 and 2.4. Based on this setup and even more important in the context of the following chapters, the Randall-Sundrum model provides one of the best explanations for the Flavor structure in the SM we have today. The hierarchies in quark masses and mixing angles can be reproduced and associated therewith, FCNCs from higher dimensional operators are suppressed. In Section 2.5 will be explained how this works and the connection with the concept of partial compositeness as introduced in Section 1.1 will be established.

2.1 Why this and not that?

The geometrical setup of the RS model has already been introduced in Section 1.1. This section serves to describe the motivation for this particular geometry and the choice of localization of the SM fields (whether they are bulk fields or why they should be confined to one brane or the other).

On first sight, the metric in (1.49) seems to be constructed and the question arises if it corresponds to a generic approach to assume such a metric or if it is based on very special assumptions. In other words, is there some hidden tuning like in the case of large extra dimensions in the specific choice of the geometry?

In order to check this, we will make the most general ansatz compatible with 4D Poincaré invariance and the \mathbb{Z}_2 orbifold symmetry,¹

$$ds^2 = G_{MN} dx^M dx^N = a(\phi) \eta_{\mu\nu} dx^\mu dx^\nu - b(\phi) d\phi^2. \quad (2.1)$$

¹Remember, that the orbifold is a necessity if one wants to describe chiral fermions in an odd number of spacetime dimensions.

and see what choices we have, given a few sensible conditions.² Because ϕ is a dimensionless variable, dimensional analysis tells us, that the mass dimensions of $[a(\phi)] = 0$ and $[b(\phi)] = -2$. Another condition we can surely impose is that in the decoupling limit $r_c \rightarrow 0$, we must recover flat Minkowski spacetime, so $\lim_{r_c \rightarrow 0} b(\phi) = 0$ and $\lim_{r_c \rightarrow 0} a(\phi) = 1$. Further $b(\phi)$ can be chosen constant, since every function of ϕ can be absorbed in the differential element with a suitable coordinate transformation. With only the dimensionful quantities r_c and k at hand, this leaves only the choice $b \sim r_c^2$. For the other coefficient function, we can conclude that up to constant coefficients a_i , one can write $a(\phi) = 1 + a_1 k r_c |\phi| + \dots$, where the ellipsis stands for higher powers of $k r_c |\phi|$ with the corresponding coefficients, and the absolute value is dictated by the orbifold symmetry. These arguments are not a rigorous derivation, but after all, (1.49) does not seem all that strange.

One result of [55] was, that (1.49) is a solution to the 5D Einstein equations with a large, $\mathcal{O}(M_{\text{Pl}})$, negative cosmological constant, which corresponds to an extremely curved *Anti de Sitter* space. This sounds very puzzling, because we assume a stable compact extra dimension with flat four dimensional boundaries. Wouldn't the two branes not immediately be smashed together? After all we know, our universe is slightly de Sitter and expands with an observable rate. And what tells us that the brane metric should be flat?

Answers for these questions can be found by considering Einsteins equations. Making use of such a coordinate transformation as mentioned above, $|z| = e^\sigma(\phi)/k$, the metric can be put in the form

$$ds^2 = \left(\frac{R}{|z|} \right)^2 (\eta_{\mu\nu} dx^\mu dx^\nu - dz^2) . \quad (2.2)$$

The UV brane is localized at $z = 1/k \equiv R$ and the IR brane at $z = \Lambda_{\text{UV}}/(k\Lambda_{\text{IR}}) \equiv R'$ in these coordinates. They are particular well suited for the calculation of the Einstein tensor, because the metric is *conformally flat*, that is it can be written as $G_{MN} = \Omega^2 \eta_{MN}$ with η_{MN} the flat five dimensional metric and Ω a smooth function, and are therefore often called *conformal coordinates*. In order to differentiate between the notations, we will refer to the notation introduced in (1.49) as ϕ -notation. Applying [78] and $A(z) = \log(|z|/R)$, the Einstein tensor \mathcal{G} becomes a one-liner,

$$\begin{aligned} \mathcal{G}_{MN} &= R_{MN} - \frac{1}{2} G_{MN} R \\ &= 3 [\partial_M A \partial_N A + \partial_M \partial_N A - \eta_{MN} (\partial_K \partial^K A - \partial_K A \partial^K A)] . \end{aligned} \quad (2.3)$$

The only non-vanishing components are

$$\mathcal{G}_{55} = 6(A')^2 , \quad (2.4)$$

$$\mathcal{G}_{\mu\nu} = -3\eta_{\mu\nu} [A'' - (A')^2] . \quad (2.5)$$

Even if we assume the SM fields to propagate in the bulk, in the presence of an order Planck scale cosmological constant one can neglect the matter contributions to the

²If not stated otherwise, the convention for the 5D metric signature in this thesis is (+, -, -, -, -).

stress-energy tensor as a first approximation, so that

$$\mathcal{G}_{MN} = \frac{1}{2M_{\text{Pl}(5)}^3} \Lambda G_{MN}, \quad (2.6)$$

which implies for the 55 component

$$(A')^2 = -\frac{1}{12M_{\text{Pl}(5)}^3} \Lambda \left(\frac{R}{z}\right)^2 \Rightarrow \Lambda = -12M_{\text{Pl}(5)}^3 k^2. \quad (2.7)$$

The cosmological constant must therefore be negative, $\Lambda < 0$ in order to find a real solution. The $\mu\nu$ components of the Einstein tensor gives

$$\mathcal{G}_{\mu\nu} = 6\eta_{\mu\nu} \left[-\frac{1}{z^2} + \frac{1}{|z|} (\delta(z-R) - \delta(z-R')) \right]. \quad (2.8)$$

Here, a negative contribution to the term in brackets is equivalent to a positive contribution to the stress energy tensor, which is equivalent to a positive contribution to the cosmological constant and thus leads to an attractive potential. Therefore, the above calculation supports our intuition and the branes should collapse. Further, the delta functions correspond to induced cosmological constants at the branes at $z = R$ and $z = R'$, which will make them (anti-) de Sitter and not flat.

This situation can be remedied by introducing brane tensions λ_{UV} and λ_{IR} , which balance the contribution from the bulk cosmological constant in (2.8).³ These brane tensions act like brane-localized four dimensional cosmological constants in the action, which now reads

$$S \ni - \int d^4x \int_R^{R'} dz \sqrt{|G|} \left(M_{\text{Pl}(5)}^3 R_5 + \Lambda \right) - \int d^4x \sqrt{|g_{\text{IR}}|} \lambda_{\text{IR}} - \int d^4x \sqrt{|g_{\text{UV}}|} \lambda_{\text{UV}}, \quad (2.9)$$

with g_{IR} and g_{UV} the determinant of the 4D block of G_{MN} evaluated at $z = R'$ and $z = R$ respectively. In order to balance the contribution from the 5D cosmological constant, the values of the brane tensions must be chosen to be

$$\lambda_{\text{UV}} = -\lambda_{\text{IR}} = -12k M_{\text{Pl}(5)}^3 = \frac{\Lambda}{k}. \quad (2.10)$$

There is no reason for such a coincidence other than the stabilization of the setup and the requirement for a flat brane metric. Tuning the brane tensions against the bulk cosmological constant to achieve this relation is the equivalent of the tuning of the 4D cosmological constant in the SM. It does not set the compactification radius, but ensures that once the radius is set, the setup remains stable. The radius itself is the vacuum expectation value of the 55 component of the metric tensor, the radion. It can be fixed via a Goldberger-Wise mechanism [83], which introduces a potential for this field by the interaction with an additional bulk scalar, see [84] for details.

We will now turn to the localization of the Standard Model fields and in this context return to the notation (1.49). In the model discussed in this thesis, we will assume

³Equation (2.8) including the brane tension terms is sometimes called *Israel junction condition* in the literature, referring to its first mention in [82].

that all SM fields are bulk fields, apart from the Higgs, which will be realized as a separate brane-localized scalar (in contrast to EWSB by boundary conditions). As a 5D warped model, this derives its justification from the goal to cut off quadratic radiative corrections at the weak scale. Like all dimensionful scales in the warped background, the cutoff depends on the fifth coordinate and only a brane-localized Higgs sector guarantees that ultraviolet divergences are cut off at $\Lambda_{\text{IR}} = e^{-kr_c\pi} M_{\text{Pl}}$. In the dual description of the theory, we will see that this corresponds to a fully composite Higgs with no elementary scalar component.

Promoting gauge fields to bulk fields means that each is described by a 5D Lorentz vector. The vector representation of the 5D Lorentz group decomposes in a four dimensional Lorentz vector and a Lorentz scalar, compare [85, p.1119-1120], so that $A_M(x_\mu, z) = (A_\mu(x_\mu, z), A_5(x_\mu, z))$. Note that the scalar component in ϕ -notation carries a different mass dimension, $A_\phi(x_\mu, \phi) = r_c A_5(x_\mu, z)$. For the vector components we are forced to choose Neumann BCs at both branes. This can be explained by analogy with a Schrödinger particle in a box. In the box a constant solution for a zero energy eigenvalue is only possible if the wavefunction has Neumann BCs on both ends. In the case of a bulk field, the energy eigenfunctions correspond to the KK modes, and the energy eigenvalues to their masses. We would like to identify the SM gauge fields with massless zero modes and therefore need to impose Neumann BCs on both branes. The scalar components must then have Dirichlet BCs on both branes, because they have opposite orbifold parity, if the theory is supposed to be 5D gauge invariant, as $A_M \rightarrow A_M + \partial_M \alpha_M$ and ∂_ϕ is odd under the action of \mathbb{Z}_2 . With

$$S = \int dx \int_{-\pi}^{\pi} d\phi \sqrt{|G|} \left(\mathcal{L}_{\text{Gauge}} + \mathcal{L}_{\text{Higgs}} + \mathcal{L}_{\text{Matter}} \right), \quad (2.11)$$

the gauge sector reads

$$\mathcal{L}_{\text{Gauge}} = G^{KM} G^{LN} \left(-\frac{1}{4} \mathcal{G}_{KL}^r \mathcal{G}_{MN}^r - \frac{1}{4} W_{KL}^a W_{MN}^a - \frac{1}{4} B_{KL} B_{MN} \right). \quad (2.12)$$

Here, the indices at the corresponding field strength tensors⁴ $r = 1, \dots, 8$ run over the generators of $SU(3)_C$ and $a = 1, 2, 3$ over the generators of $SU(2)_L$. Breaking of the electroweak symmetry is implemented by couplings to the Higgs sector on the IR brane,

$$\mathcal{L}_{\text{Higgs}} = \frac{\delta(|\phi| - \pi)}{r_c} \left[g^{\mu\nu} (D_\mu H)^\dagger (D_\nu H) + \mu^2 H^\dagger H - \lambda (H^\dagger H)^2 \right]. \quad (2.13)$$

The matter sector includes the kinetic terms of the bulk fermions and the Yukawa couplings. Moving the fermions from the brane in the bulk is especially well motivated, because it allows for an explanation of the Yukawa hierarchies in terms of order one parameters, the localization of the zero modes along the extra dimension. This ansatz explains retroactively why the gauge bosons should be in the bulk as well, since a brane localized gauge sector would have localization dependent and thus flavor non-diagonal gauge couplings for all excitations and the zero mode, which would be

⁴Please do not confuse the gluon fields strength tensor with the Einstein tensor.

in conflict with the flavor-diagonal couplings of the photon and the gluon.

A bulk fermion however cannot be chiral, because the fundamental spinor representation of the 5D Lorentz group is a four component Dirac spinor, see for example [86, Appendix A]. One way to see this is that in order to satisfy the Clifford algebra in 5D,

$$\{\Gamma_M, \Gamma_N\} = 2\eta_{MN}, \quad (2.14)$$

one needs five gamma matrices and the only choice allowed by the anticommutation relation is $\Gamma_M = (\gamma_\mu, i\gamma_5)$. As a consequence, one cannot construct a projection operator. The orbifold however allows for a projection via BCs, because a 5D fermion will decompose into two Weyl representations in four dimensions, which must have opposite BCs in order to write down a kinetic term (again because ∂_ϕ is \mathbb{Z}_2 odd). For the SM quarks in the bulk, that means that both the 5D $SU(2)_L$ doublet Q and singlet q^c are Dirac spinors. But the \mathbb{Z}_2 even component of Q will be identified with a left-handed SM field and the even component of q^c with its right-handed counterpart. Each KK excitation however will be a Dirac fermion and thus a doubling of the degrees of freedom for each fermionic resonance is a tell tale sign of an orbifold (or of an odd number of spacetime dimensions in general). Further, because the Clifford algebra is defined over the tangent space, the curvature of the space is communicated to the fermions via a *vielbein* and the equivalent of a Christoffel symbol for spinors, the *spin connection*, (for a comprehensive discussion see [87]). A kinetic term for a bulk fermion is then given by

$$\mathcal{L}_{\text{matter}} \ni E_a^A \left[\frac{i}{2} \bar{Q} \Gamma^a (\partial_{A-} \overleftarrow{\partial}_A) Q + \frac{\omega_{bcA}}{8} \bar{Q} \{\gamma^a, \sigma^{bc}\} Q \right] - m \operatorname{sgn}(\phi) \bar{Q} Q, \quad (2.15)$$

where $E_a^A = \operatorname{diag}(e^\sigma, e^\sigma, e^\sigma, e^\sigma, 1/r)$ denotes the five dimensional inverse vielbein. It does not depend on x , since we have no dynamic gravitational background. Since it is diagonal, it will simply assign different prefactors to the derivatives ∂_μ and ∂_ϕ . For a diagonal metric the only non-vanishing components of the spin connection ω_{bcA} are $b = c = A$ and give no contribution to the action, see for example [88]. Note, that the signum in front of the mass term is necessary due to the parity assignments. Equation (2.15) for an $SU(2)$ doublet Q and an $SU(2)$ singlet q^c , together with the Yukawa couplings will be the starting point for our discussion in section 2.4,

$$\begin{aligned} \mathcal{L}_{\text{matter}} = & \sum_{q=u,d} \frac{i}{2} E_a^A \left[\bar{Q} \Gamma^a (\partial_{A-} \overleftarrow{\partial}_A) Q + \bar{q}^c \Gamma^a (\partial_{A-} \overleftarrow{\partial}_A) q^c \right] \\ & - \operatorname{sgn}(\phi) (\bar{Q} \mathbf{M}_Q Q + \bar{q}^c \mathbf{M}_q q^c) \\ & - \frac{\delta(|\phi| - \pi)}{r_c} \left[\epsilon_{ab} \bar{Q}_a H_b^\dagger \mathbf{Y}_u^{(5D)} u^c + \bar{Q} H \mathbf{Y}_d^{(5D)} d^c + \text{h.c.} \right]. \end{aligned} \quad (2.16)$$

Here, \mathbf{M}_A , $A = Q, q$ denote the generalization of the mass term for three generations. The last line contains the Yukawa interactions before EWSB with the 5D Yukawa matrices $\mathbf{Y}_u^{(5D)}$ and $\mathbf{Y}_d^{(5D)}$. The setup is illustrated in Figure 2.1, and we will now turn to the dual interpretation of this model in order to understand the physics in the later sections from both sides of the duality.

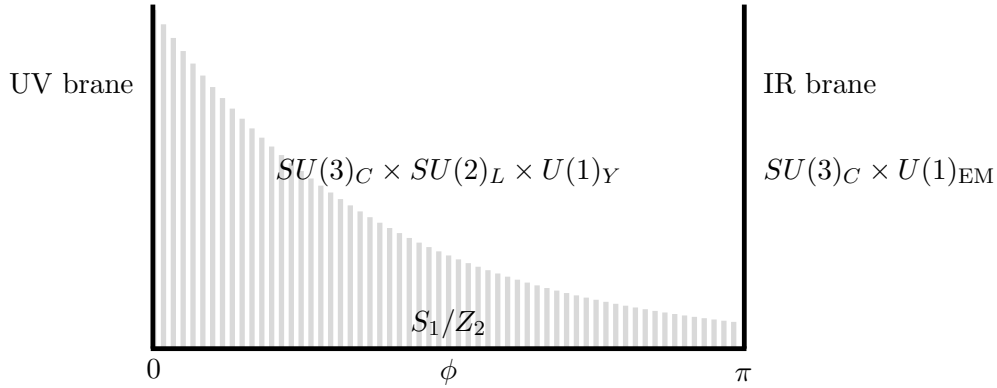


Figure 2.1: Illustration of the minimal RS model considered in this thesis. All fermions and gauge bosons are assumed to be bulk fields and the symmetry is broken at the IR brane by a Higgs boson. The effect of the warp factor for dimensionful parameters is indicated by gray lines.

2.2 AdS/CFT

I have found that in the arena of warped compactifications, the qualitative insight gained from the AdS/CFT connection between such compactifications and strongly coupled 4D dynamics, has saved me time and time again from errors. Its like checking units as an undergraduate, in principle its not necessary, but in practice indispensable

————— *Raman Sundrum*

The term AdS/CFT duality originates from a conjecture of Maldacena [95] and means in its broadest sense, that a weakly coupled theory of fields defined in the bulk of a d dimensional AdS space is equivalent to a strongly coupled CFT on its $d-1$ dimensional boundary.

This section will be a bottom-up introduction to the AdS/CFT duality, meaning that we will not go into detail about the original Maldacena conjecture, but keep the discussion close to the applications in this thesis. We will however need some of the original framework in order to motivate the conclusions in the later parts of the section. In its original formulation, the weakly coupled bulk theory is the decoupling (SUGRA) limit of a certain type of string theory on an $AdS_5 \times S_5$ space and the corresponding boundary theory is a maximally supersymmetric conformal $SU(N)$ -Yang-Mills theory in the large N limit. With $R = 1/k$ the AdS curvature radius, ℓ_s the string length and g_{YM} the coupling of the boundary Yang-Mills theory, it follows the relation

$$\frac{R^4}{\ell_s^4} = 4\pi N g_{YM}^2. \quad (2.17)$$

It tells us, that if the string length $\ell_s \ll R$, the Yang-Mills gauge coupling times the number of colors N (the *t'Hooft coupling*) becomes large and the Yang-Mills theory is strongly coupled. In addition, nonperturbative string states with masses proportional to the inverse string coupling $m \sim 1/g_s$, are required to decouple as well [107, p.22]. This means $g_s \rightarrow 0$ and therefore we have necessarily a *large N* boundary theory, because $g_s \sim 1/N$. The picture becomes much more intuitive once one examines the spacetime symmetries on both sides. Consider the AdS metric in conformal coordinates (2.2). It is evident, that this metric is invariant under the rescaling

$$x^\mu \rightarrow \lambda x^\mu, z \rightarrow \lambda z. \quad (2.18)$$

Fields transform under such a rescaling according to their scaling dimension Δ_ϕ , $\phi(x_\mu, z) \rightarrow \lambda^{-\Delta_\phi} \phi(\lambda x_\mu, \lambda z)$. In contrast to flat space, every Lorentz invariant action will turn out to be invariant under rescalings as well due to this property of the metric. For example

$$\begin{aligned} S_{\text{AdS}} &= \int d^4x dz \left(\frac{R}{z} \right)^5 \left(\frac{1}{2} G^{MN} \partial_M \phi \partial_N \phi - \frac{M^2}{2} \phi^2 - \frac{\lambda}{4!} \phi^4 \right) \\ &\rightarrow \int \lambda d^4x d\lambda z \left(\frac{R}{\lambda z} \right)^5 \left(\frac{1}{2} \lambda^{-2} G^{MN} (\lambda \partial_M) \lambda^{-\Delta_\phi} \phi (\lambda \partial_N) \lambda^{-\Delta_\phi} \phi \right. \\ &\quad \left. - \frac{M^2}{2} \lambda^{-2\Delta_\phi} \phi^2 - \frac{\lambda}{4!} \lambda^{-4\Delta_\phi} \phi^4 \right), \end{aligned} \quad (2.19)$$

which is invariant upon absorption of a factor $\lambda^{-\Delta_\phi}$ in each field, in contrast to flat space, where additional factors from the metric appear. This implies, that regardless of the mass dimension of whatever operator we write down in the bulk Lagrangian, the action will remain scale invariant. In the dual boundary theory the fifth coordinate is identified with the inverse of an energy scale and thus we will have a scale invariant boundary action. In general, it is still an open question whether scale invariance in 4D already implies conformal invariance (see *e.g.* [108]), however this is a strong hint that we are dealing with a CFT on the boundary.

In fact it can be shown, that the 15 generators of the spacetime symmetry (isometry) group of AdS₅ correspond to the 15 generators of the conformal group of the dual boundary theory, whereas the $SO(6)$ isometry of the additional S_5 corresponds to the R -symmetry group of the $\mathcal{N} = 4$ supersymmetry [109, p.187-188]. Changing the non-AdS part of the manifold will therefore only cut down the amount of supersymmetry on the CFT side and we can consider the duality on AdS₅ alone without losing essential ingredients. At this point it should be pointed out, that there is no rigorous mathematical proof of the original conjecture as of this writing and for the stripped down versions we are considering here it could be that the corresponding CFT does not even exist. However, we will see that it is very insightful to switch to the CFT view in order to get a deeper understanding of the RS model.

In a more precise formulation, the conjecture states that the 5D partition function of bulk fields $\phi(x^\mu, z)$ with boundary conditions at the AdS₅ boundary $\phi(x^\mu, z)|_{z=0} =$

$\varphi(x_\mu)$,

$$Z_{\text{bulk}} \left[\phi(x, z) \Big|_{z=0} = \varphi(x) \right] = \int \mathcal{D}\phi e^{iS_{\text{AdS}}(\phi)} \equiv e^{iS(\varphi)}, \quad (2.20)$$

corresponds to the generating functional of the correlation functions of a boundary CFT, where the boundary values of the bulk fields act as sources for the operators $\mathcal{O}(x)$,

$$Z_{\text{bulk}} \left[\phi(x, z) \Big|_{z=0} = \varphi(x) \right] = \left\langle e^{\int d^4x \varphi(x) \mathcal{O}(x)} \right\rangle_{\text{CFT}}. \quad (2.21)$$

In other words it is possible to derive all n -point functions of the strongly coupled boundary CFT by varying (2.20) with respect to the boundary values φ of the bulk fields ϕ , and setting them to zero

$$\langle \mathcal{O}_1 \mathcal{O}_2 \dots \mathcal{O}_n \rangle = \frac{1}{n!} \frac{\delta^n \ln Z_{\text{bulk}}}{\delta \varphi_1 \delta \varphi_2 \dots \delta \varphi_n} \Big|_{\varphi=0}. \quad (2.22)$$

We will go through this exercise with the example of a free massive bulk scalar $\phi \equiv \phi(x, z)$, with corresponding 5D action in euclidean signature,

$$S_{\text{AdS}} = \frac{1}{2} \int d^4x dz \left(\frac{R}{z} \right)^5 (G^{MN} \partial_M \phi \partial_N \phi + M^2 \phi^2). \quad (2.23)$$

Applying a Fourier transform along the flat space-time directions

$$\phi(x, z) = \int d^4p e^{ipx} \tilde{\phi}(p, z), \quad (2.24)$$

leads to the bulk equations of motion (EOM),

$$\left(-p^2 - \frac{c^2}{z^2} + z^3 \partial_z \frac{1}{z^3} \partial_z \right) \tilde{\phi}(p, z) = 0, \quad (2.25)$$

where $c \equiv MR$ denotes the dimensionless 5D mass parameter. With the substitution $\tilde{\phi}(p, z) = (zp)^2 f(zp)$, the equation of motion is recognizable as a Bessel PDE,

$$(pz)^2 \frac{\partial^2}{\partial (pz)^2} f(pz) + (pz) \frac{\partial}{\partial (pz)} f(pz) - [(pz)^2 + c^2 + 4] f(pz) = 0, \quad (2.26)$$

with the solution

$$\tilde{\phi}(p, z) = p^2 z^2 \left(I_{\Delta-2}(pz) C_1 + K_{\Delta-2}(pz) C_2 \right), \quad (2.27)$$

where

$$\Delta(\Delta - 4) = c^2, \quad \Delta_{\pm} = 2 \pm \sqrt{4 + c^2}. \quad (2.28)$$

It should be noted, that one of the strange properties of Anti de Sitter space is that bulk masses as low as the *Breitenlohner Freedman* bound $c^2 > -4$, are compatible with unitarity [90]. This leaves us with the two solutions $\Delta_+ \geq 2$ and $\Delta_- < 2$,

from which we will pick the larger root Δ_+ , but will come back to the significance of the other one later in this section. The coefficients C_1 and C_2 have to be fixed by appropriate boundary conditions. At the moment we are dealing with pure AdS₅, meaning that there is no IR boundary and the UV boundary is identified with the AdS boundary $z = 0$ (no compactification). One of our boundary conditions is therefore that the solution remains regular at the deep interior $z \rightarrow \infty$, so that $C_1 = 0$. Fixing the second boundary condition forces us to move the UV brane slightly into the bulk, $z = \epsilon$, because the solution becomes irregular at the AdS boundary (in the dual picture this corresponds to the introduction of a cutoff $\Lambda_{\text{UV}} \sim 1/\epsilon$ at which the CFT is broken). At the end of the day we will take the limit $\epsilon \rightarrow 0$ and everything will be finite. Choosing the UV boundary condition as above, $\tilde{\phi}(p, z)|_{z=\epsilon} = \tilde{\varphi}(p)$, yields

$$\tilde{\phi}(p, z) = \tilde{\varphi}(p) \frac{z^2 K_{\Delta-2}(pz)}{\epsilon^2 K_{\Delta-2}(p\epsilon)}. \quad (2.29)$$

Upon integration by parts, we obtain from the action

$$S_{\text{AdS}} = \frac{1}{2} \int d^4x dz \phi \left(\partial_N \frac{R^3}{z^3} \partial^N + \frac{R^3}{z^3} \frac{c^2}{z^2} \right) \phi + \frac{1}{2} \int d^4x \frac{R^3}{z^3} \phi \partial_z \phi \Big|_{z=\epsilon}, \quad (2.30)$$

where the first integral vanishes by the EOM. It should be emphasized that we use the EOM here. That means we are working with a *on-shell* five dimensional theory and the duality will give us an *off shell* boundary theory! Inserting (2.29), the second part, which is called *flux* in the literature due to its resemblance with particle number flux in scattering theory [97, p.7] gives

$$\begin{aligned} \frac{1}{2} \int d^4x \frac{R^3}{z^3} \phi \partial_z \phi \Big|_{z=\epsilon} &= \frac{1}{2} \int d^4x d^4q d^4p \frac{R^3}{z^3} e^{ipx} \tilde{\phi}(p, z) \partial_z e^{iqx} \tilde{\phi}(q, z) \Big|_{z=\epsilon} \\ &= \frac{1}{2} \int d^4q d^4p (2\pi)^4 \delta(p+q) \frac{R^3}{z^3} \tilde{\phi}(p, z) \partial_z \tilde{\phi}(q, z) \Big|_{z=\epsilon} \\ &= -\frac{1}{2} \int d^4q d^4p (2\pi)^4 \delta(p+q) \frac{R^3 z}{\epsilon^3} \tilde{\varphi}(q) \tilde{\varphi}(p) \\ &\quad \times \frac{K_{\Delta-2}(pz)}{K_{\Delta-2}(p\epsilon)} \left(q \frac{K_{\Delta-3}(qz)}{K_{\Delta-2}(q\epsilon)} + \frac{(\Delta-4)}{z} \frac{K_{\Delta-2}(qz)}{K_{\Delta-2}(q\epsilon)} \right) \Big|_{z=\epsilon} \\ &= -\frac{1}{2} \int d^4q d^4p (2\pi)^4 \delta(p+q) \tilde{\varphi}(q) \tilde{\varphi}(p) \frac{R^3}{\epsilon^3} \\ &\quad \times \left(q \frac{K_{\Delta-3}(q\epsilon)}{K_{\Delta-2}(q\epsilon)} + \frac{(\Delta-4)}{\epsilon} \right). \end{aligned} \quad (2.31)$$

For non-integer order ν , the modified Bessel function has an expansion for small arguments,

$$K_\nu(x) = x^\nu 2^{-\nu-1} \Gamma(-\nu) [1 + \mathcal{O}(x^2)] + x^{-\nu} 2^{\nu-1} \Gamma(\nu) [1 + \mathcal{O}(x^2)]. \quad (2.32)$$

So that in Fourier space the two point function reads

$$\begin{aligned}
 \langle \mathcal{O}(p)\mathcal{O}(q) \rangle &= -(2\pi)^4 \delta(p+q) \frac{R^3}{\epsilon^4} \\
 &\times \left(\frac{\Delta-4}{2} + \frac{(q\epsilon)^{\Delta-2} 2^{2-\Delta} \Gamma(3-\Delta) + \dots + (q\epsilon)^{4-\Delta} 2^{\Delta-4} \Gamma(\Delta-3) + \dots}{(q\epsilon)^{\Delta-2} 2^{2-\Delta} \Gamma(2-\Delta) + \dots + (q\epsilon)^{2-\Delta} 2^{\Delta-2} \Gamma(\Delta-2) + \dots} \right) \\
 &= -(2\pi)^4 \delta(p+q) \frac{R^3}{\epsilon^4} \\
 &\times \left(\frac{\Delta_+ - 4}{2} + \frac{1}{\Delta_+ - 3} \left(\frac{q\epsilon}{2} \right)^2 + \frac{\Gamma(3 - \Delta_+)}{\Gamma(\Delta_+ - 2)} \left(\frac{q\epsilon}{2} \right)^{2\Delta_+ - 4} + \dots \right), \tag{2.33}
 \end{aligned}$$

where in the last step from the expansion only the leading non-analytic and leading analytic terms have been kept for the larger solution of (2.28). Constant terms, will give rise to contact terms in position space and local polynomials in q have to be subtracted by an appropriate boundary counter term. In a properly regularized action only the non-analytic piece remains. This solution can be analytically continued to integer values of ν , see *i.e.* [96, p.30-33] as well as for Δ_- (the latter is not as straightforward as one might think and has been first and extensively worked out in [94]). The bottom line of the above calculation is now that the non-analytic part of (2.33) in position space reads (in the following ignoring the subscript of Δ_+)

$$\langle \mathcal{O}(x)\mathcal{O}(y) \rangle = \frac{R^3}{\pi^2} (2 - \Delta) \frac{\Gamma(\Delta)}{\Gamma(\Delta - 2)} \epsilon^{2\Delta-8} \frac{1}{|x - y|^{2\Delta}}, \tag{2.34}$$

which should be interpreted as the two point correlation function of the unknown strongly coupled CFT. And it is in fact the 2-point correlation function of a CFT, once numerical factors and especially the cutoff dependence is absorbed into the operators, which corresponds to $\phi(x, z)|_{z=\epsilon} = \epsilon^{4-\Delta} \varphi(x)$. Since even if one cannot say much about strongly interacting theories, conformal invariance fixes the 1-point correlation function to zero and the 2- and 3-point correlation functions up to numerical constants [89, p.11f.],

$$\langle \mathcal{O}(x) \rangle = 0, \tag{2.35}$$

$$\langle \mathcal{O}_i(x_1)\mathcal{O}_j(x_2) \rangle = \frac{\delta_{ij}}{r_{12}^{2\Delta_i}}, \tag{2.36}$$

$$\langle \mathcal{O}_i(x_1)\mathcal{O}_j(x_2)\mathcal{O}_k(x_3) \rangle = \frac{\lambda_{ijk}}{r_{12}^{\Delta_i+\Delta_j-\Delta_k} r_{13}^{\Delta_i-\Delta_j-\Delta_k} r_{23}^{-\Delta_i+\Delta_j+\Delta_k}}, \tag{2.37}$$

with $r_{ab} \equiv |x_a - x_b|$ and Δ_i denoting the conformal dimension (scaling dimension) of the operators $\mathcal{O}_i(x)$. The result (2.34) is the same as the two point function derived from the Lagrangian

$$\mathcal{L} = \varphi(x)\mathcal{O}(x) + \mathcal{L}_{\text{CFT}}, \tag{2.38}$$

which is therefore called the *dual Lagrangian* to (2.23). Here, $\varphi(x)$ denotes some source field (sometimes also denoted J_φ). Therefore, we can relate the sources with the boundary values of the bulk fields at the UV brane and the scaling dimension with the localization in the bulk. Note that the one-point function (*i.e.* the vacuum expectation

value of the operator \mathcal{O}) comes trivially out to be zero, because (2.31) is quadratic in the sources due to the regularity condition fixing C_1 to zero in (2.29), which is analogous to the statement, that the conformal symmetry is not spontaneously broken. Higher order correlation functions can be computed by including self-interactions in the bulk Lagrangian with an elegant technique introduced by Witten [99].

In the RS model, the UV brane is however not at $z = 0$, but at some non-zero position $z = R$. We should expect that this affects the dual theory, so that it is not conformally invariant anymore above some scale $\Lambda_{\text{UV}} \sim 1/R$, because the 5D theory is not scale invariant in this region. In this situation, the analytic terms in (2.33) gain importance. The first term, independent of the momentum q , can be interpreted as a mass term for the source field in the dual Lagrangian, while the second expression can be obtained by a kinetic term for the source field. They correspond to the usual propagator of a 4D scalar field with

$$m_{\text{eff}}^2 = \frac{2(\Delta - 4)(\Delta - 3)}{R^2}, \quad (2.39)$$

and not explicitly given higher order analytic terms correspond to terms with additional derivatives. Thus, the source field becomes dynamical and the dual theory describes a conformal sector, probed by some field $\varphi(x)$, called *elementary* for reasons to become clear soon, which explicitly breaks conformal invariance at the scale at which we placed the UV brane. Accordingly, the two-point function on the left-hand side of (2.33) does not only describe the propagator of the conformal operators, but of the mixed conformal-elementary states, with the elementary parts generating the analytic contributions. In the 5D picture, the source fields can be understood as degrees of freedom confined to the UV brane, while the conformal states probe the bulk. In this case, the dual Lagrangian reads

$$\mathcal{L} = \partial_\mu \varphi(x) \partial^\mu \varphi(x) + m_{\text{eff}}^2 \varphi(x)^2 + \frac{\omega}{\Lambda^{\Delta-3}} \varphi(x) \mathcal{O}(x) + \mathcal{L}_{\text{CFT}}, \quad (2.40)$$

with $m \sim k$ and ω some dimensionless parameter. Note, that in order for the mixing term to form a singlet under all symmetry groups, ϕ and \mathcal{O} need to have the same conformal and gauge quantum numbers. The amount of mixing of elementary and conformal sector in the mass eigenstates depends on the scaling dimension of \mathcal{O} , which in the 5D theory is equivalent to its localization along the extra dimension. The generalization for more general bulk fields is straightforward (although the construction of the dual CFT for chiral fermions requires some care [104]). From Equation (2.39) it is evident, that a scaling dimension/localization of $\Delta = 3$ and $\Delta = 4$ gives rise to purely massless eigenstates and it turns out, that these are the exact scaling dimensions for gauge fields and gravitons, respectively, compare Section (2.3). The computation is actually really similar to the case of a bulk scalar, only the relation between scaling dimension and the bulk mass (2.28) differ from the spin 0 case due to the different EOM for different spin bulk fields, see Table 2.1. For a bulk gauge field however, we can deduce additional information about the dual CFT. The dual Lagrangian in this case reads

$$\mathcal{L} = -\frac{1}{4} F_{\mu\nu}^a(x) F_a^{\mu\nu}(x) + \omega A_\mu^a(x) \mathcal{O}_a^\mu(x) + \mathcal{L}_{\text{CFT}}, \quad (2.41)$$

Scalar	$(j_1, j_2) = (0, 0)$	$\Delta_{\pm} = 2 \pm \sqrt{4 + c^2}$
Vector	$(j_1, j_2) = (\frac{1}{2}, \frac{1}{2})$	$\Delta_{\pm} = 2 \pm \sqrt{1 + c^2}$
Spin 2	$(j_1, j_2) = (1, 1)$	$\Delta_{\pm} = 2 \pm \sqrt{4 + c^2}$
Chiral Spinor $s = \frac{1}{2}$	$(j_1, j_2) = (\frac{1}{2}, 0)$ or $(0, \frac{1}{2})$	$\Delta = \frac{3}{2} + c - \frac{1}{2} $

Table 2.1: Relation between scaling dimension of the conformal fields and bulk mass parameter (localization) in AdS₅. Note, that for general BCs, left- and right-handed chiral spinors will have different relations, see (*e.g.* [104, p.7&13]). This will be obsolete for our definition of the c-parameter, compare section 2.4. This table was first given in [93, p.2-3].

where the source fields A_{μ}^a are gauge fields, so that they must couple to conserved currents \mathcal{O}_a^{μ} in the CFT. Therefore, the existence of a bulk gauge group implies a corresponding global symmetry of the dual CFT, where only a subgroup is gauged, namely the one whose gauge bosons have Neumann boundary conditions on the UV brane and thus possess a source field (which corresponds to the gauge boson in the elementary sector). If only for a subgroup of a global symmetry gauge fields are introduced, this global symmetry is explicitly broken scenario, which, if the gauge couplings are small is in the literature called *weakly gauging* the global symmetry. Note however, that for the composite sector alone \mathcal{L}_{CFT} , the global symmetry is preserved. The fact, that one can impose a global symmetry in the composite sector by choosing the appropriate bulk gauge group, was the original inspiration for the $SU(2)_L \times SU(2)_R$ bulk group in the *custodial* extension of the RS model [105] and its at first sight arbitrary breaking pattern. It is just the holographic implementation of the global custodial symmetry of the SM Higgs sector with the $SU(2)_L \times U(1)_Y$ weakly gauged. Likewise, the extensions proposed in this thesis will translate in this way to global symmetries of the dual theory.

At this point we have still not introduced an IR brane, but applications of the duality without one can already be found in the literature. The 5D formulation of a set-up without IR brane, where gravity is closely localized at the UV brane (SM fields play no role but would reside on the UV brane in a complete realistic model) is called RS2 model, due to a follow-up paper by Randall and Sundrum in 1999 [56] and is described by a dual strongly coupled CFT together with 4D gravity (first mentioned in the Acknowledgements of [98]). If one assumes the SM confined to the UV brane and adds non SM fields into the bulk, one describes the holographic dual of a class of new physics models proposed by Georgi in 2007, called *unparticles* [101], which proposes the existence of a new conformal sector coupled to the SM.

Analogue to the explicit breaking of the CFT by the introduction of a UV brane at high energies, the introduction of an IR brane $z = R'$ should lead to a breaking of conformal invariance at low energy scales $\Lambda_{\text{IR}} \sim 1/R'$, below which scaling invariance in the bulk is broken. As a first consequence, regarding our bulk scalar example above, we observe that the introduction of an IR brane will replace the regularity condition at $z = \infty$, which fixes C_1 to zero in (2.27) by a boundary condition at $z = R'$ and thus leads to $C_1 \neq 0$. Since the regularity condition in the non-compactified theory is

the reason for the one-point function (2.35) to be zero (the flux (2.31) contains only terms quadratic in the source fields), this means that

an IR brane brings about an operator vev proportional to the coefficient C_1 (sometimes, one finds therefore the expressions vev for C_1 and source for C_2 in the literature). In contrast to the UV brane, the introduction of an IR brane is therefore connected to a *spontaneous* breaking of the conformal symmetry in the dual theory, similar to the breaking of classical conformal invariance through confinement in QCD. However, the spontaneous breaking of a conformal symmetry is connected with the existence of a Goldstone boson, the *dilaton*.⁵ In the holographic approach, this scalar is identified with the radion, which is the fluctuation about the radius of the extra dimension, [92]. Moreover, we know that a compactified extra dimension leads to an infinite tower of KK states with linear mass splitting. In the dual CFT, that is reflected by the fact, that the operators $\mathcal{O}(x)$ do not describe a continuum CFT eigenstate anymore, but an infinite tower of composite mass eigenstates, the equivalent of mesons. It is actually known since the seventies that in the large N limit, the two point function of a confining $SU(N)$ gauge theory can be written as the infinite sum (see [100, p.20])

$$\langle \mathcal{O}(p)\mathcal{O}(-p) \rangle = \sum_{n=1}^{\infty} \frac{a_n^2}{p^2 - m_n^2} \approx \sum_{n=1}^{\infty} \frac{N}{p^2 - m_n^2}, \quad (2.42)$$

where m_n are the masses of the n th meson state and $a_n = \langle 0|\mathcal{O}|n \rangle$ is the matrix element for \mathcal{O} to create the n th meson from the vacuum⁶. The fact that we have a spontaneous breakdown of conformal invariance in the dual CFT and a 2-point correlation function with discretely separated poles, tells us that the IR brane describes a confining phase in the dual CFT. In the KK decomposition introduced in this thesis (2.88), the zero mode can thereby be understood as dual to a mainly elementary state, the equivalent of the elementary field $\varphi(x)$ in (2.40), while the dual of the KK modes mainly consist of composite states, the equivalent of $\mathcal{O}(x)$ in (2.40)⁷. The zero mode and likewise the KK modes can thus be considered superpositions of composite and elementary states with the same quantum numbers, similar to $\gamma - \rho$ mixing in the SM, as illustrated in Figure 2.2. The mixing angle or equivalently the amount of compositeness is dictated by the localization in the bulk, which controls in the dual theory whether the mixing term is a relevant, marginal or irrelevant operator. This realizes the concept of *partial compositeness*. For the example of a bulk fermion, before introduction of an IR brane, one finds a dual Lagrangian

⁵It is named like this, because it corresponds to the broken generator from the dilation invariance of the CFT. In this context it is interesting to note, that the number of Goldstone bosons from the breaking of a spacetime symmetry will not follow from the Goldstone theorem, which is rooted in the fact that the generators are linearly independent, but the long-wavelength excitations they produce need not be [106].

⁶However, in large N QCD the meson masses show straight *Regge behavior*, meaning $m_n^2 \sim n$, while the hard wall RS model has KK mass spectra $m_n \sim n$. This is the reason why AdS/QCD is modeled by *soft wall* RS models, which introduce a quadratic radion profile, leading to a linear mass splitting [103].

⁷It should be mentioned, that in the AdS/CFT literature, the term “zero mode” often denotes *only* the elementary state, located *at* the UV brane, which goes back to a different KK decomposition as the one used in this thesis, the so-called *holographic basis* introduced by Batell and Ghergetta [102].



Figure 2.2: Illustration of $\gamma - \rho$ mixing and the mixing of elementary and composite states in the dual theory of the RS1 scenario.

$$\mathcal{L} \ni \mathcal{L}_{\text{el}} + \omega M^{1-|c-\frac{1}{2}|} (\bar{\psi}_L^0 \mathcal{O}_R + h.c.) + \mathcal{L}_{\text{CFT}}, \quad (2.43)$$

where $M \sim \Lambda_{\text{UV}}$ is of order Planck scale and c is the localization parameter of the bulk field which is dual to $\mathcal{O}_R(x)$. In this notation the scaling dimension of the composite fermion operator reads $\dim \mathcal{O}_R(x) = 4 - 3/2 - 1 + |c - 1/2| = 3/2 + |c - 1/2|$. After introducing an IR brane, and therefore spontaneous breaking of the CFT, $\mathcal{O}_R(x)$ represents a composite bound state in a strongly coupled theory with a mass gap dictated by the IR scale Λ_{IR} . In the following, we will therefore make use of the symbolic notation introduced in Section 1.1 and write the Lagrangian at the compositeness scale Λ_{IR} as

$$\mathcal{L} \ni \mathcal{L}_{\text{el}} + \omega M \left(\frac{\Lambda_{\text{IR}}}{M} \right)^{|c-\frac{1}{2}|} (\bar{\psi}_L^0 \mathcal{O}_R + h.c.) + \mathcal{L}_{\text{CFT}}. \quad (2.44)$$

This corresponds to attributing the varying scaling dimension of the composite operator to the power law running in a strongly coupled theory close to the conformal window, compare [37, p.4-5]. With the identification

$$\gamma = |c - 1/2|, \quad (2.45)$$

the Lagrangian (2.44) can now directly be compared to the Lagrangian (1.24), which shows how the localization in the bulk is connected to the mixing between elementary and composite states. As illustrated in Figure 2.3, for a localization parameter $c < -1/2$, the mixing operator becomes irrelevant and therefore there is next to no mixing between the CFT and the elementary sector. As a consequence, in the mass eigenbasis, the light eigenstate will correspond to a mostly elementary field. This is the case for the light quarks and leptons in the RS model with an IR localized Higgs. For a bulk mass $-1/2 < c < 1/2$, which corresponds to a IR localized fermion, the mixing becomes relevant and maximal mixing is achieved for $c = 1/2$, which will be dual to roughly a 50% composite, 50% elementary eigenstate. From (2.44), one would expect, that even more IR localized fields the mixing decreases again, however for localizations $c > 1/2$, the dual theory will look different and (2.44) does not hold. We will not go into detail concerning the construction of the dual Lagrangian in this case, but refer to the relevant literature [104]. We note, that in this case the spectrum of the composite theory contains a light field, with negligible admixture from the elementary sector, which in turn develops a mass term of the order of the cutoff. One can therefore consider a fermion localized at $c > 1/2$ to be almost completely composite [91].

This scenario is related to the two possible branches Δ_{\pm} , which we found in the scalar

example. For the root Δ_+ the CFT part of the scalar correlation function computed above encodes a massless pole – this can be seen explicitly by doing a small momentum expansion of (2.33), see [107, Sec. 4.2.2] – and the mass term for the elementary scalar is given by (2.39). The correlation function of the Δ_- branch in (2.28) has not been computed here, but would neither develop such a pole nor generate a mass term. The calculation can be found in [107, Sec. 4.2.1].

Note, that the right- and left-handed elementaries are generated from different 5D fields and therefore the bulk mass parameters can differ in general. One can therefore write the mass term as

$$M \begin{pmatrix} \bar{\psi}_L^0 & \bar{\mathcal{O}}_L \end{pmatrix} \begin{pmatrix} 0 & (\Lambda_{\text{IR}}/M)^{|c_R-1/2|} \\ (\Lambda_{\text{IR}}/M)^{|c_L-1/2|} & \Lambda_{\text{IR}}/M \end{pmatrix} \begin{pmatrix} \psi_R^0 \\ \mathcal{O}_R \end{pmatrix}, \quad (2.46)$$

which can be diagonalized with rotations analogue to (1.25). Thus we conclude, that a localization very close to the IR brane, $c > -1/2$ for fermions, corresponds to a large scaling dimension and thus a mainly composite state in the dual theory, while localization close to the UV brane, $c < -1/2$ for fermions, results in a mainly elementary zero mode and for values in between those limits, various amount of mixing can be achieved.

The Holographic Dual of the Minimal RS Model

We can now understand the strongly coupled dual of the RS model described in Section 2.1, which will be used throughout the main part of this thesis. It has a Higgs scalar confined to the IR brane, which is to be understood as the limit of an extremely IR localized bulk scalar. This corresponds to a purely composite state in the dual theory. Furthermore, this state has a scaling dimension $\Delta_H > 4$, which tells us that in terms of the classification of composite Technicolor theories, we deal with the opposite of walking technicolor, in the sense that in WTC one needs $\Delta_H < 3$ in order to generate the top mass.⁸

Large fermion masses are consequently implemented by mixing and the Higgs does not couple at all to the elementary sector. Such a coupling would be gauge invariant, but the large scaling dimension of the Higgs composite renders them irrelevant. As discussed in Section 1.1, such an argument cannot be made if all fields are strongly coupled bound states, as it is the case for the Higgs couplings to composite fermions. The top is thus mainly composite in this setup and the light quarks are dominantly elementary states. As such, the Yukawa coupling of the right-handed top to the Higgs is of order one, while light fermions can feel the presence of the Higgs only through mixing with their composites, which induces Yukawas suppressed by the corresponding mixing angles. Diagrammatically, this is illustrated in Figure 2.4. Referring to these diagrams, we find for the effective Yukawa couplings

$$y_t \sim f(c_{t_L}) Y, \quad y_u \sim f(c_{u_L}) f(c_{u_R}) Y, \quad (2.47)$$

⁸In an unfortunate notation (because the couplings still walk), it is sometimes called *speeding technicolor* [29, p.4]

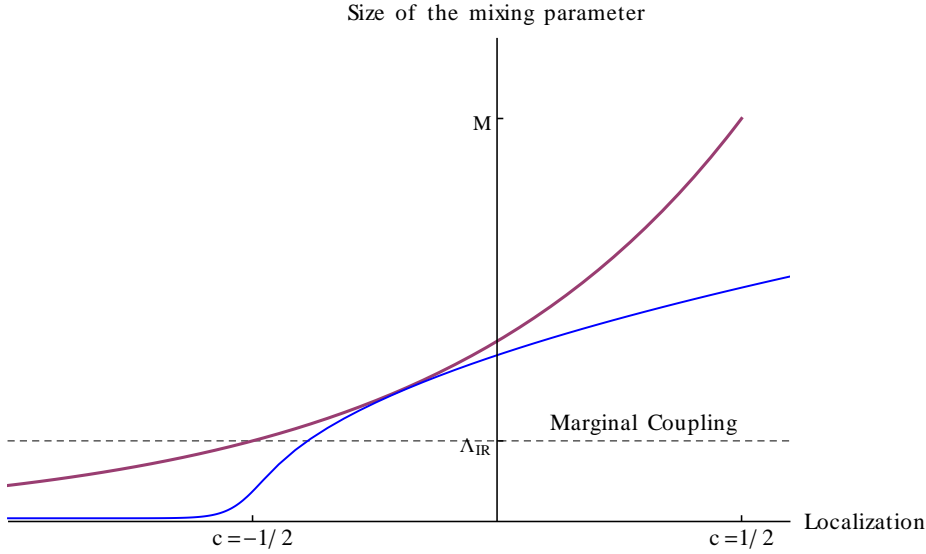


Figure 2.3: Sketch showing the size of the mixing parameters $M^{1-|c-\frac{1}{2}|}$ in the Lagrangian (2.44) in purple and $F(c)$ as defined in (2.150) in blue, depending on the bulk localization of the 5D fermion. The dashed black line crosses the purple plot at $c = -1/2$, which implies marginal mixing. In the vicinity of $c = -1/2$, the fermion is either slightly UV or IR localized and $F(c)$ grows exponentially, while localization parameters $c < -1/2$ will lead to irrelevant mixing corresponding to a negligibly small $F(c)$ and for $c > -1/2$, $F(c)$ becomes linear. At $c = 1/2$ the mixing becomes maximal and localization parameters $c > 1/2$ correspond to a different dual theory with mainly composite fermions.

where Y denotes the $\mathcal{O}(1)$ *proto*- or 5D Yukawa coupling, the coefficient of the three-vertex operator $\mathcal{O}_R \mathcal{O}_L \mathcal{O}_H$, and $f(c_i) \sim \omega (\Lambda_{\text{IR}}/M)^{|c_i-\frac{1}{2}|}$ for i the flavor index, quantifies the mixing between elementary and composite state. This explains the hierarchy of effective 4D Yukawas in terms of the dual theory.

Gauge fields have by construction marginal mixing with the composite sector and only the W s and the Z gauge bosons do directly feel the composite sector due to their coupling to the Higgs.

In contrast to the Higgs however, the elementary gauge bosons have direct couplings to the elementary sector. As a consequence we have two possible ways for the fermion zero modes to couple to composite vector currents, depicted in Figure 2.5. The diagram on the left gives rise to a flavor-universal (enforced by gauge symmetry) coupling in the elementary sector and a mixing of order one (must be marginal) with the composite vector. On the right, the three vertex is the composite-composite coupling while the elementary fermions mix in with suppression factors $f(c_i)$, just like in Figure 2.4, because the mixing operator is irrelevant or at most marginal (apart from the left handed bottom/top). Upon diagonalization of the mass mixing terms (1.27), the light mass eigenstates which are identified with the SM fields will have flavor non-diagonal

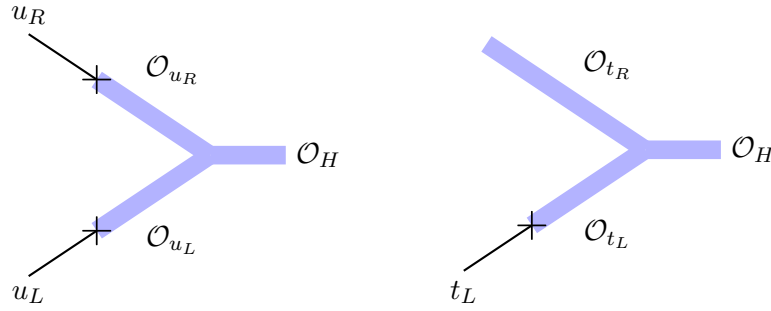


Figure 2.4: Three vertices relevant for the effective Yukawa couplings of UV-localized quarks (left panel) and for the top quark (right panel).

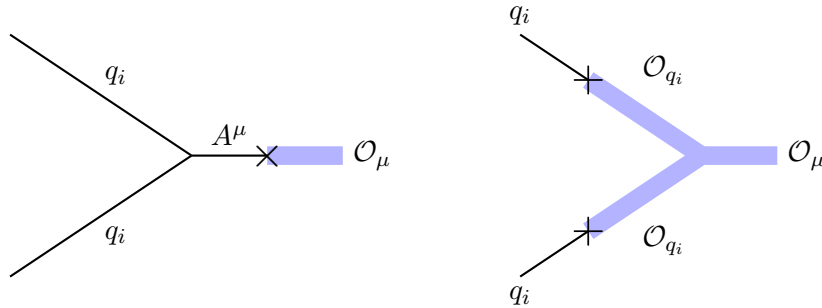


Figure 2.5: Diagrams responsible for flavor universal (left panel) and flavor non-universal couplings to the composite vector current.

couplings, which are represented by these diagrams, because the mixings are in general not flavor universal, $f(c_i) \neq f(c_j)$, if $i \neq j$. This is the dual picture for the RS-GIM mechanism, which will be discussed in detail in Section 2.5: Both the coupling to the Higgs and the flavor non-universal couplings to composite vector bosons, feel the same suppression factors.

In Section 2.3 we will be able to identify the different contributions to the sum over the gauge boson tower with the three different combinations of the two diagrams in order to construct a four-fermion operator.

The Holographic Dual of Higgsless, Custodially Protected, Composite Higgs and Little Higgs Theories

It is instructive to identify the holographic dual of the other concepts connected to strongly coupled theories presented in Section 1.1.

It is very straightforward to replace the Higgs operator in our model by a non-linear sigma field, which would correspond to a higgsless TC theory with only 3 scalar degrees of freedom, which are eaten by the electroweak gauge bosons. One can alternatively realize this model by breaking of the electroweak bulk symmetry via BCs (without a scalar brane field). In the following we will use this description and label Dirichlet (D) BCs on the UV brane and Neumann (N) BCs on the IR brane by (DN) and likewise

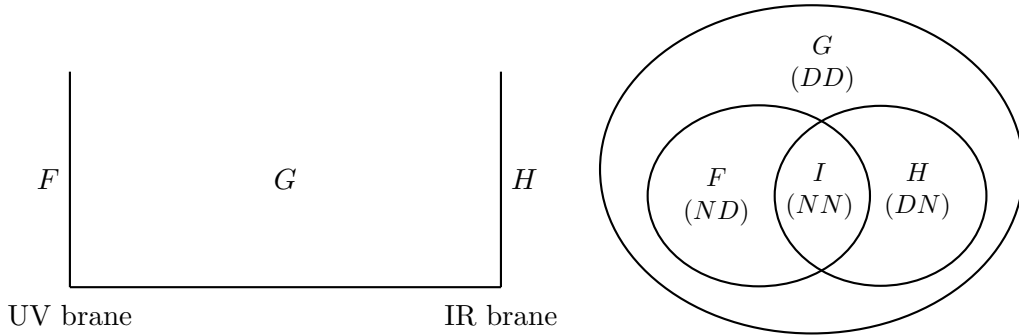


Figure 2.6: Illustration of the breaking by BCs at the UV and IR brane. In the dual theory, the subgroup F is gauged by elementary fermions and the group H leaves the composite sector invariant after confinement. The right hand side shows a Venn diagram of the groups. The BCs of the fields living in the corresponding complements are also given (For example, fields in G may have any combination of BCs, but fields in $G \setminus (F \cup H)$ must have Dirichlet BCs on both branes).

for all other combinations. We will consider the consequences of Goldstones theorem in a situation in which breaking on both branes can appear, and its implications for the dual theory.

In general, one has a bulk gauge group G , which is broken down to the subgroup F on the UV brane by explicit breaking through weakly gauging this subgroup in the elementary sector, see Figure 2.6. The dual theory is given by the Lagrangian (2.41), where a denotes the indices of the generators of F . On the IR brane, G is broken down to the subgroup H , which is the subgroup that still leaves the composite sector invariant after confinement sets in. We will call the intersection of these groups $I = F \cap H$. One therefore expects $\dim G/H = \dim G - \dim H$ Goldstone bosons from the spontaneous symmetry breaking. However, $\dim F/I$ of those will be eaten, because there exist elementary gauge fields corresponding to the generators of this spontaneously broken subgroup. In the end, one thus has $\dim I$ massless gauge bosons in the elementary sector and $N_{\text{PNGB}} = \dim G/H - \dim F/I$ pseudo-Nambu Goldstone bosons, since they correspond to explicitly broken generators. The general setup is depicted in Figure 2.6, where the corresponding BCs for the vector part of the bulk gauge fields have been given. Since the breaking takes place via BCs, there are no scalar degrees of freedom on the brane. The longitudinal degrees of freedom of the gauge bosons are in this setup provided by the A_5 components of the residual $\dim G/(F \cup H)$, which must have Neumann BCs on both branes and thus develop zero modes, compare Section 4 of [62]. Both approaches, symmetry breaking via a brane field or via BCs, give the same number of degrees of freedoms. One can further infer, that the A_5 mode of a bulk gauge field is the holographic dual of a composite pseudo Nambu Goldstone boson.

Higgsless TC is therefore described by an RS model without a brane scalar and the following symmetries realized in the bulk and on the branes respectively (here, and in the following scenarios, only the electroweak sector plays a role and the not noted

$SU(3)_C$ is considered to be unbroken on both branes)

$$\begin{aligned} G &= SU(2)_L \times U(1)_{B-L} \\ F &= SU(2)_L \times U(1)_{B-L} \\ H &= U(1)_Y \end{aligned} \quad \Rightarrow \quad \frac{\dim G/H = 3}{\dim F/I = 3} \cdot \quad (2.48)$$

$$N_{\text{PNGB}} = 0$$

In this scenario, the $U(1)$ charges are chosen in a way that ensures that the single massless gauge boson, $I = U(1)_Q$, corresponds to the photon. The remaining three gauge bosons correspond to W^\pm and the Z and are massive only due to BCs on the IR brane, which will put their masses in the right range (compare the upper left panel of Figure 2.8 and the discussion in Section 2.3).

The extension to a model with a custodial global symmetry is straightforward. Consider the setup [63],

$$\begin{aligned} G &= SU(2)_L \times SU(2)_R \times U(1)_{B-L} \\ F &= SU(2)_L \times U(1)_Y \\ H &= SU(2)_V \times U(1)_{B-L} \end{aligned} \quad \Rightarrow \quad \frac{\dim G/H = 3}{\dim F/I = 3} \cdot \quad (2.49)$$

$$N_{\text{PNGB}} = 0$$

Here, the spontaneous breaking preserves a custodial $SU(2)_V$ symmetry, just like in the SM. The group F tells us for which composite Goldstone bosons there are elementary gauge bosons. This is again a W^\pm and the Z (there is not much room for choosing F). The intersection I will again be the electromagnetic $U(1)_Q$. But now there are three gauge bosons, corresponding to the bulk $SU(2)_R$, which do not have a zero mode due to Dirichlet BCs on both branes. They will lead to a tower of massive W^\pm 's and Z 's, which will couple with the same coupling strength as the KK modes of the electroweak gauge bosons and therefore cancel their contributions to the T parameter, see Section 3.1 for details.

In the holographic dual of the composite Higgs scenario, which realizes the Higgs as a Nambu Goldstone boson, we expect to have a fully unbroken electroweak gauge group in the theory and the confining phase will only give us 4 Goldstone Bosons in the correct representation to form a composite Higgs. We will demonstrate this by means of a scenario which also implements custodial symmetry, see [37, Sec. 2],

$$\begin{aligned} G &= SO(5) \times U(1)_X \\ F &= SU(2)_L \times U(1)_Y \\ H &= SO(4) \times U(1)_X \end{aligned} \quad \Rightarrow \quad \frac{\dim G/H = 4}{\dim F/I = 0} \cdot \quad (2.50)$$

$$N_{\text{PNGB}} = 4$$

Here, the $U(1)$ charges are chosen in a way that results in $I = SU(2)_L \times U(1)_Y$. Obviously, this choice of groups will leave all four electroweak gauge bosons massless, preserves the $SU(2)_V \sim SO(4)$ custodial symmetry in the composite sector, and four PNGBs remain in the theory.

One can construct the holographic dual of models which implement the collective breaking mechanism in an analogous way. For example, the corresponding scenario

presented in Section 1.1 has the symmetry breaking pattern

$$\begin{aligned} G &= SU(3) \times SU(3) \times U(1) \\ F &= SU(3) \times U(1) \\ H &= SU(2) \times SU(2) \times U(1) \end{aligned} \quad \Rightarrow \quad \begin{array}{l} \dim G/H = 10 \\ \dim F/I = 5 \\ N_{\text{PNGB}} = 5 \end{array} . \quad (2.51)$$

The charges must again be chosen in a way which guarantees $I = SU(2)_L \times U(1)_Y$. One also finds five PNGBs, which in agreement with (1.36) will form the composite Higgs doublet and a singlet. One might be alarmed by the fact that we now have a large elementary gauge group F , possibly implying that there are additional gauge bosons with masses at the electroweak scale in the theory. However, in both the composite Higgs scenarios (with and without collective breaking), the IR BCs will not break the electroweak symmetry (that is what the composite Higgs is for), but the larger global symmetry G at some scale $f > v$. The five additional gauge bosons in the collective breaking scenario are just what we found in (1.41) with masses in the multiple TeV range.

2.3 Profiles of Gauge Bosons

In the later discussion of flavor observables, we will compute the Wilson coefficients of four fermion operators. The leading coefficients come from tree-level diagrams in the full theory, with external fermion zero modes, but with gauge boson zero modes (which are just the SM contributions), as well as their KK excitations or composite resonances propagating between the vertices. At the matching scale, the momenta in these propagators can be neglected compared to the masses. In this section, the general 5D propagator with all possible boundary conditions for a generic bulk gauge boson will be given and interpreted in the dual theory.

We assume a bulk gauge field transforming as a 5D Lorentz vector $A_M(x_\mu, \phi)$ with suppressed gauge indices (as they play no role in deriving the propagator) and add a gauge fixing term as well as an explicit mass term, to the Lagrangian. Both gauge breaking terms are kept, so that the solution can be adapted to different situations,

$$\begin{aligned} \mathcal{L}_{\text{Gauge}} + \mathcal{L}_{\text{GF}} + \mathcal{L}_{\text{Mass}} &= G^{KM} G^{LN} \left(-\frac{1}{4} F_{KL} F_{MN} \right) + \frac{1}{2} G^{MN} M_A^2 A_M A_N \\ &\quad - \frac{r_c}{2\xi \sqrt{|G|}} \left(\partial_\mu A^\mu - \frac{\xi}{r_c^2} \partial_\phi e^{-2\sigma} A_\phi \right)^2 . \end{aligned} \quad (2.52)$$

Note, that the gauge fixing is specifically chosen in a way that the A_ϕ independent term represents the usual 4D gauge fixing and the cross terms cancel the mixing between vector and scalar components of A_M which will arrange for diagonal propagators [111].

After integration by parts, one finds [112]

$$\begin{aligned} \sqrt{|G|}(\mathcal{L}_{\text{Gauge}} + \mathcal{L}_{\text{GF}} + \mathcal{L}_{\text{Mass}}) = \\ \frac{r_c}{2} \left[A_\nu \left(\partial^2 \eta^{\mu\nu} - \left(1 - \frac{1}{\xi}\right) \partial^\mu \partial^\nu - \partial_\phi \frac{e^{-2\sigma}}{r_c^2} \partial_\phi \eta^{\mu\nu} + M_A^2 e^{-2\sigma} \right) A_\mu \right. \\ \left. + A_\phi \left(-\frac{e^{-2\sigma}}{r_c^2} \partial^2 + \frac{\xi}{r_c^4} e^{-2\sigma} \partial_\phi^2 e^{-2\sigma} - \frac{e^{-4\sigma}}{r_c^2} M_A^2 \right) A_\phi \right]. \end{aligned} \quad (2.53)$$

Boundary terms from partial integration vanish as long as the fields have either Dirichlet or Neumann BCs and the fields are well behaved at 4D infinity.

We will once more change notation, because it is sensible for the numerics to have all expressions in dimensionless variables. Therefore, let $t \equiv M_{\text{KK}} z = M_{\text{KK}} e^\sigma / k$ with $M_{\text{KK}} = \epsilon k$ defined in (1.54), and $\epsilon \equiv \Lambda_{\text{IR}} / \Lambda_{\text{UV}}$. The line element in this t -notation reads

$$ds^2 = \left(\frac{\epsilon}{t}\right)^2 (\eta_{\mu\nu} dx^\mu dx^\nu - M_{\text{KK}}^{-2} dt^2), \quad (2.54)$$

and the positions of the branes are now intuitively expressed by ratios of scales, $t = \epsilon$ for the UV and $t = 1$ for the IR brane. In addition, we define the *volume* of the extra dimension as $L = -\ln \epsilon = kr_c \pi \approx 36$. Finally, we redefine the scalar component of A_M ,

$$A_5(x_\mu, t) = \frac{\epsilon}{t r_c} A_\phi(x_\mu, \phi), \quad (2.55)$$

in order to adjust the mass dimension and simplify the following calculations. With these conventions, equation (2.53) reads

$$\begin{aligned} S = \int d^4x \int d\phi \sqrt{|G|} (\mathcal{L}_{\text{Gauge}} + \mathcal{L}_{\text{GF}}) &= \frac{1}{2} \int d^4x \int_{-\pi}^{\pi} r_c d\phi A_M K_\xi^{MN} A_N \\ &= \frac{1}{2} \int d^4x \frac{2\pi r_c}{L} \int_\epsilon^1 \frac{dt}{t} A_M K_\xi^{MN} A_N, \end{aligned} \quad (2.56)$$

in which

$$K_\xi^{MN} = \begin{pmatrix} (\partial^2 - M_{\text{KK}}^2 t \partial_t \frac{1}{t} \partial_t) \eta^{\mu\nu} - \left(1 - \frac{1}{\xi}\right) \partial^\mu \partial^\nu + \frac{\epsilon^2}{t^2} M_A^2 \eta^{\mu\nu} & 0 \\ 0 & -\partial^2 + \xi M_{\text{KK}}^2 \partial_t t \partial_t \frac{1}{t} - \frac{\epsilon^2}{t^2} M_A^2 \end{pmatrix} \quad (2.57)$$

is the inverse of the Feynman propagator in R_ξ gauge. After a Fourier transformation of the coordinates of the non-compact directions, $p_\mu = i\partial_\mu$, the following two equations

define the propagator of the vector and scalar components,

$$\left[\left(-p^2 - M_{\text{KK}}^2 t \partial_t \frac{1}{t} \partial_t + \frac{\epsilon^2}{t^2} M_A^2 \right) \eta^{\mu\nu} + \left(1 - \frac{1}{\xi} \right) p^\mu p^\nu \right] D_{\nu\rho}^\xi(p, t; t') = \frac{Lt'}{2\pi r_c} \delta_\rho^\mu \delta(t - t'), \quad (2.58)$$

$$\left[p^2 + \xi M_{\text{KK}}^2 \partial_t t \partial_t \frac{1}{t} - \frac{\epsilon^2}{t^2} M_A^2 \right] D_{55}^\xi(p, t; t') = \frac{Lt'}{2\pi r_c} \delta(t - t'). \quad (2.59)$$

We further define the dimensionless quantities $q_\mu \equiv p_\mu/M_{\text{KK}}$ and $c_A \equiv \epsilon M_A/M_{\text{KK}}$ and simplify,

$$\left[\left(-q^2 - t \partial_t \frac{1}{t} \partial_t + \frac{c_A^2}{t^2} \right) \eta^{\mu\nu} + \left(1 - \frac{1}{\xi} \right) q^\mu q^\nu \right] D_{\nu\rho}^\xi(q, t; t') = \frac{Lt'}{2\pi r_c M_{\text{KK}}^2} \delta_\rho^\mu \delta(t - t'), \quad (2.60)$$

$$\left[\frac{1}{\xi} q^2 + t \partial_t \frac{1}{t} \partial_t - \frac{c_A^2/\xi - 1}{t^2} \right] \xi D_{55}^\xi(q, t; t') = \frac{Lt'}{2\pi r_c M_{\text{KK}}^2} \delta(t - t'). \quad (2.61)$$

For the vector component, one can read off an ansatz for the solution [112],

$$D_{\nu\rho}^\xi(q, t; t') = A_\xi(q, t; t') \frac{q_\nu q_\rho}{q^2} + B(q, t; t') \left(\eta_{\nu\rho} - \frac{q_\nu q_\rho}{q^2} \right), \quad (2.62)$$

which, after inserting in (2.60) yields two independent equations,

$$\left(-\frac{1}{\xi} q^2 - t \partial_t \frac{1}{t} \partial_t + \frac{c_A^2}{t^2} \right) A_\xi = \left(-q^2 - t \partial_t \frac{1}{t} \partial_t + \frac{c_A^2}{t^2} \right) B, \quad (2.63)$$

$$\left(-q^2 - t \partial_t \frac{1}{t} \partial_t + \frac{c_A^2}{t^2} \right) B = \frac{Lt'}{2\pi r_c M_{\text{KK}}^2} \delta(t - t'). \quad (2.64)$$

The first one tells us that $A_\xi(q, t; t') = B(q/\sqrt{\xi}, t; t')$ and therefore

$$D_{55}^\xi(q, t; t') = -\frac{1}{\xi} A_\xi(q, t; t') = -\frac{1}{\xi} B(q/\sqrt{\xi}, t; t') \quad \text{with} \quad c_A \rightarrow \sqrt{c_A^2/\xi - 1}. \quad (2.65)$$

Solving the second equation (2.64), is sufficient to compute both propagators. Evaluated for $t \neq t'$ the equation can be put in the form

$$\left((qt)^2 \partial_{qt}^2 + (qt) \partial_{qt} + [(qt^2) - (c_A^2 + 1)] \right) \frac{B(qt)}{qt} = 0, \quad (2.66)$$

which is a Bessel PDE with solutions (compare (2.27))

$$B_{>}(qt_{>}) = (qt_{>}) \left[C_1^> J_{\Delta-2}(qt_{>}) + C_2^> Y_{\Delta-2}(qt_{>}) \right], \quad \text{for } t > t', \quad (2.67)$$

$$B_{<}(qt_{<}) = (qt_{<}) \left[C_1^< J_{\Delta-2}(qt_{<}) + C_2^< Y_{\Delta-2}(qt_{<}) \right], \quad \text{for } t < t', \quad (2.68)$$

in which $t_{>} \equiv \text{Max}[t, t']$, $t_{<} \equiv \text{Min}[t, t']$ and $\Delta = 2 + \sqrt{1 + c_A^2}$, which is chosen in a way that makes it easily comparable with the results from Section 2.2. Note, that for the scalar propagator, $\Delta = 2 \pm c_A/\sqrt{\xi}$. This is not what we found for a bulk scalar,

see Table 2.1. But the A_5 component will also not propagate in the unitary gauge, $\xi \rightarrow \infty$, which is the exact behavior of a Goldstone boson and confirms therefore our findings of Section 2.2, that A_5 can be considered to be the holographic dual of a Goldstone boson. In this limit, the KK excitations of the vector fields will eat the KK modes of the A_5 s and become massive, compare [62]. The behavior of the zero modes will depend on the BCs.

The propagator is symmetric in t and t' and a viable ansatz for the bulk solution is therefore

$$B(q, t_>, t_<) = N_B(q^2, t_>, t_<) [C_1^> J_{\Delta-2}(qt_>) + C_2^> Y_{\Delta-2}(qt_>)] \\ \times [C_1^< J_{\Delta-2}(qt_<) + C_2^< Y_{\Delta-2}(qt_<)] , \quad (2.69)$$

where the normalization is fixed by the jump condition,

$$\lim_{\delta \rightarrow 0} \int_{t'-\delta}^{t'+\delta} dt \left(-q^2 - t \partial_t \frac{1}{t} \partial_t + \frac{c_A^2}{t^2} \right) B(q, t_>, t_<) = \frac{L t'}{2\pi r_c M_{\text{KK}}^2} \quad (2.70)$$

$$\Rightarrow \lim_{\delta \rightarrow 0} \left[(\partial_{t_<} - \partial_{t_>}) B(q, t_>, t_<) \Big|_{t_<=t_>-\delta} \right] = \frac{L t_>}{2\pi r_c M_{\text{KK}}^2} , \quad (2.71)$$

so that

$$N_B = \frac{L}{4M_{\text{KK}}^2 q^2 r_c} \frac{1}{C_1^> C_2^< - C_1^< C_2^>} . \quad (2.72)$$

The remaining coefficients are fixed by the boundary conditions. We will be mainly interested in gauge bosons, that is $\Delta = 3$. However, a mass term may be induced by a bulk Higgs, and can then be written as

$$c_A^2 \rightarrow L \frac{v_4 g_4^2}{4M_{\text{KK}}^2} , \quad (2.73)$$

in which we follow [57] in defining $g_5 = \sqrt{2\pi r_c} g_4$, and further use $v_4 = \epsilon v_5$ as well as adjusting the mass dimension by $\langle H \rangle = v_5 \sqrt{k}/\sqrt{2}$. Note, that this expression is not general, but true for the SM.⁹ In the case of such a spontaneous symmetry breaking in the bulk, one also has to introduce the corresponding Goldstone bosons φ_A in the gauge fixing term in (2.52),

$$\left(\partial_\mu A^\mu - \frac{\xi}{r_c^2} \partial_\phi e^{-2\sigma} A_\phi \right)^2 \rightarrow \left(\partial_\mu A^\mu - \xi \left[\sqrt{k} \frac{v_5 g_5}{2} \varphi_A + \frac{1}{r_c^2} \partial_\phi e^{-2\sigma} A_\phi \right] \right)^2 . \quad (2.74)$$

Note, that in this model a linear combination of A_ϕ and the Goldstone boson φ_A , which has mass dimension $[\varphi_A] = 3/2$, is absorbed by the KK modes of the A_μ , while the other combination remains physical, see [50, App. A]. As a consequence, there is a tower of additional pseudo scalars, which is a distinctive signal of a bulk Higgs mechanism.

This is not the case if brane Higgs fields are introduced, which can be implemented

⁹Other gauge groups and symmetry breaking patterns induce different numerical factors, compare Section 3.6.

in the above equations by replacing

$$c_A^2 \rightarrow L \frac{v_4^2 g_4^2}{4M_{\text{KK}}^2} \delta(t - 1^-) + L \frac{v_4^2 g_4^2}{4M_{\text{KK}}^2} \delta(t - \epsilon^+). \quad (2.75)$$

and

$$\left(\partial_\mu A^\mu - \frac{\xi}{r_c^2} \partial_\phi e^{-2\sigma} A_\phi \right)^2 \rightarrow \left(\partial_\mu A^\mu - \xi \left[\frac{v_4 g_5}{2r_c} (\delta(|\phi| - \pi) + \delta(|\phi|)) \varphi_A + \frac{1}{r_c^2} \partial_\phi e^{-2\sigma} A_\phi \right] \right)^2. \quad (2.76)$$

This will only affect the propagator of the vector component, because in contrast to the bulk Higgs, the kinetic term only needs couplings to the vector, in order to be 4D Lorentz invariant, as in (2.13). Note also, that here $\langle H \rangle = v_5/\sqrt{2}$ and $[\varphi_A] = 1$, because H is a brane localized scalar. As a consequence, there will be no Higgs KK modes and only one Goldstone boson for the zero mode of the gauge field. Squaring the delta function in (2.76) looks worrisome, but is unproblematic, because the resulting terms will cancel in the KK decomposed theory, as discussed in Section 2.3. Alternatively, a brane Higgs can also be implemented with brane gauge fixing terms, as in [113, Sec. 2.3]. Note also, that the bulk solution has always $\Delta = 3$ in case of a brane Higgs.

If the replacement (2.75) is made in (2.60), it basically corresponds to invoking BCs for the gauge field. Similar to (2.70), they can be found by integrating over small intervals around the branes (in ϕ -notation), or from a infinitesimally displaced point in the bulk to the brane (in t -notation)

$$\partial_t D_{\mu\nu}^\xi(q, t; t') \Big|_{t=\epsilon^+} = L \frac{v_4^2 g_4^2}{4M_{\text{KK}}^2} D_{\mu\nu}^\xi(q, \epsilon^+; t'), \quad (2.77)$$

$$\partial_t D_{\mu\nu}^\xi(q, t; t') \Big|_{t=1^-} = -L \frac{v_4^2 g_4^2}{4M_{\text{KK}}^2} D_{\mu\nu}^\xi(q, 1^-; t'). \quad (2.78)$$

The δ -function should be implemented in a way that does not clash with the boundary conditions of the fields, which is induced by the orbifold symmetry – and guarantees the vanishing of boundary terms from integration by parts. This is denoted by the superscripts at 1^- and ϵ^+ , which indicate a regularization of the δ function, for example $\delta(t - 1^-) \equiv \lim_{\eta \rightarrow 0} \delta(t - 1 + \eta)$, with

$$\delta(t - 1 + \eta) = \begin{cases} \frac{1}{\eta}, & \text{for } t \in [1 - \eta, 1], \\ 0, & \text{otherwise,} \end{cases} \quad (2.79)$$

so that the second equation in (2.77) makes sense, even though the orbifold symmetry fixes the propagator or its derivative to vanish at the fixed points. See section 2.4 for more details.

Symmetry breaking via BCs and by a brane Higgs field implies a different physical spectrum, because the former will not generate a Higgs resonance in the spectrum. However, for the following discussion, we will omit this distinction and choose a general

parametrization for the BCs,

$$\partial_t D_{\mu\nu}^\xi(q, t; t') \Big|_{t=\epsilon^+} = v_{\text{UV}} D_{\mu\nu}^\xi(q, \epsilon^+; t'), \quad \partial_t D_{\mu\nu}^\xi(q, t; t') \Big|_{t=1^-} = -v_{\text{IR}} D_{\mu\nu}^\xi(q, 1^-; t'), \quad (2.80)$$

and an equivalent set of equations for $t \leftrightarrow t'$. Here, v_{UV} and v_{IR} can either be understood as functions of the vevs of some UV or IR brane localized scalars or as to be taken in the limit where they are 0 or ∞ and represent Neumann or Dirichlet BCs. The results derived in the following paragraphs will apply for both scenarios. It follows for general bulk mass Δ , that

$$\begin{aligned} C_1^> &= -q Y_{\Delta-3}(q) + (-v_{\text{IR}} + \Delta - 3) Y_{\Delta-2}(q), \\ C_2^> &= q J_{\Delta-3}(q) - (-v_{\text{IR}} + \Delta - 3) J_{\Delta-2}(q), \\ C_1^< &= -q\epsilon Y_{\Delta-3}(q\epsilon) + (v_{\text{UV}}\epsilon + \Delta - 3) Y_{\Delta-2}(q\epsilon), \\ C_2^< &= q\epsilon J_{\Delta-3}(q\epsilon) - (v_{\text{UV}}\epsilon + \Delta - 3) J_{\Delta-2}(q\epsilon). \end{aligned} \quad (2.81)$$

The limit $\Delta \rightarrow 3$ for gauge bosons is straightforward.

We will study the gauge boson propagator in the effective theory, $q \ll 1$, and will elaborate an interpretation in the dual theory depending on different BCs. In general, the small momentum limit yields

$$D_{\mu\nu}^\xi(q, t; t') = \eta_{\mu\nu} \frac{L}{4\pi r_c M_{\text{KK}}^2} (c_1 t_{<}^2 + c_2 t^2 t'^2 + c_3 (t^2 + t'^2) + c_4) + \mathcal{O}(q^2) \quad (2.82)$$

with

$$\begin{aligned} c_1 &= \frac{v_{\text{UV}}(2 + v_{\text{IR}}) + v_{\text{IR}}\epsilon(2 - v_{\text{UV}}\epsilon)}{v_{\text{UV}}(2 + v_{\text{IR}}) + v_{\text{IR}}\epsilon(2 - v_{\text{UV}}\epsilon)} = 1, & c_2 &= \frac{-v_{\text{IR}}v_{\text{UV}}}{v_{\text{UV}}(2 + v_{\text{IR}}) + v_{\text{IR}}\epsilon(2 - v_{\text{UV}}\epsilon)}, \\ c_3 &= \frac{v_{\text{IR}}\epsilon(v_{\text{UV}}\epsilon - 2)}{v_{\text{UV}}(2 + v_{\text{IR}}) + v_{\text{IR}}\epsilon(2 - v_{\text{UV}}\epsilon)}, & c_4 &= \frac{(2 + v_{\text{IR}})\epsilon(2 - v_{\text{UV}}\epsilon)}{v_{\text{UV}}(2 + v_{\text{IR}}) + v_{\text{IR}}\epsilon(2 - v_{\text{UV}}\epsilon)}. \end{aligned} \quad (2.83)$$

The correct way to read these different contributions is to imagine a four quark diagram with one vertex labeled by t and the other by t' , as shown in Figure 2.10. Integration over t and t' will cause flavor violation at the corresponding vertex. If a coefficient multiplies neither t nor t' , the corresponding term describes two flavor diagonal vertices, which is the case for c_4 .¹⁰ Coefficients which multiply either t or t' can refer to diagrams with a flavor change at either one vertex, as in the case for c_3 . Finally, the coefficient of terms with both t and t' can induce flavor change at both vertices. This is the case for c_1 and c_2 in (2.82).

It makes not much sense to keep terms that are ϵ suppressed and neglect $\mathcal{O}(q^2)$ terms in the expressions above, since $\epsilon \sim 10^{-16}$. However, a vev on the UV brane is naturally order Planck scale and therefore factors $\sim v_{\text{UV}}\epsilon$ may become relevant and the ϵ

¹⁰It is a $\mathbb{1}$ in flavor space and the integral over the profiles of the external fermions vanishes, due to the orthonormality relation (2.125), derived in the next section.

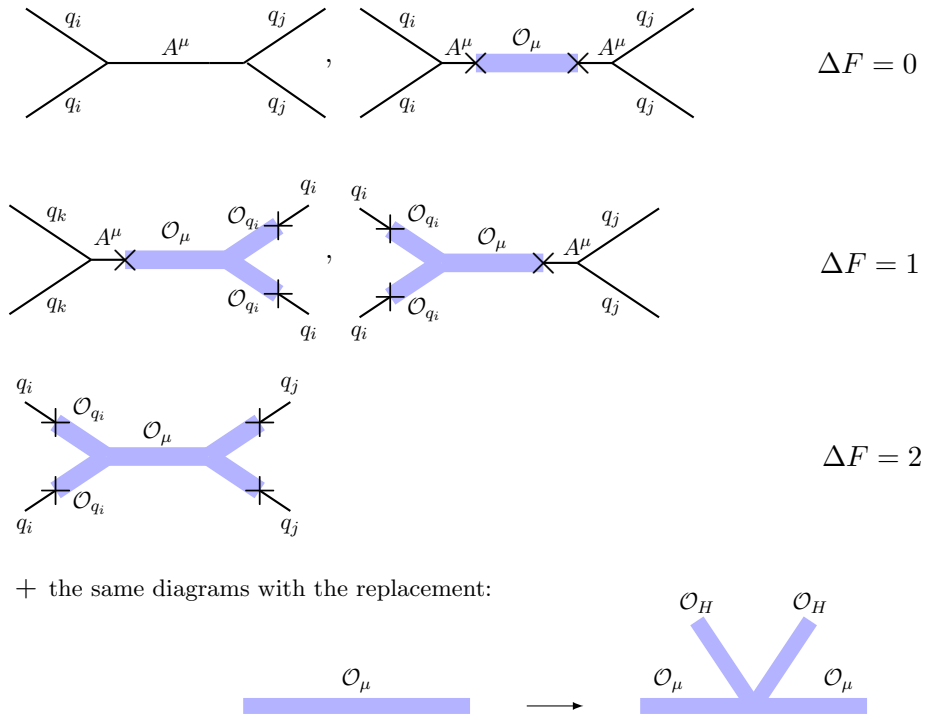


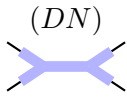
Figure 2.7: Collection of the contributions to the full four fermion operator in the strongly coupled dual theory with at most one \mathcal{O}_μ propagator, constructed from the building blocks given in Figures 2.5 and 2.4. Thick lines represent composites and thin lines elementary fields.

dependence has been kept at this point. It is also puzzling on first sight, why the coefficient c_1 would be exactly one, regardless of the BCs, which seems not motivated at all from the 5D theory. This will however become clearer by considering the strongly coupled dual theory. Before we discuss specific limits, let us therefore collect the different contributions we would expect in the dual theory. In terms of diagrams, they are given in Figure 2.7.

In principle, fermion lines are not directly relevant for the following discussion (we only compute the boson propagator), but they are included to illustrate the different contributions. If there is an elementary gauge boson, that is the propagator has Neumann BCs in the UV, there exist contributions which can only be flavor diagonal, shown in the first line of Figure 2.7. They consist of a pure gauge boson contribution and a contribution from mixing in the composite state. Following the discussion of section 2.2, composite states are always in the theory. Boundary conditions will only tell us whether there is a gauge boson to mix into or not, and if the composites get mass corrections from a composite Higgs coupling (depicted in the last line of Figure 2.7). Also, in our model, fermions are bulk fields and therefore the elementary quarks mix into corresponding composite states. This allows for flavor violation at either one vertex, see the second line of Figure 2.7, or $\Delta F = 2$ contributions from

pure composite exchange, which can be found in the third line of Figure 2.7. Keep in mind, that these diagrams are flavor-diagonal in Figure 2.7, but not flavor universal, which will lead to the described flavor violation after rotation into the basis in which the Yukawa matrices are diagonal. Also, the diagrams in the second and third line of Figure 2.7 can give flavor conserving and $\Delta F = 1$ contributions as well, the right hand side only denotes the maximal number of vertices at which flavor violation can occur simultaneously. Further diagrams can be constructed through additional mixing from composites into the elementary states and back. However, each additional \mathcal{O}_μ propagator carries another factor M_{KK}^{-2} and will the corresponding terms will thus be suppressed.

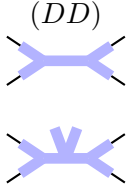
An interesting result of this thesis is, that we are able to assign diagrams in the dual theory to the different contributions of (2.82), by systematically considering different BCs. In the following, the respective BCs and the contributing diagrams are shown on the left hand side. Also, after performing the limits for the respective BCs, ϵ -suppressed factors will be omitted and the results are given in Feynman-'t Hooft gauge, $\xi = 1$. Let us start with the ‘‘cleanest’’ scenario.



Dirichlet BCs in the UV imply, that there is no elementary gauge boson in the theory. Consequentially, there is no mixing as in (2.41). If there were no composite fermions, the elementary and composite sector would not talk to each other at all. There is also no symmetry breaking in the composite sector, because all fields (for all possible gauge indices) have Neumann BCs in the IR. Referring to Figure (2.7), that means, that we do only expect the exchange of composite states, *i.e.* only the diagram in the third line. Interestingly, for these BCs, (2.82) reduces to

$$D_{\mu\nu}^{\xi=1}(q, t; t') = \frac{\eta_{\mu\nu} L}{4\pi r_c M_{\text{KK}}^2} t_{<}^2, \quad (2.84)$$

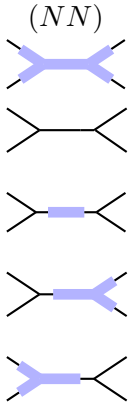
which represents the term which we found to appear in (2.82) with always the same coefficient regardless of the BCs. In the dual theory, this corresponds to the exchange of exclusively composites, which is only controlled by the bulk. That means, one can check that a different localization, $\Delta \neq 3$, will in general change this factor. This term will however always be present as long as $\Delta = 3$ and a change of BCs will only generate additional diagrams.



When a Higgs vev is turned on on the IR brane, the higgsing generates mass correction to the bosonic composites. We expect therefore the same contributions as in the (DN) scenario, however additional $\Delta F = 2$ contributions should appear. The situation in the UV is unchanged (still Dirichlet BCs) and since there is no mixing, no extra flavor diagonal or $\Delta F = 1$ terms should appear. Accordingly, we find,

$$D_{\mu\nu}^{\xi=1}(q, t; t') = \frac{\eta_{\mu\nu} L}{4\pi r_c M_{\text{KK}}^2} (t_{<}^2 - t^2 t'^2), \quad (2.85)$$

which perfectly agrees with the expectations.

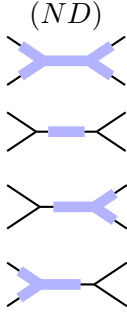


If one allows for Neumann BCs on both branes, the situation changes significantly. There is still the exclusively composite exchange like in the (DN) scenario, however as Neumann BCs in the UV correspond to gauge fields in the elementary sector the mixing term in (2.41) becomes active and allows for all the additional diagrams shown on the left hand side. We cannot reproduce a one-to-one correspondence for each diagram here, because there exist many diagrams contributing to the same terms. However, one can infer that in contrast to the (DD) scenario no additional $\Delta F = 2$ contributions should appear. Also, the existence of a pure gauge boson diagram will lead to a flavor diagonal term independent of the KK scale. There should be additional flavor-diagonal contributions as well, from the diagram with mixing into the composite boson and back. We find

$$D_{\mu\nu}^{\xi=1}(q, t; t') = -\frac{\eta_{\mu\nu}}{2\pi r_c p^2} \quad (2.86)$$

$$+ \frac{\eta_{\mu\nu}}{4\pi r_c M_{\text{KK}}^2} \left(Lt_{<}^2 - t^2 \left[\frac{1}{2} - \ln t \right] - t'^2 \left[\frac{1}{2} - \ln t' \right] + \frac{1}{2L} \right),$$

which agrees with these expectations. Note, that the (NN) scenario cannot be extracted from (2.82) by inserting the BCs directly, because the equation has a singularity for $v_{\text{UV}} = v_{\text{IR}} = 0$. Equation (2.86) is therefore the result of a limiting procedure.



and all possible Higgs insertions

This is the “messiest” scenario, in the sense that all possible diagrams in Figure 2.7 contribute to the propagator, besides the pure gauge boson propagator, because it will be massive due to mixing with a composite which breaks the gauge symmetry. In the language of Section 2.2, the group I is empty here. The corresponding propagator should have flavor-diagonal, $\Delta F = 1$ and additional $\Delta F = 2$ contributions and we find

$$D_{\mu\nu}^{\xi=1}(q, t; t') = \frac{\eta_{\mu\nu} L}{4\pi r_c M_{\text{KK}}^2} (t_{<}^2 - t^2 - t'^2 + 1). \quad (2.87)$$

This is not exactly what one would expect. The Higgs corrections to the $\Delta F = 2$ contributions we found for (*DD*) BCs are absent. This can not be explained by a direct cancellation between diagrams, because all other diagrams will not lead to $\Delta F = 2$ effects. Also, the flavor-diagonal factor is much larger compared to (*NN*) BCs, which can only be explained by the Higgs insertions there having a large effect.

We will close this section with the introduction of the KK decomposition for the different scenarios just introduced and a discussion of the behavior of the profile functions for the lightest modes.

The generic bulk Lagrangian (2.53) suggests a KK decomposition in t -notation

$$\begin{pmatrix} A_\mu(x_\mu, t) \\ A_5(x_\mu, t) \end{pmatrix} = \frac{1}{\sqrt{r_c}} \sum_n \begin{pmatrix} A_\mu^n(x_\mu) \chi_n(t) \\ M_{\text{KK}} A_5^n(x_\mu) \partial_t \chi_n(t) \end{pmatrix}. \quad (2.88)$$

If this decomposition is inserted into equation (2.53), one finds the important relation (valid in Feynman gauge)

$$iD_{\mu\nu}(q, t; t') = \sum_{n=0}^{\infty} \frac{-i\eta_{\mu\nu}}{q^2 - x_n^2 + i\epsilon} \chi_n(t) \chi_n(t'), \quad (2.89)$$

in which $x_n \equiv m_n/M_{\text{KK}}$ and m_n denotes the mass of the n th KK mode. This shows how the 5D propagator is equivalent to the exchange of the whole KK tower and represents another connection to the strongly coupled dual theory, compare (2.42). It also follows that the normalization of the kinetic terms imposes the orthonormality relation

$$\frac{2\pi}{L} \int_\epsilon^1 \frac{dt}{t} \chi_m(t) \chi_n(t) = \delta_{mn}. \quad (2.90)$$

Further, all terms including derivatives with respect to ϕ and the bulk mass have to be matched to a 4D mass term for each mode. The resulting equations are called EOM, and read for the vector component

$$\left(-t\partial_t \frac{1}{t} \partial_t + \frac{c_A^2}{t^2} \right) \chi_n(t) = x_n^2 \chi_n(t). \quad (2.91)$$

We can concentrate on the vector component, as the EOM for the scalar can again be derived by the replacement $c_A^2 \rightarrow c_a^2/\xi - 1$ and $x_n^2 \rightarrow \xi x_n^2$. A solution to (2.91) can be guessed by comparison with (2.64), which has the same form,

$$\chi_n(t) = t \left(J_{\Delta-2}(tx_n) + \alpha_n Y_{\Delta-2}(tx_n) \right), \quad (2.92)$$

where again $\Delta = 2 + \sqrt{1 + c_A^2}$. The coefficient α_n is fixed by the UV BC and the IR BC gives the mass eigenvalues. In general, they read

$$\partial_t \chi_n(t) \Big|_{t=\epsilon^+} = v_{\text{UV}} \chi_n(\epsilon^+), \quad \partial_t \chi_n(t) \Big|_{t=1^-} = -v_{\text{IR}} \chi_n(1^-). \quad (2.93)$$

One can infer, that the mass eigenvalues have a splitting dictated by the zeros of Bessel functions, which means the mass splitting approaches $\delta m_n = \pi M_{\text{KK}}$ for large n .

The mass of the first excitation is controlled by both BCs as shown in Figure 2.8. The plots show the mass of the lightest mode depending on one BC, while the other one is kept fixed. In all cases, x_1 , which denotes the mass of the lightest KK mode in units of M_{KK} approaches a limit and the units on the x-axis are chosen in a way that this limit is shown in the respective plot. In the upper left panel the UV BC is Neumann and the IR BC varies, showing the transition from the (NN) to the (ND) scenario. From the dual picture, we expect the lightest mode to correspond to a massless gauge boson if $v_{\text{IR}} = 0$, and to become massive due to spontaneous symmetry breaking once a vev is turned on on the IR brane. Its mass will therefore not grow arbitrarily, but will always be a fraction of the symmetry breaking scale, which does agree with the plot. The limit is at $m_n \sim 0.235 M_{\text{KK}}$ and is more or less satisfied at $v_{\text{IR}} \sim 10$.

For the reverse situation, Dirichlet BCs in the UV and Neumann BCs in the IR, the dual theory predicts no elementary gauge boson and no Higgs contribution to the masses of the KK modes. This scenario should yield a straight line in the $v_{\text{UV}} - x_1$ plane at the mass of the first composite, unless v_{UV} becomes so small, that Dirichlet BCs are not a good approximation. This happens only for extremely small values of $v_{\text{UV}} = \mathcal{O}(10\epsilon)$, as shown in the upper right panel of Figure 2.8. In this plot, the values of v_{UV} are unnaturally small in order to show the region in which the mass approaches zero. That corresponds to a situation, in which the breaking on the UV brane is so small, that the dual theory has an approximate massless gauge boson. For all other values, the limit is reached. From (2.93), it is evident that this limit is given by the first zero of $J_0(x_n)$, $x_1 \approx 2.4$. Therefore the plot shows the rapid transition from the (NN) to the (DN) scenario.

The last panel (in the second row) shows the plot for the situation where v_{UV} is of $\mathcal{O}(1)$ and v_{IR} is free to vary. It illustrates the transition from (DN) to (DD) BCs. The lowest mass in this plot is consequentially the limit from the upper right plot. Turning on the Higgs vev in the IR seems to have a considerable effect on the first KK mass, the limiting value is shifted to the first zero of $J_1(x_n)$ at $x_1 \approx 3.8$. This can again easily be extracted from the equations (2.93). In the dual theory one can argue that stronger couplings between the composites may allow for larger corrections to the masses compared to the (ND) scenario, in which the contributions

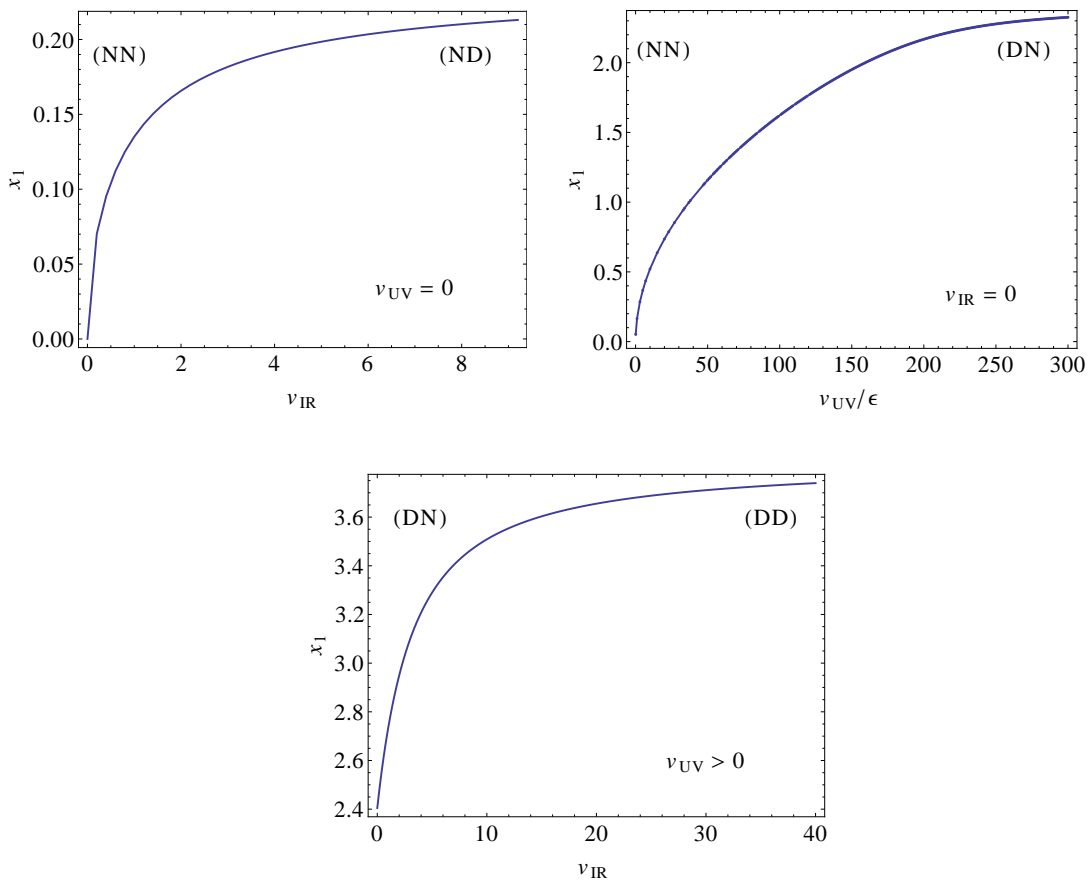


Figure 2.8: Mass of the lightest excitation for different BCs. See text for details.

from symmetry breaking are given by a marginal mixing operator. Note, that we also found a substantial effect from the Higgs in the discussion of the (DD) propagator limit, in contrast to the (ND) scenario, which is in line with our findings here. It should be stressed, that the behavior can change significantly once one allows for a non-zero bulk mass parameter.

The Electroweak Gauge Sector of the SM

The electroweak gauge sector of the SM is completely shifted into the bulk in the minimal RS model. Following the above analysis, one would expect gauge boson masses of the order of the electroweak scale, as given in the upper left panel of Figure 2.8, if we start with (NN) BCs and couple to a IR localized Higgs. It will turn out, that this proves true and the zero mode masses agree with the SM up to small

modifications.

The 5D Lagrangian is given by the terms in (2.12) minus the $SU(3)_C$ terms and (2.13). Analogue to the SM, we define

$$\begin{aligned} W_M^\pm &= \frac{1}{\sqrt{2}} (W_M^1 \mp iW_M^2), \\ Z_M &= \frac{1}{\sqrt{g_5^2 + g_5'^2}} (g_5 W_M^3 - g_5' B_M), \\ A_M &= \frac{1}{\sqrt{g_5^2 + g_5'^2}} (g_5' W_M^3 + g_5 B_M), \end{aligned} \quad (2.94)$$

and

$$M_W = \frac{vg_5}{2}, \quad M_Z = \frac{v\sqrt{g_5^2 + g_5'^2}}{2}, \quad (2.95)$$

where g_5 and g_5' are the 5D gauge couplings of $SU(2)_L$ and $U(1)_Y$, respectively. The covariant derivative acting on the Higgs reads

$$D_\mu H = \frac{1}{\sqrt{2}} \begin{pmatrix} -i\sqrt{2} (\partial_\mu \varphi^+ + M_W W_\mu^+) \\ \partial_\mu h + i (\partial_\mu \varphi_3 + M_Z Z_\mu) \end{pmatrix} + \text{terms bi-linear in fields}, \quad (2.96)$$

and the brane Higgs involves in accordance with (2.76) the following gauge fixing terms,

$$\begin{aligned} \mathcal{L}_{\text{GF}} &= -\frac{1}{2\xi} \left(\partial^\mu A_\mu - \xi \left[M_{\text{KK}} t \partial_t \frac{1}{t} A_5 \right] \right)^2 \\ &\quad - \frac{1}{2\xi} \left(\partial^\mu Z_\mu - \frac{\xi}{2} \left[\delta(t-1) k M_Z \varphi_3 + 2M_{\text{KK}} t \partial_t \frac{1}{t} Z_5 \right] \right)^2 \\ &\quad - \frac{1}{\xi} \left(\partial^\mu W_\mu^+ - \frac{\xi}{2} \left[\delta(t-1) k M_W \varphi^+ + 2M_{\text{KK}} t \partial_t \frac{1}{t} W_5^+ \right] \right) \\ &\quad \times \left(\partial^\mu W_\mu^- - \frac{\xi}{2} \left[\delta(t-1) k M_W \varphi^- + 2M_{\text{KK}} t \partial_t \frac{1}{t} W_5^- \right] \right), \end{aligned} \quad (2.97)$$

in which (2.55) has been applied in changing to t -coordinates for all scalar components. More generally, the gauge fixing parameters could have been chosen different for each gauge fixing term, but for convenience they are set equal. We will in the following concentrate on terms quadratic in the fields. It is however straightforward to implement three and four gauge boson terms. Accounting for the kinetic terms of the gauge bosons and the Higgs, as well as for the gauge fixing terms, results in the

action

$$\begin{aligned}
 S \ni & \int d^4x r \frac{2\pi}{L} \int_{\epsilon}^1 \frac{dt}{t} \tag{2.98} \\
 & \left\{ -\frac{1}{4} F_{\mu\nu} F^{\mu\nu} - \frac{1}{2\xi} (\partial^\mu A_\mu)^2 + \frac{1}{2} (\partial_\mu A_5 \partial^\mu A_5 + M_{\text{KK}}^2 \partial_t A_\mu \partial_t A^\mu) \right. \\
 & - \frac{1}{4} Z_{\mu\nu} Z^{\mu\nu} - \frac{1}{2\xi} (\partial^\mu Z_\mu)^2 + \frac{1}{2} (\partial_\mu Z_5 \partial^\mu Z_5 + M_{\text{KK}}^2 \partial_t Z_\mu \partial_t Z^\mu) \\
 & - \frac{1}{2} W_{\mu\nu}^+ W^{-\mu\nu} - \frac{1}{\xi} \partial^\mu W_\mu^+ \partial^\nu W_\nu^- + (\partial_\mu W_5^+ \partial^\mu W_5^- + M_{\text{KK}}^2 \partial_t W_\mu^+ \partial_t W^{-\mu}) \\
 & + \frac{k}{2} \delta(t-1) \left(\frac{1}{2} \partial_\mu h \partial^\mu h - \lambda v^2 h^2 + \partial_\mu \varphi^+ \partial^\mu \varphi^- + \frac{1}{2} \partial_\mu \varphi_3 \partial^\mu \varphi_3 \right. \\
 & \qquad \qquad \qquad \left. + \frac{M_Z^2}{2} Z_\mu Z^\mu + M_W^2 W_\mu^+ W^{-\mu} \right) \\
 & - \frac{\xi}{2} \left(M_{\text{KK}} t \partial_t \frac{1}{t} A_5 \right)^2 - \frac{\xi}{8} \left(\delta(t-1) k M_Z \varphi_3 + 2 M_{\text{KK}} t \partial_t \frac{1}{t} Z_5 \right)^2 \\
 & \left. - \frac{\xi}{4} \left(\delta(t-1) k M_W \varphi^+ + M_{\text{KK}} t \partial_t \frac{1}{t} W_5^+ \right) \left(\delta(t-1) k M_W \varphi^- + M_{\text{KK}} t \partial_t \frac{1}{t} W_5^- \right) \right\}.
 \end{aligned}$$

In the next step, analogue to (2.88), we decompose the fields in KK modes,

$$\begin{aligned}
 A_\mu(x, t) &= \frac{1}{\sqrt{r_c}} \sum_n A_\mu^{(n)}(x) \chi_n^A(t), & A_5(x, t) &= \frac{M_{\text{KK}}}{\sqrt{r_c}} \sum_n a_n^A \varphi_A^{(n)}(x) \partial_t \chi_n^A(t), \\
 Z_\mu(x, t) &= \frac{1}{\sqrt{r_c}} \sum_n Z_\mu^{(n)}(x) \chi_n^Z(t), & Z_5(x, t) &= \frac{M_{\text{KK}}}{\sqrt{r_c}} \sum_n a_n^Z \varphi_Z^{(n)}(x) \partial_t \chi_n^Z(t), \\
 W_\mu^\pm(x, t) &= \frac{1}{\sqrt{r_c}} \sum_n W_\mu^{\pm(n)}(x) \chi_n^W(t), & W_5^\pm(x, t) &= \frac{M_{\text{KK}}}{\sqrt{r_c}} \sum_n a_n^W \varphi_W^{\pm(n)}(x) \partial_t \chi_n^W(t),
 \end{aligned} \tag{2.99}$$

and expand the would-be Goldstone bosons in (2.96) in the same basis of mass eigenstates as the scalars,

$$\varphi^\pm(x) = \sum_n b_n^W \varphi_W^{\pm(n)}(x), \quad \varphi_3(x) = \sum_n b_n^Z \varphi_Z^{(n)}(x). \tag{2.100}$$

We obtain the EOM (2.91) with the replacement

$$c_A^2 \rightarrow \frac{1}{2} \delta(t-1^-) k \frac{M_a^2}{M_{\text{KK}}^2} = \delta(t-1^-) L \frac{v_4^2 g_4^2}{4M_{\text{KK}}^2}, \tag{2.101}$$

where the last equality holds for $M_a = M_W$ and also for $M_a = M_Z$, if g_4^2 is replaced by $(g_4^{\prime 2} + g_4^2)$. In the following, we denote both fields by M_a , with the corresponding replacements for the couplings implied. Consequentially, the orthonormality relation

(2.90) holds and the BCs become

$$\begin{aligned} \partial_t \chi_n^a(\epsilon^+) &= 0, \\ \partial_t \chi_n^a(1^-) &= -\frac{L}{2\pi r_c} \frac{M_a^2}{M_{\text{KK}}^2} \chi_n^a(1^-) = -L \frac{v_4^2 g_4^2}{4M_{\text{KK}}^2} \chi_n^a(1^-) = -L \frac{m_a^2}{M_{\text{KK}}^2} \chi_n^a(1^-), \end{aligned} \quad (2.102)$$

where the masses of the zero modes m_a , with $a = W, Z$ have been introduced. By comparison with (2.93), the propagator can be found from (2.82), and reads

$$r_c D_{\mu\nu}^\xi(q, t; t') = \eta_{\mu\nu} \left(\frac{1}{2\pi m_{W,Z}^2} + \frac{L}{4\pi M_{\text{KK}}^2} [t_{<}^2 - t^2 - t'^2 + 1] \right) + \mathcal{O}(q^2), \quad (2.103)$$

and the propagator for the photon is given by (2.86).

The 4D effective theory is constructed by inserting the KK decomposition (2.99) into (2.98), applying the EOM and the orthonormality relation, so that after integrating out the fifth dimension one ends up with

$$\begin{aligned} S_{\text{Gauge},2} &= \sum_n \int d^4x \left\{ -\frac{1}{4} F_{\mu\nu}^{(n)} F^{\mu\nu(n)} - \frac{1}{2\xi} \left(\partial^\mu A_\mu^{(n)} \right)^2 + \frac{(m_n^A)^2}{2} A_\mu^{(n)} A^{\mu(n)} \right. \\ &\quad - \frac{1}{4} Z_{\mu\nu}^{(n)} Z^{\mu\nu(n)} - \frac{1}{2\xi} \left(\partial^\mu Z_\mu^{(n)} \right)^2 + \frac{(m_n^Z)^2}{2} Z_\mu^{(n)} Z^{\mu(n)} \\ &\quad - \frac{1}{2} W_{\mu\nu}^{+(n)} W^{-\mu\nu(n)} - \frac{1}{\xi} \partial^\mu W_\mu^{+(n)} \partial^\nu W_\nu^{-(n)} + (m_n^W)^2 W_\mu^{+(n)} W^{-\mu(n)} \\ &\quad + \frac{1}{2} \partial_\mu \varphi_A^{(n)} \partial^\mu \varphi_A^{(n)} - \frac{\xi(m_n^A)^2}{2} \varphi_A^{(n)} \varphi_A^{(n)} + \frac{1}{2} \partial_\mu \varphi_Z^{(n)} \partial^\mu \varphi_Z^{(n)} - \frac{\xi(m_n^Z)^2}{2} \varphi_Z^{(n)} \varphi_Z^{(n)} \\ &\quad \left. + \partial_\mu \varphi_W^{+(n)} \partial^\mu \varphi_W^{-(n)} - \xi(m_n^W)^2 \varphi_W^{+(n)} \varphi_W^{-(n)} \right\} + \int d^4x \left(\frac{1}{2} \partial_\mu h \partial^\mu h - \lambda v^2 h^2 \right), \end{aligned} \quad (2.104)$$

under the additional condition, that the Fourier coefficients in (2.99) and (2.100) are

$$a_n^a = -\frac{1}{m_n^a}, \quad b_n^a = \frac{M_a}{\sqrt{r}} \frac{\chi_n^a(1^-)}{m_n^a}. \quad (2.105)$$

Solving the EOM with the BCs (2.102) leads to

$$\chi_n^a(t) = N_n \sqrt{\frac{L}{\pi}} t c_n^+(t), \quad (2.106)$$

where only the UV BC is used in determining the unspecified coefficient in the homogeneous solution, so that

$$c_n^+(t) = Y_0(x_n^a \epsilon) J_1(x_n^a t) - J_0(x_n^a \epsilon) Y_1(x_n^a t), \quad (2.107)$$

$$c_n^-(t) = \frac{1}{x_n^a t} \frac{d}{dt} [t c_n^+(t)] = Y_0(x_n^a \epsilon) J_0(x_n^a t) - J_0(x_n^a \epsilon) Y_0(x_n^a t). \quad (2.108)$$

Note, that this result agrees with (2.92) for a brane Higgs up to an additional factor. The normalization is fixed by (2.90), and reads

$$N_n^{-2} = [c_n^+(1)]^2 + [c_n^-(1)]^2 - \frac{2}{x_n} c_n^+(1) c_n^-(1) - \epsilon^2 [c_n^+(\epsilon)]^2, \quad (2.109)$$

and the mass eigenvalues are the zeros of the IR BC,

$$x_n^a c_n^-(1^-) = -\frac{g_4^2 v_4^2}{4M_{\text{KK}}^2} L c_n^+(1^-). \quad (2.110)$$

One can now expand this equation in the zero mode mass $x_0 \ll 1$ and solve for the mass of the SM gauge bosons

$$(m_W^{\text{RS}})^2 \equiv \frac{g_4^2 v_4^2}{4} \left[1 - \frac{g_4^2 v_4^2}{8M_{\text{KK}}^2} \left(L - 1 + \frac{1}{2L} \right) + \mathcal{O} \left(\frac{v^4}{M_{\text{KK}}^4} \right) \right], \quad (2.111)$$

and for the mass of the Z one finds the same expression after replacing the gauge couplings accordingly. Equation (2.111) represents a correction to the SM relation $m_W^{\text{SM}} = g_4 v_4 / 2$. Direct experimental measurements will measure the left hand side of (2.111), and one can therefore absorb the universal RS corrections into $m_{W,Z}$. On a more fundamental level, this corresponds to the rescaling of the Higgs vacuum expectation value, as discussed [116]. This rescaling should consequentially also take place in the propagator, so that (2.103) becomes to leading order in v^2/M_{KK}^2 and q^2

$$r_c D_{\mu\nu}^\xi(q, t; t') = \eta_{\mu\nu} \left(\frac{1}{2\pi(m_{W,Z}^{\text{RS}})^2} + \frac{1}{4\pi M_{\text{KK}}^2} \left[Lt_{<}^2 - L(t^2 + t'^2) + 1 - \frac{1}{2L} \right] \right). \quad (2.112)$$

In [115, Sec. 2.3] this result was reproduced using an alternative method, in which the sums over the profile functions are directly evaluated by performing the sum on the right-hand side of equation (2.89), generalizing a technique introduced in [117]. Finally, we note that the ZMA expressions for the zero modes read

$$\chi_{W,Z} = \frac{1}{\sqrt{2\pi}} \left[1 + \frac{m_{W,Z}^2}{4M_{\text{KK}}^2} \left(1 - \frac{1}{L} + t^2 (1 - 2L - 2 \ln t) \right) + \mathcal{O} \left(\frac{m_{W,Z}^4}{M_{\text{KK}}^4} \right) \right]. \quad (2.113)$$

The generalization to the full SM gauge group is rather straightforward, because the quadratic terms of the effective $SU(3)_C$ Lagrangian will be an exact copy the photon part of (2.104) upon replacing the gauge coupling. Because of the BCs, the gluon propagator is given by (2.86) as well. in

2.4 Profiles of Fermions

In contrast to the gauge bosons, we will only need the zero modes of the bulk fermions in the later computations. While a comprehensive discussion of the fermion propagator

can be found elsewhere [118, Sec. 4.2], we will concentrate on the KK decomposed theory here.

As mentioned in Section 2.1, a bulk fermion is described by an irreducible Dirac spinor field, which reduces to its two Weyl components in four dimensions, due to the orbifold symmetry or equivalently, due to opposite BCs. This can be seen by considering the kinetic term (2.15), which after partial integration and in terms of the chiral components, $Q = Q_L + Q_R$ can be written as

$$\begin{aligned} \sqrt{|G|} \mathcal{L}_{\text{matter}} \ni e^{-3\sigma} \bar{Q} i \not{\partial} Q - e^{-4\sigma} m \text{sgn}(\phi) \bar{Q} Q \\ - \frac{e^{-2\sigma}}{r_c} \left[\bar{Q}_L \partial_\phi (e^{-2\sigma} Q_R) - \bar{Q}_R \partial_\phi (e^{-2\sigma} Q_L) \right]. \end{aligned} \quad (2.114)$$

In contrast to the vector boson, an explicit mass term does not break gauge invariance and we are going to keep it throughout the discussion. It is convenient to switch to t -notation, in which a viable KK decomposition reads

$$Q_L(x_\mu, t) = \frac{1}{\sqrt{r}} \frac{t^2}{\epsilon^2} \sum_n Q_L^n(x_\mu) f_L^n(t), \quad (2.115)$$

$$Q_R(x_\mu, t) = \frac{1}{\sqrt{r}} \frac{t^2}{\epsilon^2} \sum_n Q_R^n(x_\mu) f_R^n(t). \quad (2.116)$$

Therefore, the orthonormality relation from the 4D part of the kinetic term reads

$$\frac{2\pi}{L\epsilon} \int_\epsilon^1 dt f_{L/R}^n(t) \left(f_{L/R}^m(t) \right)^* = \delta^{nm}, \quad (2.117)$$

which implies for the matching conditions or EOM the system of coupled first order PDEs

$$\begin{aligned} \left(\partial_t + \frac{c}{t} \right) f_R^n(t) &= x_n f_L^n(t), \\ \left(-\partial_t + \frac{c}{t} \right) f_L^n(t) &= x_n f_R^n(t). \end{aligned} \quad (2.118)$$

Here, x_n again denotes the dimensionless ratio of the mass of the n th KK mode m_n and the KK scale M_{KK} , and $c = m/k$ the dimensionless bulk mass parameter. This leads to the second order differential equation

$$\left(-t^2 \partial_t^2 + c(c \mp 1) \right) f_{L/R}^n(t) = t^2 x_n^2 f_{L/R}^n(t). \quad (2.119)$$

It is interesting to note, that in contrast to (2.91), in the limit $c \rightarrow 0$, the left hand side reduces to a simple second derivative and one ends up with trigonometric solutions. In other words, a free fermion will not feel the AdS -curvature, if it is massless.

A solution to (2.119) reads

$$f_{L/R}^n(t) = \sqrt{t} \left(J_{c \mp \frac{1}{2}}(x_n t) + \alpha_n Y_{c \mp \frac{1}{2}}(x_n t) \right). \quad (2.120)$$

In deriving this solution, it was already used, that the integration constant α_n is the same for f_L and f_R , which follows from (2.118). The value of α_n is fixed by the BCs,

which simultaneously give the mass eigenvalues of the KK modes x_n . It follows also from (2.118), that the BCs of f_L and f_R must be opposite, so that it is enough to give one of them and in the following, the notion “BCs of Q ” will always be understood to be the BCs of its f_L component. The following choices of BCs are possible,

$$\begin{array}{cc} \hline f_L & f_R \\ \hline (NN) & (DD) \\ (DD) & (NN) \\ (ND) & (DN) \\ (DN) & (ND) \end{array}$$

But only the first two lines will give rise to a zero mode for either the f_L or f_R component. The zero modes are massless, but introducing Yukawa couplings with a brane localized Higgs will result in zero mode masses which depend on the overlap of the corresponding Bessel function with the IR brane, and thus on the bulk mass parameter c . In this context of model building, the third and last line give still interesting solutions, because the (DN) component mimics a (NN) solution with a Higgs localized on the UV brane, which implies that a IR localization $c > -1/2$ results in a very light first KK mode. These *ultralight* KK fermions have first been recognized in [119, App A.2] and can arise in theories in which the SM top is in an extended multiplet with additional fermions, which do not have a zero mode due to (DN) BCs. Candidates are GUTs as in the original reference or higgsless models as examined in [120].

An interpretation of the different BCs in the dual theory can be given in accordance with the interpretation of a bulk gauge boson. If the BC in the UV is Neumann, there exists an elementary fermion which mixes with a composite state of the same quantum number. Only for (NN) BCs will this elementary state remain massless, Dirichlet BC in the IR result in a mass depending on the scale of the IR brane and the localization along the bulk. In the case of (DN) or (DD) BCs the dual theory has no elementary fermion and the Dirichlet BC in the IR make only for a correction of the masses of the composite meson tower.

In order to model SM fermions, we will rely on the first two solutions, so that the masses and the integration constant is fixed by

$$\alpha_n = \frac{J_{c \mp \frac{1}{2}}(x_n \epsilon)}{Y_{c \mp \frac{1}{2}}(x_n \epsilon)}, \quad (2.121)$$

in which the $-$ sign holds if f_L has a zero mode and and the $+$ for the case that f_R has a zero mode.

In order to model the SM field content with two chiral zero modes for each quark generation, we will have to introduce three copies of $Q = (u, d)$ transforming as a doublet under $SU(2)_L$ and a set of three down-type and three up-type $SU(2)_L$ singlets $q^c = u^c, d^c$, as already hinted at in Section 2.1. The Yukawa interactions couple these bulk fermions to the Higgs, which should result in a Yukawa coupling for the zero modes and therefore implies, that the zero mode of Q corresponds to an f_L solution, while the zero mode of q^c is the f_R solution of the bulk EOM. The ansatz (2.16) gives

then

$$\begin{aligned}
 S \ni & \int dx \int_{-\pi}^{\pi} d\phi \sqrt{|G|} \mathcal{L}_{\text{matter}} \\
 &= \sum_{q=u,d} \int dx \int_{-\pi}^{\pi} r_c d\phi \left\{ e^{-3\sigma} \left(\bar{Q} i \not{\partial} Q + \bar{q}^c i \not{\partial} q^c \right) - e^{-4\sigma} \text{sgn}(\phi) \left(\bar{Q} \mathbf{M}_Q Q + \bar{q}^c \mathbf{M}_q q^c \right) \right. \\
 & \quad - \frac{e^{-2\sigma}}{r_c} \left[\bar{Q}_L \partial_\phi (e^{-2\sigma} Q_R) - \bar{Q}_R \partial_\phi (e^{-2\sigma} Q_L) + \bar{q}_L^c \partial_\phi (e^{-2\sigma} q_R^c) - \bar{q}_R^c \partial_\phi (e^{-2\sigma} q_L^c) \right] \\
 & \quad \left. - \delta(|\phi| - \pi) \frac{e^{-4\sigma}}{r_c} \left[\epsilon_{ab} \bar{Q}_{La} H_b^\dagger \mathbf{Y}_u^{(5D)} u_R^c + \epsilon_{ab} \bar{Q}_{Ra} H_b^\dagger \bar{\mathbf{Y}}_u^{(5D)} u_L^c \right. \right. \\
 & \quad \left. \left. + \bar{Q}_L H \mathbf{Y}_d^{(5D)} d_R^c + \bar{Q}_R H \bar{\mathbf{Y}}_d^{(5D)} d_L^c + \text{h.c.} \right] \right\}. \tag{2.122}
 \end{aligned}$$

Here, the bar on the Yukawas indicates that in principle $\mathbf{Y}_q^{(5D)}$ and $\bar{\mathbf{Y}}_q^{(5D)}$ can be chosen differently, which is suppressed in (2.4). This difference is only due to the fact, that the Higgs is a brane localized 4D field. We will in the following assume, that $\bar{\mathbf{Y}}_q^{(5D)} = \mathbf{Y}_q^{(5D)}$, which can be motivated by considering the model resulting as a limit of a theory with a bulk scalar, in which the couplings would be the same, because the bulk must respect 5D Lorentz invariance. Even without introducing this limit, this assumption should not affect the physics, because we expect the 5D Yukawas to be structureless order one coefficients anyway with no effect on the hierarchies in the flavor sector, so that even being more restrictive, for example choosing $\mathbf{Y}_u^{(5D)} = \mathbf{Y}_d^{(5D)}$ should not change the results.

Further, the real bulk mass matrices $\mathbf{M}_{Q,q}$ and the complex 5D Yukawa matrices will not be diagonal in the same basis. If not stated otherwise, we will from now on assume that we are in the *bulk mass basis*, in which the bulk mass matrices are diagonal. Due to the flavor degrees of freedom and the Higgs on the brane, The KK decomposition is more involved than in (2.115). It can be brought into the form

$$\begin{aligned}
 u_L(x_\mu, t) &= \frac{1}{\sqrt{r}} \frac{t^2}{\epsilon^2} \sum_n u_L^n(x_\mu) \mathbf{C}_n^Q(t) a_n^U, \\
 u_R(x_\mu, t) &= \frac{1}{\sqrt{r}} \frac{t^2}{\epsilon^2} \sum_n u_R^n(x_\mu) \mathbf{S}_n^Q(t) a_n^U, \\
 u_L^c(x_\mu, t) &= \frac{1}{\sqrt{r}} \frac{t^2}{\epsilon^2} \sum_n u_L^n(x_\mu) \mathbf{S}_n^u(t) a_n^u, \\
 u_R^c(x_\mu, t) &= \frac{1}{\sqrt{r}} \frac{t^2}{\epsilon^2} \sum_n u_R^n(x_\mu) \mathbf{C}_n^u(t) a_n^u, \tag{2.123}
 \end{aligned}$$

where the index n runs over all flavor and KK modes. So will for example $m_1 = m_u, m_2 = m_c, m_3 = m_t$ give the SM quark masses, and m_4, \dots, m_9 the masses of the first set of six KK modes, and likewise for downtype quarks. The 3×3 matrices $\mathbf{S}_n^{Q,q}(t)$ correspond to the solutions with (DD) BCs which do not acquire a zero mode, while $\mathbf{C}_n^{Q,q}(t)$ denote profiles with (NN) BCs that have a zero mode. The additional a -vectors $a_n^{(U,u)}$ quantify flavor mixing induced by the Yukawa couplings. Therefore,

while the profile functions must be the same for both components of the $SU(2)_L$ doublet, $\mathbf{S}_n^U = \mathbf{S}_n^D \equiv \mathbf{S}_n^Q$ and $\mathbf{C}_n^U = \mathbf{C}_n^D \equiv \mathbf{C}_n^Q$, the a -vectors are not, because the two components are treated differently in the Yukawa interactions. Also, the profile functions can be chosen diagonal and real in the bulk mass basis, whereas the a -vectors are complex. Proceeding just like in the case of a free bulk gauge boson, we will first derive the orthonormality relation by matching onto the kinetic term and then fix the mass eigenvalues using the BCs.

In contrast to the free bulk fermion, upon insertion of the KK decomposition, the matching of the first term in the second line of (2.122) onto the canonical kinetic term

$$S_{4D} = \sum_{q=u,d} \sum_n \int d^4x \bar{q}^n(x) i \not{\partial} q^n(x), \quad (2.124)$$

in which $q^n(x) \equiv q_L^n(x_\mu) + q_R^n(x_\mu)$ and $q_{L,R}^n(x_\mu)$ denoting the 4D fields in the KK decomposition, will result in the more general orthonormality relation

$$\frac{2\pi}{L\epsilon} \int_\epsilon^1 dt a_m^{(Q,q)\dagger} \mathbf{C}_m^{(Q,q)}(t) \mathbf{C}_n^{(Q,q)}(t) a_n^{(Q,q)} + a_m^{(q,Q)\dagger} \mathbf{S}_m^{(q,Q)}(t) \mathbf{S}_n^{(q,Q)}(t) a_n^{(q,Q)} = \delta_{mn}. \quad (2.125)$$

In the limit of vanishing Yukawa interactions, this expression separates into two sets of three independent equations for $q = u, d$. Since we know, that the C - and S -profiles must reduce to the solutions $f_{L,R}$ in this limit, which form complete sets of functions in the bulk and fulfill separate orthonormality conditions (2.117), we can deduce that

$$a_n^{Q\dagger} a_n^Q + a_n^{q\dagger} a_n^q = \mathbb{1}. \quad (2.126)$$

With the result (2.125), the matching of the second to last term of (2.122) onto a canonical 4D mass term gives rise to the EOM [115, 114]

$$\begin{aligned} (-t\partial_t - \mathbf{c}_Q) \mathbf{S}_n^Q(t) a_n^Q &= -x_n t \mathbf{C}_n^Q(t) a_n^Q + \delta(t-1) \frac{v}{\sqrt{2}M_{\text{KK}}} \mathbf{Y}_q \mathbf{C}_n^q(t) a_n^q, \\ (t\partial_t + \mathbf{c}_q) \mathbf{S}_n^q(t) a_n^q &= -x_n t \mathbf{C}_n^q(t) a_n^q + \delta(t-1) \frac{v}{\sqrt{2}M_{\text{KK}}} \mathbf{Y}_q^\dagger \mathbf{C}_n^Q(t) a_n^Q, \\ (t\partial_t - \mathbf{c}_Q) \mathbf{C}_n^Q(t) a_n^Q &= -x_n t \mathbf{S}_n^Q(t) a_n^Q + \delta(t-1) \frac{v}{\sqrt{2}M_{\text{KK}}} \mathbf{Y}_q \mathbf{S}_n^q(t) a_n^q, \\ (-t\partial_t + \mathbf{c}_q) \mathbf{C}_n^q(t) a_n^q &= -x_n t \mathbf{S}_n^q(t) a_n^q + \delta(t-1) \frac{v}{\sqrt{2}M_{\text{KK}}} \mathbf{Y}_q^\dagger \mathbf{S}_n^Q(t) a_n^Q, \end{aligned} \quad (2.127)$$

in which a sign has been introduced in defining $\mathbf{c}_{Q,q} \equiv \pm \mathbf{M}_{Q,q}/k$, which will prove to be convenient, as well as the dimensionless 4D Yukawa couplings have been defined by $\mathbf{Y}_q^{(5D)} \equiv 2\mathbf{Y}_q/k$. Apart from the IR brane, that is for $t \neq 1$, these equations decouple and can be reduced to two times three sets of (2.118), because the a -vectors must be proportional to unit vectors in this limit, with the corresponding solutions (2.120). One way to find a solution to (2.127) is therefore to assume these solutions in the bulk and treat the Yukawa couplings as perturbations. Alternatively, one can directly account for the Yukawa terms in the EOM, as shown above. Both approaches are

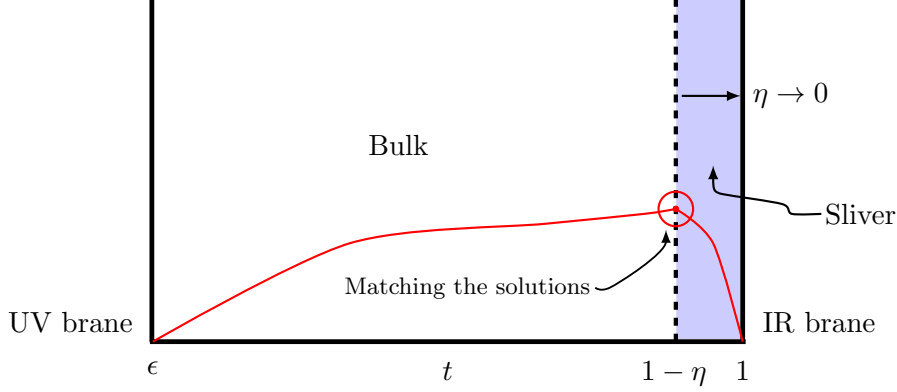


Figure 2.9: Illustration of the separation of a sliver from the bulk of the extra dimension in the context of the regularization of the delta function and the procedure of solving the coupled EOM. The red line in the bulk indicates an S -profile which solves the bulk EOM, the red line in the sliver depicts the corresponding solution of the sliver EOM, which is supposed to match the bulk solution at 1^- .

equivalent, see [122], although the latter is more straightforward and will therefore be adopted here.

As mentioned in the previous section, in a situation with a brane localized Higgs, it is crucial to properly regularize the delta functions and we will use the rectangular regularization introduced in (2.79). The importance of such a regularization procedure was first pointed out in [121, Sec. IV] and it was shown that the results are independent of the regularization method later in [114]. The following derivation is also outlined in the appendix of the latter reference. The regularized delta function effectively divides the bulk into two regions, $t \in [0, 1 - \eta]$ and a small sliver $t \in [1 - \eta, 1]$, see Figure 2.9. The solution in the sliver will generate the proper BCs for the bulk solutions at 1^- . In the sliver, only the following terms in the EOM are relevant,

$$-\partial_t \mathbf{S}_n^Q(t) a_n^Q = \delta^\eta(t-1) \frac{v}{\sqrt{2}M_{\text{KK}}} \mathbf{Y}_q \mathbf{C}_n^q(t) a_n^q, \quad (2.128)$$

$$\partial_t \mathbf{S}_n^q(t) a_n^q = \delta^\eta(t-1) \frac{v}{\sqrt{2}M_{\text{KK}}} \mathbf{Y}_q^\dagger \mathbf{C}_n^Q(t) a_n^Q, \quad (2.129)$$

$$\partial_t \mathbf{C}_n^Q(t) a_n^Q = \delta^\eta(t-1) \frac{v}{\sqrt{2}M_{\text{KK}}} \mathbf{Y}_q \mathbf{S}_n^q(t) a_n^q, \quad (2.130)$$

$$-\partial_t \mathbf{C}_n^q(t) a_n^q = \delta^\eta(t-1) \frac{v}{\sqrt{2}M_{\text{KK}}} \mathbf{Y}_q^\dagger \mathbf{S}_n^Q(t) a_n^Q. \quad (2.131)$$

Using (2.79), we obtain

$$\left[\partial_t^2 - \left(\frac{\mathbf{X}_q}{\eta} \right)^2 \right] \mathbf{S}_n^Q(t) = 0, \quad \left[\partial_t^2 - \left(\frac{\bar{\mathbf{X}}_q}{\eta} \right)^2 \right] \mathbf{S}_n^q(t) = 0, \quad (2.132)$$

in which

$$\mathbf{X}_q \equiv \frac{v}{\sqrt{2}M_{\text{KK}}} \sqrt{\mathbf{Y}_q \mathbf{Y}_q^\dagger}, \quad \bar{\mathbf{X}}_q \equiv \frac{v}{\sqrt{2}M_{\text{KK}}} \sqrt{\mathbf{Y}_q^\dagger \mathbf{Y}_q}. \quad (2.133)$$

The solutions to these PDEs are hyperbolic functions. Integration constants are fixed by the fact that at the IR brane $t = 1$, the S -profiles have Dirichlet BCS, $\mathbf{S}_n^{Q,q}(1) = 0$ and at $1 - \eta$, they must be matched onto the solution of the bulk EOM at $t = 1^-$. So that

$$\begin{aligned} \mathbf{S}_n^Q(t) &= \frac{\sinh\left(\frac{\mathbf{X}_q}{\eta}(1-t)\right)}{\sinh(\mathbf{X}_q)} \mathbf{S}_n^Q(1^-), & \mathbf{S}_n^q(t) &= \frac{\sinh\left(\frac{\bar{\mathbf{X}}_q}{\eta}(1-t)\right)}{\sinh(\bar{\mathbf{X}}_q)} \mathbf{S}_n^q(1^-). \\ \mathbf{C}_n^Q(t) &= \frac{\cosh\left(\frac{\mathbf{X}_q}{\eta}(1-t)\right)}{\cosh(\mathbf{X}_q)} \mathbf{C}_n^Q(1^-), & \mathbf{C}_n^q(t) &= \frac{\cosh\left(\frac{\bar{\mathbf{X}}_q}{\eta}(1-t)\right)}{\cosh(\bar{\mathbf{X}}_q)} \mathbf{C}_n^q(1^-), \end{aligned} \quad (2.134)$$

where the solutions for the C -profiles follow from (2.128). At the boundary between sliver and bulk, the bulk solutions are therefore related by

$$\mathbf{S}_n^Q(1^-) a_n^Q = \frac{v}{\sqrt{2}M_{\text{KK}}} \mathbf{Y}_q (\bar{\mathbf{X}}_q)^{-1} \tanh(\bar{\mathbf{X}}_q) \mathbf{C}_n^q(1^-) a_n^q, \quad (2.135)$$

$$-\mathbf{S}_n^q(1^-) a_n^q = \frac{v}{\sqrt{2}M_{\text{KK}}} \mathbf{Y}_q^\dagger (\mathbf{X}_q)^{-1} \tanh(\mathbf{X}_q) \mathbf{C}_n^Q(1^-) a_n^Q, \quad (2.136)$$

which can be re-expressed by introducing the effective Yukawa couplings

$$\tilde{\mathbf{Y}}_q \equiv \mathbf{f} \left(\frac{v}{\sqrt{2}M_{\text{KK}}} \sqrt{\mathbf{Y}_q \mathbf{Y}_q^\dagger} \right) \mathbf{Y}_q, \quad \mathbf{f}(\mathbf{A}) = \mathbf{A}^{-1} \tanh(\mathbf{A}). \quad (2.137)$$

These correspond to the bare Yukawas plus corrections of the order $\mathcal{O}(v^2/M_{\text{KK}}^2)$. One can therefore write (2.137) as

$$\mathbf{S}_n^Q(1^-) a_n^Q = \frac{v}{\sqrt{2}M_{\text{KK}}} \tilde{\mathbf{Y}}_q \mathbf{C}_n^q(1^-) a_n^q, \quad (2.138)$$

$$-\mathbf{S}_n^q(1^-) a_n^q = \frac{v}{\sqrt{2}M_{\text{KK}}} \tilde{\mathbf{Y}}_q^\dagger \mathbf{C}_n^Q(1^-) a_n^Q. \quad (2.139)$$

It is straightforward to derive the eigenvalue equation and expressions for the a -vectors from (2.138). Since the diagonal S - and C -profiles will have only nonzero entries (otherwise the corresponding SM quark would have no kinetic term), they can be inverted and it follows

$$\begin{aligned} \mathbf{S}_n^Q(1^-) a_n^Q &= -\frac{v^2}{2M_{\text{KK}}^2} \tilde{\mathbf{Y}}_u \mathbf{C}_n^q(1^-) [\mathbf{S}_n^q(1^-)]^{-1} \tilde{\mathbf{Y}}_u^\dagger \mathbf{C}_n^Q(1^-) a_n^Q, \\ \mathbf{S}_n^q(1^-) a_n^q &= -\frac{v^2}{2M_{\text{KK}}^2} \tilde{\mathbf{Y}}_u^\dagger \mathbf{C}_n^Q(1^-) [\mathbf{S}_n^Q(1^-)]^{-1} \tilde{\mathbf{Y}}_u \mathbf{C}_n^q(1^-) a_n^q. \end{aligned} \quad (2.140)$$

The mass eigenvalues x_n can then be found by solving

$$\det \left(\mathbf{1} - \frac{v^2}{2M_{\text{KK}}^2} [\mathbf{S}_n^Q(1^-)]^{-1} \tilde{\mathbf{Y}}_q \mathbf{C}_n^q(1^-) [-\mathbf{S}_n^q(1^-)]^{-1} \tilde{\mathbf{Y}}_q^\dagger \mathbf{C}_n^Q(1^-) \right) = 0, \quad (2.141)$$

and subsequently the corresponding a -vectors can be derived from (2.140).

Bulk Profiles

Considering again a simple bulk fermion with BCs examined at the beginning of the last section one can already anticipate a lot of the correct solution for the complete model. In the case of non-integer order α , the general solution (2.120) can be expressed solely by first order Bessel functions, because

$$Y_\alpha(x) = \frac{1}{\sin(\alpha\pi)} \left(\cos(\alpha\pi) J_\alpha(x) - J_{-\alpha}(x) \right), \quad (2.142)$$

so that

$$f_{L/R}^n(t) = \sqrt{t} \left(a_n^{L,R} J_{c \mp \frac{1}{2}} - b_n^{L,R} J_{-c \pm \frac{1}{2}} \right). \quad (2.143)$$

Note, that in this basis the EOM fix $a_n^L = a_n^R$, but $b_n^L = -b_n^R$. The value of the coefficients as well as the mass eigenvalues are fixed by the BCs, which in the case of Neumann BCs in the UV give

$$\frac{b_n}{a_n} = \frac{J_{c+\frac{1}{2}}(x_n\epsilon)}{J_{-c-\frac{1}{2}}(x_n\epsilon)}. \quad (2.144)$$

It is therefore straightforward to find the solutions for the components of the matrices $\mathbf{S}_n^{Q,q}(t)$ and $\mathbf{C}_n^{Q,q}(t)$ in this basis, if we choose to fix the coefficients in the UV and use the information on the IR brane in order to derive the mass eigenvalues. They will be direct generalizations of (2.143) with (2.143), because they only differ in the IR. Flavor is completely encoded in the choice of the localization parameters c_{Q_i} and c_{q_i} , so that we can omit flavor indices and find in agreement with [58, 59]

$$\begin{aligned} C_n^{Q,q}(t) &= \mathcal{N}_n(c_{Q,q}) \sqrt{\frac{L\epsilon t}{\pi}} f_n^+(t, c_{Q,q}), \\ S_n^{Q,q}(t) &= \pm \mathcal{N}_n(c_{Q,q}) \sqrt{\frac{L\epsilon t}{\pi}} f_n^-(t, c_{Q,q}), \end{aligned} \quad (2.145)$$

in which

$$f_n^\pm(t, c) = J_{-\frac{1}{2}-c}(x_n\epsilon) J_{\mp\frac{1}{2}+c}(x_n t) \pm J_{\frac{1}{2}+c}(x_n\epsilon) J_{\pm\frac{1}{2}-c}(x_n t). \quad (2.146)$$

This motivates the introduction of the extra minus sign in $c_{Q,q} = \pm M_{Q,q}/k$, because it allows for a compact notation in the case of Neumann UV BCs and regardless of the solution implies that $c_{Q,q} < -1/2$ will always mean UV localization and $c_{Q,q} > -1/2$ IR localization. However, in order to obtain a profile for $c + 1/2 \in \mathbb{N}$, one must rely

on the more general basis. The orthonormality relation (2.125) gives rise to

$$2 \int_{\epsilon}^1 dt t [f_n^{\pm}(t, c)]^2 = \frac{1}{\mathcal{N}_n^2(c)} \pm \frac{f_n^+(1^-, c) f_n^-(1^-, c)}{x_n}, \quad (2.147)$$

so that the normalization factor in (2.145) is fixed by

$$\mathcal{N}_n^{-2}(c) = [f_n^+(1^-, c)]^2 + [f_n^-(1^-, c)]^2 - \frac{2c}{x_n} f_n^+(1^-, c) f_n^-(1^-, c) - \epsilon^2 f_n^+(\epsilon, c)^2. \quad (2.148)$$

The IR BCs determine the mass eigenvalues x_n through (2.141), which for the zero modes are well approximated by $x_n \ll 1$, or equivalently $v \ll M_{\text{KK}}$. It is therefore convenient to expand (2.145) in this limit,

$$\begin{aligned} C_n^{Q,q}(t) &\approx \sqrt{\frac{L\epsilon}{\pi}} F(c_{Q,q}) t^{c_{Q,q}}, \\ S_n^{Q,q}(t) &\approx \pm \sqrt{\frac{L\epsilon}{\pi}} x_n F(c_{Q,q}) \frac{t^{1+c_{Q,q}} - \epsilon^{1+2c_{Q,q}} t^{-c_{Q,q}}}{1 + 2c_{Q,q}}, \end{aligned} \quad (2.149)$$

which is suggestively called *zero mode approximation* (ZMA). Accordingly, the function

$$F(c) \equiv \text{sgn}[\cos(\pi c)] \sqrt{\frac{1+2c}{1-\epsilon^{1+2c}}}, \quad (2.150)$$

which is proportional to the value of the zero mode C -profiles on the IR brane will be called *zero-mode profile*. Note, that the S -profiles on the IR brane are proportional to the inverse of the zero-mode profile.

We finish the discussion of the fermion profiles by giving the approximate behavior of the zero-mode profile for different regions of the localization parameters

$$F(c) \approx \begin{cases} -\sqrt{-1-2c} \epsilon^{-c-\frac{1}{2}}, & -3/2 < c < -1/2, \\ \sqrt{1+2c}, & -1/2 < c < 1/2. \end{cases} \quad (2.151)$$

Since S -profiles are suppressed by x_n compared to the C -profiles, the coupling between fermions and the Higgs is controlled by (2.151), if the Yukawas are anarchic matrices. As a consequence of the curvature of the extra dimension, the KK modes of gauge bosons are also peaked towards the IR, indicated by the t dependence of (2.106). Therefore, the behavior of the zero-mode profile shows that a UV localized fermion zero mode will have exponentially small mass compared to the electroweak scale as well as exponentially suppressed couplings to KK gauge bosons. In other words, the same mechanism responsible for light masses ensures that flavor changing couplings, which are generically mediated by the KK excitations of gauge bosons. This is the RS-GIM mechanism and will be the subject of the next section. Note, that for the IR localized top quark however, large overlaps and therefore large effects are expected, which will be further examined in Chapter 4.

2.5 Hierarchies in Quark Masses and Mixings and the RS GIM Mechanism

Presumably, there is a “Balmer series” hiding somewhere in the CKM matrix. There is a regularity between the elements which is tantalizing; those regularities hint at more fundamental relationships between the generations.

————— Dan Green

As stated in the introduction, the mass hierarchies of the quarks as well as a suppression of FCNCs mediated by new resonances can both be explained in the context of partially composite fermions. In the explicit model that Kaplan constructed, see [31, Sec. 3], the confining interactions are QCD like and the possibility to base this explanation on order one parameters, namely the anomalous dimensions of the composite quarks, was not foreseen. The fact that such a mechanism exists in Randall-Sundrum models was recognized first by Ghergetta and Pomarol in [59, Sec. 4.3]. Later on, the connection to Kaplan was made in [123]. In this section we will derive explicit expressions for the masses and mixings and discuss the consequences and implications for FCNCs.

Hierarchic Quark Masses and Mixings from Anarchic Fundamental Parameters

In Section 1.2, it was mentioned, that the mechanism of generating hierarchical masses and mixings by the localization of the bulk fermions is related to the Froggatt-Nielsen mechanism. Here, this relation will be made explicit, by rederiving the formulas in [70] in the RS model. The small expansion parameter of the CKM matrix, the Cabibbo angle $\lambda \simeq 0.2$ was chosen proportional to the vev of the Froggatt-Nielsen scalar in Section 1.2, in order to illustrate the principle. Although this is possible, we will choose the more general ansatz

$$\frac{\langle \phi \rangle}{\Lambda_{\text{FI}}} \sim \epsilon, \quad (2.152)$$

where $\epsilon \neq \lambda$, but some unspecified small parameter.¹¹ Equation (1.64) is then replaced by

$$Y_{ij} = G_{ij} \epsilon^{a_i - b_j}, \quad (2.153)$$

in which it is not to be summed over double indices, and G_{ij} denotes the entries of some fundamental matrix \mathbf{G} , which are assumed to be anarchical and of order one. In the RS model with a brane Higgs, the effective four dimensional Yukawa couplings can

¹¹Not to be confused with the ϵ introduced in (2.54).

be found by integrating the last two lines of Equation (2.122) over the fifth coordinate. Taking into account (2.149), this gives to leading order in v/M_{KK} ,

$$\left(\mathbf{Y}_q^{\text{eff}}\right)_{ij} = F(c_{Q_i}) \left(\mathbf{Y}_q^{(5D)}\right)_{ij} F(c_{q_j}), \quad (2.154)$$

in which again no sum over double indices is implied. One can therefore motivate the identification

$$\left(\mathbf{Y}_q^{(5D)}\right)_{ij} \leftrightarrow (\mathbf{G}_q)_{ij}, \quad F(c_{Q_{4-i}}) \leftrightarrow \epsilon^{a_i}, \quad F(c_{q_{4-j}}) \leftrightarrow \epsilon^{-b_j^q}, \quad (2.155)$$

where $q = u, d$ and clearly two different sets of charges for c_d and c_u and two copies of \mathbf{G} need to be introduced. The strange identification scheme of charges and bulk mass parameters is due to the fact that we follow [70] in the convention of ordering the charges in the way¹² $a_{i+1} > a_i$ and $b_{i+1} < b_i$, so that the quarks are enumerated starting with the heaviest. On the other hand, the flavor-bulk mass assignment should stay in line with the previous chapters, in which c_{q_3} denotes the localization of the heaviest generation and so forth.

One set of equations (2.153) will then hold for the up- and one for the downtype quarks, and their masses can be found using

$$\prod_{i=1}^n m_i^q = \left(\frac{v}{\sqrt{2}}\right)^n \det \mathbf{G}_q^{(n)} \epsilon^{K_n} \quad \text{with} \quad K_n = \sum_{i=1}^n a_i - b_i^q, \quad (2.156)$$

where $\mathbf{G}_q^{(n)}$ denotes the $n \times n$ submatrix formed by the first n rows and columns of \mathbf{G}_q . This yields for the n th largest quark mass

$$m_n = \frac{v}{\sqrt{2}} \frac{|\det \mathbf{G}_q^{(n)}|}{|\det \mathbf{G}_q^{(n-1)}|} \epsilon^{a_n + b_n^q}. \quad (2.157)$$

Applying (2.155) results in

$$\begin{aligned} m_u &= \frac{v}{\sqrt{2}} \frac{|\det \mathbf{Y}_u^{(5D)}|}{|(M_u^{(5D)})_{11}|} |F(c_{Q_1})F(c_{u_1})|, & m_d &= \frac{v}{\sqrt{2}} \frac{|\det \mathbf{Y}_d^{(5D)}|}{|(M_d^{(5D)})_{11}|} |F(c_{Q_1})F(c_{d_1})|, \\ m_c &= \frac{v}{\sqrt{2}} \frac{|(M_u^{(5D)})_{11}|}{|(Y_u^{(5D)})_{33}|} |F(c_{Q_2})F(c_{u_2})|, & m_s &= \frac{v}{\sqrt{2}} \frac{|(M_d^{(5D)})_{11}|}{|(Y_d^{(5D)})_{33}|} |F(c_{Q_2})F(c_{d_2})|, \\ m_t &= \frac{v}{\sqrt{2}} |(Y_u^{(5D)})_{33}| |F(c_{Q_3})F(c_{u_3})|, & m_b &= \frac{v}{\sqrt{2}} |(Y_d^{(5D)})_{33}| |F(c_{Q_3})F(c_{d_3})|, \end{aligned} \quad (2.158)$$

in which $M_q^{(5D)}$ denote the minors of the corresponding 5D Yukawa matrix. In the rest of this section, the superscript (5D) will be suppressed and every Yukawa matrix or minor is always understood to be derived from the five dimensional fundamental Yukawa, if not explicitly noted otherwise. One can find closed form expressions for

¹²For degenerate charges the following relations are only order-of-magnitude wise correct.

the unitary diagonalization matrices U_R^q and U_L^q [70], which read

$$(U_L^q)_{ij} = (u_q)_{ij} \begin{cases} \frac{F(c_{Q_i})}{F(c_{Q_j})}, & i \leq j, \\ \frac{F(c_{Q_j})}{F(c_{Q_i})}, & i > j, \end{cases} \quad \mathbf{u}_q = \begin{pmatrix} 1 & \frac{(M_q)_{21}}{(M_q)_{11}} & \frac{(Y_q)_{13}}{(Y_q)_{33}} \\ -\frac{(M_q)_{21}^*}{(M_q)_{11}^*} & 1 & \frac{(Y_q)_{23}}{(Y_q)_{33}} \\ \frac{(M_q)_{31}^*}{(M_q)_{11}^*} & -\frac{(Y_q)_{23}^*}{(Y_q)_{33}^*} & 1 \end{pmatrix}, \quad (2.159)$$

$$(U_R^q)_{ij} = (w_q)_{ij} e^{i\phi_j} \begin{cases} \frac{F(c_{q_i})}{F(c_{q_j})}, & i \leq j, \\ \frac{F(c_{q_j})}{F(c_{q_i})}, & i > j. \end{cases} \quad \mathbf{w}_q = \begin{pmatrix} 1 & \frac{(M_q)_{12}^*}{(M_q)_{11}^*} & \frac{(Y_q)_{31}^*}{(Y_q)_{33}^*} \\ -\frac{(M_q)_{12}}{(M_q)_{11}} & 1 & \frac{(Y_q)_{32}^*}{(Y_q)_{33}^*} \\ \frac{(M_q)_{13}}{(M_q)_{11}} & -\frac{(Y_q)_{32}}{(Y_q)_{33}} & 1 \end{pmatrix}, \quad (2.160)$$

in which the phase factor

$$e^{i\phi_j} = \text{sgn}[F(c_{Q_j})F(c_{f_j})] e^{-i\theta_j}, \quad \boldsymbol{\theta} = \begin{pmatrix} \arg(\det \mathbf{Y}_q) - \arg((M_q)_{11}) \\ \arg((M_q)_{11}) - \arg((Y_q)_{33}) \\ \arg((Y_q)_{33}) \end{pmatrix}, \quad (2.161)$$

appears as a consequence of the convention to choose the diagonal entries of U_L^q real. The CKM matrix $V_{\text{CKM}} = (U_L^u)^\dagger U_L^d$ can then be expressed in terms of the zero mode profiles and the 5D Yukawa couplings alone. The Wolfenstein parameters read

$$\lambda = \frac{|V_{us}|}{\sqrt{|V_{ud}|^2 + |V_{us}|^2}}, \quad A = \frac{1}{\lambda} \left| \frac{V_{cb}}{V_{us}} \right|, \quad \bar{\rho} - i\bar{\eta} = -\frac{V_{ud}^* V_{ub}}{V_{cd}^* V_{cb}}, \quad (2.162)$$

so that we obtain from (2.159)

$$\lambda = \frac{|F(c_{Q_1})|}{|F(c_{Q_2})|} \left| \frac{(M_d)_{21}}{(M_d)_{11}} - \frac{(M_u)_{21}}{(M_u)_{11}} \right|, \quad A = \frac{|F(c_{Q_2})|^3}{|F(c_{Q_1})|^2 |F(c_{Q_3})|} \left| \frac{\frac{(Y_d)_{23}}{(Y_d)_{33}} - \frac{(Y_u)_{23}}{(Y_u)_{33}}}{\left[\frac{(M_d)_{21}}{(M_d)_{11}} - \frac{(M_u)_{21}}{(M_u)_{11}} \right]^2} \right|, \\ \bar{\rho} - i\bar{\eta} = \frac{(Y_d)_{33} (M_u)_{31} - (Y_d)_{23} (M_u)_{21} + (Y_d)_{13} (M_u)_{11}}{(Y_d)_{33} (M_u)_{11} \left[\frac{(Y_d)_{23}}{(Y_d)_{33}} - \frac{(Y_u)_{23}}{(Y_u)_{33}} \right] \left[\frac{(M_d)_{21}}{(M_d)_{11}} - \frac{(M_u)_{21}}{(M_u)_{11}} \right]}. \quad (2.163)$$

Note, that ρ and η are in leading order independent of the zero mode profiles and thus of the quark localization. Since the Yukawa couplings are not supposed to add any

structure, there are nine zero mode profiles $F(c_{Q_i}), F(c_{u_i}), F(c_{d_i}), i = 1, 2, 3$, whose values determine six quark masses and the remaining two Wolfenstein parameters. We will therefore use the SM values as an input in order to fix eight of these profile functions, and randomly choose the remaining one as well as the Yukawa matrices in all numerical analyses. Since they are spectators in the process of generating hierarchies, it makes sense to randomize the Yukawas on the basis of a flat distribution, see Appendix A for details. This is not the case for all of the zero mode profiles, because of (2.151). Only for the right-handed top quark profile function $F(c_{u_3})$ we expect a linear distribution of localization parameters, because the ZMA profile depends only linearly on c_{u_3} , and it thus represents a specific choice for the unspecified degree of freedom. In other words, generating values for one of the other profile functions based on a flat distribution will result in a large rejection rate, because we know that they are not flatly distributed. However, any peaked distribution may generate results biased towards the peak value. We will therefore derive expressions for these eight profile functions depending on the Yukawas, the physical input parameters and the right handed top localization. Plots of the resulting distributions of the quark profiles are given in Figure A.1. For the profile functions of the $SU(2)_L$ doublets, this yields

$$\begin{aligned}
 |F(c_{Q_1})| &= \frac{\sqrt{2} m_t}{v} \left(|(Y_u)_{33}| \left| \frac{(Y_d)_{23}}{(Y_d)_{33}} - \frac{(Y_u)_{23}}{(Y_u)_{33}} \right| \left| \frac{(M_d)_{21}}{(M_d)_{11}} - \frac{(M_u)_{21}}{(M_u)_{11}} \right| \right)^{-1} \frac{\lambda^3 A}{|F(c_{u_3})|}, \\
 |F(c_{Q_2})| &= \frac{\sqrt{2} m_t}{v} \left(|(Y_u)_{33}| \left| \frac{(Y_d)_{23}}{(Y_d)_{33}} - \frac{(Y_u)_{23}}{(Y_u)_{33}} \right| \right)^{-1} \frac{\lambda^2 A}{|F(c_{u_3})|}, \\
 |F(c_{Q_3})| &= \frac{\sqrt{2} m_t}{v} \frac{1}{|(Y_u)_{33}|} \frac{1}{|F(c_{u_3})|}, \tag{2.164}
 \end{aligned}$$

while the up-type singlet profiles read

$$\begin{aligned}
 |F(c_{u_1})| &= \frac{m_u}{m_t} \frac{|(Y_u)_{33}| |(M_u)_{11}|}{\det \mathbf{Y}_u} \left| \frac{(Y_d)_{23}}{(Y_d)_{33}} - \frac{(Y_u)_{23}}{(Y_u)_{33}} \right| \left| \frac{(M_d)_{21}}{(M_d)_{11}} - \frac{(M_u)_{21}}{(M_u)_{11}} \right| \frac{|F(c_{u_3})|}{\lambda^3 A} \\
 |F(c_{u_2})| &= \frac{m_c}{m_t} \frac{|(Y_u)_{33}|^2}{|(M_u)_{11}|} \left| \frac{(Y_d)_{23}}{(Y_d)_{33}} - \frac{(Y_u)_{23}}{(Y_u)_{33}} \right| \frac{|F(c_{u_3})|}{\lambda^2 A} \tag{2.165}
 \end{aligned}$$

and the down-type singlet profiles are

$$\begin{aligned}
 |F(c_{d_1})| &= \frac{m_d}{m_t} \frac{|(Y_u)_{33}| |(M_d)_{11}|}{\det \mathbf{Y}_d} \left| \frac{(Y_d)_{23}}{(Y_d)_{33}} - \frac{(Y_u)_{23}}{(Y_u)_{33}} \right| \left| \frac{(M_d)_{21}}{(M_d)_{11}} - \frac{(M_u)_{21}}{(M_u)_{11}} \right| \frac{|F(c_{u_3})|}{\lambda^3 A}, \\
 |F(c_{d_2})| &= \frac{m_s}{m_t} \frac{|(Y_u)_{33}| |(Y_d)_{33}|}{|(M_d)_{11}|} \left| \frac{(Y_d)_{23}}{(Y_d)_{33}} - \frac{(Y_u)_{23}}{(Y_u)_{33}} \right| \frac{|F(c_{u_3})|}{\lambda^2 A}. \\
 |F(c_{d_3})| &= \frac{m_b}{m_t} \frac{|(Y_u)_{33}|}{|(Y_d)_{33}|} |F(c_{u_3})|. \tag{2.166}
 \end{aligned}$$

The hierarchies advertised in the introduction can now be read off directly from these expressions, as

$$\frac{|F(c_{Q_1})|}{|F(c_{Q_2})|} \sim \lambda \quad \frac{|F(c_{Q_2})|}{|F(c_{Q_3})|} \sim \lambda^2 \quad \frac{|F(c_{Q_1})|}{|F(c_{Q_3})|} \sim \lambda^3, \tag{2.167}$$

and

$$\begin{aligned} \frac{|F(c_{u_1})|}{|F(c_{u_3})|} &\sim \frac{m_u}{m_t} \frac{1}{\lambda^3} & \frac{|F(c_{u_2})|}{|F(c_{u_3})|} &\sim \frac{m_c}{m_t} \frac{1}{\lambda^2} \\ \frac{|F(c_{d_1})|}{|F(c_{u_3})|} &\sim \frac{m_d}{m_t} \frac{1}{\lambda^3} & \frac{|F(c_{d_2})|}{|F(c_{u_3})|} &\sim \frac{m_s}{m_t} \frac{1}{\lambda^2} & \frac{|F(c_{d_3})|}{|F(c_{u_3})|} &\sim \frac{m_b}{m_t}, \end{aligned} \quad (2.168)$$

which in turn make the hierarchical structure of the rotation matrices (2.159) and (2.160) clearly visible.

Because only ratios or products of profile functions are fixed by the above relations, there is some freedom in rescaling a given set of profile functions and Yukawa matrices and still end up with a set of parameters, that reproduces all physical input parameters. From (2.158) it is evident that this can either be done by reshuffling between the singlet and doublet profiles and keeping the Yukawas unchanged,

$$F(c_{Q_i}) \rightarrow \eta F(c_{Q_i}), \quad F(c_{q_i}) \rightarrow \frac{1}{\eta} F(c_{q_i}), \quad (2.169)$$

or by rescaling both the profiles and the Yukawas

$$F(c_{Q_i}) \rightarrow \eta F(c_{Q_i}), \quad F(c_{q_i}) \rightarrow \eta_q F(c_{q_i}), \quad \mathbf{Y}_q \rightarrow \frac{1}{\eta \eta_q} \mathbf{Y}_q. \quad (2.170)$$

This freedom will be referred to as *reparametrization invariance* and will be a convenient tool in estimating whether regions of parameter space which are not covered directly in the numerical analyses would change the conclusions without the need to generate a whole new set of parameter points. One should be careful in taking advantage of this freedom, because a rescaling of the Yukawa matrix should not clash with the assumption of order one Yukawa couplings. Also, one should be aware that a large reparametrization of the zero mode profiles implies changes of the localization parameters, which can lead to a shift of some profiles from the UV in the IR and result in severe bounds from FCNCs, as we will see in the next section. The range of sensible values for η and η_q is therefore not unlimited.

In the dual theory, the zero mode profiles are equivalent to the functions defined below (2.47) and the bulk parameters to the anomalous dimensions of the composite quark partners. Referring to Section 1.1, the profile functions can be understood as the mixing angles (1.30), so that the equations (1.31), (2.47) and (2.154) are basically the same in different languages.

The derivation of hierarchies in the quark sector in the dual theory is explained in the corresponding Sections 1.1 and 2.2. Reparametrization invariance is the freedom of choosing the degree of compositeness in the dual theory and corresponds to a reshuffling between the c -parameters in (2.46). Therefore, the dual theory allows for a better understanding of the the limitations of the rescaling parameters η, η_q . Based on Figure 2.3, one can see that a rescaling of the profile functions of the light quarks towards the IR will not affect the generation of the masses and mixing angles, but will make the light quarks more and more composite, which in turn would not only lead to

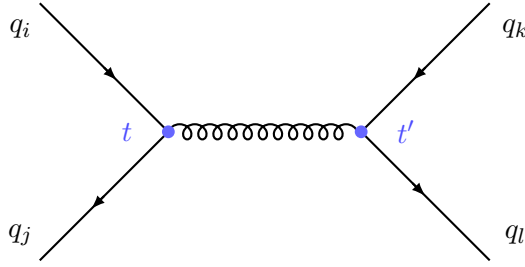


Figure 2.10: Four fermion diagram leading to $\Delta F = 1$ and $\Delta F = 2$ processes.

FCNCs, but also imply form factors (see [125, Sec. 3.3] for explicit calculations) clearly in tension with the most recent experimental limits on quark compositeness [126].

The RS-GIM Mechanism

The Higgs, being confined to the IR brane is in the dual theory interpreted as a fully composite state, and its overlap with the zero modes of the light flavor quarks is small, because they correspond to mostly elementary states which do not couple to the Higgs. Similarly, gauge boson KK modes are almost entirely composites and are therefore localized towards the IR brane. As a byproduct of the mass generation by an IR brane localized Higgs, this also keeps the couplings between light flavor quarks and these new resonances small. Most importantly, FCNCs which appear at tree level due to the couplings being non-universal in flavor space are exponentially suppressed by the zero mode profile functions (2.151). This is called the RS-GIM mechanism, in reference to the SM GIM mechanism, which explains why loop-level FCNCs in the SM are small. Both rely on the fact, that small quark masses enter in the couplings. In both cases, the absence or even the equality of all quark masses (bulk mass parameters) would eliminate FCNCs.

One could worry that effects in the RS model might still be significantly too large, because they appear at tree level, while SM FCNCs are suppressed by a loop factor. This is however balanced by the KK modes being heavy, so that the new physics scale provides an additional suppression. All experimental evidence points in the direction of small FCNCs in very good agreement with the SM and thus the requirement

$$\frac{1}{M_{\text{KK}}^2} \times m_q^2 \approx \frac{1}{16\pi^2} \times \frac{m_q^2}{M_W^2} \quad (2.171)$$

can be understood as a very rough estimate of the new physics scale expected if an RS-GIM mechanism is realized in nature. Remarkably, this puts it in the ballpark of $M_{\text{KK}} \sim 4\pi M_W$, which is what one would expect from a model designed to solve the gauge hierarchy problem. It should be stressed, that it is especially noteworthy if not unique, that flavor points to the TeV scale in a new physics model with no additional assumptions regarding couplings in the flavor sector (*a.k.a.* MFV).

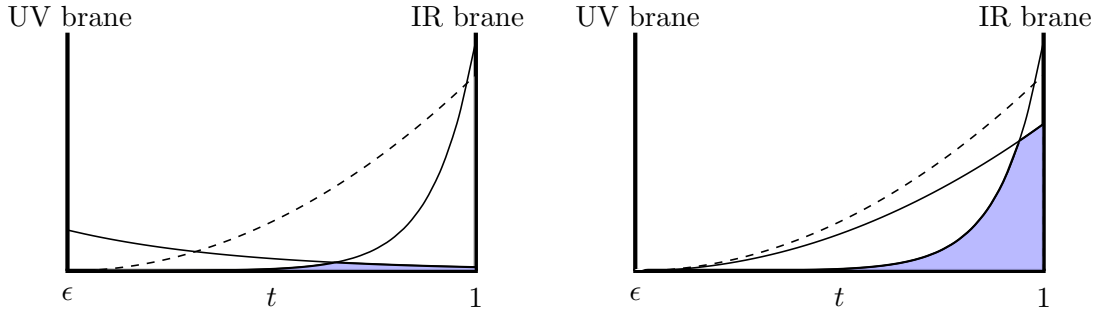


Figure 2.11: Qualitative illustration of the RS-GIM mechanism. The dashed lines represent a t^2 term from the 5D gauge boson propagator. The solid lines show the profile of a UV and an IR localized fermion zero mode in the left panel and of to IR localized zero modes in the right panel. The blue shaded area can be interpreted as an indicator of the size of the FCNC coupling resulting from the overlap integral including the three functions.

Moreover does the 5D description allow for a particularly illustrative explanation of the RS-GIM mechanism in geometric terms. In order to understand this let us analyze all possible contributions arising from tree level diagrams as shown in Figure 2.10. It describes a process in which external zero mode fermions couple to the tower of all KK modes of a gauge boson, which in the effective theory is given by the first term in the expansion of the 5D propagator for small momenta (2.82). The couplings will therefore be rescaled by an integral over the fifth dimension including the t -dependent terms of the zero modes (2.149) and the expressions (2.86) or (2.103). As an example, the Wilson coefficient of a four quark operator with four $SU(2)_L$ singlet external quarks

$$\mathcal{H}_{\text{eff}} \ni \sum_{i,j,k,l=1}^3 c_{ijkl} (\bar{q}_i^c \gamma_\mu q_j^c) (\bar{q}_k^c \gamma_\mu q_l^c), \quad (2.172)$$

with i, j, k, l flavor indices, gets contributions from KK photon exchange proportional to the following *overlap integral*

$$c_{ijkl} \sim \frac{\alpha}{M_{\text{KK}}^2} \int_\epsilon^1 dt \int_\epsilon^1 dt' t^{c_{q_i} + c_{q_j}} t'^{c_{q_k} + c_{q_l}} \left[Lt_{<}^2 - t^2 \left(\frac{1}{2} - \ln t \right) - t'^2 \left(\frac{1}{2} - \ln t' \right) + \frac{1}{2L} \right], \quad (2.173)$$

in which only the leading C -profiles are included and the 5D coordinates are assigned to the two vertices as shown in Figure 2.10. The integral

$$\int_\epsilon^1 dt t^{c_{q_i} + c_{q_j}} \times \text{constant} \quad (2.174)$$

will not lead to FCNCs, because in the case of the photon, the operator in (2.172) with only $SU(2)_L$ doublets gives rise to a similar integral with S -profiles which in the sum completes the orthonormality relation of the fermion profiles (2.125).

FCNCs can therefore only arise if the gauge boson couplings distinguish between

$SU(2)_L$ doublets and singlets or from propagator terms proportional to t or t' . Terms proportional to only one of the coordinates t or t' should therefore be read as $t^2 \rightarrow t^2 \times \mathbb{1}$ in flavor space and since we will concentrate on the photon, which has vectorial couplings, can at most generate contributions to $\Delta F = 1$ processes. Consequentially, only the term proportional to $t_{<}^2 = \text{Min}[t^2, t'^2]$ in equation (2.173) will contribute to $\Delta F = 2$ processes, while the second and third term will lead to flavor violation at the respective vertex and the constant is flavor diagonal.

Note, that there are no negative powers of t or t' in the propagator. This implies, that the function becomes large in the IR and small in the UV. For the fermion zero modes, the sign of the exponent depends on the localization. The factor $t^{c_{q_i} + c_{q_j}}$ becomes large in the IR only if both q_i and q_j are IR localized, which is generically only the case if both are top quarks. If one of them or even both are UV localized, this factor drags the whole integral kernel into the UV which leads to small overlap integrals. As a rough guide one can assume that if the shared enclosed area of the function curves of the propagator term and the two zero modes is small (large), the overlap integral becomes small (large). This rule of thumb is illustrated in Figure 2.11. It works only because the propagators are IR localized. The zero mode of the graviton for example is localized in the UV, which makes the overlap integrals with SM fermion profiles even smaller, so that the conclusions drawn from Figure 2.11 are not applicable.

The discussion in this section is based on the exchange of the whole KK tower, but would have led to the same qualitative results if only a single gauge boson KK mode was exchanged instead. In this case, the propagator in (2.173) is replaced by one summand of the right hand side of (2.89). The profiles of the gauge boson KK modes are given in (2.106), and are already IR localized due to the t in front of the Bessel functions.¹³ Certain aspects of the full sum can however not be estimated by considering the exchange of a single KK mode. For example, the enhancement by the volume factor $L \approx 36$ in front of the $t_{<}^2$ - term is hidden in a mode-by-mode inspection, and will lead to somewhat surprisingly large effects in $\Delta F = 2$ observables, because such a factor clearly spoils the naive estimate (2.171). One can however check, that the sum must not extend to infinity in order to reproduce these effects.

It can even be considered wrong to sum up all modes, because this would contradict the perception of the RS model as an effective theory. At what point the tower should be cut off however is not uniquely defined. In the 5D description, it depends on the localization of the involved fields in the bulk and is therefore process dependent. Based on this argument, a process involving the Higgs describes physics close to the IR brane and should thus be cutoff at $m_n \sim$ a few TeV. Processes involving only light fermions (and a graviton for example) would however require a cutoff close to the Planck scale $m_n \sim M_{\text{Pl}}$.

Regarding these considerations, one should keep in mind, that dual theory is a walking TC theory, which means it remains strongly coupled over a large range of scales, namely over the whole bulk due to the identification of the fifth coordinate with an inverse energy scale. From this point of view it would be sensible to cut off at the scale

¹³This is a direct effect of the warped metric. In the limit of vanishing curvature $k \rightarrow 0$, the Bessel functions become trigonometric functions and $t \rightarrow 1$. As a result, there is no localization.

at which the theory becomes asymptotically free, which is indicated by the position of the UV brane. Independent on what position one takes, it will be a good approximation to evaluate the whole propagator, as very heavy modes do not contribute much.

In order to give precise expressions for the integrals in (2.173), we will in the following collect formulas for overlap integrals involving all possible terms which appear in the propagators derived in Section 2.3, including the full fermion profiles (2.149). It will be referred to those in the next sections, when effective Hamiltonians are constructed. Flavor changing at one vertex is described by the integrals

$$\begin{aligned}
 (\Delta_Q)_{ij} &= \frac{2\pi}{L\epsilon} \int_{\epsilon}^1 dt t^2 \left[a_i^{(Q)\dagger} C_i^{(Q)}(t) C_j^{(Q)}(t) a_j^{(Q)} + a_i^{(q)\dagger} S_i^{(q)}(t) S_j^{(q)}(t) a_j^{(q)} \right], \quad (2.175) \\
 (\Delta_q)_{ij} &= \frac{2\pi}{L\epsilon} \int_{\epsilon}^1 dt t^2 \left[a_i^{(q)\dagger} C_i^{(q)}(t) C_j^{(q)}(t) a_j^{(q)} + a_i^{(Q)\dagger} S_i^{(Q)}(t) S_j^{(Q)}(t) a_j^{(Q)} \right], \\
 (\Delta'_Q)_{ij} &= \frac{2\pi}{L\epsilon} \int_{\epsilon}^1 dt t^2 \left[\frac{1}{2} - \ln t \right] \left[a_i^{(Q)\dagger} C_i^{(Q)}(t) C_j^{(Q)}(t) a_j^{(Q)} + a_i^{(q)\dagger} S_i^{(q)}(t) S_j^{(q)}(t) a_j^{(q)} \right], \\
 (\Delta'_q)_{ij} &= \frac{2\pi}{L\epsilon} \int_{\epsilon}^1 dt t^2 \left[\frac{1}{2} - \ln t \right] \left[a_i^{(q)\dagger} C_i^{(q)}(t) C_j^{(q)}(t) a_j^{(q)} + a_i^{(Q)\dagger} S_i^{(Q)}(t) S_j^{(Q)}(t) a_j^{(Q)} \right],
 \end{aligned}$$

in which i, j refer to the flavor indices in Figure 2.10. The other vertex gets only flavor diagonal contributions from these structures. Recall also, that on the profiles of $SU(2)_L$ doublet fermions no distinction is made between $Q = U, D$. Propagator terms proportional to $t^2_{<}$ lead to non-factorizable overlap integrals, for example

$$\begin{aligned}
 (\tilde{\Delta}_Q)_{ij} \otimes (\tilde{\Delta}_{q'})_{kl} &= \frac{2\pi^2}{L^2\epsilon^2} \int_{\epsilon}^1 dt \int_{\epsilon}^1 dt' t^2_{<} \\
 &\times \left[a_i^{(Q)\dagger} C_i^{(Q)}(t) C_j^{(Q)}(t) a_j^{(Q)} + a_i^{(q)\dagger} S_i^{(q)}(t) S_j^{(q)}(t) a_j^{(q)} \right] \\
 &\times \left[a_k^{(q')\dagger} C_k^{(q')}(t') C_l^{(q')}(t') a_l^{(q')} + a_k^{(Q')\dagger} S_k^{(Q)}(t') S_l^{(Q)}(t') a_l^{(Q')} \right], \quad (2.176)
 \end{aligned}$$

in which the flavor indices are again chosen in line with Figure 2.10. If the couplings to $SU(2)_L$ singlets and doublets differ, as in the case of the Z boson, the couplings can be expressed by the equivalent of the above integrals with the C -profiles omitted, denoted by the replacement $\Delta \rightarrow \varepsilon$. The expressions $\varepsilon^{(l)}$, $\tilde{\varepsilon} \otimes \tilde{\Delta}$ and variations thereof are then defined in an obvious manner. Finally, couplings to the Higgs involve the profiles evaluated directly at the brane and we define

$$(g_h^q)_{ij} = \sqrt{2} \frac{\pi}{L\epsilon} \int_{\epsilon}^1 dt \delta(t-1) \left[a_i^{Q\dagger} C_i^Q(t) Y_q C_j^q(t) a_j^q + a_i^{q\dagger} S_i^q(t) Y_q^\dagger S_j^Q(t) a_j^Q \right]. \quad (2.177)$$

in order to describe them. Using the EOM, (2.177) can be reformulated as

$$(g_h^q)_{ij} = \delta_{ij} \frac{m_i^q}{v} - \frac{m_i^q}{v} (\delta_q)_{ij} - (\delta_Q)_{ij} \frac{m_j^q}{v} + (\Delta g_h^q)_{ij}, \quad (2.178)$$

with the overlap integrals

$$\begin{aligned}
 (\delta_q)_{ij} &= \frac{2\pi}{L\epsilon} \int_{\epsilon}^1 dt a_i^{Q\dagger} \mathbf{S}_i^Q(t) \mathbf{S}_j^Q(t) a_j^Q \\
 (\delta_Q)_{ij} &= \frac{2\pi}{L\epsilon} \int_{\epsilon}^1 dt a_i^{q\dagger} \mathbf{S}_i^q(t) \mathbf{S}_j^q(t) a_j^q \\
 (\Delta g_h^q)_{ij} &= \frac{2\pi}{L\epsilon} \int_{\epsilon}^1 dt \delta(t-1) a_i^{q\dagger} \mathbf{S}_i^q(t) \mathbf{Y}_q^\dagger \mathbf{S}_j^Q(t) a_j^Q.
 \end{aligned} \tag{2.179}$$

The last integral corresponds to the second Yukawa coupling in (2.177) and must be evaluated with a properly regularized delta function, see [118, p.135f.]. It will represent the leading term in Higgs mediated flavor violating processes, because it is not chirally suppressed. However, for all processes considered it can still be neglected, because in the case of $\Delta F = 1$ currents the flavor-conserving vertex is chirally suppressed and for $\Delta F = 2$ currents it is smaller than the tensor structure (2.176) by a factor v^2/M_{KK}^2 . It is however important in Higgs physics [127].

In the ZMA, the above matrices simplify considerably,

$$\begin{aligned}
 \Delta_Q &\rightarrow U_L^{q\dagger} \text{diag} \left[\frac{F^2(c_{Q_i})}{3 + 2c_{Q_i}} \right] U_L^q, \\
 \Delta_q &\rightarrow U_R^{q\dagger} \text{diag} \left[\frac{F^2(c_{q_i})}{3 + 2c_{q_i}} \right] U_R^q, \\
 \Delta'_Q &\rightarrow U_L^{q\dagger} \text{diag} \left[\frac{5 + 2c_{Q_i}}{2(3 + 2c_{Q_i})^2} F^2(c_{Q_i}) \right] U_L^q, \\
 \Delta'_q &\rightarrow U_R^{q\dagger} \text{diag} \left[\frac{5 + 2c_{q_i}}{2(3 + 2c_{q_i})^2} F^2(c_{q_i}) \right] U_R^q,
 \end{aligned} \tag{2.180}$$

and

$$(\tilde{\Delta}_Q)_{mn} \otimes (\tilde{\Delta}_{q'})_{m'n'} \rightarrow \sum_{i,j} (U_L^{q\dagger})_{mi} (U_L^q)_{in} (\tilde{\Delta}_{Qq})_{ij} (U_R^{q\dagger})_{m'j} (U_R^q)_{j'n'}, \tag{2.181}$$

where

$$(\tilde{\Delta}_{Qq})_{ij} = \frac{F^2(c_{Q_i})}{3 + 2c_{Q_i}} \frac{3 + c_{Q_i} + c_{q_j}}{2(2 + c_{Q_i} + c_{q_j})} \frac{F^2(c_{q_j})}{3 + 2c_{q_j}}, \tag{2.182}$$

and analogue for the remaining combinations of indices Q and q . Because of the v/M_{KK} suppression in (2.150), the ϵ structures vanish in the ZMA. Using the fact that all c_i parameters except c_{u_3} are very close to $-1/2$, it is a reasonable approximation to replace $(3 + c_{Q_i} + c_{q_j})/(2 + c_{Q_i} + c_{q_j})$ by 2, in which case we obtain the approximate result

$$\tilde{\Delta}_A \otimes \tilde{\Delta}_B \rightarrow \Delta_A \Delta_B, \tag{2.183}$$

as well as $\Delta'_A \approx \Delta_A$, both for $A, B \in \{Q, q\}$. For completeness, the matrices (2.179) are given

$$\begin{aligned}\delta_Q &\rightarrow \mathbf{x}_q U_R^{q\dagger} \text{diag} \left[\frac{1}{1-2c_{q_i}} \left(\frac{1}{F^2(c_{q_i})} - 1 + \frac{F^2(c_{q_i})}{3+2c_{q_i}} \right) \right] U_R^q \mathbf{x}_q, \\ \delta_q &\rightarrow \mathbf{x}_q U_L^{q\dagger} \text{diag} \left[\frac{1}{1-2c_{Q_i}} \left(\frac{1}{F^2(c_{Q_i})} - 1 + \frac{F^2(c_{Q_i})}{3+2c_{Q_i}} \right) \right] U_L^q \mathbf{x}_q, \\ \Delta \mathbf{g}_h^q &\rightarrow \frac{\sqrt{2}v^2}{3M_{\text{KK}}^2} U_L^{q\dagger} \text{diag} [F(c_{Q_i})] \mathbf{Y}_q \mathbf{Y}_q^\dagger \mathbf{Y}_q \text{diag} [F(c_{q_i})] U_R^q,\end{aligned}\tag{2.184}$$

where \mathbf{x}_q denotes a vector in flavor space with $x_q = m_q/M_{\text{KK}}$ as its entries.

2.6 Four Fermion Interactions

Given the flavor mixing matrices introduced in the last section and the expressions for the SM gauge boson propagators (2.103) and (2.86), it is straightforward to derive effective Hamiltonians featuring all dimension six operators with four fermion legs. In matching the full with the effective theory, one has to evaluate all diagrams in the full theory, and take into account possible symmetry factors for the effective diagrams, which are process dependent. Therefore, a common prefactor $S(\bar{q}_i, q_j; \bar{q}'_k, q'_l)$ depending on the flavor indices i, j, k, l of all external quarks in a given process, is introduced. In order not to clutter up the notation we will write the external quarks q and q' as vectors in flavor space and the sum implicitly assumes a sum over all KK modes as well. For the photon one finds,

$$\begin{aligned}\mathcal{H}_{\text{eff}}^{(\gamma)} &= \frac{2\pi\alpha}{M_{\text{KK}}^2} \sum_{q, q'} S(\bar{q}_i, q_j; \bar{q}'_k, q'_l) Q_q Q_{q'} \left\{ \frac{1}{2L} (\bar{q}\gamma^\mu q) (\bar{q}'\gamma_\mu q') \right. \\ &\quad - 2 (\bar{q}_L\gamma^\mu \Delta'_Q q_L + \bar{q}_R\gamma^\mu \Delta'_q q_R) (\bar{q}'\gamma_\mu q') \\ &\quad \left. + 2L (\bar{q}_L\gamma^\mu \tilde{\Delta}_Q q_L + \bar{q}_R\gamma^\mu \tilde{\Delta}_q q_R) \otimes (\bar{q}'_L\gamma_\mu \tilde{\Delta}_{Q'} q'_L + \bar{q}'_R\gamma_\mu \tilde{\Delta}_{q'} q'_R) \right\}.\end{aligned}\tag{2.185}$$

The same expression holds for the gluon, with $\alpha \rightarrow \alpha_s$ and the electromagnetic charges replaced by the color matrices $T^a \otimes T^a$ inserted in the respective quark bilinears. The

induced interactions arising from the exchange of a Z -boson read

$$\begin{aligned}
 \mathcal{H}_{eff}^{(Z)} = & \frac{4\pi\alpha}{s_w^2 c_w^2 m_Z^2} \left[1 + \frac{m_Z^2}{2M_{KK}^2} \left[1 - \frac{1}{2L} + \mathcal{O}\left(\frac{m_Z^4}{M_{KK}^4}\right) \right] \right] \quad (2.186) \\
 & \times \sum_{q,q'} S(\bar{q}_i, q_j; \bar{q}'_k, q'_l) \left[\bar{q}_L \gamma^\mu T_3^q (\mathbf{1} - \delta_Q) q_L + \bar{q}_R \gamma^\mu T_3^q \delta_q q_R - s_w^2 Q_q \bar{q} \gamma^\mu q \right] \\
 & \times \left[\bar{q}'_L \gamma^\mu T_3^{q'} (\mathbf{1} - \delta_{Q'}) q'_L + \bar{q}'_R \gamma^\mu T_3^{q'} \delta_{q'} q'_R - s_w^2 Q_{q'} \bar{q}' \gamma^\mu q' \right] \\
 & + \frac{4\pi\alpha L}{s_w^2 c_w^2 M_{KK}^2} \sum_{q,q'} S(\bar{q}_i, q_j; \bar{q}'_k, q'_l) \\
 & \left\{ - \left[\bar{q}_L \gamma^\mu T_3^q (\mathbf{1} - \delta_Q) q_L + \bar{q}_R \gamma^\mu T_3^q \delta_q q_R - s_w^2 Q_q \bar{q} \gamma^\mu q \right] \right. \\
 & \times \left[\bar{q}'_L \gamma^\mu T_3^{q'} (\Delta_{Q'} - \varepsilon_{Q'}) q'_L + \bar{q}'_R \gamma^\mu T_3^{q'} \varepsilon_{q'} q'_R - s_w^2 Q_{q'} (\bar{q}'_L \gamma^\mu \Delta_{Q'} q'_L + \bar{q}'_R \gamma^\mu \Delta_{q'} q'_R) \right] \\
 & + \left[\bar{q}_L \gamma^\mu T_3^q (\tilde{\Delta}_Q - \tilde{\varepsilon}_Q) q_L + \bar{q}_R \gamma^\mu T_3^q \tilde{\varepsilon}_q q_R - s_w^2 Q_q (\bar{q}_L \gamma^\mu \tilde{\Delta}_Q q_L + \bar{q}_R \gamma^\mu \tilde{\Delta}_q q_R) \right] \\
 & \left. \otimes \left[\bar{q}'_L \gamma^\mu T_3^{q'} (\tilde{\Delta}_{Q'} - \tilde{\varepsilon}_{Q'}) q'_L + \bar{q}'_R \gamma^\mu T_3^{q'} \tilde{\varepsilon}_{q'} q'_R - s_w^2 Q_{q'} (\bar{q}'_L \gamma^\mu \tilde{\Delta}_{Q'} q'_L + \bar{q}'_R \gamma^\mu \tilde{\Delta}_{q'} q'_R) \right] \right\}.
 \end{aligned}$$

Here, the δ and ε matrices appear due to the non-vectorial coupling of the Z . Also, by writing m_Z , we implicitly assume the RS corrections (2.111) to be absorbed. Here and in the following, $m_{W,Z} \equiv m_{W,Z}^{\text{RS}}$. To a good approximation one can neglect these terms and ends up with a considerably simpler expression, which holds up to order v^4/M_{KK}^4 corrections,

$$\begin{aligned}
 \mathcal{H}_{eqq}^{(Z)} = & \frac{4\pi\alpha}{s_w^2 c_w^2 m_Z^2} \left[1 + \frac{m_Z^2}{2M_{KK}^2} \left[1 - \frac{1}{2L} + \mathcal{O}\left(\frac{m_Z^4}{M_{KK}^4}\right) \right] \right] S(\bar{q}, q; \bar{q}', q') J_Z^\mu J_{Z\mu} \quad (2.187) \\
 & - \frac{8\pi\alpha}{s_w^2 c_w^2 m_Z^2} \sum_q S(\bar{q}_i, q_j; \bar{q}'_k, q'_l) \left[\bar{q}_L \gamma^\mu T_3^q \delta_q q_L - \bar{q}_R \gamma^\mu T_3^q \delta_q q_R \right] J_{Z\mu} \\
 & - \frac{4\pi\alpha L}{s_w^2 c_w^2 M_{KK}^2} \sum_q S(\bar{q}, q; \bar{q}', q') \left[(T_3^q - s_w^2 Q_q) \bar{q}_L \gamma^\mu \Delta_Q q_L - s_w^2 Q_q \bar{q}_R \gamma^\mu \Delta_q q_R \right] J_{Z\mu} \\
 & + \frac{4\pi\alpha L}{s_w^2 c_w^2 M_{KK}^2} \sum_{q,q'} S(\bar{q}, q; \bar{q}', q') \left\{ \left[(T_3^q - s_w^2 Q_q) \bar{q}_L \gamma^\mu \tilde{\Delta}_Q q_L - s_w^2 Q_q \bar{q}_R \gamma^\mu \tilde{\Delta}_q q_R \right] \right. \\
 & \left. \otimes \left[(T_3^{q'} - s_w^2 Q_{q'}) \bar{q}'_L \gamma^\mu \tilde{\Delta}_{Q'} q'_L - s_w^2 Q_{q'} \bar{q}'_R \gamma^\mu \tilde{\Delta}_{q'} q'_R \right] \right\},
 \end{aligned}$$

in which

$$J_Z^\mu \equiv \sum_q \left[(T_3^q - s_w^2 Q_q) \bar{q}_L \gamma^\mu q_L - s_w^2 Q_q \bar{q}_R \gamma^\mu q_R \right]. \quad (2.188)$$

Finally, Higgs exchange leads to the Hamiltonian

$$\begin{aligned}
 \mathcal{H}_{\text{eff}}^{(h)} &= \frac{1}{m_h^2} \sum_{q,q'} S(\bar{q}_i, q_j; \bar{q}'_k, q'_l) \left[\bar{q}_L \frac{\mathbf{m}_q}{v} q_R - \bar{q}_L \left(\frac{\mathbf{m}_q}{v} \boldsymbol{\delta}_q + \boldsymbol{\delta}_Q \frac{\mathbf{m}_q}{v} + \boldsymbol{\Delta} \mathbf{g}_h^q \right) q_R + \text{h.c.} \right] \\
 &\quad \times \left[\bar{q}'_L \frac{\mathbf{m}_{q'}}{v} q'_R - \bar{q}'_L \left(\frac{\mathbf{m}_{q'}}{v} \boldsymbol{\delta}_{q'} + \boldsymbol{\delta}_{Q'} \frac{\mathbf{m}_{q'}}{v} + \boldsymbol{\Delta} \mathbf{g}_h^{q'} \right) q'_R + \text{h.c.} \right] \\
 &\approx \frac{1}{m_h^2 v^2} \sum_{q,q'} S(\bar{q}_i, q_j; \bar{q}'_k, q'_l) \\
 &\quad \times \left[(\bar{q} \mathbf{m}_q q - 2 [\bar{q}_L (\mathbf{m}_q \boldsymbol{\delta}_q + \boldsymbol{\delta}_Q \mathbf{m}_q + v \boldsymbol{\Delta} \mathbf{g}_h^q) q_R + \text{h.c.}]) (\bar{q}' \mathbf{m}_{q'} q') \right],
 \end{aligned} \tag{2.189}$$

in which the second line is an approximation valid up to $\mathcal{O}(v^4/M_{\text{KK}}^4)$ corrections.

Since we are mainly interested in studying FCNCs, we refrain from giving explicit expressions for the effective Hamiltonians describing the exchange of charged gauge bosons, but refer to [150, Sec. 3.3] for the relevant expressions.

One might also expect the previously mentioned radion to give significant contributions to FCNCs, especially since it is often considered the lightest new resonance in RS models in the literature. However, it will only have a mass in the range of the Higgs mass if the Goldberger-Wise potential is tuned,¹⁴ while in a general setup the mass of the radion is of $\mathcal{O}(\text{TeV})$, compare [84, Sec. 6]. Moreover, one finds that the radion couplings to fermions are chirally suppressed, similar to the Higgs, see [128] for a detailed discussion. Since we find that Higgs contributions to FCNCs are negligible, we will also neglect the effects of radion exchange in the analyses in the next chapter.

¹⁴Which is done in many analyses, because it allows for an analytic solution.

3 Solving the Flavor Problem in Strongly Coupled Theories

In this chapter, which I consider the core of the thesis, the flavor problem of strongly coupled theories will be discussed at the hand of the holographic dual RS model. A solution will be proposed, which is successful in theories which do have a dual 5D theory and the consequences of this mechanism for models without holographic interpretation will be explained.

In the first Section 3.1, the compatibility of such models with electroweak precision tests is reviewed. Updates to the published results will be presented as well as a discussion of the significance of those tests for strongly coupled theories.

Section 3.2 collects some examples which show how the RS-GIM mechanism successfully suppresses tree-level mediated flavor changing processes both for $\Delta F = 1$ and for $\Delta F = 2$ currents. For this analysis processes involving b quarks have been chosen which are good tests of the RS-GIM mechanism, as the b is still fairly IR localized. It will be shown that almost all flavor observables can be brought in agreement with a KK scale of a few TeV, with a single exception, ϵ_K , which measures CP-violation in $K - \bar{K}$ -mixing. Even though the quarks involved are in the first and second generation, and therefore UV localized, the traditional pitfall in the flavor sector, the hugely enhanced mixed-chirality operators in $\Delta S = 2$ processes push the KK scale to $M_{\text{KK}} = \mathcal{O}(10)$ TeV.

Section 3.3 will explain this problem and list some solutions proposed in the literature, pointing out their strengths and weaknesses both from the perspective of a strongly coupled theory as well as from the holographic point of view. Subsequently, in Section 3.4 a novel solution will be motivated and discussed in detail. It will be shown how the same mechanism can also solve the flavor problem in composite Higgs models without partial compositeness in Section 3.5, even if they can not be described by a holographic extra dimensional model.

In Section 3.6 a discussion about the implications for the scalar sector will be given and in Section 3.7 the consequences for direct searches of KK particles at the LHC, as well as for flavor violating observables in other sectors are explained.

It should be emphasized that the discussion throughout this chapter concentrates on tree level diagrams and observables which are generated by loops are not computed. The calculation of loops in warped extra dimensions is very involved due to nested sums over internal KK modes and we will be content with quoting important results and otherwise refer to the literature, *e.g.* [129] and [130]. Likewise are lepton flavor violating observables not considered, as the implementation of the lepton sector requires further model building (the localization along the extra dimension does not readily yield the correct mixing angles). For this is also referred to the relevant literature [131].

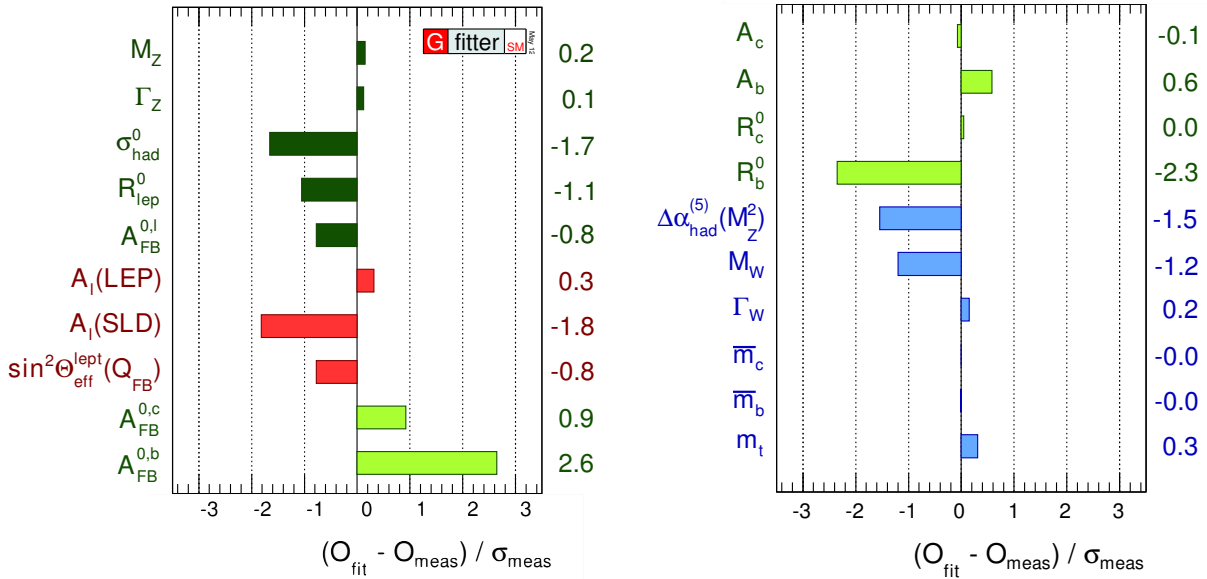


Figure 3.1: This is a list of electroweak precision observables published by the GFitter group [133]. A definition of the observables can be found in the original paper or for example in [132, Sec.3A]. The bars show the deviation of the measurements from the SM predictions in standard deviation.

3.1 Electroweak Precision Observables

The main focus of this thesis is on flavor changing processes. It is nevertheless important to consider implications from flavor conserving observables, especially if they have direct impact on the later discussions. Electroweak precision tests are a measure of new physics contributions to flavor conserving four fermion scattering processes, including both propagator and vertex corrections. They are an important check for new physics models and a particularly hard one for strongly coupled theories. In this section the reasons for this and the implications for the Randall Sundrum model will be discussed.

It is assumed that the reader is familiar with the list of electroweak observables compiled in Figure 3.1. A detailed explanation for each observable can for example be found in [132, Sec.3A]. Indicated by the bars are the degrees of compatibility of the experimental values with the SM predictions measured in standard deviations, the so-called *pull*. Historically, fits to these observables have been used to successfully predict the mass of the top quark before its direct observation [132, Sec.3A]. Likewise, a global fit to these data has been used to constrain the Higgs mass window before its discovery. However, since Higgs-induced loops lead to logarithmic corrections, *e.g.* $\sim \ln m_h/m_Z$, while quark loops induce quadratic corrections $\sim m_t^2/m_Z^2$, the top mass was a rather precise prediction, whereas the Higgs mass bound from the latest fit

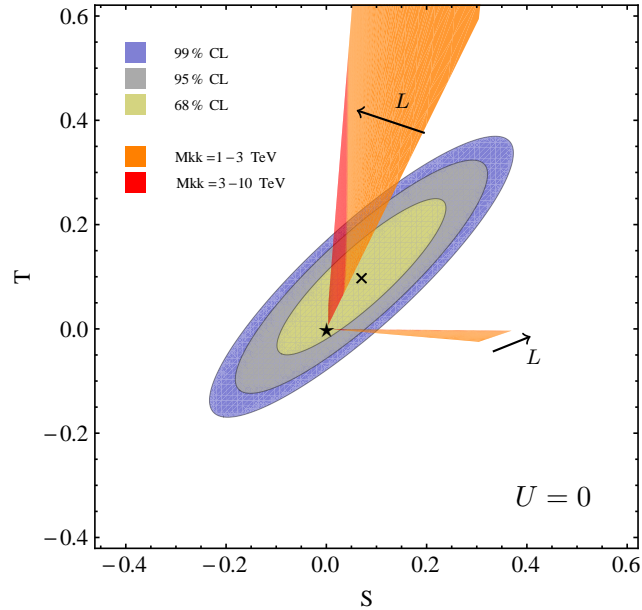


Figure 3.2: The plots show regions of 68%, 95% and 99% probability in the $S - T$ plane. Shaded red (orange) are the accessible regions for $M_{KK} \in [1 - 3]$ TeV ($M_{KK} \in [3 - 10]$ TeV) for the minimal model (growing vertically towards large T) and for the custodially protected model (the horizontal stripe). The black arrows point in the direction of growing volume $L \in [5, 36]$.

[133],

$$m_h = 96_{-24}^{+31} \text{ GeV}, \quad (3.1)$$

can only be considered a rough guide pointing towards a rather light Higgs. These global fits do not only constrain the masses of hypothetical SM particles, but also of new physics resonances which contribute through radiative corrections. Basically every light new resonance with an electroweak quantum number is supposed to show up as a discrepancy in Figure 3.1. Possible cancellations of these contributions could therefore still have explained why the Higgs would be heavier than allowed by the SM fit (3.1), until it was finally found at $m_h \approx 126$ GeV [134, 135]. This makes electroweak precision test an even more powerful tool to constrain new physics, because every possible cancellation must occur between the new resonances and should therefore be predicted by the model at hand.

Oblique Parameters

All observables in Figure 3.1 show very good agreement with the SM, which is synonym with no deviation at 3σ or more. Apart from couplings of the Z to bottom quarks,

measured by $R_b^0 = \Gamma_{Z \rightarrow b\bar{b}}^{\text{had}} / \Gamma_Z^{\text{had}}$, which denotes the ratio of $Z \rightarrow b\bar{b}$ decays and the full hadronic Z branching ratio, as well as $A_{\text{FB}}^{b\bar{b}}$, the forward-backward asymmetry of the same decay channel, not even a 2σ discrepancy is observed. Both of these observables are sensitive to vertex corrections. New contributions to the electroweak gauge boson propagators should therefore exhibit a particular good agreement with the SM. Following Peskin and Takeuchi [136, 137], it makes therefore sense to define parameters, which quantify New Physics contributions to the electroweak gauge boson propagators (1.7), in writing

$$\Pi_{ab}(q^2) = \Pi_{ab}^{\text{SM}}(q^2) + \delta\Pi_{ab}(q^2), \quad (3.2)$$

for all allowed combinations $ab = \gamma\gamma, Z\gamma, ZZ$ and WW . Assuming that the new physics scale is large compared to the gauge boson masses, one can expand its contribution in (3.2) up to linear order in q^2 ,

$$\delta\Pi_{ab}(q^2) \approx \delta\Pi_{ab}(0) + q^2\delta\Pi'_{ab}(0). \quad (3.3)$$

From the eight parameters $\delta\Pi_{ab}(0), \delta\Pi'_{ab}(0)$, three are fixed by the renormalization of the three SM input parameters G_F, α and m_Z . Two are zero by gauge invariance, $\delta\Pi_{\gamma\gamma}(0) = \delta\Pi_{\gamma Z}(0) = 0$, and therefore all New Physics effects can be described by three linear combinations. The values of the SM contributions $\Pi_{ab}^{\text{SM}}(q^2)$ are normalized to zero, so that we can define the *oblique parameters* [137],

$$\begin{aligned} S &= \frac{4s_w^2 c_w^2}{\alpha} \left[\Pi'_{ZZ}(0) + \frac{s_w^2 - c_w^2}{s_w c_w} \Pi'_{Z\gamma}(0) - \Pi'_{\gamma\gamma}(0) \right], \\ T &= \frac{1}{\alpha c_w^2 m_Z^2} \left[\Pi_{WW}(0) - c_w^2 \Pi_{ZZ}(0) \right], \\ U &= \frac{4s_w^2}{\alpha} \left[\Pi'_{WW}(0) - c_w^2 \Pi'_{ZZ}(0) - 2s_w c_w \Pi'_{Z\gamma}(0) - s_w^2 \Pi'_{\gamma\gamma}(0) \right]. \end{aligned} \quad (3.4)$$

The SM values are by construction $S = T = U = 0$, and we anticipate that $U = 0$ to leading order in the RS model as well. In this case, the best fit to the experimental input values results in [133]

$$\begin{aligned} S_{\text{exp}} &= 0.07 \pm 0.09, \\ T_{\text{exp}} &= 0.10 \pm 0.08, \end{aligned} \quad \rho = \begin{pmatrix} 1.00 & 0.88 \\ 0.88 & 1.00 \end{pmatrix}, \quad (3.5)$$

in which ρ denotes the correlation matrix and a Higgs mass of $m_h = 120$ GeV was used as an input.

One can think of the S parameter as the number of degrees of freedom running in the loop. In strongly coupled theories typically the number of colors and the number of flavors tends to be large, in order to allow for a walking coupling and an embedding in an ETC group. Therefore one finds using naive dimensional analysis (NDA) [138], that $S \sim N_F N_C / \pi$ in TC theories, or alternatively $S \sim 0.3$ extrapolated from QCD [136, Sec.VII]. This makes the S parameter, besides the top mass, one of the most difficult challenges for strongly coupled theories. The T parameter can be considered a measure of additional isospin breaking from fermions running in the loops. In TC models, $T \sim 1/(4\pi)$ and thus negligible in most cases. The reason is, that the T

parameter is related to $\rho = m_W^2/(m_Z^2 c_w^2) = 1 + \alpha T$, which is protected by the approximate global $SU(2)_L \times SU(2)_R$ symmetry of the Higgs sector. This global symmetry, is generally assumed to be realized in TC extensions of the SM as well, which leads to small deviations.

In the minimal RS model, the leading contributions to the oblique parameters arise from mixing of the KK excitations into the zero mode gauge bosons, [115, 140, 139],

$$S = \frac{2\pi v^2}{M_{\text{KK}}^2} \left(1 - \frac{1}{L}\right), \quad T = \frac{\pi^2 v}{2c_w^2 M_{\text{KK}}^2} \left(L - \frac{1}{L}\right). \quad (3.6)$$

The result is shown in Figure 3.2, in which the cross is at the best fit point with 68%, 95% and 99% confidence level (CL) ellipses in shades of yellow, gray and blue respectively, the star is the SM prediction and the orange (red) band rising in the direction of a large T parameter shows (3.6) for a KK scale of 3 – 10 TeV (1 – 3) TeV. In addition, the effect of varying the volume of the extra dimension $L \in [5, 36]$ is plotted with increasing L in the direction of the arrow. Two things are remarkable here. First, the S parameter seems to be under control. This can be interpreted as an unexpected nice result from the holographic theory, because it seems to contradict the estimates relying on NDA or upscaled QCD (keep in mind that the RS model is dual to a large N_c strongly coupled theory). However, it was shown for holographic higgsless models, that if one localizes the fermions on the UV brane, a large positive contribution to S in very good agreement with the naive estimates occurs, compare [141, Sec.3]. On the other hand, models with IR brane localized fermions give large (order L) negative contributions to S , as discovered in [142, Sec.3].

In [143] these results could be explained by showing that the contributions to the S parameter are sensitive to the localization of the fermions and vanish for $c \approx -1/2$. This dependence is not visible in (3.6), because we only consider universal corrections there. It can be motivated in the dual theory described in Section 2.2, how a different fermion localization may affect the S parameter. If the quarks are confined to the UV brane, they are elementary fermions with direct couplings to the electroweak gauge bosons and reproduce the SM quark contributions to S , while the composite fields live in the IR and contribute in agreement with what we expect from a strongly interacting theory. Confining the quarks to the IR brane makes them fully composite and couplings to the electroweak gauge bosons can only occur through mixing with composite vector bosons (there is no direct coupling due to the large anomalous dimension of IR localized fields). Therefore, the contribution from the elementary quarks to the reference value $S = 0$ is not present in this model, resulting in a negative value of S , even though the technifermions still give positive corrections. The possibility to achieve moderate S can therefore be viewed as another advantage of partially composite fermions.

The second remark is, that the T parameter is enhanced by a volume factor and therefore significantly larger than expected from NDA. An explanation can also be found from the dual description. In Section 2.2 it was shown that a global symmetry in the strongly coupled theory is described by a bulk gauge symmetry. As pointed out above, the T parameter is small because it is protected by a global symmetry, the custodial $SU(2)_L \times SU(2)_R$. The minimal model as shown in Figure 2.1, with the SM gauge

group only, does not correspond to a theory with such a protection and therefore the T parameter turns out to be large. One can therefore consider a custodial symmetry indispensable for any extension of the SM, and in the custodially protected RS model with an corresponding extended bulk group one finds [114],

$$S = \frac{2\pi v^2}{M_{\text{KK}}^2} \left(1 - \frac{1}{L}\right), \quad T = -\frac{\pi^2 v}{2c_w^2 M_{\text{KK}}^2} \frac{1}{L}, \quad (3.7)$$

as shown in Figure 3.2 by the orange band extending from the SM prediction towards larger S .

One can think of other solutions, for example a version of the RS model in which the volume factor L is smaller than 36. The effect of this modification is shown in Figure 3.2 as well, in which the volume factor grows from $L = 5$ to $L = 36$ along the black arrows. The physical meaning of such a truncation is that the gauge hierarchy problem will only be cured up to some intermediate scale $\Lambda_{\text{UV}} = e^L$ TeV. Based on little Higgs models, these models are called *little RS* (LRS) models and just like the little Higgs model they need some UV completion already at $\Lambda_{\text{UV}} = e^L$ TeV. Since lowering the volume factor will affect many observables also in the flavor sector, we will come back to this option when we discuss FCNCs.

Corrections to $Z \rightarrow b\bar{b}$

The only observables with at least moderate deviations from the SM in 3.1 are sensitive to corrections to the $Zb\bar{b}$ vertex. Since the left-handed b quark is the weak isospin partner of the top, they share the same 5D mass or localization parameter c_{Q_3} in the RS model. In order to generate the large top mass, c_{Q_3} is shifted towards the IR compared to the light quark localizations. Consequentially, one should expect sizable corrections from the RS model.

From (2.113) and the structures defined in (2.175) it follows that the Z -vertex correction for general external quark flavors can be written in the form

$$\begin{aligned} \mathcal{L}_{4\text{D}} \ni & \frac{g}{\cos \theta_W} \left[1 + \frac{m_Z^2}{4M_{\text{KK}}^2} \left(1 - \frac{1}{L}\right) \right] Z_\mu^0 \\ & \times \sum_{ij} \left[(g_L^q)_{ij} \bar{q}_{L,i} \gamma^\mu q_{L,j} + (g_R^q)_{ij} \bar{q}_{R,i} \gamma^\mu q_{R,j} \right], \end{aligned} \quad (3.8)$$

in which

$$\begin{aligned} \mathbf{g}_L^q &= (T_3^q - \sin^2 \theta_W Q_q) \left[\mathbf{1} - \frac{m_Z^2}{2M_{\text{KK}}^2} (L \mathbf{\Delta}_Q - \mathbf{\Delta}'_Q) \right] - T_3^q \left[\mathbf{\delta}_Q - \frac{m_Z^2}{2M_{\text{KK}}^2} (L \mathbf{\epsilon}_Q - \mathbf{\epsilon}'_Q) \right], \\ \mathbf{g}_R^q &= -\sin^2 \theta_W Q_q \left[\mathbf{1} - \frac{m_Z^2}{2M_{\text{KK}}^2} (L \mathbf{\Delta}_q - \mathbf{\Delta}'_q) \right] + T_3^q \left[\mathbf{\delta}_q - \frac{m_Z^2}{2M_{\text{KK}}^2} (L \mathbf{\epsilon}_q - \mathbf{\epsilon}'_q) \right], \end{aligned} \quad (3.9)$$

with $i, j = 1, 2, 3$ denoting flavor indices and $T_3^d = -\frac{1}{2}$ and $Q^d = -\frac{1}{3}$ the corresponding weak isospin and charge for down type quarks. Relevant for the $Zb\bar{b}$ vertex are the 33

elements of these matrices, that is the modifications to the flavor universal couplings. In general the Z coupling to light quarks is modified as well. However, because of the UV localization of the corresponding bulk fields, the SM expressions $(g_L^q)_{11} = T_3^q - \sin_W \theta_W Q^q$ and $(g_R^q)_{11} = -\sin^2 \theta_W Q^q$ are excellent approximations and the production can assumed to be SM like.¹ With the help of the ZMA (2.180) and (2.184), we obtain

$$g_L^b \equiv (g_L^d)_{33} \rightarrow \left(-\frac{1}{2} + \frac{\sin^2 \theta_W}{3} \right) \left[1 - \frac{m_Z^2}{2M_{\text{KK}}^2} \frac{F^2(c_{b_L})}{3 + 2c_{b_L}} \left(L - \frac{5 + 2c_{b_L}}{2(3 + 2c_{b_L})} \right) \right] \quad (3.10)$$

$$+ \frac{m_b^2}{2M_{\text{KK}}^2} \left[\frac{1}{1 - 2c_{b_R}} \left(\frac{1}{F^2(c_{b_R})} - 1 + \frac{F^2(c_{b_R})}{3 + 2c_{b_R}} \right) + \sum_{i=1,2} \frac{|(Y_d)_{3i}|^2}{|(Y_d)_{33}|^2} \frac{1}{1 - 2c_{d_i}} \frac{1}{F^2(c_{b_R})} \right],$$

$$g_R^b \equiv (g_R^d)_{33} \rightarrow \frac{\sin^2 \theta_W}{3} \left[1 - \frac{m_Z^2}{2M_{\text{KK}}^2} \frac{F^2(c_{b_R})}{3 + 2c_{b_R}} \left(L - \frac{5 + 2c_{b_R}}{2(3 + 2c_{b_R})} \right) \right] \quad (3.11)$$

$$- \frac{m_b^2}{2M_{\text{KK}}^2} \left[\frac{1}{1 - 2c_{b_L}} \left(\frac{1}{F^2(c_{b_L})} - 1 + \frac{F^2(c_{b_L})}{3 + 2c_{b_L}} \right) + \sum_{i=1,2} \frac{|(Y_d)_{i3}|^2}{|(Y_d)_{33}|^2} \frac{1}{1 - 2c_{Q_i}} \frac{1}{F^2(c_{b_L})} \right],$$

in which the notation $c_{b_L} \equiv c_{Q_3}$ and $c_{b_R} \equiv c_{d_3}$ is introduced. The terms in the second lines in (3.10) and (3.11) come from the ZMA expressions of the δ matrices and are further suppressed by m_b/m_Z , so that the leading terms are controlled by the zero mode profiles $F(c_{b_L})$ and $F(c_{b_R})$.

The ratio of the width of the Z^0 -boson decay into bottom quarks and the total hadronic width R_b^0 , the bottom quark left-right asymmetry parameter A_b , and the forward-backward asymmetry for bottom quarks $A_{\text{FB}}^{0,b}$, are given in terms of the left- and right-handed bottom quark couplings as [145]

$$R_b^0 = \left[1 + \frac{4 \sum_{q=u,d} [(g_L^q)^2 + (g_R^q)^2]}{\eta_2 \eta_{\text{QCD}} \eta_{\text{QED}} [(1 - 6z_b)(g_L^b - g_R^b)^2 + (g_L^b + g_R^b)^2]} \right]^{-1},$$

$$A_b = \frac{2\sqrt{1 - 4z_b} \frac{g_L^b + g_R^b}{g_L^b - g_R^b}}{1 - 4z_b + (1 + 2z_b) \left(\frac{g_L^b + g_R^b}{g_L^b - g_R^b} \right)^2}, \quad A_{\text{FB}}^{0,b} = \frac{3}{4} A_e A_b, \quad (3.12)$$

where $\eta_{\text{QCD}} = 0.9954$ and $\eta_{\text{QED}} = 0.9997$ are QCD and QED radiative correction factors. The factor $\eta_2 = 0.99386$ takes into account the recently published fermionic two loop contributions computed in [147], which are the only reason for the significant pull of R_b^0 in Figure 3.1. The parameter $z_b \equiv m_b^2(m_Z)/m_Z^2 = 0.997 \cdot 10^{-3}$ describes the effects of the non-zero bottom quark mass. As explained above, left- and right-handed couplings of the light quarks, g_L^q and g_R^q , and the asymmetry parameter of the electron, A_e can be assumed SM like and we fix these quantities to their SM values. In what follows we will employ $g_L^u = 0.34674$, $g_R^u = -0.15470$, $g_L^d = -0.42434$, $g_R^d = 0.077345$ and $A_e = 0.1473$ for the SM predictions [146, Table G3].

¹For electrons as initial state the modifications are even smaller.

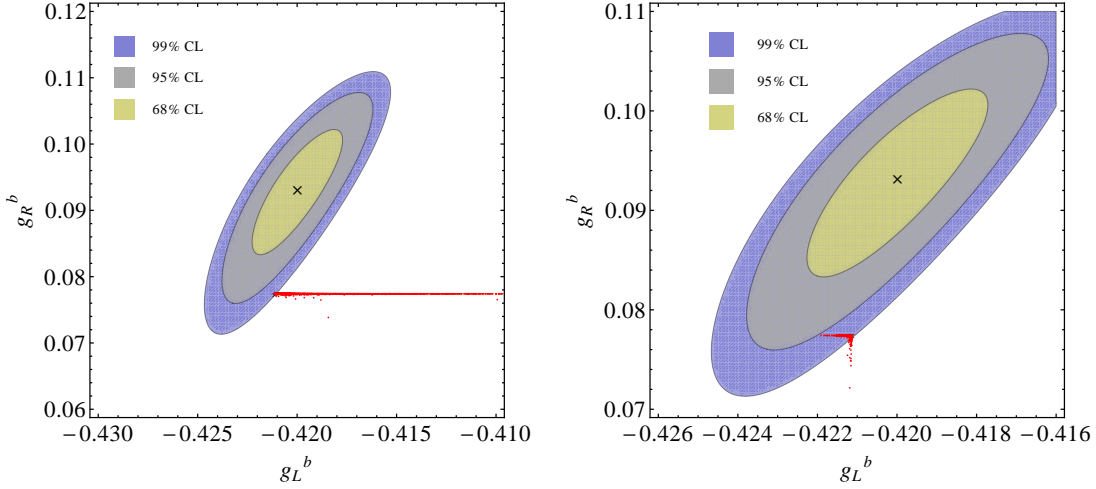


Figure 3.3: The plots show regions of 68%, 95% and 99% probability in the $g_L^b - g_R^b$ plane. The best fit value is denoted with a cross and the experimental value with a star. The red colored regions indicate the predicted values of a large set of parameter points for the minimal RS model in the left panel and for the RS model with custodial protection in the right panel.

Inserting the predicted SM values $g_L^b = -0.42114$ and $g_R^b = 0.077420$ [146, Table G3] for the left- and right-handed bottom-quark couplings into the relations (3.12), we obtain for the central values of the quantities in question

$$R_b^0 = 0.21474, \quad A_b = 0.935, \quad A_{FB}^{0,b} = 0.1032. \quad (3.13)$$

In comparison, the experimentally extracted values for the three “pseudo observables” read [146]

$$\begin{aligned} R_b^0 &= 0.21629 \pm 0.00066, \\ A_b &= 0.923 \pm 0.020, \\ A_{FB}^{0,b} &= 0.0992 \pm 0.0016, \end{aligned} \quad \rho = \begin{pmatrix} 1.00 & -0.08 & -0.10 \\ -0.08 & 1.00 & 0.06 \\ -0.10 & 0.06 & 1.00 \end{pmatrix}, \quad (3.14)$$

where ρ is the correlation matrix. This reproduces the deviations listed in Table 3.1. In contrast to the original analysis in [115, Sec. 6.4], the theoretical corrections to R_b^0 pull the best fit value 3σ away from the experimental SM value, as can be seen in Figure 3.3, in which the best fit is denoted by a cross and the experimental value by a star.

A new physics contribution that would improve this situation needs a large positive correction to g_R^b of the order of 20% and no contribution to g_L^b (while a small negative shift would also improve the fit). As becomes clear from (3.10) and (3.11), RS corrections reduce the SM value of both g_R^b and g_L^b in magnitude, which corresponds to a negative shift of g_R^b and a positive one for g_L^b , pointing in exactly the opposite direction. In addition, the corrections to g_R^b are smaller by a factor of roughly

$\delta g_R^b / \delta g_L^b \sim F(c_{b_R})^2 / F(c_{b_L})^2$ for $\delta g^b = (g_{\text{RS}}^b - g_{\text{SM}}^b) / g_{\text{SM}}^b$, which is typically of the order of a few percent, because c_{b_L} is more IR localized in order to help realizing the large top mass in (2.158). The scaling on the plot in the left panel of Figure 3.3 however makes the g_R^b corrections completely invisible. As a consequence, our set of parameter points, which is chosen so that the correct quark masses and mixings are reproduced (see Appendix A for details), lies entirely in the red band shown in the left panel of Figure 3.3 and therefore fails to agree with the experiment within 3σ for the majority of points.

Note, that the scaling of Figure 3.3 distorts the fact that there are still 10% of the parameter points in the 3σ ellipse. Translating this into a constraint for M_{KK} would yield a very strong bound. One can invoke the reparametrization invariance introduced in section 2.5 in order to examine the characteristics of the parameter corner which is in agreement with this constraint. By reshuffling between $F(c_{b_L})$ and $F(c_{b_R})$ using (2.169), for $\eta < 1$, one increases $\delta g_R^b / \delta g_L^b$. For $\eta = 1/2(1/3)$, about 35(45)% of the parameter points do at least not aggravate the already large discrepancy between the SM and the experiment. Thus, parameter points with strongly IR localized right-handed bottom quarks tend to give less dangerous corrections to the global fit in (3.14).

It is interesting to discuss the implications for the dual theory of such a considerable reparametrization. Scaling down $F(c_{b_L})$ will not only enlarge $F(c_{b_R})$, but also $F(c_{t_R})$, the zero mode of the right-handed top, which is already strongly IR localized. In a generalization of this shift to all generations, one can assume that all doublets are extremely UV localized and all singlets shifted towards the IR. The dual theory of such a model would have, to a good approximation, only right-handed quarks composites, while the left-handed quarks are elementaries. This *right-handed compositeness* was found to be a very attractive idea in [149], in which the relevance for the $Z\bar{b}b$ vertex was however not pointed out. In the later sections we will get back to this scenario and check the compatibility with other observables.

This situation is also ameliorated by the mixing between the Z zero mode and the additional neutral composite vector bosons of the $SU(2)_R$ present in the custodially protected RS model [148]. This is especially intriguing, because as discussed in the previous section, the scalar sector of any extension of the SM should respect the custodial symmetry in order to not get into conflict with the oblique parameters. The mixing eliminates completely the L enhanced term in g_L^b and increases the L enhanced term in g_R^b by $L \rightarrow \frac{3c_w^2}{s_w^2} L \approx 10L$. Therefore, corrections to g_L^b are dominated by the terms in the second line of (3.10), which can now account for both negative and positive modifications, controlled by the interplay of the singlet down quark localization parameters of all generations. Choosing the correct quark representations under the enlarged symmetry group and assuming the bulk symmetric under the exchange $SU(2)_L \leftrightarrow SU(2)_R$, will further reduce the correction to g_L^b and make them purely

negative, so that one finds to leading order (see [114] for details and the derivation)

$$g_L^b = \left(-\frac{1}{2} + \frac{s_w^2}{3} \right) \left[1 + \frac{m_Z^2}{2M_{\text{KK}}^2} \frac{F^2(c_{b_L})}{3 + 2c_{b_L}} \frac{5 + 2c_{b_L}}{2(3 + 2c_{b_L})} \right] + \frac{m_b^2}{2M_{\text{KK}}^2} \frac{1}{1 - 2c_{b_R}} \left(\frac{F^2(c_{b_R})}{3 + 2c_{b_R}} - 1 \right), \quad (3.15)$$

$$g_R^b = \frac{s_w^2}{3} \left[1 - \frac{m_Z^2}{2M_{\text{KK}}^2} \frac{F^2(c_{b_R})}{3 + 2c_{b_R}} \left(\frac{3c_w^2}{s_w^2} L - \frac{5 + 2c_{b_R}}{2(3 + 2c_{b_R})} \right) \right] - \frac{m_b^2}{2M_{\text{KK}}^2} \left[\frac{1}{1 - 2c_{b_L}} \left(\frac{1}{F^2(c_{b_L})} - 1 + \frac{F^2(c_{b_L})}{3 + 2c_{b_L}} \right) + \sum_{i=1,2} \frac{|(Y_d)_{i3}|^2}{|(Y_d)_{33}|^2} \frac{1}{1 - 2c_{Q_i}} \frac{1}{F^2(c_{b_L})} \right]. \quad (3.16)$$

Here, $\delta g_R^b / \delta g_L^b > 1$, and the right-handed corrections will lead to a worse than 3σ discrepancy for some parameter points. Despite the misleading scatterplot however, more than 99% of the parameter points are in the 3σ CL ellipsis in Figure 3.3.

Interestingly, with the new fit, the corrections to g_L^b tend to slightly improve the situation compared to the SM. Both is evident from the plot on the right hand side of Figure 3.3, which shows the same set of parameter points as the left plot for the couplings in the custodially protected RS model (3.15) and (3.16). Note, that an improvement can be achieved for small M_{KK} , which should be contrasted with the model without custodial symmetry discussed above, in which a large new physics scale is preferred in order to not spoil the fit. Also, the reparametrization invariance can be used in favor of an IR shift of the left-handed profiles for even better agreement with the measurements.²

This shows that the custodial protection is sufficient to protect the T parameter and allows for an even slight attenuation of the tension from the fit to R_b^0 , A_b and $A_{FB}^{0,b}$. Even though other solutions exist, we will assume that the custodial protection in the SM is not broken by the underlying theory, in order not to be pushed to a corner of parameter space or having to resort to a large M_{KK} scale for agreement with electroweak precision tests.

3.2 RS GIM Working

The present status of flavor physics is characterized by a large number of precision results on B , D and K decays which are in tantalizing agreement with the SM picture of flavor and CP violation. In the RS model, the KK modes generate tree-level FCNCs, which are ultimately caused by the flavor non-universal couplings in (1.34), and are suppressed by the mixing angles in (1.34) or equivalently by the zero-mode profiles (2.150) in the context of the RS-GIM mechanism.

In the following it will be demonstrated how the RS-GIM mechanism successfully suppresses FCNCs by using observables involving b quarks, which have a large composite

²It should be pointed out, that in the custodial model without the P_{LR} symmetry, many parameter points end up in the 2σ ellipsis in Figure 3.3. Since this is not a consequence of a physically motivated parameter choice, but depends on the random relative size of the right-handed localization parameters and Yukawa matrices, we will not discuss this scenario.

component and therefore the RS-GIM suppression is weak compared to the lighter flavors. In addition, constraints derived from the analysis in section 3.1 will have the most immediate impact. We will concentrate on observables which have recently been measured very precisely at LHCb and lead to stringent bounds on any new physics which allow for FCNCs. A very comprehensive analysis of flavor observables can be found in the original paper [150].

$B_s - \bar{B}_s$ Mixing

We will demonstrate the effectiveness of the RS-GIM mechanism first on the example of $B_s - \bar{B}_s$ mixing. A short review of neutral meson mixing is given in Appendix B and we will concentrate on the characteristics of the B_s system here.

Since no first generation quarks are involved, it is the perfect place to test the limits of the RS-GIM mechanism. In the original analysis, the constraints from the $Zb\bar{b}$ vertex have been employed as a filter for viable parameter points, however the updated experimental situation makes it necessary to enlarge the electroweak bulk gauge group to $SU(2)_L \times SU(2)_R \times U(1)_X$ in order to not introduce fine-tuning in this observable, as discussed in the last section. That means, we discard parameter points which lie outside of the 99% CL ellipse in the right panel of Figure 3.3.

While in the SM only left-handed currents contribute through box diagrams with W^\pm exchange, in the RS model also right-handed currents appear, because contributions arise already from tree-level diagrams mediated by KK gluons, KK photons as well as the Z zero mode and KK modes. We therefore adopt the following general parametrization of new physics effects in neutral meson mixing [151, 152, 153]

$$\mathcal{H}_{eff}^{\Delta B=2} = \sum_{i=1}^5 C_i Q_i^{bs} + \sum_{i=1}^3 \tilde{C}_i \tilde{Q}_i^{bs}, \quad (3.17)$$

where

$$\begin{aligned} Q_1^{bs} &= (\bar{s}_L \gamma^\mu b_L) (\bar{s}_L \gamma_\mu b_L), \\ \tilde{Q}_1^{bs} &= (\bar{s}_R \gamma^\mu b_R) (\bar{s}_R \gamma_\mu b_R), \\ Q_4^{bs} &= (\bar{s}_R b_L) (\bar{s}_L b_R), \\ Q_5^{bs} &= (\bar{s}_R^\alpha b_L^\beta) (\bar{s}_L^\beta b_R^\alpha). \end{aligned} \quad (3.18)$$

A summation over color indices α, β is understood and the Wilson coefficients are denoted as a sum of a SM and a new physics contribution, $C_i \equiv C_i^{\text{SM}} + C_i^{\text{RS}}$ (where in the SM only C_1^{SM} is non-zero). After splitting the gluon propagator into $U(N_C)$ and $U(1)$ part,

$$\sum_a T_{\alpha\beta}^a T_{\sigma\rho}^a = \frac{1}{2} \left(\delta_{\alpha\rho} \delta_{\beta\sigma} - \frac{1}{N_C} \delta_{\beta\alpha} \delta_{\rho\sigma} \right), \quad (3.19)$$

one can obtain from the general results (2.185) and (2.187) along with standard Fierz identities and a symmetry factor³ $S_{sbsb} = 1/2$, the contributions arising in the RS model

$$\begin{aligned}
C_1^{\text{RS}} &= \frac{2\pi L}{M_{\text{KK}}^2} (\tilde{\Delta}_D)_{23} \otimes (\tilde{\Delta}_D)_{23} \left[\frac{\alpha_s}{2} \left(1 - \frac{1}{N_c} \right) + Q_d^2 \alpha + \omega_Z^{DD} \frac{(T_3^D - s_w^2 Q_d)^2 \alpha}{s_w^2 c_w^2} \right], \\
\tilde{C}_1^{\text{RS}} &= \frac{2\pi L}{M_{\text{KK}}^2} (\tilde{\Delta}_d)_{23} \otimes (\tilde{\Delta}_d)_{23} \left[\frac{\alpha_s}{2} \left(1 - \frac{1}{N_c} \right) + Q_d^2 \alpha + \omega_Z^{dd} \frac{(s_w^2 Q_d)^2 \alpha}{s_w^2 c_w^2} \right], \\
C_4^{\text{RS}} &= \frac{2\pi L}{M_{\text{KK}}^2} (\tilde{\Delta}_D)_{23} \otimes (\tilde{\Delta}_d)_{23} [-2\alpha_s], \\
C_5^{\text{RS}} &= \frac{2\pi L}{M_{\text{KK}}^2} (\tilde{\Delta}_D)_{23} \otimes (\tilde{\Delta}_d)_{23} \left[\frac{2\alpha_s}{N_c} - 4Q_d^2 \alpha + \omega_Z^{Dd} \frac{4s_w^2 Q_d (T_3^D - s_w^2 Q_d) \alpha}{s_w^2 c_w^2} \right],
\end{aligned} \tag{3.20}$$

where $Q_d = -1/3$, $T_3^D = -1/2$, $\omega_{qq'}^Z = 1$ for all $q, q' \in \{d, D\}$ and $N_c = 3$ in the minimal model. For the custodially protected model [167, App. C],

$$\omega_{qq'}^Z = 1 + \frac{1}{c_w^2 - s_w^2} \left(\frac{s_w^2 (T_{3L}^q - Q_d) - c_w^2 T_{3R}^q}{T_{3L}^q - s_w^2 Q_d} \right) \left(\frac{s_w^2 (T_{3L}^{q'} - Q_d) - c_w^2 T_{3R}^{q'}}{T_{3L}^{q'} - s_w^2 Q_d} \right), \tag{3.21}$$

in which the $SU(2)_R \times SU(2)_L$ quantum numbers are completely fixed if the P_{LR} parity is imposed. It follows $T_{3L}^D = T_3^D = -1/2$, $T_{3R}^D = 1/2$, $T_{3L}^d = 0$, $T_{3R}^d = 1$, compare [114, Table 2].

In (3.20) the expressions in brackets refer, in an obvious way, to the contributions from KK gluons, KK photons, and from the Z boson and its KK excitations. As stated before, $\Delta F = 2$ contributions from flavor-changing Higgs-boson exchange are of $\mathcal{O}(v^4/M_{\text{KK}}^4)$ and we thus will not give them explicitly.

In the language of the dual theory, the overlap integrals (2.176) correspond to the exchange of the infinite tower of composites described by the diagram in the third line of Figure 2.7.

Note, that the leading contributions to (3.20) clearly result from KK gluon exchange, but in the custodial model one finds $\omega_{DD}^Z \approx 3$, $\omega_{dd}^Z \approx 129$ and $\omega_{Dd}^Z \approx -15$, so that the right-handed currents are subject to sizable corrections from the new $SU(2)_R$ KK modes, which also partially cancel the gluon contributions to C_5^{RS} , because they enter with opposite signs [154].

The tree-level expressions for the Wilson coefficients given above refer to a renormalization scale $\mu_{\text{KK}} = \mathcal{O}(M_{\text{KK}})$. They must be evolved down to a scale $\mu \approx m_b$, where the hadronic matrix elements of the four-quark operators can be evaluated using lattice QCD. The renormalized coefficients are given by [155],

$$C_i(m_b) = \sum_{j,k} \left(b_k^{(i,j)} + \eta c_k^{(i,j)} \right) \eta^{a_k} C_j(M_{\text{KK}}), \tag{3.22}$$

³In the full theory, a t and an s channel diagram provide an equal contribution and the effective theory four quark vertex can be constructed in four different ways.

in which $\eta \equiv (\alpha_s(M_{KK})/\alpha_s(m_t))$ and the $a_k, b_k^{(i,j)}$ and $c_k^{(i,j)}$ denote the “magic numbers” collected in Appendix C, which basically parameterize the anomalous dimension matrix.

The hadronic matrix elements of the various operators are customarily expressed in terms of the *bag parameters* B_i . For the operators relevant to our analysis, one has⁴

$$\begin{aligned}\langle B_s^0 | Q_1(\mu) | \bar{B}_s^0 \rangle &= \langle B_s^0 | \tilde{Q}_1(\mu) | \bar{B}_s^0 \rangle = \left(1 + \frac{1}{N_c}\right) \frac{m_{B_s} f_{B_s}^2}{4} B_1^{bs}(\mu), \\ \langle B_s^0 | Q_4(\mu) | \bar{B}_s^0 \rangle &= \left[\frac{m_{B_s}}{m_b(\mu) + m_s(\mu)} \right]^2 \frac{m_{B_s} f_{B_s}^2}{4} B_4^{bs}(\mu), \\ \langle B_s^0 | Q_5(\mu) | \bar{B}_s^0 \rangle &= \frac{1}{N_c} \left[\frac{m_{B_s}}{m_b(\mu) + m_s(\mu)} \right]^2 \frac{m_{B_s} f_{B_s}^2}{4} B_5^{bs}(\mu).\end{aligned}\quad (3.23)$$

These definitions are such that in the vacuum-insertion approximation (VIA)

$$\begin{aligned}\left[B_1^{bs}(\mu) \right]_{\text{VIA}} &= 1, \\ \left[B_4^{bs}(\mu) \right]_{\text{VIA}} &= 1 + \frac{1}{2N_c} \left[\frac{m_b(\mu) + m_s(\mu)}{m_{B_s}} \right]^2, \\ \left[B_5^{bs}(\mu) \right]_{\text{VIA}} &= 1 + \frac{N_c}{2} \left[\frac{m_b(\mu) + m_s(\mu)}{m_{B_s}} \right]^2,\end{aligned}\quad (3.24)$$

Lattice simulations quantify the deviation from the naive VIA results parameterized by the bag parameters B_i^{bs} [156] which are collected in Appendix C. Furthermore, we use $m_{B_s} = 5366.8 \text{ MeV}$ [157] and $f_{B_s} = 231 \text{ MeV}$ [160] for the B_s meson mass and decay constant [157].

Working with the standard phase convention for the CKM matrix [157], the mass difference and the weak phase of the B_s system are related to the absolute value and the argument of the effective Hamiltonian (3.17) respectively,

$$\Delta m_{B_s} = 2 \left| \langle B_s | \mathcal{H}_{\text{eff,full}}^{\Delta B=2} | \bar{B}_s \rangle \right|, \quad 2\varphi_s = \arg \left(\langle B_s | \mathcal{H}_{\text{eff,full}}^{\Delta B=2} | \bar{B}_s \rangle \right). \quad (3.25)$$

In all cases the effective Hamiltonian contains the SM contribution plus contributions from the RS model, as indicated by the subscript “full”. We will normalize the matrix elements of the full effective Hamiltonian to those of only the SM contribution,

$$C_{B_s} e^{2i\phi_{B_s}} = \frac{\langle B_s | \mathcal{H}_{\text{eff,full}}^{\Delta B=2} | \bar{B}_s \rangle}{\langle B_s | \mathcal{H}_{\text{eff,SM}}^{\Delta B=2} | \bar{B}_s \rangle}, \quad (3.26)$$

so that

$$C_{B_s} = \frac{\Delta m_s}{(\Delta m_s)_{\text{SM}}} \quad (3.27)$$

⁴Here the meson states are normalized to $\langle M^0 | M^0 \rangle = \langle \bar{M}^0 | \bar{M}^0 \rangle = 1$ for general mesons M^0 . The expressions (3.23) differ therefore from the ones used in lattice calculations by a factor $1/(8m_M)$, because there a normalization $\langle M^0 | M^0 \rangle = 1/(2m_M)$ is common and the extra $1/4$ stems from a different operator basis [176].

measures the magnitude of the mass difference Δm_s relative to the one in the SM, while the phase ϕ_{B_s} affects the coefficients of $\sin(\Delta M_s t)$ in the time-dependent asymmetry of $B_s \rightarrow \psi\phi$. One obtains [161]

$$S_{\psi\phi} = \sin(2|\beta_s| - 2\phi_{B_s}), \quad (3.28)$$

where

$$V_{ts} = -|V_{ts}| e^{-i\beta_s}, \quad (3.29)$$

and $\beta_s \approx -1^\circ$. In the presence of a non-vanishing phase ϕ_{B_s} , the time-dependent asymmetry measures therefore $\varphi_s = |\beta_s| - \phi_{B_s}$, and not β_s . Generally, (3.28) is only correct if only a negligible weak phase is present in the decay amplitude $B_s \rightarrow \psi\phi$, which is the case for the SM. This assumption can be adopted in the RS model, because corrections to charged-current interactions are suppressed by m_W^2/M_{KK}^2 and numerically $\arg(V_{cb}^* V_{cs}) < 0.001^\circ$, and also the matrix elements in right-handed charged-current interactions $(V_R)_{22}$ and $(V_R)_{23}$ do not exceed the level of 10^{-5} in magnitude [115]. These tiny corrections can be safely neglected for all practical purposes.

The width differences $\Delta\Gamma_s$ and the semileptonic CP asymmetries A_{SL}^s take the form

$$\begin{aligned} \frac{\Delta\Gamma_s}{\Gamma_s} &= - \left(\frac{\Delta m_s}{\Gamma_s} \right)_{\text{exp}} \left[\text{Re} \left(\frac{\Gamma_{12}^s}{M_{12}^s} \right)_{\text{SM}} \frac{\cos 2\phi_{B_s}}{C_{B_s}} - \text{Im} \left(\frac{\Gamma_{12}^s}{M_{12}^s} \right)_{\text{SM}} \frac{\sin 2\phi_{B_s}}{C_{B_s}} \right], \\ A_{\text{SL}}^s &= \text{Im} \left(\frac{\Gamma_{12}^s}{M_{12}^s} \right)_{\text{SM}} \frac{\cos 2\phi_{B_s}}{C_{B_s}} - \text{Re} \left(\frac{\Gamma_{12}^s}{M_{12}^s} \right)_{\text{SM}} \frac{\sin 2\phi_{B_s}}{C_{B_s}}, \end{aligned} \quad (3.30)$$

with [158]

$$\text{Re} \left(\frac{\Gamma_{12}^s}{M_{12}^s} \right)_{\text{SM}} = (-4.97 \pm 0.94) \cdot 10^{-3}, \quad \text{Im} \left(\frac{\Gamma_{12}^s}{M_{12}^s} \right)_{\text{SM}} = (2.06 \pm 0.57) \cdot 10^{-5}. \quad (3.31)$$

In Figure 3.4, the width difference of the mass eigenstates normalized to the total width (3.30) is plotted against $S_{\psi\phi}$ as given in (3.28), which encodes the CP violation from mixing (see Appendix B for details). The SM prediction for this phase is extremely small and precise [160],

$$2\beta_s^{\text{SM}} = 0.0363_{-0.0015}^{+0.0016}. \quad (3.32)$$

and therefore a good place to constrain new physics effects. Shaded yellow and blue are the 68% and 95% CL regions obtained from a global fit based on the most recent combination of measurements of the semileptonic CP asymmetry A_{SL}^s , the mass difference Δm_{B_s} , the phase ϕ_{B_s} as well as $\Delta\Gamma_s$ [159]. Shown in red are parameter points which fulfill the constraints from $Z \rightarrow b\bar{b}$ and from ϵ_K , which is discussed in Section 3.3.

It is interesting to note, that the phase showed a 3σ deviation from the SM phase, based on a combination of almost one third of the $D\bar{D}$ and CDF data back in 2008 [162]. New physics in general can accommodate a large phase. However it is hard to

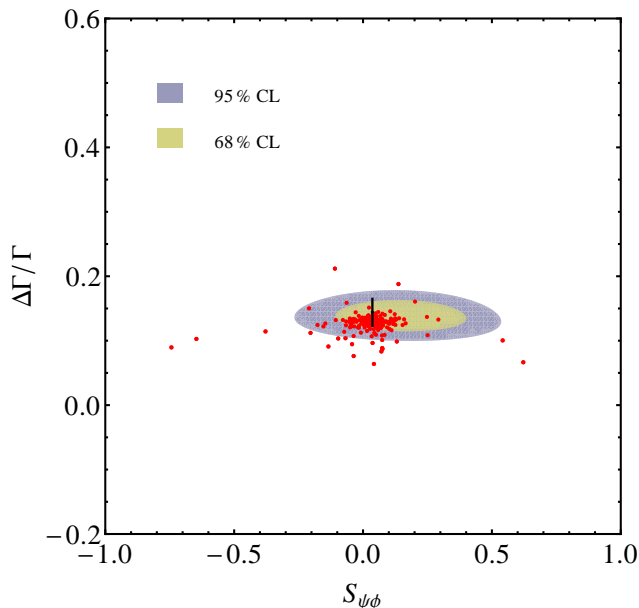


Figure 3.4: Predictions for $S_{\psi\phi}$ versus $\Delta\Gamma_s/\Gamma_s$ in the custodially protected RS model with extended electroweak symmetry group. The red points reproduce the measured value of the $Zb\bar{b}$ couplings and of ϵ_K at the 99% and 95% CL. The black bar indicates the SM prediction and error and the yellow (gray) contours the experimentally preferred regions of 68% (95%) probability.

generate in the RS model once the constraints from the $Z \rightarrow b\bar{b}$ analysis and $K - \bar{K}$ -mixing are taken into account, as becomes clear from Figure 3.4, but can already be seen in our analysis in [150, Sec.5.4.2]. The 3σ discrepancy slowly melted away over the years by analyzing more and more data and the full CDF dataset (10fb^{-1}) finally shows agreement with the SM within 1σ [163]. Even smaller errors could be obtained from the LHCb measurements [164], which also provide the dominant input for the combination [159] and are therefore the root for the small errors in our global fit⁵. The fact that the RS prediction does generically agree with this very constraining experimental results even for a KK scale of a few TeV, is an indication of the impressive range of the RS-GIM mechanism.

B Meson Decays to Muons

One might object, that $\Delta F = 2$ observables are not the best place for a stress test of the RS-GIM mechanism, because the tensor structures (2.176) which enter the Wilson coefficients are sensitive to the fermion localization on both vertices, *i.e.* proportional to $\sim m_b m_s/v^2$ in the case of $B_s - \bar{B}_s$ mixing. We will therefore examine $\Delta F = 1$ observables, again selected by the criteria that they depend on the localization of the

⁵It should be noted, that the LHCb analysis did also resolve the long standing sign ambiguity of $\Delta\Gamma_s$ in favor of the SM [165].

b quark as well as being constrained by very precise measurements.

The branching ratios of both the B_d and B_s mesons to muons meet these criteria. Not only is the experimental limit very close to the SM prediction, which excludes large new physics effects and cuts deep into the parameter space of many extensions of the SM ⁶, but also did CDF observe an excess of events in $\mathcal{B}(B_s \rightarrow \mu^+ \mu^-)$, which allows for the first time to establish a two sided bound on the branching ratio with a central value slightly above the SM prediction.

In the RS model, there are the following operators contributing to the effective Hamiltonian for $b \rightarrow s \ell^+ \ell^-$ transitions

$$\begin{aligned} \mathcal{H}_{\text{eff}}^{b \rightarrow s \ell^+ \ell^-} &= C_{\ell 1} (\bar{s}_L \gamma^\mu b_L) \sum_{\ell} (\bar{\ell}_L \gamma_\mu \ell_L) + C_{\ell 2} (\bar{s}_L \gamma^\mu b_L) \sum_{\ell} (\bar{\ell}_R \gamma_\mu \ell_R) \\ &+ \tilde{C}_{\ell 1} (\bar{s}_R \gamma^\mu b_R) \sum_{\ell} (\bar{\ell}_R \gamma_\mu \ell_R) + \tilde{C}_{\ell 2} (\bar{s}_R \gamma^\mu b_R) \sum_{\ell} (\bar{\ell}_L \gamma_\mu \ell_L) \\ &+ C_{\ell 3} (\bar{s}_L b_R) \sum_{\ell} (\bar{\ell} \ell) + \tilde{C}_{\ell 3} (\bar{s}_R b_L) \sum_{\ell} (\bar{\ell} \ell). \end{aligned} \quad (3.33)$$

The Wilson coefficients can only get contributions from the Z and its KK excitations, the photon KK modes and from the Higgs, see Section 2.6. They depend on the overlap integrals (2.175) and (2.184), which are described in the dual theory by the diagrams in the second line of Figure 2.7. Note, that we do not implement leptons as bulk fields. However, non-universal contributions at the lepton vertex are suppressed by $m_\mu^2/(m_s m_b)$ relative to the leading contributions and can be neglected to very good approximation and for the same reason the tensor structures which are proportional to $m_s m_b m_\mu^2/v^4$ give only subleading corrections. One obtains

$$\begin{aligned} C_{\ell 1}^{\text{RS}} &= -\frac{4\pi\alpha}{3M_{\text{KK}}^2} (\Delta'_D)_{23} - \frac{2\pi\alpha(1-2s_w^2)}{s_w^2 c_w^2 M_{\text{KK}}^2} (\Sigma_D)_{23}, \\ C_{\ell 2}^{\text{RS}} &= -\frac{4\pi\alpha}{3M_{\text{KK}}^2} (\Delta'_D)_{23} + \frac{4\pi\alpha}{c_w^2 M_{\text{KK}}^2} (\Sigma_D)_{23}, \\ \tilde{C}_{\ell 1}^{\text{RS}} &= -\frac{4\pi\alpha}{3M_{\text{KK}}^2} (\Delta'_d)_{23} - \frac{4\pi\alpha}{c_w^2 M_{\text{KK}}^2} (\Sigma'_d)_{23}, \\ \tilde{C}_{\ell 2}^{\text{RS}} &= -\frac{4\pi\alpha}{3M_{\text{KK}}^2} (\Delta'_d)_{23} + \frac{2\pi\alpha(1-2s_w^2)}{s_w^2 c_w^2 M_{\text{KK}}^2} (\Sigma'_d)_{23}, \\ C_{\ell 3}^{\text{RS}} &= -\frac{2m_\ell}{m_h^2 v} \left[\frac{m_s}{v} (\delta_d)_{23} + \frac{m_b}{v} (\delta_D)_{23} + (\Delta g_h^d)_{23} \right], \\ \tilde{C}_{\ell 3}^{\text{RS}} &= -\frac{2m_\ell}{m_h^2 v} \left[\frac{m_b}{v} (\delta_d)_{23} + \frac{m_s}{v} (\delta_D)_{23} + (\Delta g_h^d)_{23} \right], \end{aligned} \quad (3.34)$$

in which

$$\Sigma_{Q,q} \equiv \omega_{LL}^Z L \left(\frac{1}{2} - \frac{s_w^2}{3} \right) \Delta_{Q,q} + \frac{M_{\text{KK}}^2}{m_Z^2} \delta_{Q,q} \quad \Sigma'_{Q,q} \equiv \omega_{RR}^Z L \frac{s_w^2}{3} \Delta_{Q,q} + \frac{M_{\text{KK}}^2}{m_Z^2} \delta_{Q,q}, \quad (3.35)$$

⁶For example in the MSSM, the branching ratio (3.36) grows with $\tan \beta^6$.

with $\omega_{LL}^Z = \omega_{RR}^Z = 1$ in the minimal model and if the electroweak gauge group is extended in order to comprise a custodial symmetry, $\omega_{LL}^Z = 0$ and $\omega_{RR}^Z = \frac{3c_w^2}{s_w^2}$, as in (3.15) and (3.16), compare also [167, App. B].

Corrections to $b \rightarrow s\ell^+\ell^-$ arising from $C_{\ell 3}^{\text{RS}}$ and $\tilde{C}_{\ell 3}^{\text{RS}}$ are either $\mathcal{O}(m_\mu m_b/M_{\text{KK}}^2)$ or $\mathcal{O}(v^4/M_{\text{KK}}^4)$ and will consequentially also be ignored in the numerical analysis.

The branching ratios for the $B_q \rightarrow \mu^+\mu^-$ decays can be expressed as

$$\begin{aligned} \mathcal{B}(B_q \rightarrow \mu^+\mu^-) &= \frac{G_F^2 \alpha^2 m_{B_q}^3 f_{B_q}^2 \tau_{B_q}}{64\pi^3 s_w^4} |\lambda_t^{(qb)}|^2 \sqrt{1 - \frac{4m_\mu^2}{m_{B_q}^2}} \\ &\times \left(\frac{4m_\mu^2}{m_{B_q}^2} |C_A - C'_A|^2 + m_{B_q}^2 \left[1 - \frac{4m_\mu^2}{m_{B_q}^2} \right] \left| \frac{m_b C_S - m_q C'_S}{m_b + m_q} \right|^2 \right), \end{aligned} \quad (3.36)$$

where m_{B_q} , f_{B_q} , and τ_{B_q} are the mass, decay constant, and lifetime of the B_q meson and $\lambda_q^{(pr)} \equiv V_{qp}^* V_{qr}$. The electromagnetic coupling α entering the branching ratios should be evaluated at m_Z . The expressions for the coefficients $C_{A,S}$ and $C'_{A,S}$ read

$$\begin{aligned} C_A &= c_A - \frac{s_w^4 c_w^2 m_Z^2}{\alpha^2 \lambda_t^{(qb)}} (C_{\ell 1}^{\text{RS}} - C_{\ell 2}^{\text{RS}}), & C'_A &= \frac{s_w^4 c_w^2 m_Z^2}{\alpha^2 \lambda_t^{(qb)}} (\tilde{C}_{\ell 1}^{\text{RS}} - \tilde{C}_{\ell 2}^{\text{RS}}), \\ C_S &= \frac{2s_w^4 c_w^2 m_Z^2}{\alpha^2 m_b \lambda_t^{(qb)}} C_{\ell 3}^{\text{RS}}, & C'_S &= \frac{2s_w^4 c_w^2 m_Z^2}{\alpha^2 m_q \lambda_t^{(qb)}} \tilde{C}_{\ell 3}^{\text{RS}}, \end{aligned} \quad (3.37)$$

where $c_A = 0.96 \pm 0.02$ denotes the SM contribution to the Wilson coefficient of the axial-vector current [169, 170], and the coefficients $C_{\ell 1-3}^{\text{RS}}$ and $\tilde{C}_{\ell 1-3}^{\text{RS}}$ contain the 13 or 23 elements of the mixing matrices in the case of $B_d \rightarrow \mu^+\mu^-$ and $B_s \rightarrow \mu^+\mu^-$, respectively.⁷

The SM branching ratios of the $B_q \rightarrow \mu^+\mu^-$ decay channels evaluate to [171, 172]

$$\mathcal{B}(B_d \rightarrow \mu^+\mu^-)_{\text{SM}} = (1.0 \pm 0.1) \cdot 10^{-10}, \quad (3.38)$$

$$\mathcal{B}(B_s \rightarrow \mu^+\mu^-)_{\text{SM}} = (3.2 \pm 0.2) \cdot 10^{-9}. \quad (3.39)$$

These predictions are obtained by normalizing the decay rates to the well-measured meson mass differences $(\Delta m_q)_{\text{exp}}$. This eliminates the dependence on CKM parameters and the bulk of the hadronic uncertainties by trading the decay constants for less uncertain hadronic parameters. The dominant source of error is nevertheless still provided by the hadronic input.

The result is plotted in Figure 3.5 and shows again very good agreement with the current bounds, which however start to cut into the parameter space. Experimental bounds refer to the very precise limit from LHCb measurements, obtained including the full 2011 dataset [166], and the two-sided bound from CDF [168] respectively. It is

⁷While C_A and C'_A are scale independent, the coefficients C_S and C'_S have a non-trivial RG evolution. We can ignore that because they are numerically insignificant.

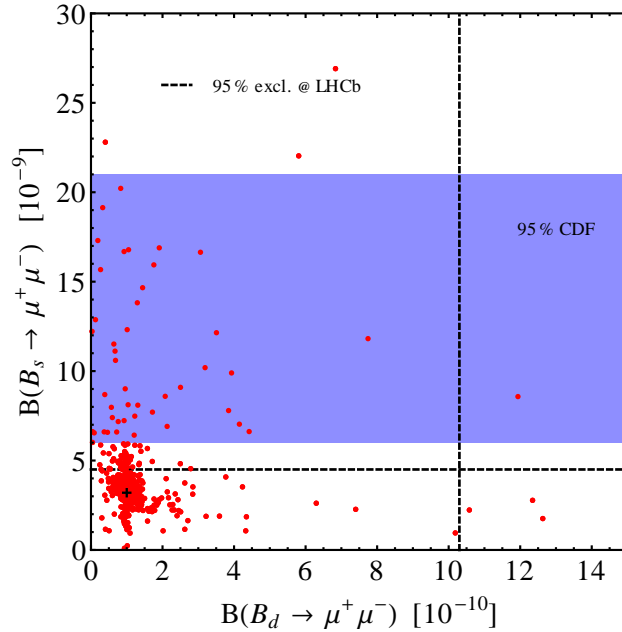


Figure 3.5: The red points correspond to the parameter set constrained by the $Zb\bar{b}$ couplings and $|\epsilon_K|$ at the 99% and 95% CL, for the custodially protected RS model. The black star indicates the SM prediction and the black dashed lines denote the experimental upper limits as measured by LHCb at 95% CL. The blue band shows the preferred region at 95% CL measured by CDF.

impressive that also rare decays are sufficiently suppressed by the RS-GIM mechanism even for reasonably small new physics scales with the measurements reaching a stage which will soon test the SM.

shown

3.3 Limitations of the RS GIM Mechanism

In summary of the previous sections, one can say that the RS-GIM mechanism proves to be a successful protection from large tree level FCNCs, even if the heavy b quark is involved. However, already from Table 1.1 it is clear that the most restrictive bound on new physics from the flavor sector does not come from heavy quarks, but from $K - \bar{K}$ mixing. The reason is twofold, and both aspects are related to the mixed left-right operators Q_4 and Q_5 in (3.18). First, the corresponding Wilson coefficients are subject to a large chiral enhancement from the matrix elements (3.23) (which translate to the case of $K - \bar{K}$ mixing with the obvious replacements), because in contrast to the B-mesons, the Kaon is much heavier than the sum of its constituents,

$$\left[\frac{m_K}{m_s + m_d} \right]^2 \approx 15. \quad (3.40)$$

Second, renormalization group running from the KK scale down to 2 GeV, where the matrix elements are evaluated, results in a considerably larger factor than the running down to m_b , the scale at which the bag parameters for B mesons are computed. Therefore, one finds for a reference point of $M_{\text{KK}} = 2$ TeV,

$$\langle K^0 | \mathcal{H}_{\text{eff,RS}}^{\Delta S=2} | \bar{K}^0 \rangle \propto C_1^{\text{RS}} + \tilde{C}_1^{\text{RS}} + 150 \left(C_4^{\text{RS}} + \frac{C_5^{\text{RS}}}{N_C} \right). \quad (3.41)$$

These enhancements are a problem for all new physics models which allow for right-handed currents, but are even large enough to overcome the RS-GIM suppression and push the KK scale in the range of $M_{\text{KK}} = \mathcal{O}(10)$ TeV.

The Flavor Problem of the RS Model

In the case of the Kaon system one finds for the mass difference and the CP violating quantity ϵ_K (see Appendix B for details)

$$\Delta m_K = 2 \text{Re} \langle K^0 | \mathcal{H}_{\text{eff,full}}^{\Delta S=2} | \bar{K}^0 \rangle, \quad \epsilon_K = \frac{\kappa_\epsilon e^{i\varphi_\epsilon}}{\sqrt{2} \Delta m_K^{\text{exp}}} \text{Im} \langle K^0 | \mathcal{H}_{\text{eff,full}}^{\Delta S=2} | \bar{K}^0 \rangle, \quad (3.42)$$

in which $\varphi_\epsilon = (43.51 \pm 0.05)^\circ$ and $\kappa_\epsilon = 0.92 \pm 0.02$ [173]. The suppression factor κ_ϵ parametrizes the effects due to the imaginary part of the isospin-zero amplitude in $K \rightarrow \pi\pi$ decays [174].

The theoretical values for both m_K and ϵ_K are dependent on uncalculable long-distance contributions, which make a precise prediction on the level of the experimental uncertainty impossible. The best one can do, is compare the theoretical value including the best estimate for the short-distance contributions [177], with the experimental values [157],

$$\Delta m_K^{\text{SM}} = (3.1 \pm 1.2) \times 10^{-15}, \quad \Delta m_K^{\text{exp}} = (3.483 \pm 0.0059) \times 10^{-15}, \quad (3.43)$$

$$|\epsilon_K^{\text{SM}}| = (1.81 \pm 0.28) \times 10^{-3}, \quad |\epsilon_K^{\text{exp}}| = (2.228 \pm 0.011) \times 10^{-3}. \quad (3.44)$$

It is therefore only meaningful to impose an order of magnitude upper limit on new physics contributions, a lower limit in order to explain the deviation from the experimental value cannot be obtained. Consequentially, we will require that the pure RS-contributions do not exceed

$$|\epsilon_K^{\text{RS}}| < 1 \times 10^{-3}, \quad |\Delta m_K^{\text{RS}}| < 1 \times 10^{-15}. \quad (3.45)$$

The contributions from the RS model are given by the Wilson coefficients (3.20), with the replacement of the mixing matrices $(\tilde{\Delta}_D)_{23} \rightarrow (\tilde{\Delta}_D)_{12}$. Renormalization group running is implemented by (3.22), in which the left hand side is replaced by $C_i(2 \text{ GeV})$, at which the matrix elements for Kaon final and initial states are evaluated. These are given by (3.23) with the replacements $B_s^0 \rightarrow K^0$, $B_i^{sd}(\mu)$, $m_{B_s} \rightarrow m_K = 497.6$ MeV, $m_b \rightarrow m_d$ and $f_{B_s} \rightarrow f_K = 156.3$ MeV [157, 160]. The definition of the $B_i^{sd}(\mu)$ is given by (3.24) with the same replacements. Note, that significant progress has

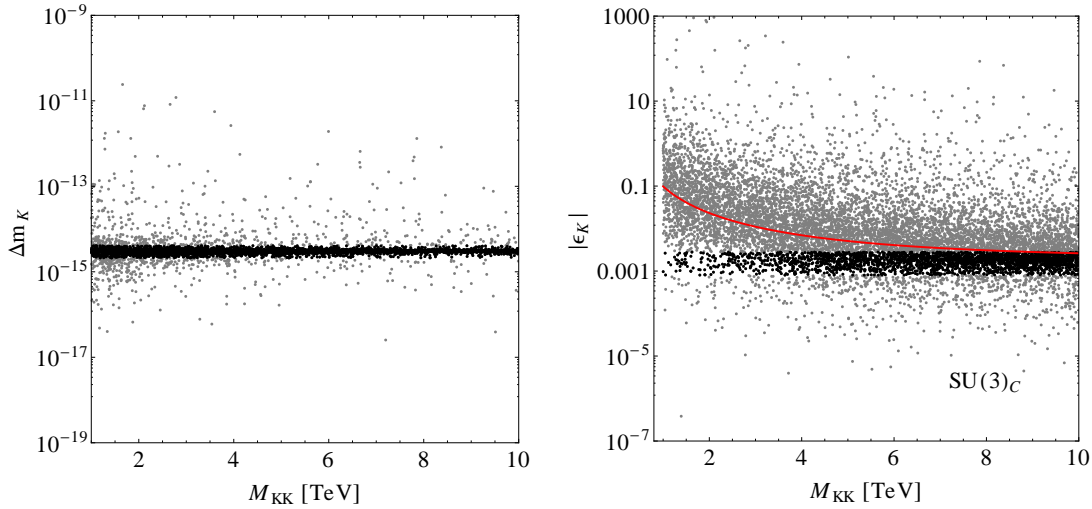


Figure 3.6: Plots showing the observables Δm_K (left panel) and $|\epsilon_K|$ (right panel) plotted against the KK scale for the full parameter set, both in the more restrictive case of the custodially protected RS model with enlarged electroweak bulk group. Parameter points which do (not) agree with the bounds (3.45) are black (gray), and in the right panel, a fit to the median value of the parameter points in 500 GeV bins is plotted in red. For the minimal model, this bound is shifted by roughly 1 TeV towards a lower KK scale.

been made in the last few years regarding the calculation of the bag parameters using lattice QCD. In particular the matrix elements for $K - \bar{K}$ mixing have been very recently computed with considerably improved precision [175, 176]. The new results (C.3) also tend to increase the contribution from the new physics operators compared to the SM and thus further aggravate the bound on the new physics scale.

In Figure 3.6 scatterplots of our parameter set are shown for $\Delta m_K = \Delta m_K^{\text{SM}} + \Delta m_K^{\text{RS}}$ on the left panel and $|\epsilon_K| = |\epsilon_K^{\text{SM}} + \epsilon_K^{\text{RS}}|$ versus M_{KK} on the right panel, in which parameter points (not) consistent with (3.45) are colored (gray) black. The plot ranges have been chosen in order to make the results easily comparable. While the corrections to Δm_K generically agree with the imposed bound and a KK scale of the order of a TeV, the bound from ϵ_K is much more severe. In order to guide the eye, a fit to the median values for 500 GeV bins of M_{KK} has been plotted in red, and the point at which it crosses the black “band” can be considered a rough estimate of the lower bound on the KK scale. This gives $M_{\text{KK}} > 6 - 7$ TeV, which translates into a mass for the lowest lying KK mode of roughly $m_{\mathcal{G}(1)} > 15$ TeV. For the custodial model, this bound becomes even worse, $M_{\text{KK}} > 8$ TeV and $m_{\mathcal{G}(1)} > 15$ TeV, because the cancellation in C_5 is overcome by the $\mathcal{O}(100)$ enhancement of \tilde{C}_1 .

Because this is the only observable in the flavor sector which is not compatible with a TeV-ish new physics scale as suggested by the gauge hierarchy problem, the resulting constraint is called the *RS flavor problem* and a lot of effort was put in modifications of the minimal RS in order to somehow attenuate this bound.

A List of Solutions to the Flavor Problem

The situation described in the last section has triggered many new ideas in order to make the bound from ϵ_K compatible with a KK scale in the ballpark of a TeV. This section will contain a comprehensive review of these ideas. They will be separated in three categories. First, parametric suppressions of the relevant Wilson coefficients. Second, global symmetries which ensure that the coefficients of the dangerous mixed chirality operators are either zero or extremely small and finally, alternative solutions, which rely on mechanisms that can not be categorized in one of the above.

Parametric Suppressions

A key observation is, that the enhancement of ϵ_K is almost solely due to the Wilson coefficient C_4 and, to a lesser extent (especially with a custodial protection), C_5 in (3.20) (which is always understood with the corresponding replacements if cited in the context of $K - \bar{K}$ mixing and the RS superscript will be dropped if no confusion is possible). The parametric dependence of them becomes clearest using the ZMA and (2.158), so that

$$C_4 = -N_c C_5 \approx -\frac{4\pi\alpha_s}{M_{\text{KK}}^2} L \frac{2m_d m_s}{v^2} \frac{|(Y_d^{(5D)})|}{|\det \mathbf{Y}_d^{(5D)}|} \approx -\frac{4\pi\alpha_s}{M_{\text{KK}}^2} L \frac{2m_d m_s}{v^2 Y_d^2}, \quad (3.46)$$

where Y_d denotes an order one parameter sensitive to the 5D Yukawa couplings in the down sector. One possibility, which was first mentioned in [178], is therefore to increase the down sector Yukawas, which corresponds to the application of the reparametrization invariance (2.170). In terms of the 5D language, the overlap between zero modes and the gauge boson KK tower becomes smaller, because the down type quarks or the 5D electroweak doublets are more UV localized. In the dual theory this is to be interpreted as decreasing the mixing angle and thus making the down-type quarks or the doublets more elementary and less composite. As a consequence, given the relation between zero mode profiles induced by the masses of the quarks (2.158), either the Yukawas in the up-sector have to be larger as well or the electroweak singlet up-type quarks must be localized closer to the IR brane, *i.e.* must be more composite. Both seems like a good trade-off, because bounds on FCNCs in the up-sector are considerably less constraining. In the numerical analysis, the Yukawa couplings for both sectors are randomized, so that the absolute values of all entries are in the range $|Y| \in [0.3, 3]$, see Appendix A for details. However, one cannot arbitrarily increase the value of the fundamental Yukawa couplings. One reason is that the Yukawa couplings should not become non-perturbative, because the above analysis cannot be made if one loses perturbative control. The point at which this happens depends on the normalization chosen in defining the dimensionless Yukawa couplings in (2.127) and therefore there is some freedom, see the discussion in [115, Sec 3.4] and [181, App E.4]. However, in order to balance out the enhancement in (3.41), one would need to enhance the Yukawas by a factor of ten. Larger Yukawas might therefore ameliorate the bound from ϵ_K , but at some point one simply shifts the tuning over to the Yukawa sector. Even if this would be accepted, there are upper bounds on the

absolute value of the Yukawa couplings from observables which are proportional to positive powers of them, typically $\Delta F = 1$ observables, which arise at the one loop level with mass insertions. The authors of [180] find that direct CP violation from Kaon decay, measured by ϵ'/ϵ_K gives the most severe upper bound. At $Y_d \approx 6$, the derived bound on M_{KK} becomes stronger than the one from $|\epsilon_K|$, so that the best one can arrange for would be a KK scale of $M_{KK} \geq 3$ TeV.

This problem can be avoided if instead of enhancing the Yukawa couplings, one lowers the value of the volume of the extra dimension $L = -\ln \epsilon$, which appears linearly in both the Wilson coefficients in $\Delta F = 1$ and $\Delta F = 2$ effective Hamiltonians [144]. This is the idea of the LRS models, which have been introduced in Section 3.1 as a means to reduce the contributions to the oblique parameters. The reason for this linearity is, that the coupling of the KK modes to a good approximation reads $g\sqrt{L}$, which becomes apparent if one computes the contributions mode by mode instead of using the full 5D propagators. This coupling will therefore be smaller if the bulk is truncated at scales $\epsilon_{LRS} = \Lambda_{EW}/\Lambda_{LRS}$, with $\Lambda_{LRS} \ll M_{Pl}$. In the dual theory this means, that the range of scales over which the theory is strongly coupled is smaller, *i.e.* asymptotic freedom sets in already at the scale Λ_{LRS} .

However, for the zero mode profiles of the light quarks holds $F(c) \sim \epsilon^{-c-1/2}$ and if $\epsilon \rightarrow \epsilon_{LRS}$ which is orders of magnitude smaller, the localization parameters must adjust, because the values of the zero mode profiles are fixed by the mass relations (2.158). Considering the original proposal [144], $\epsilon_{LRS} = 10^3$ ($L_{LRS} \approx 7$), this means that the c -parameters are by a factor of two larger in magnitude than in the original model. However, the RS-GIM mechanism, illustrated by the naive picture 2.11 assumes, that the integrand of the overlap integrals in (2.173) is proportional to a positive power of the bulk coordinates t and t' . This will only be true as long as $c_{q_i} + c_{q_j} + 2 > 0$ (remember, all light flavors have $c_{Q,q} < -1/2$). If the c parameters become smaller, the overlap integrals (2.176) will not be dominated by the IR localization of the gluon KK modes, but by the extreme UV localization of the fermion zero modes, so that the main contributions arise from the region where $t \approx \epsilon$ and the RS-GIM suppression is undermined. This phenomenon is called *UV dominance* and its implications for flavor changing as well as flavor diagonal neutral currents, for example the $Zb\bar{b}$ coupling, have been analyzed in [179]. One can turn this argument around and formulate a lower bound on the volume $L_{LRS} > 8.2$, above which the bound from ϵ_K is at least not stronger, but the enhancement in (3.41) cannot be balanced out by lowering L alone.

Global Symmetries and MFV

The dangerous coefficients C_4 and C_5 appear only if flavor changing vertices with both right- and left-handed down quarks are present. This can be prevented, either by imposing a global symmetry which arranges for the singlet or doublet bulk mass parameters to be equal or by aligning them with the down-type Yukawa matrix [184]. The latter is an implication of minimal flavor violation, which was introduced in Section 1.2. Several variants have been proposed, in which the alignment is assumed only in the down sector, is extended to the up sector, or holds only for the first two

generations [182, 183, 184]. In the dual theory, such an alignment means that not the mixing angles in (1.27) alone are responsible for the structure in the flavor sector, but also the fundamental Yukawa couplings denoted by λ in (1.27) in the composite sector have some structure. As in the SM, the origin of this structure is not explained, which at least partially abrogates one of the strengths of the RS model, namely the capability to explain flavor structure and FCNC suppression by the same fundamental order one parameters.

If alternatively the bulk masses of all 5D fermions are chosen equal in the down-sector, $c_{d_i} = c_d$, the couplings \mathbf{g}_R in (1.34) will be universal or equivalently, the corresponding matrices in (2.180) and (2.181), both for $q = d$, are diagonal in flavor space [186]. An alignment can equally well be imposed for the doublet bulk mass parameters c_{Q_i} , but not for both the up- and the down singlet localizations at once without introducing additional structure in the Yukawa matrices. In essence, the reparametrization invariance (2.169) can be applied once in order to redistribute between the down-type singlets and the doublets. This ansatz is from the point of view of the dual theory, related to the idea of only electroweak singlet or doublet quarks having composite partners, as proposed by Redi and Weiler [149], which was already quoted as a possible way to reduce the tension from the $Zb\bar{b}$ coupling in Section 3.1.

Alignment of the bulk mass parameters c_{d_i} corresponds to having an equal anomalous dimension for all composite down-type singlet partners. In the bulk, this can be assured by imposing a global symmetry, which does however not translate to a symmetry in the dual theory. Only for local bulk symmetries one knows that they are present in the composite sector as well, which for example makes it necessary to gauge the $SU(2)_R$ in order to realize the custodial protection in the dual theory. Gauged bulk flavor symmetries have therefore gained some attention, see [185] and references therein. The symmetry must also be exact, because small deviations from the alignment will already imply large corrections, because the bulk mass parameters enter the Wilson coefficients in the exponents. Such a symmetry can only be considered stable in the dual theory, if the localization of the singlet down-quarks is not only equal, but also they are confined to the UV brane, which removes the composite singlet down-quarks from the dual theory, a.k.a. left-handed compositeness (and vice versa for the left-handed partners being confined to the UV brane).

Whether or not such a symmetry would be enough to balance the enhancement in (3.41) can be estimated by considering the effect of higher order operators such as $(\bar{Q}_L Y_d H d_R)^2$ which are encoded in the $\mathcal{O}(v^2/M_{\text{KK}}^2)$ corrections to (2.181). One finds

$$(\tilde{\delta}_D)_{mn} \otimes (\tilde{\delta}_d)_{mn} = \frac{m_{d_m} m_{d_n}}{M_{\text{KK}}^2} \left[(U_d^{L\dagger})_{mi} (U_d^L)_{in} (\tilde{\delta}_D)_{ij} (U_d^{L\dagger})_{mj} (U_d^L)_{jn} + (U_d^{R\dagger})_{mi} (U_d^R)_{in} (\tilde{\delta}_d)_{ij} (U_d^{R\dagger})_{mj} (U_d^R)_{jn} \right] \quad (3.47)$$

from the terms in (2.176) involving both even $\mathbf{C}_m^{(A)}(\phi)$ and odd $\mathbf{S}_m^{(A)}(\phi)$ fermion profiles. Here a summation over the indices i, j is understood. Neglecting terms suppressed by $F^2(c_{Q_i})$ and $F^2(c_{Q_i})F^2(c_{Q_j})$, which are small for the light flavors, the

elements of $(\tilde{\delta}_D)_{ij}$ take the form

$$(\tilde{\delta}_D)_{ij} = \frac{2(3 + c_{Q_i} - c_{Q_j})}{(3 + 2c_{Q_i})(3 - 2c_{Q_j})(2 + c_{Q_i} - c_{Q_j})} \frac{F^2(c_{Q_i})}{F^2(c_{Q_j})}. \quad (3.48)$$

An analogous expression holds in the case of $(\tilde{\delta}_d)_{ij}$ with c_{Q_i} replaced by c_{d_i} . Since all bulk mass parameters are close to $-1/2$ it is also a good approximation to replace the rational function of c_{Q_i} and c_{Q_j} in (3.48) by the numerical factor $3/8$. Using the mass relations (2.158) as well as (2.159), it is straightforward to deduce from (3.47) that (3.46) is replaced by

$$C_4^{\text{al}} = -N_c C_5^{\text{al}} \approx -\frac{4\pi\alpha_s}{M_{\text{KK}}^4} L m_d m_s \approx \frac{v^2 Y_d^2}{2M_{\text{KK}}^2} C_4, \quad (3.49)$$

in which the last expression gives the relation to the Wilson coefficient in the RS model with anarchical bulk mass parameters. Depending on the size of the Yukawa couplings, this allows to cancel the enhancement from renormalization group running and the matrix elements for KK scales in the range of $1 - 2$ TeV. Notice that the $\mathcal{O}(v^2/M_{\text{KK}}^2)$ corrections from $(\tilde{\delta}_d)_{ij}$ have been neglected in (3.49), which is justified, because the universality of $(\tilde{\delta}_d)_{ij} \sim 1$ in combination with the unitarity of the U_d^R matrices renders them negligibly small.

Alternative Solutions

One of the alternative strategies to ameliorate the RS flavor problem is to allow for the Higgs to be shifted into the bulk [187]. In the case of a brane Higgs, the Yukawa interactions are brane-localized operators, because the overlap with a brane Higgs and the bulk fermions are given by the values of the fermion zero modes and the IR brane. For a bulk Higgs, the overlap integral does include the Higgs profile, which is typically exponentially peaked towards the IR brane, and will therefore be numerically larger than the value of the fermion profiles at the brane (the “tail” of the Higgs profile will always make for a larger overlap). In order for the mass relations to hold, this means that the fermion profiles must be shifted towards the UV. One can imagine the effect of a bulk Higgs by multiplying the zero mode profiles $F(c_{Q_i})$ and $F(c_{q_i})$ in (2.158) by the value of the overlap integral with the Higgs. This factor must be compensated by the zero mode profiles, which, as in the case of larger Yukawas, results in a negative shift in the bulk masses c_{Q_i} and c_{q_i} .

The Wilson coefficient C_4 in (3.20) is generated by KK gluon exchange alone, and since the gluon KK modes are not affected at all by the localization of the Higgs, they are unchanged for a bulk Higgs compared to the brane Higgs scenario. Consequently, the UV shift of the quark profiles leads to smaller overlap integrals with the KK tower of the gluon and therefore the more the Higgs is shifted into the bulk, the more are FCNC constraints defused, compare [181, Table 1].

In the dual theory, promoting the Higgs to a bulk field makes it a mixed state of an elementary and a composite scalar. One might object, that an elementary scalar in the theory is contrary to the original idea of a composite Higgs as a solution to the hierarchy problem. However, as long as the Higgs stays close to the IR brane the

mixing angle is tiny and the elementary mode has a mass of the order Planck scale, see (2.39), so that the hierarchy problem is not reintroduced.

A related mechanism is provided in models with a *soft wall* [189]. Originally inspired by the modeling of the Regge trajectories in AdS/QCD models (see the footnote on page p.47), a soft wall model assumes in contrast to the RS model, that the backreaction of the dilaton on the metric is not small, but large enough to distort the metric in the IR, so that the action (2.11) is replaced by

$$S = \int d^5x \sqrt{|G|} e^{-\Phi} \mathcal{L}, \quad (3.50)$$

in which Φ denotes the dilaton/radion field and \mathcal{L} stands for the whole bulk Lagrangian. As a consequence, the metric is no longer pure AdS, but changes in the IR, and the bulk is not cut off by a delta-function potential (a brane), but by a smooth potential wall, depending on the coordinate dependent vev of Φ . Because the bulk coordinate runs between $t \in [\epsilon, \infty]$ in this setup, the IR boundary conditions are replaced by integrals up to $t = \infty$, or by overlap integrals with a bulk Higgs respectively. This bulk Higgs and the distorted metric both induce a shift of the fermion profiles towards the UV brane and as a result further suppress FCNCs [188, 190]. The change in the warp factor generated by the backreaction of the dilaton will however lead to considerable fine-tuning in order to solve the gauge hierarchy problem in such models [189].

3.4 A Solution in the Gauge Sector

A qualitatively different solution to the RS flavor problem is to consider an extension of the strong interaction gauge group in the bulk. It is based on the idea, that the contributions from the gluon KK excitations to the coefficients C_4 and C_5 of the mixed chirality operators in (3.20) can be canceled by a KK tower of a strongly interacting gauge boson, which couples with opposite sign to left- and right-handed quarks, but with the same coupling strength as the gluon. The zero mode of this new bulk field can be projected out by choosing the appropriate BCs. In contrast to gauged flavor symmetries in the bulk, this model does neither affect the order one Yukawa couplings nor does it impose a symmetry on the bulk masses which generate the hierarchies in the quark masses and mixings. Therefore, instead of a widespread implementation of the SM flavor structure with all its features and shortcomings, this solution specifically targets the single operator which is not sufficiently suppressed by the RS-GIM mechanism. Some of the results derived in the following sections have been published in [191].

Extension of the Color Gauge Group

The goal is to find an extension of the strong interaction gauge group, which will be able to accommodate the RS gluon as well as another gauge boson with couplings

of opposite sign but equal magnitude to left- and right-handed bulk quarks. In SM extensions, such an *axial* coupling is encountered in *axigluon* or *chiral color* models, which have been considered first in [192]. In the following we will see if a 5D implementation of the corresponding extension of the color gauge group will have the desired characteristics.

Therefore, the color gauge group in the bulk is replaced by

$$SU(3)_C \rightarrow SU(3)_D \times SU(3)_S, \quad (3.51)$$

where the subscripts D, S indicate that the corresponding gauge bosons only couple to 5D electroweak singlets or doublets, respectively. The quarks do therefore transform as $Q \sim (\mathbf{3}, 1)$ and $q^c \sim (1, \mathbf{3})$ under the extended gauge group. From now on, a sum over flavor $q^c = u^c, d^c$ as in (2.122) is understood if the singlets appear in the Lagrangian and will not be denoted explicitly. As a consequence, the interaction terms of the 5D gluon and the bulk fermions in the Lagrangian

$$\sqrt{|G|}\mathcal{L}_{\text{int}} \ni e^{-3\sigma} g_{s5} \left(\bar{Q} \gamma^\mu \mathcal{G}_\mu^a T^a Q + \bar{q}^c i \gamma^\mu \mathcal{G}_\mu^a T^a q^c \right), \quad (3.52)$$

in which \mathcal{G}_μ is the bulk gluon field, g_{s5} denotes the 5D strong coupling constant and $T^a = \lambda^a/2$, $a = 1, \dots, 8$, the generators of $SU(3)_C$ (so that λ^a are the Gellmann matrices), has to be replaced by

$$\sqrt{|G|}\mathcal{L}_{\text{int}} \ni e^{-3\sigma} \left(g_{D5} \bar{Q} \gamma^\mu (G_D)_\mu^a T^a Q + g_{S5} \bar{q}^c i \gamma^\mu (G_S)_\mu^a T^a q^c \right). \quad (3.53)$$

Here, the 5D gauge bosons of the $SU(3)_D$ and $SU(3)_S$ are denoted by G_D and G_S and the corresponding couplings by g_{D5} and g_{S5} . The bulk gluon field is a linear combination of these new gauge fields. Introducing the mixing matrix

$$\begin{pmatrix} G_D^\mu \\ G_S^\mu \end{pmatrix} = \begin{pmatrix} \cos \theta & -\sin \theta \\ \sin \theta & \cos \theta \end{pmatrix} \begin{pmatrix} \mathcal{G}^\mu \\ \mathcal{A}^\mu \end{pmatrix}, \quad (3.54)$$

in which \mathcal{G}^μ denotes the gluon and \mathcal{A}^μ the remaining linear combination, one can therefore rewrite (3.53),

$$\begin{aligned} \sqrt{|G|}\mathcal{L}_{\text{int}} \ni e^{-3\sigma} \left(g_{D5} \bar{Q} \gamma^\mu [\mathcal{G}_\mu^a \cos \theta - \mathcal{A}_\mu^a \sin \theta] T^a Q \right. \\ \left. + g_{S5} \bar{q}^c \gamma^\mu [\mathcal{G}_\mu^a \sin \theta + \mathcal{A}_\mu^a \cos \theta] T^a q^c \right), \quad (3.55) \end{aligned}$$

and find that the strong coupling constant must be defined as

$$g_{s5} \equiv g_{D5} \cos \theta = g_{S5} \sin \theta. \quad (3.56)$$

With this definition,

$$\begin{aligned} \sqrt{|G|}\mathcal{L}_{\text{int}} \ni e^{-3\sigma} g_{s5} \left(\bar{Q} \gamma^\mu \mathcal{G}_\mu^a T^a Q + \bar{q}^c \gamma^\mu \mathcal{G}_\mu^a T^a q^c \right. \\ \left. - \tan \theta \bar{Q} \gamma^\mu \mathcal{A}_\mu^a T^a Q + \cot \theta \bar{q}^c \gamma^\mu \mathcal{A}_\mu^a T^a q^c \right). \end{aligned} \quad (3.57)$$

It is obvious, that the linear combination \mathcal{A}_μ will couple with opposite signs to 5D doublets and singlets. These will in the case of the zero modes decompose into left-handed and right-handed 4D fields respectively, apart from small admixtures from the other chirality. This is due to the fact, that the other chirality enters with the S -profiles in (2.123), which for the zero modes are suppressed by $x_0 \approx v/M_{\text{KK}}$, see (2.149). The magnitude of the couplings depends on the form of the propagator and the mixing angle θ . For $\theta = \pi/4$, the couplings become purely axial and one could speak of a 5D *axigluon*. In a slight abuse of language, in the following, this notation will also be used for differing mixing angles. Interestingly, however, in contributions to the diagrams responsible for C_4 , the dependence on the mixing angle cancels, while the contributions to the purely left- and right-handed operators show the proportionality $C_1 \sim \tan^2 \theta$ and $\tilde{C}_1 \sim \cot^2 \theta$.

Whether or not the contributions to C_4 from the axigluon KK tower will lead to a cancellation of the contribution from the gluon KK tower will therefore only depend on the terms of the corresponding propagators which can induce flavor changes at both vertices. These terms are fixed by the boundary conditions of \mathcal{G}_μ and \mathcal{A}_μ . As discussed in Section 2.3, the gluon must have Neumann BCs on both branes, with the corresponding propagator (2.86). The only contribution to $\Delta F = 2$ processes arise therefore from overlap integrals with the fermion profiles and the first term in the second line of (2.86), which is $\sim t_\leq^2$. However, one of the central results of Section (2.3) was, that the $\sim t_\leq^2$ part always appears with the same coefficient for all possible combinations of BCs. The reason is, that this term could be assigned to the purely composite part of the propagator in the dual theory, which is always present, independently of the particle content of the elementary sector and whether or not there is a composite Higgs (which both is reflected in the BCs in the 5D theory).

As a consequence, already the Lagrangian (3.57) ensures that there happens a cancellation of the contributions to C_4 between the gluon and axigluon KK modes, which does neither depend on the mixing angle in (3.54) nor on the BCs still to be chosen in order to fix the axigluon propagator. This can be better understood from the dual theory, in which the global symmetry corresponding to the bulk symmetry group (3.51) forbids these mixed chirality operators. Section 3.5 will address this underlying explanation.

In a specific model, the BCs of the axigluon propagator need to be fixed and there are physical motivations other than the flavor problem which leave not much room for choice here. For details regarding the following discussion refer to Section 2.3, in which all combinations of BCs and their implications are discussed. We will assume the axigluon propagator to have the most general form (2.82) to begin with and determine the values of the coefficients gradually. We will also adopt the notation (ND) for Neumann (Dirichlet) BCs in the UV (IR) and likewise for all other combinations.

Choosing Neumann BCs on both branes implies a massless axigluon zero mode, which is clearly not seen in experiments and the (NN) scenario is therefore ruled out. Switching on a Higgs vev in the IR, which implies that the axigluons are massive due to a spontaneous symmetry breaking, will only achieve a mass of the first mode of the order of the electroweak scale. The current mass limit for an axigluon from dijet resonance searches at LHC is [193]

$$m_{\mathcal{A}}^{\text{exp}} > 3.28 \text{ TeV}. \quad (3.58)$$

We extracted an upper limit of $m_1^{\mathcal{A}} < 0.235 M_{\text{KK}}$ for the lowest lying KK mode in the (ND) scenario, as becomes visible from the plot in the upper left panel of Figure 2.8. Clearly, if the only source of breaking was an IR localized Higgs the most recent mass bounds would therefore push the KK scale already above 10 TeV, in which case the flavor problem wouldn't pose itself to begin with. This makes sense from the perspective of the dual theory as well, because Neumann BCs in the UV correspond to an elementary gauge boson which gets massive by coupling to the composite Higgs, just as the W^\pm and the Z , resulting in masses in the same range. Imposing Dirichlet BCs in the UV eliminates this gauge boson from the theory, which in this case only has composite axigluons, identified with the corresponding KK modes. Consequentially, the (DN) scenario allows for an upper bound of $m_{\mathcal{A}^1} < 2.4 M_{\text{KK}}$ as shown in the upper right panel of Figure 2.8, which is still in agreement with the current bounds for a TeV-ish KK scale.⁸

One source of breaking in the IR can however not be avoided. Yukawa interactions on the IR brane can only be invariant operators, if the $SU(3)_D$ and $SU(3)_S$ quantum numbers of the doublet and singlet quarks are saturated. The implementation of the Yukawa couplings requires therefore an extended scalar sector. One possibility is to introduce an additional colored scalar $S \sim (\mathbf{3}, \bar{\mathbf{3}}, 1)_0$, where the transformation properties are denoted according to $(SU(3)_D, SU(3)_S, SU(2)_L)_Y$, such that the last two lines of (2.122) have to be replaced by

$$\left[\dots \right] \longrightarrow \left[\frac{S}{M_{\text{KK}}} \left\{ \epsilon_{ab} \bar{Q}_{La} H_b^\dagger \mathbf{Y}_u^{(5D)} u_R^c + \epsilon_{ab} \bar{Q}_{Ra} H_b^\dagger \bar{\mathbf{Y}}_u^{(5D)} u_L^c + \bar{Q}_L H \mathbf{Y}_d^{(5D)} d_R^c + \bar{Q}_R H \bar{\mathbf{Y}}_d^{(5D)} d_L^c \right\} + \text{h.c.} \right], \quad (3.59)$$

in which $H \sim (\mathbf{1}, \mathbf{1}, \mathbf{2})_{\frac{1}{2}}$ denotes the SM Higgs and the Yukawa interactions are higher dimensional operators. Alternatively, one can avoid the appearance of higher dimensional brane-localized operators and write down dimension four operators,

$$\left[\dots \right] \longrightarrow \left[\bar{Q}_L H_u \mathbf{Y}_u^{(5D)} u_R^c + \bar{Q}_R H_u \bar{\mathbf{Y}}_u^{(5D)} u_L^c + \bar{Q}_L H_d \mathbf{Y}_d^{(5D)} d_R^c + \bar{Q}_R H_d \bar{\mathbf{Y}}_d^{(5D)} d_L^c \right] + \text{h.c.}, \quad (3.60)$$

in which two Higgs doublets have to be introduced, transforming under the representations $H_u \sim (\mathbf{3}, \bar{\mathbf{3}}, \mathbf{2})_{-\frac{1}{2}}$ and $H_d \sim (\mathbf{3}, \bar{\mathbf{3}}, \mathbf{2})_{\frac{1}{2}}$. In both cases will the colored scalars

⁸In addition, such a heavy first KK mode is already localized much closer to the IR brane and will therefore dominantly decay into top pairs, so that (3.58) does not apply and the bounds are considerably weaker, see Section 3.7.

contribute to the breaking of the extended bulk symmetry and therefore to the axigluon mass if they take on their vevs. A detailed discussion of both variants of the extended scalar sector can be found in Section 3.6.

For now, we note that the only physically viable BCs are Dirichlet BCs in the UV and mixed BCs in the IR. That means, that the breaking from the IR localized scalars dictates the IR boundary condition, completely analogous to the case of EWSB, only that the electroweak gauge bosons have Neumann BCs in the UV. The propagator of the axigluon \mathcal{A}_μ follows from (2.82) and yields, expanded for small momenta,

$$D_{\mu\nu}^{\xi=1}(q, t; t') = \frac{\eta_{\mu\nu} L}{4\pi r_c M_{\text{KK}}^2} \left(t_{<}^2 - \frac{v_{\text{IR}}}{2 + v_{\text{IR}}} t^2 t'^2 \right), \quad (3.61)$$

in which v_{IR} depends on the value of the $SU(3)_D \times SU(3)_S$ breaking vev on the IR brane, compare (2.93) and (2.102).

Given the expression (3.61), the effective Hamiltonian for four fermion operators from integrating out the axigluon KK excitations can be computed as described in Section (2.6). One finds

$$\begin{aligned} \mathcal{H}_{\text{eff}}^{(A)} = & \frac{2\pi\alpha_s}{M_{\text{KK}}^2} \sum_{q,q'} S(\bar{q}_i, q_j; \bar{q}'_k, q'_l) \frac{t^a \otimes t^a}{s_\theta^2 c_\theta^2} \\ & \left\{ 2L(\bar{q}_L \gamma^\mu [\tilde{\Delta}_Q s_\theta^2 - \tilde{\varepsilon}_Q] q_L - \bar{q}_R \gamma^\mu [\tilde{\Delta}_q c_\theta^2 - \tilde{\varepsilon}_q] q_R) \right. \\ & \quad \otimes (\bar{q}'_L \gamma_\mu [\tilde{\Delta}_{Q'} s_\theta^2 - \tilde{\varepsilon}_{Q'}] q'_L - \bar{q}'_R \gamma_\mu [\tilde{\Delta}_{q'} c_\theta^2 - \tilde{\varepsilon}_{q'}] q'_R) \\ & \quad - \frac{v_{\text{IR}}}{2 + v_{\text{IR}}} L (\bar{q}_L \gamma^\mu [\Delta_Q s_\theta^2 - \varepsilon_Q] q_L - \bar{q}_R \gamma^\mu [\Delta_q c_\theta^2 - \varepsilon_q] q_R) \\ & \quad \left. \times (\bar{q}'_L \gamma_\mu [\Delta_{Q'} s_\theta^2 - \varepsilon_{Q'}] q'_L - \bar{q}'_R \gamma_\mu [\Delta_{q'} c_\theta^2 - \varepsilon_{q'}] q'_R) \right\}. \end{aligned} \quad (3.62)$$

As in the case of the Z boson, terms proportional to $\varepsilon_{Q,q}$ can be discarded to very good approximation, because they are of $\mathcal{O}(v^2/M_{\text{KK}}^2)$. In this approximation one obtains the simpler expression

$$\begin{aligned} \mathcal{H}_{\text{eff}}^{(A)} = & \frac{2\pi\alpha_s}{M_{\text{KK}}^2} \sum_{q,q'} S(\bar{q}_i, q_j; \bar{q}'_k, q'_l) t^a \otimes t^a \\ & \left\{ 2L(\bar{q}_L \gamma^\mu \tilde{\Delta}_Q \tan \theta q_L - \bar{q}_R \gamma^\mu \tilde{\Delta}_q \cot \theta q_R) \right. \\ & \quad \otimes (\bar{q}'_L \gamma_\mu \tilde{\Delta}_{Q'} \tan \theta q'_L - \bar{q}'_R \gamma_\mu \tilde{\Delta}_{q'} \cot \theta q'_R) \\ & \quad - \frac{v_{\text{IR}}}{2 + v_{\text{IR}}} L (\bar{q}_L \gamma^\mu \Delta_Q \tan \theta q_L - \bar{q}_R \gamma^\mu \Delta_q \cot \theta q_R) \\ & \quad \left. \times (\bar{q}'_L \gamma_\mu \Delta_{Q'} \tan \theta q'_L - \bar{q}'_R \gamma_\mu \Delta_{q'} \cot \theta q'_R) \right\}, \end{aligned} \quad (3.63)$$

which is valid up to $\mathcal{O}(v^4/M_{\text{KK}}^4)$ corrections. By comparing the second line of equation (3.63) with the last line of (2.185), one can clearly see how the cancellation of the tensor structures for the mixed-chirality operators works.

However, if the coefficient $v_{\text{IR}}/(2 + v_{\text{IR}})$ is of order one, the $\Delta F = 2$ contributions to

the Wilson coefficients C_4 and C_5 induced by the second term in (3.61) will become of the same size as the terms which cancel out and thus reintroduce the flavor problem.

The value of v_{IR} depends sensitively on the modeling of the extended scalar sector, but with reference to (2.102) and Section 3.6, we can anticipate that it can be written as

$$v_{\text{IR}} = L \frac{g_s^2}{2N_C c_\theta^2 s_\theta^2} \frac{v_4^2}{M_{\text{KK}}^2} \xi = \frac{2\pi\alpha_s L}{N_C c_\theta^2 s_\theta^2} \frac{v_4^2}{M_{\text{KK}}^2} \xi, \quad (3.64)$$

in which v_4 denotes the vev of the scalar which couples to the strong sector (either H_u and H_d in (3.60) or S in (3.59)), $N_C = 3$ the number of colors, $g_s = g_{s5}/\sqrt{2\pi r_c}$ the strong coupling constant and ξ some for now unspecified order one factor, parameterizing the effects from modeling the extended scalar sector. With the additional assumption that v_4 is proportional to the electroweak breaking scale (which will turn out to be true for the scenario (3.60)), the contributions induced by the BCs are suppressed by v^2/M_{KK}^2 with respect to the gluon KK mode contributions to C_4 . The combined contributions to the Wilson coefficients of the operators (3.18) from the KK towers of the gluon (2.185) and the axigluon (3.63) read⁹

$$\begin{aligned} C_1^{\mathcal{G}+\mathcal{A}} &= \frac{2\pi L}{M_{\text{KK}}^2} \left[\frac{\alpha_s}{2} \left(1 - \frac{1}{N_C} \right) \right] \frac{1}{c_\theta^2} \left\{ (\tilde{\Delta}_D)_{12} \otimes (\tilde{\Delta}_D)_{12} - 2(\tilde{\Delta}_D)_{12} \otimes (\tilde{\varepsilon}_D)_{12} \right. \\ &\quad \left. + \frac{1}{s_\theta^2} (\tilde{\varepsilon}_D)_{12} \otimes (\tilde{\varepsilon}_D)_{12} - \frac{1}{2} \frac{v_{\text{IR}}}{2 + v_{\text{IR}}} \left[s_\theta^2 (\Delta_D)_{12}^2 - 2(\Delta_D)_{12} (\varepsilon_D)_{12} + \frac{1}{s_\theta^2} (\varepsilon_D)_{12}^2 \right] \right\}, \\ \tilde{C}_1^{\mathcal{G}+\mathcal{A}} &= \frac{2\pi L}{M_{\text{KK}}^2} \left[\frac{\alpha_s}{2} \left(1 - \frac{1}{N_C} \right) \right] \frac{1}{s_\theta^2} \left\{ (\tilde{\Delta}_d)_{12} \otimes (\tilde{\Delta}_d)_{12} - 2(\tilde{\Delta}_d)_{12} \otimes (\tilde{\varepsilon}_d)_{12} \right. \\ &\quad \left. + \frac{1}{c_\theta^2} (\tilde{\varepsilon}_d)_{12} \otimes (\tilde{\varepsilon}_d)_{12} - \frac{1}{2} \frac{v_{\text{IR}}}{2 + v_{\text{IR}}} \left[c_\theta^2 (\Delta_d)_{12}^2 - 2(\Delta_d)_{12} (\varepsilon_d)_{12} + \frac{1}{c_\theta^2} (\varepsilon_d)_{12}^2 \right] \right\}, \\ C_4^{\mathcal{G}+\mathcal{A}} &= -N_C C_5^{\text{RS}} = \frac{2\pi L}{M_{\text{KK}}^2} 2\alpha_s \left\{ -\frac{1}{c_\theta^2} (\tilde{\Delta}_D)_{12} \otimes (\tilde{\varepsilon}_d)_{12} - \frac{1}{s_\theta^2} (\tilde{\Delta}_d)_{12} \otimes (\tilde{\varepsilon}_D)_{12} \right. \\ &\quad \left. + \frac{1}{s_\theta^2 c_\theta^2} (\tilde{\varepsilon}_D)_{12} \otimes (\tilde{\varepsilon}_d)_{12} - \frac{1}{2} \frac{v_{\text{IR}}}{2 + v_{\text{IR}}} \left[(\Delta_D)_{12} (\Delta_d)_{12} - \frac{1}{s_\theta^2} (\Delta_D)_{12} (\varepsilon_d)_{12} \right. \right. \\ &\quad \left. \left. - \frac{1}{c_\theta^2} (\Delta_d)_{12} (\varepsilon_D)_{12} + \frac{1}{c_\theta^2 s_\theta^2} (\varepsilon_D)_{12} (\varepsilon_d)_{12} \right] \right\}, \end{aligned} \quad (3.65)$$

⁹The electroweak contributions are not repeated as they are unchanged from (3.20).

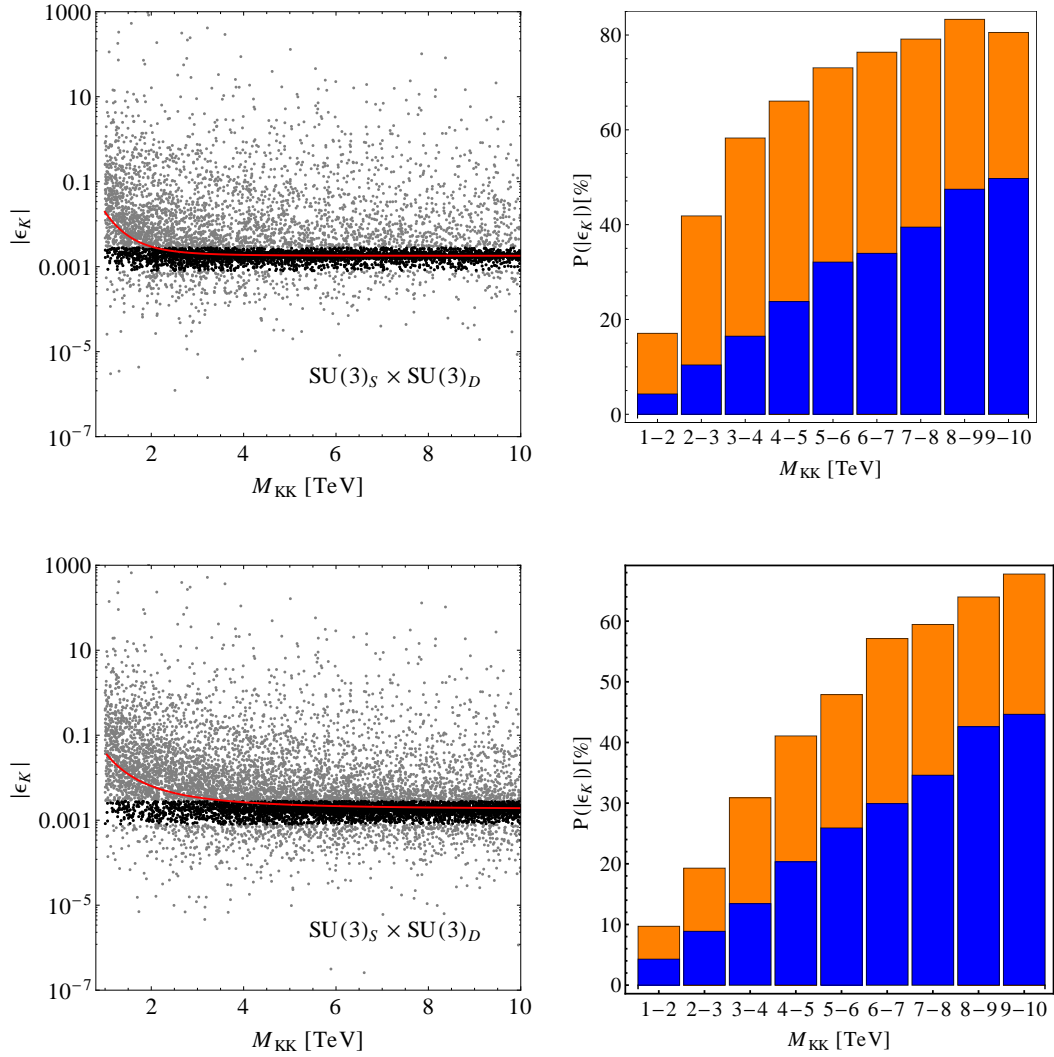


Figure 3.7: The upper row refers to the minimal RS model, the lower row to the custodially protected extension. The left panels show the observable $|\epsilon_K|$ plotted against the KK scale for the full parameter set and the extended color gauge group (3.51). A fit to the median value of the parameter points in 500 GeV bins is plotted in red and parameter points which do (not) agree with the bound (3.45) are black (gray). The right panels shows the percentages of parameter points in agreement with this bound for the RS model with (orange) and without (blue) extended color gauge group.

which again considerably simplify if one keeps only the leading terms in the v^2/M_{KK}^2 expansion,

$$\begin{aligned}
 C_1^{\mathcal{G}+\mathcal{A}} &= \frac{2\pi L}{M_{\text{KK}}^2} \left[\frac{\alpha_s}{2} \left(1 - \frac{1}{N_C} \right) \right] \frac{1}{c_\theta^2} (\tilde{\Delta}_D)_{12} \otimes (\tilde{\Delta}_D)_{12}, \\
 \tilde{C}_1^{\mathcal{G}+\mathcal{A}} &= \frac{2\pi L}{M_{\text{KK}}^2} \left[\frac{\alpha_s}{2} \left(1 - \frac{1}{N_C} \right) \right] \frac{1}{s_\theta^2} (\tilde{\Delta}_d)_{12} \otimes (\tilde{\Delta}_d)_{12}, \\
 C_4^{\mathcal{G}+\mathcal{A}} &= -N_C C_5^{\text{RS}} = \frac{2\pi L}{M_{\text{KK}}^2} 2\alpha_s \left\{ -\frac{1}{c_\theta^2} (\tilde{\Delta}_D)_{12} \otimes (\tilde{\varepsilon}_d)_{12} - \frac{1}{s_\theta^2} (\tilde{\Delta}_d)_{12} \otimes (\tilde{\varepsilon}_D)_{12} \right. \\
 &\quad \left. - \frac{1}{2} \frac{v_{\text{IR}}}{2 + v_{\text{IR}}} (\Delta_D)_{12} (\Delta_d)_{12} \right\}.
 \end{aligned} \tag{3.66}$$

In (3.66), the first two terms in C_4, C_5 include the $\varepsilon_{Q,q}$ structure and the last one is proportional to the IR BC v_{IR} , which both are of the order v^2/M_{KK}^2 . Using (3.64) and $v_{\text{IR}} < 1$, this results in the relation

$$C_4^{\mathcal{G}+\mathcal{A}} \approx \frac{\alpha_s \pi L}{2N_C c_\theta^2 s_\theta^2} \xi \frac{v_4^2}{M_{\text{KK}}^2} C_4 \sim \begin{cases} \frac{2}{3} \alpha_s \pi L \xi \frac{v_4^2}{M_{\text{KK}}^4} C_4, & \theta = 45^\circ, \\ \frac{8}{9} \alpha_s \pi L \xi \frac{v_4^2}{M_{\text{KK}}^4} C_4, & \theta = 30^\circ \text{ or } \theta = 60^\circ, \end{cases} \tag{3.67}$$

where in the last step $N_C = 3$ has been inserted and the value of the mixing angle has been fixed for two examples. As noted above, in principle one is free to choose the mixing angle because the cancellation of the leading order terms of C_4 does not depend on θ . From (3.67) one can see that also the term induced by the BCs is largely independent, however in the parameter corner of very large or very small mixing angles, the terms enhanced by c_θ^{-2} and s_θ^{-2} in the Wilson coefficients (3.66) become too large. The smallest overall contributions are achieved for $\theta = 45^\circ$, which will be the default setting for the following numerical analyses. Equation (3.67) has to be compared with the equivalent relation for the scenario of aligned right-handed localization parameters (3.49), for which we estimated, that the suppression is sufficient for a KK scale of 1 – 2 TeV.

In the upper row and left panel of Figure 3.7, the scatter plot in the right panel of Figure 3.6 has been redone with the gluon contributions in the Wilson coefficients (3.20) replaced by the exact expressions in (3.65) and assuming the minimal RS model without a custodial protection. For the numerical analysis the same parameter points have been used and $\xi = 1$, $\theta = 45^\circ$ as well as $v_4 = 246$ GeV have been employed for the parameters of the extended gauge sector. From the red curve, which is again fitted to the median of eighteen 500 GeV bins of M_{KK} one can see that the estimate above was sharp. The approximate bound on M_{KK} above which the parameter points on average fulfill the ϵ_K constraint (3.45) is $M_{\text{KK}} > 2$ TeV. In the left panel of the lower row, the same plot has been made with the additional assumption of a custodial protection induced by an extended electroweak gauge group. The bound is stronger than from the minimal model for two reasons. Already without the extended color gauge group, is the bound from ϵ_K stronger, because of the huge enhancement of the \tilde{C}_1 , as discussed in Section 3.3. This is partially canceled by a cancellation of the gluon

and the electroweak contributions to C_5 in the custodially protected model. However, the extended color gauge group already cancels the gluon contributions to C_5 , so that in the electroweak corrections will reinforce the corrections from this mixed-chirality operator, with the result of a bound of roughly $M_{\text{KK}} > 3$ TeV.

The right panels in Figure 3.7 show the improvement even clearer as they compare the percentages of parameter points which fulfill the ϵ_K constraint in 1 TeV bins of M_{KK} in the minimal (upper row) or custodially protected (lower row) RS model (blue) and the corresponding RS model with extended gauge sector (orange). While in the RS model, less than 5% of parameter points in the lowest bin agree with the constraint from ϵ_K roughly 17% (9% with custodial protection) agree in the RS model with an extended color group.

ff

This RS model with extended color gauge group does therefore not require fine-tuning in order to agree with the bounds from $\Delta F = 2$ observables, although a tension prevails if a custodial protection is assumed.

3.5 Implications for Other Theories

In Chapter 2, below equation (2.41) is discussed, how a gauge symmetry in the bulk of the RS model corresponds to a global symmetry in the composite sector of the dual theory. This is the starting point for the understanding of the absence of any contributions to the dangerous Wilson coefficients in (3.20) in the strongly coupled dual of the RS model with an extended color gauge symmetry. Theories without a holographic dual (in particular CTC), as described towards the end of Section 1.1 might also evade exclusion if this mechanism is applied.

Let us remind ourselves, that the composite sector must be a strongly coupled large N theory in order for the AdS/CFT duality to hold. The two-point function of a conserved current can be described in such a large N theory by the exchange of an infinite tower of vector meson states, which carry the quantum numbers of the corresponding global symmetry, compare (2.42). This is dual to the KK modes of the respective gauge boson, up to mixing with the elementary gauge boson, which corresponds to the zero mode. We can resume, that due to the AdS/CFT duality, there exists a correspondence between

$$\left\{ \begin{array}{c} \text{A bulk symmetry } G \\ \text{in the} \\ \text{5D theory} \end{array} \right\} \text{ and } \left\{ \begin{array}{c} \text{A global symmetry } G \\ \text{of the} \\ \text{4D theory} \end{array} \right\} \text{ and } \left\{ \begin{array}{c} \text{A tower of composite} \\ \text{vector mesons in the adjoint} \\ \text{of } G \text{ in the 4D theory} \end{array} \right\} .$$

Therefore, a quark bilinear (by quark we will denote fermions in the elementary sector in this section),

$$\bar{\psi} \gamma_\mu T^a \psi, \tag{3.68}$$

for an arbitrary element of some Lie algebra $T^a \in \mathfrak{g}$ with dimension a , can couple to a tower of composite mesons if the corresponding group G is a global symmetry of

the composite sector. A four quark operator

$$\frac{1}{\Lambda^2} (\bar{\psi} \gamma_\mu T^a \psi) (\bar{\psi} \gamma^\mu T^a \psi), \quad (3.69)$$

will consequentially only have a non-zero coefficient, if the composite sector is invariant under the corresponding global symmetry. Note, that here the composite scale Λ is to be identified with the KK scale.

If now as an example, the 5D gauge boson of some bulk gauge symmetry only couples to left-handed zero modes, this will translate to composites which will only couple to left-handed quarks in the dual theory and from the list (3.20) only C_1 would receive contributions. One might object, that in the minimal RS model the bulk $SU(2)_L$ gauge bosons seem to contribute to all Wilson coefficients in (3.20), except C_4 because of the color structure, but this does not hold true. The electroweak neutral current is described by the exchange of the KK excitations of the photon and the Z , which in return are mixtures of the hypercharge $U(1)_Y$ and the neutral $SU(2)_L$ gauge bosons, just as in the SM. The hypercharge $U(1)_Y$ gives rise to vector couplings and its admixture is the sole reason for the Z to couple to right-handed fermions. In the limit of vanishing hypercharge, in which $c_w^2 \rightarrow 1$, $s_w^2 \rightarrow 0$ and $Q_d \rightarrow T_3^D$, one can check that all electroweak contributions vanish apart from the one for C_1 , for which

$$Q_d^2 \alpha + \frac{(T_3^D - s_w^2 Q_d)^2 \alpha}{s_w^2 c_w^2} \rightarrow (T_3^D)^2 \frac{g^2}{4\pi}, \quad (3.70)$$

as one would expect. In the dual theory, there are only composite mesons with couplings to left-handed quarks and thus a four quark interaction involving right-handed quarks will not occur.

For the same reason purely left-handed, purely right-handed and mixed chirality four fermion interactions get contributions from color-charged composite mesons, because the gluon couples vectorially. If this group is now extended to $SU(3)_L \times SU(3)_R$, the composite sector will again only allow for four quark operators with only quarks of the same chirality as external legs, because

$$\frac{1}{\Lambda^2} (\bar{\psi}_L \gamma_\mu T_L^a \psi_L) (\bar{\psi}_R \gamma^\mu T_R^a \psi_R), \quad (3.71)$$

vanishes if T_L^a and T_R^a belong to different Lie groups. This is independent of the gauge couplings for the two bulk $SU(3)$ s and therefore of the mixing angle θ in (3.56), because in this basis the mixed chirality operators can simply not be constructed from the meson fields available in the composite sector. Extreme values of $\tan \theta$ will only affect the contributions to C_1 and \tilde{C}_1 .

This is hidden by the fact that we choose the linear combination with vector and the one with axial vector couplings in (3.54) to have different BCs. In terms of these combinations, which correspond to the equivalent linear combinations of vector mesons in the dual theory, it looks like their contributions to C_4 and C_5 cancel. In other words, considering only the bulk symmetry, the composite sector has vector mesons which couple either to left- or to righthanded currents and a change of basis may not alter the fact, that the Wilson coefficients of four-quark operators which include both chiralities are zero.

One can also understand the remaining terms in C_4 in (3.66). The first two terms

would vanish, if the 5D doublet and singlet would decompose into purely left- and right-handed 4D fields. The mixing induced by the couplings to a brane-localized Higgs are the reason for the cancellation being not perfect, and those terms do also appear for the example of a purely left-handed coupling above. This is however rooted in the fermion implementation, which can be seen by the fact that one can not find these terms based on the propagator (3.61) alone.

Moreover, the IR localized Higgs has another effect, not directly evident from (3.61). Because it gives masses to the linear combination with axial vector couplings, the corresponding composite mesons will have a different mass than the ones with vectorial couplings which do not interact with the composite Higgs. The term in the last line of (3.66) measures the amount by which this mass splitting sets off the cancellation, which explains why it must be proportional to the Higgs vev. In the propagator we encountered the responsible terms in the analysis of the (DD) BCs in Section 2.3.

There is good reason to believe that these conclusions carry over to a composite theory which cannot be described by a holographic dual. Conformal Technicolor, which was shortly discussed in section 1.1 is such a small N strongly coupled theory, which features a composite Higgs but no composite fermions. It does therefore not explain the hierarchies in the quark sector and has no built in RS-GIM, but it solves the hierarchy problem by assuming that the scaling dimension of the Higgs mass operator is $\Delta_{H^\dagger H} = 4$, while $\Delta_H \gtrsim 1$. If it were possible to describe CTC by a 5D theory, it would correspond to a model in which the whole SM model field content is on the UV brane and only the Higgs extends into the bulk, but stays close to the UV brane in order to allow for it to have a small scaling dimension, so that the Yukawa interactions are only slightly irrelevant [29]. We concluded, that it may be the only feasible way to bring an explanation of the hierarchy problem based on a strongly coupled theory in agreement with experimental constraints if it should turn out that quarks of all flavors are elementary particles. It is however strongly constrained from numerical analyses in combination with flavor constraints and already ruled out, if the new resonances do not respect additional flavor symmetries [30].

Whether the results obtained in the last section will also hold for a small N theory can not be computed. It is however encouraging that QCD, which isn't exactly a large N theory does not only exhibit rho-photon mixing in complete analogy with the elementary-composite mixing in the dual descriptions of RS models, but also features a vector meson octet, which corresponds to the global $SU(3)_V$ symmetry of (quantum) QCD. In the holographic dual, this octet would be the first KK mode of a gauged bulk flavor $SU(3)_V$.

If the global symmetry of such a small N theory were $SU(3)_D \times SU(3)_S$, it is not too far fetched to assume that there would be mesons for these global charges as well. The resulting loosening of the flavor bounds is shown by the available parameter space for the extended model in the $\Delta_{H^\dagger H} - \Delta_H$ plane in Figure 3.8, shaded in green. It is achieved by eliminating the coefficients of the dangerous mixed chirality operators from the analysis. For comparison, the bound for minimal CTC as shown in Figure 1.4 is also plotted, the blue shaded region is generically excluded by numerical analyses. Only a small corner of parameter space opens up, but the situation is actually better

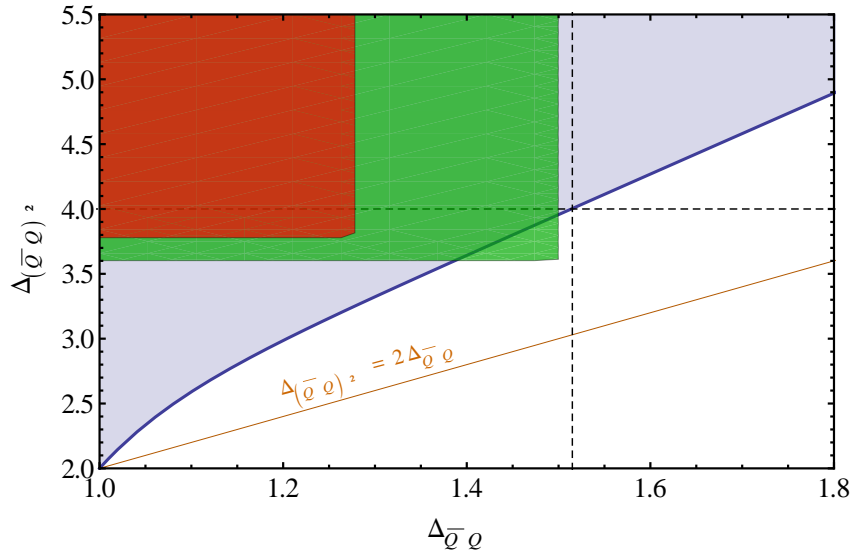


Figure 3.8: Region in the $\Delta_H - \Delta_{H^\dagger H}$ plane which is excluded using numerical methods, shown in blue. These bounds depend on the global symmetry of the technicolor condensate (and become weaker for a larger symmetry group), which is assumed to be $SU(2)$ in this plot. The red region in the upper left corner is the preferred region by flavor bounds on the ETC scale and a natural top mass. The green region shows the improvement assuming a global $SU(3)_D \times SU(3)_S$ symmetry. The dashed cross indicates the lowest possible value of $\Delta_H \equiv \Delta_{\bar{Q}Q}$, while $\Delta_{H^\dagger H} \equiv \Delta_{(\bar{Q}Q)^2} = 4$, and the orange line depicts the large N limit $\Delta_{H^\dagger H} = 2\Delta_H$.

then it appears, because the scalar sector needs to respect the enlarged global symmetry as well and this will lead to a weaker bound from the numerical analysis, which means the thick blue line in Figure 3.8 shifts up. This has not been implemented in the plot, because the fit function has not been given in the original paper, however compare [30, Fig. 4].

We can resume that the dual interpretation of the extended gauge sector proposed for RS models suggests that the associated suppression of the coefficients of mixed chirality operators can be achieved in a wider class of strongly coupled models. Experimentally, such a global symmetry would reveal itself either by the additional mesonic resonances or by the variety of scalars in the extended Higgs sector, which will be the subject of Section 3.6.

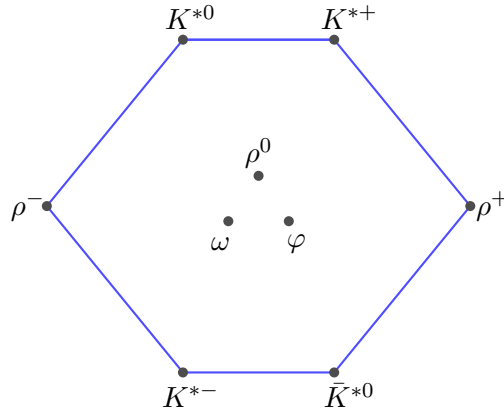


Figure 3.9: In QCD, the global $SU(3)_V$ symmetry leads to an octet of vector mesons, and a singlet corresponding to the $U(1)_B$. In the same way, vector mesons of a strongly coupled extension of the SM could be realized which correspond to a global $SU(3)_D \times SU(3)_S$ and therefore do not lead to excessive contributions to ϵ_K .

3.6 The Extension of the Scalar Sector

In order to implement Yukawa couplings on the IR brane, the Higgs sector of the extended RS model has to include color charged scalars, which saturate the quantum numbers of the bulk quarks under $SU(3)_D \times SU(3)_S$

$$Q \sim (\mathbf{3}, \mathbf{1}), \quad q^c \sim (\mathbf{1}, \mathbf{3}). \quad (3.72)$$

The same fields will also contribute to the axigluon KK masses by inducing IR BCs once they take on their vev. The most minimal extension of the scalar sector that allows for gauge invariant Yukawa couplings is to introduce an electroweak singlet with hypercharge $Y = 0$, but transforming as a bitriplet under $SU(3)_D \times SU(3)_S$. This is analogue to the most popular extension of the scalar sector in four dimensional implementations of chiral color models [194]. In addition to the SM Higgs Lagrangian on the IR brane and the Yukawa couplings (3.59), this introduces the following terms,

$$\mathcal{L}_S = \frac{\delta(|\phi| - \pi)}{r_c} \left\{ \text{Tr} \left[(D_\mu S)^\dagger (D^\mu S) \right] - V(S, H) \right\}. \quad (3.73)$$

Here, the trace is taken over the indices of the $SU(3)_D \times SU(3)_S$ generators, which by a slight abuse of language will collectively be called color indices hereafter. The potential $V(S, H)$ is given in Appendix D because it is not important for the following discussion. It is a priori not necessary to confine S to the IR brane, but it would lead to chiral color breaking by a bulk mass instead of a BC if it was a bulk field, which would change the analysis in the Sections 3.4 and 3.5 considerably, because a broken gauge symmetry in the bulk will not correspond to a global symmetry in the dual theory. We will therefore always assume the whole scalar sector to be localized on the IR brane.

The covariant derivative in (3.73) reads

$$(D_\mu S)_{\alpha a} = \left(\delta_{ab} \delta_{\alpha\beta} \partial_\mu - i g_{D5} \delta_{\alpha\beta} (G_D)_\mu^r T_{ab}^r + i g_{S5} (G_S)_\mu^r (T_{\alpha\beta}^r)^* \delta_{ab} \right) S_{b\beta}, \quad (3.74)$$

in which the color indices of the $SU(3)_D$ ($SU(3)_S$) are denoted by greek (latin) letters and the index $r = 1 \dots, 8$ runs over the number of generators of the respective group. If the vev of S is supposed to break the bulk $SU(3)_D \times SU(3)_S$ down to its diagonal subgroup, it must read

$$\langle S_{a\alpha} \rangle = \frac{v_S}{\sqrt{2N_C}} \delta_{a\alpha}. \quad (3.75)$$

Inserting the linear combinations (3.54) and using

$$\cos \theta = \frac{g_{S5}}{\sqrt{g_{S5}^2 + g_{D5}^2}}, \quad \sin \theta = \frac{g_{D5}}{\sqrt{g_{S5}^2 + g_{D5}^2}}, \quad (3.76)$$

and (3.56), it follows from the kinetic term

$$\text{Tr} \left[(D_\mu S)^\dagger (D^\mu S) \right] \ni \frac{1}{2} \frac{g_{S5}^2 v_S^2}{2N_C c_\theta^2 s_\theta^2} \mathcal{A}_\mu^r \mathcal{A}^{r\mu}. \quad (3.77)$$

Comparing this with the expressions (2.93) and (2.102), one can infer that for the axigluon

$$v_{\text{IR}} = L \frac{m_A^2}{M_{\text{KK}}^2} = L \frac{g_s^2}{2N_C c_\theta^2 s_\theta^2} \frac{v_S^2}{M_{\text{KK}}^2}, \quad (3.78)$$

which we already anticipated in (3.64). In SM implementations of chiral color, v_S is directly proportional to the axigluon mass. This is also true for an axigluon implemented in an RS model, if the IR brane provides the only source of $SU(3)_D \times SU(3)_S$ breaking. However, we could rule out this choice of BCs for the model at hand in Section 3.4, because it leads to a too light first KK mode. This is rooted in the fact that the IR brane is connected to the electroweak breaking scale. The vev of every scalar confined to the IR is naturally bounded from above by the cutoff $v_S \leq M_{\text{KK}}$. However, if the axigluon has Dirichlet BCs in the UV, the mass of its first excitation will be in the TeV range even for v_S well below M_{KK} , as discussed in Section 2.3.

Already in the SM it is questionable to assume such a minimal extension of the Higgs sector, even if the vev of S can in principle be chosen arbitrarily large. The problem arises not from the axigluon mass, but from the top quark mass. If the Yukawa interactions are dimension five operators as in (3.59), the ratio $\langle S \rangle / \Lambda$ should be of order one if the top mass is to be generated with a perturbative Yukawa coupling. That makes it problematic to neglect higher dimensional operators with additional S insertions.

In the extension of the RS model it brings about another drawback. If $v_S / M_{\text{KK}} \sim 1$, the contributions to the mixed chirality Wilson coefficients in (3.66) do not have an additional suppression and become equally large as the original terms in (3.20) so that

the RS flavor problem is not solved.

The scalar sector introduced in the next section will allow for dimension four Yukawa couplings, so that the vev is necessarily connected to the electroweak scale and a sufficient suppression of the dangerous FCNCs is achieved.

A Realistic Higgs Sector

In order to evade the tension between a realistic top Yukawa coupling and the suppression of contributions to ϵ_K , we consider a scalar sector in which the Higgs which is responsible for EWSB also carries color charges. Such an extension is shortly mentioned for a chiral color extension of the SM in [195]. The corresponding Yukawa couplings have already been given in (3.60), and the additional terms in the Lagrangian read

$$\mathcal{L}_S = \frac{\delta(|\phi| - \pi)}{r_c} \left\{ \text{Tr} \left[(D_\mu H_u)^\dagger (D^\mu H_u) \right] + \text{Tr} \left[(D_\mu H_d)^\dagger (D^\mu H_d) \right] + (D_\mu h)^\dagger (D^\mu h) - V(h, H_u, H_d) \right\}, \quad (3.79)$$

where the potential will again be given in Appendix D. The three scalar fields carry the quantum numbers

	$SU(3)_D$	$SU(3)_S$	$SU(2)_L$	$U(1)_Y$
H_u	3	$\bar{\mathbf{3}}$	2	$-\frac{1}{2}$
H_d	3	$\bar{\mathbf{3}}$	2	$\frac{1}{2}$
h	1	1	2	$\frac{1}{2}$

The Higgs with SM quantum numbers will in this section be denoted by h for a better differentiation, and the corresponding covariant derivative given by (2.96) does not include couplings to the color group gauge bosons. Notice also, that the Dirichlet BCs in the UV can be modeled by putting the Lagrangian (3.73) on the UV brane and consequentially introducing a vev $\langle S \rangle \approx M_{\text{Pl}}$.¹⁰

There need to be different color charged Higgs fields for up and down quarks, because the complex conjugated H_d transforms as $H_d^\dagger \sim (\bar{\mathbf{3}}, \mathbf{3})$ under $SU(3)_D \times SU(3)_S$ and therefore if it is inserted in the up-Yukawa interactions it will not saturate the quark color charges¹¹. The SM Higgs h will give Yukawa interactions for the leptons. In principle one could write down effective lepton Yukawas with only the two color charged fields, because $h \sim H_d H_d H_u$ since $\mathbf{3} \otimes \mathbf{3} \otimes \mathbf{3} = (\mathbf{6} \oplus \bar{\mathbf{3}}) \otimes \mathbf{3} \ni \mathbf{1}$. However, the potential $V(H_u, H_d)$ has a global $U(3) \times U(3)$ symmetry, while the vacuum is invariant under $SU(3)_C \times U(1)$. This will lead to nine Goldstone bosons from which only eight will be absorbed by the axiglons in order to become massive. It is therefore necessary

¹⁰A scalar sector on the UV brane may not include an electroweak doublet, because this would introduce Yukawa interactions on the UV brane.

¹¹Notice, that for a Higgs bidoublet as in the custodial model, there is no problem in writing down both Yukawa terms with one field, because for $SU(2)$ the fundamental and anti-fundamental representation are isomorphic.

to introduce an additional scalar which is either a singlet under the color groups or under the $SU(2)_L$, in order to break the residual $U(1)$ in the potential.

The vacuum expectation values of the three scalars are dictated by the symmetries of the vacuum

$$\begin{aligned}\langle (H_u)_{a\alpha}^i \rangle &= \frac{v_u}{\sqrt{2N_C}} \delta_{a\alpha} \delta^{i1}, \\ \langle (H_d)_{a\alpha}^i \rangle &= \frac{v_d}{\sqrt{2N_C}} \delta_{a\alpha} \delta^{i2}, \\ \langle h^i \rangle &= \frac{v_\ell}{\sqrt{2}} \delta^{i2}.\end{aligned}\tag{3.80}$$

Here, small latin letters from the middle of the alphabet denote $SU(2)_L$ indices. The mass term for the electroweak gauge bosons (2.102) and for the axigluon (3.77) change accordingly and one finds,

$$M_W = \frac{g_5 \sqrt{v_u^2 + v_d^2 + v_\ell^2}}{2}, \quad M_Z = \frac{M_W}{c_w}, \quad M_A = \frac{g_{s5} \sqrt{v_u^2 + v_d^2}}{\sqrt{2N_C} s_\theta c_\theta}.\tag{3.81}$$

All three scalars are electroweak doublets and consequentially give mass to the electroweak gauge bosons, while only the color-charged fields couple to the axigluon. It follows therefore for the SM vev $v = 246$ GeV,

$$v = \sqrt{v_u^2 + v_d^2 + v_\ell^2},\tag{3.82}$$

from which one can already infer for the factor introduced in (3.64) that $\xi < 1$. In order to make this explicit, we will repeat the matching of the 5D to the 4D Lagrangian, which was performed for the electroweak sector in (2.3), for the extended color sector. Therefore, the rotation (3.54) has to be introduced in the Lagrangian for the $SU(3)_D \times SU(3)_S$ bulk gauge fields

$$\mathcal{L}_{SU(3)_D \times SU(3)_S} = G^{KM} G^{LN} \left(-\frac{1}{4} (G_D^r)_{KL} (G_D^r)_{MN} - \frac{1}{4} (G_S^r)_{KL} (G_S^r)_{MN} \right),\tag{3.83}$$

which yields

$$\begin{aligned}
 \mathcal{L}_{SU(3)_D \times SU(3)_S} = G^{KM} G^{LN} & \left\{ -\frac{1}{4} \mathcal{G}_{KL}^r \mathcal{G}_{MN}^r - \frac{1}{4} (\partial_K \mathcal{A}_L^r - \partial_L \mathcal{A}_K^r) (\partial_M \mathcal{A}_N^r - \partial_N \mathcal{A}_M^r) \right. \\
 & - g_{s5} \left[f^{rst} (\partial_K \mathcal{G}_L^r) \mathcal{A}_M^s \mathcal{A}_N^t + (\cot \theta - \tan \theta) f^{rst} (\partial_K \mathcal{A}_L^r) \mathcal{A}_M^s \mathcal{A}_N^t \right. \\
 & \quad \left. + \frac{1}{2} f^{rst} (\partial_K \mathcal{A}_L^r - \partial_L \mathcal{A}_K^r) (\mathcal{G}_M^s \mathcal{A}_N^t - \mathcal{G}_N^s \mathcal{A}_M^t) \right] \\
 & - g_{s5}^2 \left[\frac{1}{4} (\cot^2 \theta + \tan^2 \theta) f^{rst} f^{rpq} \mathcal{A}_K^s \mathcal{A}_L^t \mathcal{A}_M^p \mathcal{A}_N^q \right. \\
 & \quad + \frac{1}{4} f^{rst} f^{rpq} (\mathcal{G}_K^s \mathcal{A}_L^t - \mathcal{G}_L^s \mathcal{A}_K^t) (\mathcal{G}_M^p \mathcal{A}_N^q - \mathcal{G}_N^p \mathcal{A}_M^q) \\
 & \quad + \frac{1}{2} (\cot \theta - \tan \theta) f^{rst} f^{rpq} (\mathcal{G}_K^s \mathcal{A}_L^t - \mathcal{G}_L^s \mathcal{A}_K^t) \mathcal{A}_M^p \mathcal{A}_N^q \\
 & \quad \left. + \frac{1}{2} f^{rst} f^{rpq} \mathcal{G}_K^s \mathcal{G}_L^t \mathcal{A}_M^p \mathcal{A}_N^q \right] \left. \right\}. \tag{3.84}
 \end{aligned}$$

Here, the first line corresponds to the color gauge sector of the minimal RS model and the axigluon kinetic term, the second and third line to $\mathcal{G}\mathcal{A}\mathcal{A}$ and $\mathcal{A}\mathcal{A}\mathcal{A}$ vertices and the remaining terms to vertices with four legs.

The color-charged scalars are bitriplets under $SU(3)_D \times SU(3)_S$, so that they can be decomposed into a singlet ϕ and an octet O^r under the diagonal subgroup $SU(3)_C$,

$$\begin{aligned}
 (H_u)_{a\alpha} &= \phi_u \frac{\delta_{a\alpha}}{\sqrt{2N_C}} + O_u^r T_{a\alpha}^r \\
 (H_d)_{a\alpha} &= \phi_d \frac{\delta_{a\alpha}}{\sqrt{2N_C}} + O_d^r T_{a\alpha}^r \\
 (S)_{a\alpha} &= \phi_S \frac{\delta_{a\alpha}}{\sqrt{2N_C}} + O_S^r T_{a\alpha}^r, \tag{3.85}
 \end{aligned}$$

in which the electroweak singlet Higgs is included in order to model the UV BC. The relevant terms in the action are quadratic in the fields. Mass terms for the scalars are omitted, because they depend non-trivially on the various parameters of the Higgs potential given in Appendix D. Including only color charged fields, one finds

$$S \ni \int d^4x r \frac{2\pi}{L} \int_{\epsilon}^1 \frac{dt}{t} \left\{ \mathcal{L}_G + \mathcal{L}_A + \frac{k}{2} \delta(t-1) \mathcal{L}_{\text{IR}} + \frac{k}{2} \delta(t-\epsilon) \mathcal{L}_{\text{UV}} + \mathcal{L}_{\text{GF}} \right\}, \tag{3.86}$$

in which

$$\mathcal{L}_{\mathcal{G}} = -\frac{1}{4}\mathcal{G}_{\mu\nu}^r\mathcal{G}^{r\mu\nu} + \frac{1}{2}\left(\partial_\mu\mathcal{G}_5^r\partial^\mu\mathcal{G}_5^r + M_{\text{KK}}^2\partial_t\mathcal{G}_\mu^r\partial_t\mathcal{G}^{r\mu}\right) - M_{\text{KK}}\partial^\mu\mathcal{G}_\mu^r t\partial_t\frac{1}{t}\mathcal{G}_5^r, \quad (3.87)$$

$$\begin{aligned} \mathcal{L}_{\mathcal{A}} = & -\frac{1}{4}\left(\partial_\mu\mathcal{A}_\nu^r - \partial_\nu\mathcal{A}_\mu^r\right)^2 + \frac{1}{2}\left(\partial_\mu\mathcal{A}_5^r\partial^\mu\mathcal{A}_5^r + M_{\text{KK}}^2\partial_t\mathcal{A}_\mu^r\partial_t\mathcal{A}^{r\mu}\right) \\ & - M_{\text{KK}}\partial^\mu\mathcal{A}_\mu^r t\partial_t\frac{1}{t}\mathcal{A}_5^r, \end{aligned} \quad (3.88)$$

$$\begin{aligned} \mathcal{L}_{\text{IR}} = & \text{Tr}\left[\partial_\mu H_u\partial^\mu H_u^\dagger\right] + \text{Tr}\left[\partial_\mu H_d\partial^\mu H_d^\dagger\right] \\ & + M_{\mathcal{A}}^u\mathcal{A}_\mu^r\partial^\mu\text{Im}O_u^r + M_{\mathcal{A}}^d\mathcal{A}_\mu^r\partial^\mu\text{Im}O_d^r + \frac{1}{2}M_{\mathcal{A}}^2\mathcal{A}_\mu^r\mathcal{A}^{r\mu}, \end{aligned} \quad (3.89)$$

$$\mathcal{L}_{\text{UV}} = \text{Tr}\left[\partial_\mu S\partial^\mu S^\dagger\right] + M_{\mathcal{A}}^S\mathcal{A}_\mu^r\partial^\mu\text{Im}O_S^r + \frac{1}{2}M_{\mathcal{A}}^{S^2}\mathcal{A}_\mu^r\mathcal{A}^{r\mu}. \quad (3.90)$$

Here, $\mathcal{G}_{\mu\nu}^r$ denotes the gluon fields strength tensor and the mass terms are defined by (3.81) and

$$M_{\mathcal{A}}^i \equiv \frac{g_{s5}v_i}{\sqrt{2N_{CS\theta}c_\theta}}, \quad (3.91)$$

for $i = u, d, S$. The gauge fixing terms must take care of the mixing terms between the scalar and vector component of the bulk gluon and axigluon and the mixing between the imaginary part of the scalar octets and the vector component of the bulk fields. It follows,

$$\begin{aligned} \mathcal{L}_{\text{GF}} = & -\frac{1}{2\xi}\left(\partial^\mu\mathcal{G}_\mu^r - \xi\left[M_{\text{KK}}t\partial_t\frac{1}{t}\mathcal{G}_5^r\right]\right)^2 \\ & -\frac{1}{2\xi}\left(\partial^\mu\mathcal{A}_\mu^r - \frac{\xi}{2}\left[\delta(t-1)k\left\{M_{\mathcal{A}}^u\text{Im}O_u^r + M_{\mathcal{A}}^d\text{Im}O_d^r\right\}\right.\right. \\ & \left.\left.+ \delta(t-\epsilon)kM_{\mathcal{A}}^S\text{Im}O_S^r + 2M_{\text{KK}}t\partial_t\frac{1}{t}\mathcal{A}_5^r\right]\right)^2, \end{aligned} \quad (3.92)$$

in accordance with (2.76). This eliminates the mixing terms and one finds an analogue expression to (2.98). Upon insertion of the KK decomposition, which for the gauge fields is given by

$$\begin{pmatrix} X_\mu^r(x, t) \\ X_5^r(x, t) \end{pmatrix} = \frac{1}{\sqrt{r_c}}\sum_n \begin{pmatrix} X_\mu^{r(n)}(x)\chi_n^X(t) \\ M_{\text{KK}}a_n^X\varphi_X^{r(n)}(x)\partial_t\chi_n^X(t) \end{pmatrix}, \quad (3.93)$$

for $X = \mathcal{A}, \mathcal{G}$, and one finds for the scalar octets analogue to (2.100),

$$\begin{aligned} \text{Im}O_u^r(x) = \sum_n b_n^{\text{Im}O_u} \varphi_{\mathcal{A}}^{r(n)}(x), \quad \text{Im}O_d^r(x) = \sum_n b_n^{\text{Im}O_d} \varphi_{\mathcal{A}}^{r(n)}(x), \\ \text{Im}O_S^r(x) = \sum_n b_n^{\text{Im}O_S} \varphi_{\mathcal{A}}^{r(n)}(x), \end{aligned} \quad (3.94)$$

the boundary conditions take the form

$$\partial_t \chi_n^{\mathcal{G}}(\epsilon^+) = 0, \quad \partial_t \chi_n^{\mathcal{G}}(1^-) = 0, \quad (3.95)$$

$$\partial_t \chi_n^{\mathcal{A}}(\epsilon^+) = \frac{L}{2\pi r_c} \frac{\epsilon M_S^2}{M_{\text{KK}}^2} \chi_n^{\mathcal{G}}(\epsilon^+), \quad (3.96)$$

$$\partial_t \chi_n^{\mathcal{A}}(1^-) = -\frac{L}{2\pi r_c} \frac{M_A^2}{M_{\text{KK}}^2} \chi_n^{\mathcal{A}}(1^-), \quad (3.97)$$

and the action reads (ignoring the kinetic terms for the scalars)

$$\begin{aligned} S_{\text{Gauge},2} = \sum_n \int d^4x \left\{ -\frac{1}{4} \mathcal{G}_{\mu\nu}^{r(n)} \mathcal{G}^{r\mu\nu(n)} - \frac{1}{2\xi} \left(\partial^\mu \mathcal{G}_\mu^{r(n)} \right)^2 + \frac{(m_n^{\mathcal{G}})^2}{2} \mathcal{G}_\mu^{r(n)} \mathcal{G}^{r\mu(n)} \right. \\ \left. + \frac{1}{2} \partial_\mu \varphi_{\mathcal{G}}^{r(n)} \partial^\mu \varphi_{\mathcal{G}}^{r(n)} - \frac{\xi (m_n^{\mathcal{G}})^2}{2} \varphi_{\mathcal{G}}^{r(n)} \varphi_{\mathcal{G}}^{r(n)} \right. \\ \left. - \frac{1}{4} \left(\partial_\mu \mathcal{A}_\nu^{r(n)} - \partial_\nu \mathcal{A}_\mu^{r(n)} \right)^2 - \frac{1}{2\xi} \left(\partial^\mu \mathcal{A}_\mu^{r(n)} \right)^2 + \frac{(m_n^{\mathcal{A}})^2}{2} \mathcal{A}_\mu^{r(n)} \mathcal{A}^{r\mu(n)} \right. \\ \left. + \frac{1}{2} \partial_\mu \varphi_{\mathcal{A}}^{r(n)} \partial^\mu \varphi_{\mathcal{A}}^{r(n)} - \frac{\xi (m_n^{\mathcal{A}})^2}{2} \varphi_{\mathcal{A}}^{r(n)} \varphi_{\mathcal{A}}^{r(n)} \right\}, \end{aligned}$$

under the additional condition for the Fourier coefficients in (3.93) and (3.94)

$$\begin{aligned} \alpha_n^{\mathcal{A}} = -\frac{1}{m_n^{\mathcal{A}}}, \quad \alpha_n^{\mathcal{G}} = -\frac{1}{m_n^{\mathcal{G}}}, \quad (3.98) \\ b_n^{\text{Im}O_S} = \frac{M_S^S}{\sqrt{r_c}} \frac{\chi_n^{\mathcal{A}}(\epsilon^+)}{m_n^{\mathcal{A}}}, \quad b_n^{\text{Im}O_u} = \frac{M_A^u}{\sqrt{r_c}} \frac{\chi_n^{\mathcal{A}}(1^-)}{m_n^{\mathcal{A}}}, \quad b_n^{\text{Im}O_d} = \frac{M_A^d}{\sqrt{r_c}} \frac{\chi_n^{\mathcal{A}}(1^-)}{m_n^{\mathcal{A}}}. \end{aligned}$$

The masses $m_n^{\mathcal{A}}$ and $m_n^{\mathcal{G}}$ are fixed by the IR BCs in (3.95) and (3.97), while the UV BCs determine the coefficients α_n in the profiles (2.92). For the gluon, the UV and the IR BCs are Neumann and the masses of the KK modes are consequentially equal to the minimal RS scenario with a first excitation at $x_1 \approx 2.4$. For the axigluon, the BCs read

$$\partial_t \chi_n^{\mathcal{A}}(\epsilon^+) = L \frac{\epsilon v_S^2 g_s^2}{2N_C s_\theta^2 c_\theta^2 M_{\text{KK}}^2} \chi_n^{\mathcal{G}}(\epsilon^+), \quad (3.99)$$

$$\partial_t \chi_n^{\mathcal{A}}(1^-) = -L \frac{(v_u^2 + v_d^2) g_s^2}{2N_C s_\theta^2 c_\theta^2 M_{\text{KK}}^2} \chi_n^{\mathcal{A}}(1^-), \quad (3.100)$$

which shows that Dirichlet BCs are successfully reproduced by a UV brane localized scalar because naturally $v_S \sim M_{\text{Pl}}$, so that $v_{\text{UV}} \approx M_{\text{Pl}}/M_{\text{KK}}$ and as shown in the upper right panel of Figure 2.8, every value of v_{UV} which is not extremely small, $v_{\text{UV}} \approx \mathcal{O}(\epsilon)$, will effectively lead to Dirichlet BCs in the UV. The IR BCs tell us that

$$v_{\text{IR}} = L \frac{g_s^2}{2N_C s_\theta^2 c_\theta^2} \frac{(v_u^2 + v_d^2)}{M_{\text{KK}}^2}, \quad (3.101)$$

which compared with (3.64) shows that for a thorough implementation of the Higgs sector

$$\xi = \frac{v_u^2 + v_d^2}{v^2} < 1. \quad (3.102)$$

Since $v_{\text{IR}} < 1$ in this scenario, one can expand (3.97) and also give an approximate mass for the first axigluon KK mode of

$$x_{\mathcal{A}}^{(1)} \approx 2.4 + v_{\text{IR}}/2.4. \quad (3.103)$$

Adjusting the Fermion Profiles

Introducing different Higgs fields for the up- and down-type quarks will change the mass relations (2.158), because the vacuum expectation value is now replaced by the corresponding line of (3.80). In the extended model, the mass relations read

$$m_{q_{u_i}} = \frac{v_u}{\sqrt{2N_C}} Y_u |F(c_{Q_i})F(c_{u_i})|, \quad m_{q_{d_i}} = \frac{v_d}{\sqrt{2N_C}} Y_d |F(c_{Q_i})F(c_{d_i})|, \quad (3.104)$$

in which Y_u, Y_d are again order one parameters sensitive to the respective Yukawa couplings. In order for the physical quark masses to be reproduced, that is the left hand side of (3.104) to be unchanged, a factor

$$\begin{aligned} \frac{v\sqrt{N_C}}{v_d} &= \sqrt{\frac{v^2 N_C}{v^2 - v_u^2 - v_\ell^2}} \approx \sqrt{N_C} (1 + \tan^2 \beta)^{1/2} \equiv p_d, \\ \frac{v\sqrt{N_C}}{v_u} &= \sqrt{\frac{v^2 N_C}{v^2 - v_d^2 - v_\ell^2}} \approx \sqrt{N_C} (1 + \cot^2 \beta)^{1/2} \equiv p_u, \end{aligned} \quad (3.105)$$

has to be absorbed into the variable parameters on the right-hand side of (3.104). In writing (3.105), the standard notation $\tan \beta = v_u/v_d$ has been introduced and it was assumed that $v_\ell^2/v^2 \ll 1$.¹² Note that for all $\tan \beta$, it follows $p_d > \sqrt{N_C}$ and $p_u > \sqrt{N_C}$. One possibility is to rescale the Yukawa couplings

$$Y_d \rightarrow p_d Y_d, \quad Y_u \rightarrow p_u Y_u, \quad (3.106)$$

which however will lead to the consequences described in Section 3.3. Another way to absorb these factors is to rescale the zero mode profiles and therefore ultimately the bulk mass parameters which will correspond to moving some of the profiles closer to the IR brane. A third way would be a combination of both.

We will refrain from rescaling the Yukawa couplings. Although for small $\tan \beta \sim 1$, this will not require a rescaling by a factor of ten, as the proposal discussed in Section 3.3, it will still lead to a tension with observables which scale with positive powers of

¹²Whether this is viable or not depends on the size of the lepton Yukawas and the constraints from lepton flavor violation. A sizable v_ℓ would even lead to a smaller ξ in (3.102), and therefore at first sight bring about a less severe bound from ϵ_K , but this effect might be compensated for by the rescaling of the quark profiles as argued above.

the Yukawa couplings, as ϵ'/ϵ_K .

Instead, we will rescale the singlet profile functions,

$$F(c_{q_i}) \rightarrow p_q F(c_{q_i}), \quad (3.107)$$

and therefore all singlet zero modes will be located closer to the IR brane, while the localization parameters of the doublets remain unaffected. This may reintroduce contributions to the Wilson coefficients which are sensitive to the singlet localization. For the overlap integrals, one finds on the basis of the ZMA relations (2.180), that

$$\begin{aligned} \Delta_Q &\rightarrow \Delta_Q, & \Delta'_Q &\rightarrow \Delta'_Q, \\ \Delta_q &\rightarrow p_q^2 \Delta_q, & \Delta'_q &\rightarrow p_q^2 \Delta'_q. \end{aligned} \quad (3.108)$$

The ϵ and δ structures have an additional v^2/M_{KK}^2 suppression, which was the reason why we have not given ZMA expressions for them in Section 2.5. They can be approximated by

$$\begin{aligned} (\epsilon_Q)_{mn} \sim (\epsilon'_Q)_{mn} \sim (\delta_Q)_{mn} &\approx \frac{Y_q v^2}{M_{\text{KK}}^2} F(c_{Q_m}) F(c_{Q_n}), \\ (\epsilon_q)_{mn} \sim (\epsilon'_q)_{mn} \sim (\delta_q)_{mn} &\approx \frac{Y_q v^2}{M_{\text{KK}}^2} F(c_{q_m}) F(c_{q_n}). \end{aligned} \quad (3.109)$$

In the extended model not only the profiles change, but also these suppression factors. This means that we have to replace

$$(\epsilon_Q, \epsilon'_Q, \delta_Q) \rightarrow \frac{1}{p_q^2} (\epsilon_Q, \epsilon'_Q, \delta_Q), \quad (\epsilon_q, \epsilon'_q, \delta_q) \rightarrow (\epsilon_q, \epsilon'_q, \delta_q). \quad (3.110)$$

For the tensor structures the factorization property in the ZMA (2.183) does also hold for the integrals in (3.66), so that one ends up with the rescaling of the Wilson coefficients

$$\begin{aligned} C_1^{\mathcal{G}+\mathcal{A}} &\rightarrow C_1^{\mathcal{G}+\mathcal{A}} \\ \tilde{C}_1^{\mathcal{G}+\mathcal{A}} &\rightarrow p_d^4 \tilde{C}_1^{\mathcal{G}+\mathcal{A}}, \\ C_4^{\mathcal{G}+\mathcal{A}} = -N_C C_5^{\text{RS}} &\rightarrow \frac{2\pi L}{M_{\text{KK}}^2} 2\alpha_s \left\{ -\frac{1}{c_\theta^2} (\tilde{\Delta}_D)_{12} \otimes (\tilde{\varepsilon}_d)_{12} - \frac{1}{s_\theta^2} (\tilde{\Delta}_d)_{12} \otimes (\tilde{\varepsilon}_D)_{12}, \right. \\ &\quad \left. - \frac{p_d^2}{2} \frac{v_{\text{IR}}}{2 + v_{\text{IR}}} (\Delta_D)_{12} (\Delta_d)_{12} \right\}, \end{aligned}$$

for a correctly implemented Higgs sector. Clearly, large values of $\tan \beta$ will enhance the dangerous mixed-chirality Wilson coefficients as well as \tilde{C}_1 , which is sensitive to $\tan^4 \beta$. In Figure 3.10, the resulting bound on the KK scale from ϵ_K is plotted for different values of $\tan \beta = 0.1, 0.5, 1, 2, 5$. All of the curves correspond to a fit to the complete set of parameter points for the minimal RS model without custodial protection but with extended color gauge group and with relocated quarks and have to be compared with the red curves in Figure 3.7. The lower bound on $p_d^2 > N_C$ leads to a stronger bound on the KK scale, even for extremely small $\tan \beta$ and already

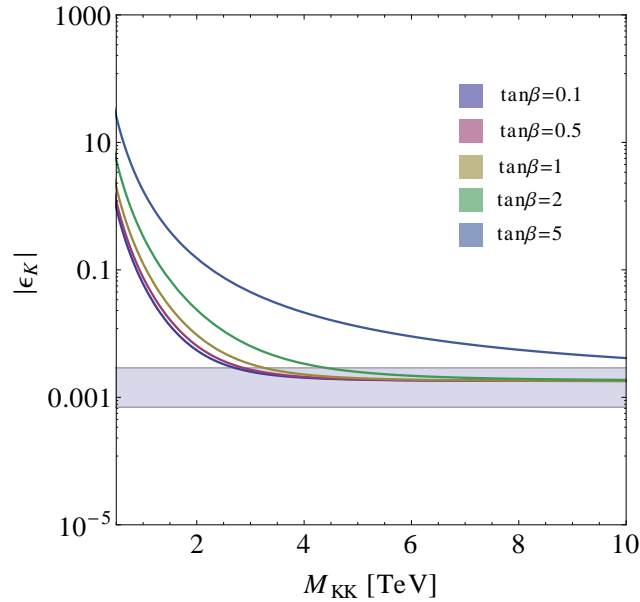


Figure 3.10: Plot of the fit to $|\epsilon_K|$ versus M_{KK} for six different values of $\tan\beta$, in which the curves are from left to right for $\tan\beta = 0.1, 0.5, 1, 2, 5$.

for $2 < \tan\beta < 5$, the bound becomes as bad as in the minimal model. Therefore, if the extended color symmetry group is realized in nature, very small $\tan\beta < 2$ are a necessary prediction for the minimal Higgs sector. Note, that implementing a custodial protection will shift the extracted value for M_{KK} from Figure 3.7 by roughly a TeV, for the reasons explained in Section 3.7. This induces a tension, because even for $\tan\beta < 1$ the extracted bound becomes $M_{\text{KK}} > 4$ TeV.

Another new source of contributions to ϵ_K arise from the exchange of the neutral color octets in the extended Higgs sector. In general, such a new scalar can lead to large FCNCs, but not if it couples proportional to the Yukawas, for details compare the model-independent analysis [197]. Such a MFV coupling is naturally implemented here and the flavor changing couplings arise only due to the mixing between fermion zero mode and KK modes as in the case of a brane-localized color singlet [196]. It is straightforward to determine the size of these FCNCs by inserting (3.85) into (3.60) and compare the result with the FCNC inducing couplings of the brane localized SM Higgs in (2.189). One can immediately read off that the couplings will be enhanced compared to the singlet scalars by a factor of $\sqrt{2N_C}$. However, on the basis of (2.189) and (2.184), this still results in an overall suppression of $v^4/(m_O^2 M_{\text{KK}}^4)$ for the octet contribution to the Wilson coefficients, in which m_O denotes the mass of the octet scalar.¹³ We find that they can be neglected for realistic masses for the color octet.

¹³Note, that the mass of the octet depends sensitively on the choice of parameters in the Higgs potential and is not trivially connected to the SM Higgs mass.

3.7 Flavor Observables and LHC Bounds

As elaborated in the last section, the extension of the color gauge group in the bulk makes it necessary to introduce an extended scalar sector and as a consequence changes the localization of the quarks along the extra dimension. Therefore not only observables in which the new axigluon resonances directly mediate FCNCs change in the extended model, but also processes which involve only photon or Z exchange.

In this section we will therefore comment on the new contributions to observables discussed in the earlier sections of this chapter and repeat the numerical analyses with the axigluon contributions as well as the fermion localization implemented.

We will also analyze the bounds from direct detection experiments for the color octet and axigluon resonances at the LHC.

Electroweak Precision Observables

The modification of the strongly coupled sector will not give direct contributions to the oblique parameters and the relocalization of the fermions does also not affect the analysis in Section 3.1, because only flavor universal contributions have been considered there.

In principle, a color octet, electroweak doublet scalar leads to modifications of the electroweak gauge boson propagators via loop insertions. A model independent analysis yields an upper bound on the mass splitting between charged and neutral color octets of $\mathcal{O}(50)$ GeV in order to agree with the T parameter [198]. This splitting depends on the parameters in the Higgs potential and can be used as a constraint for generating the physical spectrum. Note also, that we have not considered loops of KK fermions or gauge bosons in Section 3.1, which might change these conclusions.

Corrections to the $Z \rightarrow b\bar{b}$ vertex depend sensitively on the localization of the bottom quark. The extended color sector shifts all right-handed quarks closer to the IR brane, so that effectively only modifications to the coupling of the Z to right-handed b quarks g_R^b in (3.11) play a role.¹⁴ From (3.108) one can infer that the relocalization amounts to a factor p_d^2 of the RS contribution δg_R^b . Since these corrections go in the wrong direction and are already enhanced in the custodial model, the $Z\bar{b}b$ constraint also prefers small $\tan\beta$, which is in line with the parameter region favored by ϵ_K . The resulting scatter plot in the extended model is shown for $\tan\beta = 1/2$ and $\theta = 45^\circ$ in Figure 3.11, and despite the misleading scaling, still more than 95% do agree with the measurements at 99% CL.

Flavor Violating Observables

Although the extended gauge sector leads to smaller values for ϵ_K , the contributions to $\Delta B = 2$ observables as discussed in Section 2.6 may be even larger in the RS model with extended color gauge group. The reason is, that for $K - \bar{K}$ mixing the mixed

¹⁴There is also a modification for the second term in (3.10), but this term is suppressed by m_b^2/m_Z^2 .

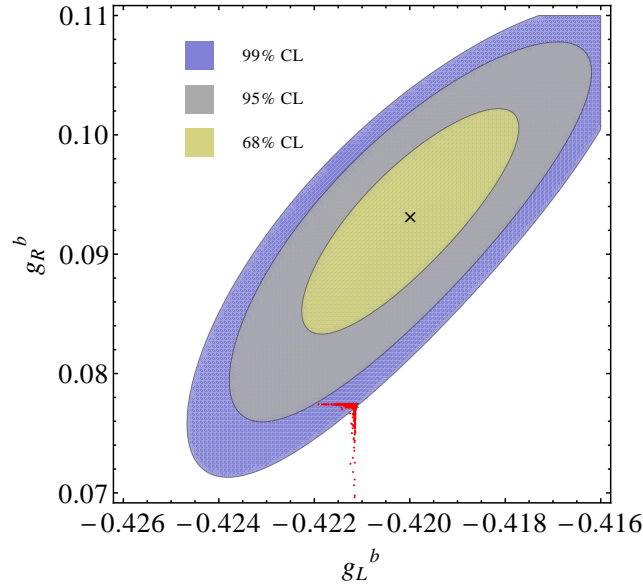


Figure 3.11: The plot shows regions of 68%, 95% and 99% probability in the $g_L^b - g_R^b$ plane. The best fit value is denoted with a cross and the experimental value with a star. The red colored regions indicate the predicted values of a large set of parameter points for the custodially protected RS model with extended color gauge group in the bulk and relocalized fermions for $\tan \beta = 1/2$ and $\theta = 45^\circ$.

chirality Wilson coefficients are enhanced by renormalization group running from M_{KK} to 2 GeV and from chirally enhanced matrix elements, which both yield significantly smaller factors if the Kaons are replaced by B_s mesons. The matrix elements are in this case evaluated at $\mu = m_b$ and the chiral enhancement is negligible. Instead of (3.41) one finds thus

$$\langle B_s^0 | \mathcal{H}_{\text{eff,RS}}^{\Delta S=2} | \bar{B}_s^0 \rangle \propto C_1^{\text{RS}} + \tilde{C}_1^{\text{RS}} + 7.4 \left(C_4^{\text{RS}} + \frac{C_5^{\text{RS}}}{2.55} \right), \quad (3.111)$$

which tells us, that the coefficients are more or less equally important. In the extended model, the contributions to C_4 and C_5 from the KK gluon and axigluon cancel, which by itself will lead to an enhancement of C_5 with respect to the custodially protected model. In addition, the coefficients C_1 and \tilde{C}_1 are enhanced by $\cos \theta^{-2}$ and $\sin \theta^{-2}$ respectively, which for values $\theta \approx 45^\circ$ are close to a factor of 2. Further, the IR shift of the c_{d_i} induced by the extended Higgs sector will result in an equivalent enhancement as in the case of $K - \bar{K}$ mixing.

Regarding the branching ratios $\mathcal{B}(B_s \rightarrow \mu^+ \mu^-)$ and $\mathcal{B}(B_d \rightarrow \mu^+ \mu^-)$ discussed in Section 2.6 only slightly larger effects are expected, because they are mediated by electroweak gauge bosons and therefore only affected by the relocalization of the right-handed down quarks. From the equations (3.108), (3.34) and (3.37) one can

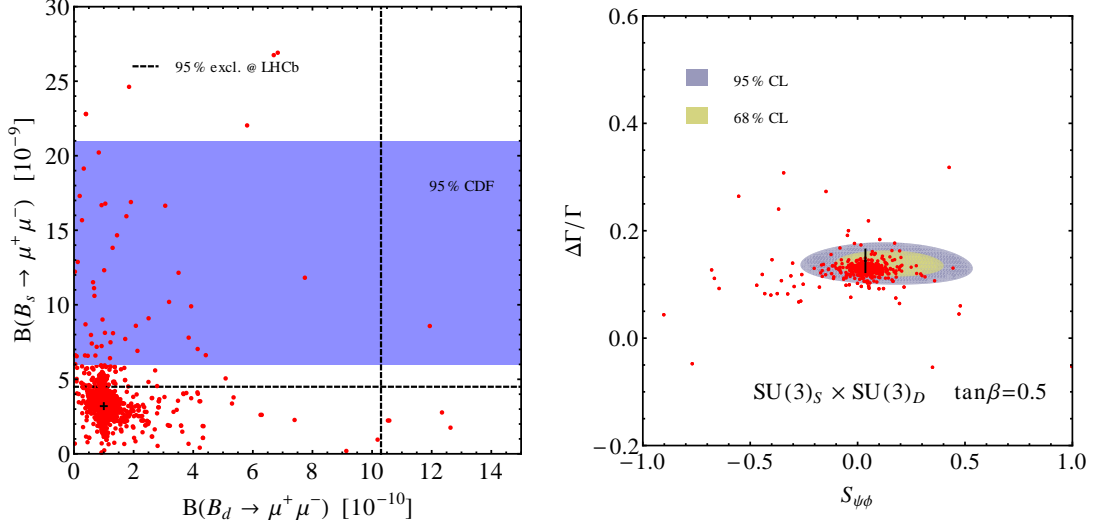


Figure 3.12: The red points indicate the predicted values of a large set of parameter points for the custodially protected RS model with extended color gauge group in the bulk and relocalized fermions for $\tan\beta = 1/2$ and $\theta = 45^\circ$, in the $\mathcal{B}(B_s \rightarrow \mu^+\mu^-)$ - $\mathcal{B}(B_d \rightarrow \mu^+\mu^-)$ plane (left panel) and in the $S_{\psi\phi} - \Delta\Gamma/\Gamma$ plane (right panel). The SM predictions are indicated by black bars, and the yellow (gray) contours the experimentally preferred regions of 68% (95%) probability in the right panel. In the left panel, the black dashed lines denote the experimental upper limits as measured by LHCb at 95% CL, and the blue band shows the preferred region at 95% CL measured by CDF.

find that to leading order in v^2/M_{KK}^2 the effect of the relocalization amounts to an enhancement of $C_{A'} \rightarrow p_d^2 C_{A'}$, while C_A remains unchanged.

Scatterplots for the extended model with relocalized fermions for the reference values of $\tan\beta = 1/2$ and $\theta = 45^\circ$, for the observables described in Section 2.6 and 2.6 are shown in Figure 3.12. One can see that slightly larger effects are possible, however the RS-GIM mechanism does still sufficiently suppress FCNCs in order to not alter the conclusions in the mentioned sections.

Bounds from Direct Detection

Besides agreement with the bounds from flavor observables, the masses of the new resonances must be below the constantly improving mass limits of the LHC experiments. This primarily concerns the KK excitations of the axigluon and the color octet scalars.

Interestingly, both axigluons as well as color octet, electroweak doublet scalars are among the most weakly constrained new physics resonances. This can be understood by considering that the best exclusion limits from the LHC come from dijet analyses, which in return are strongest if the new resonance can be produced at tree level

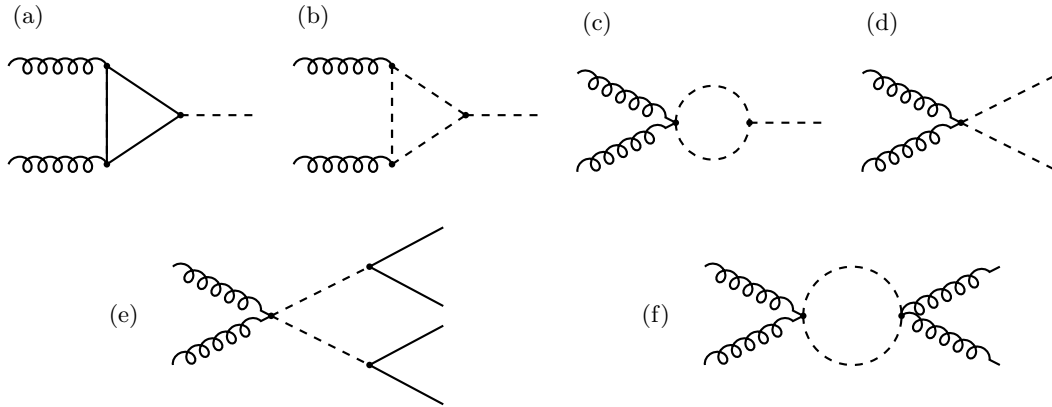


Figure 3.13: In the first row, the leading diagrams for the single and pair production of axigluon or scalar octet resonances are shown for gluon initial states. Coiled lines represent gluons, straight lines quarks and dashed lines can be either an axigluon KK mode or a scalar octet. The diagrams (b) and (c) exist also for an axigluon (octet) in the loop and a octet (axigluon) final state. The second line shows the favored decay channels for the pair production, with the straight lines in (e) denoting top quarks in case of a neutral octet and top-bottom pairs if the octets are charged.

from gluon initial states [193]. However, even though they are color charged, the new scalars are electroweak doublets and can therefore only be produced from gluon initial states via loop suppressed gluon-gluon fusion, or in pairs, see Figure 3.13.

The same holds true for the axigluon. From the second line of (3.84) it is clear that a $\mathcal{G}\mathcal{G}\mathcal{A}$ vertex is forbidden, as well as any vertex with an odd number of axigluons if $\theta = 45^\circ$, that is, if the new resonance couples purely axial. This is a result of parity conservation, since the axigluon must have negative parity. As a consequence the production channels from gluon initial states for a heavy axigluon resonance are also given by the diagrams in the first row of Figure 3.13.

Regarding the decays one can say, that the color octet will decay primarily into tops, because its couplings are proportional to the Yukawa couplings. This is also true for the axigluon in the RS model, because it will be strongly IR localized and the RS-GIM mechanism suppresses couplings to the light flavors. Both will therefore also evade the usual dijet bounds, because a top pair final state will not look like two jets in the detector and is often not reconstructed in these analyses. Possible signatures would be seen in resonance searches in top pair final states for the gluon-fusion production channel, or in four top final states if the resonances are pair-produced at tree-level. There is also the diagram (f) in Figure 3.13, but this will not produce a narrow resonance in the dijet spectrum. Scalar octets can also radiate off an electroweak gauge boson before they decay, which is however suppressed if the decay in top pairs is kinematically accessible, see [200, Fig.4] and the analysis therein.

In order to estimate whether the extended RS model is in conflict with the direct detection limits we will concentrate on the axigluon KK mode. For this resonance the

model predicts a mass which depends only on M_{KK} , while the masses of the scalar octets are not connected to the KK scale but depend on a large number of parameters in the Higgs potential. We will therefore only refer to the literature on color octet electroweak doublets [197, 199, 200, 201] and note that a dedicated analysis using the LHC dataset is still to be undergone and the current upper limits from LEP searches are in the $m_O > 100$ GeV range ¹⁵.

For the axigluon KK mode, we will compare the tree-level production cross section times the branching ratio into light flavors with the latest dijet bounds from the ATLAS collaboration based on 5.8fb^{-1} integrated luminosity at $\sqrt{s} = 8$ TeV [202]. In order to do this we adapt the analysis done in [203, Sec. 5] to the case of a heavy axigluon with flavor non-universal couplings to quarks.

The total cross section for tree-level production includes only $q\bar{q} \rightarrow G$, and reads

$$\sigma = \sum_q \mathcal{F}_{q\bar{q}}((m_{\mathcal{A}}^{(1)})^2/s, \mu_f) \frac{C_F}{N_c} \frac{2\pi^2\alpha_s}{s} ((g_L^{\mathcal{A}})_q^2 + (g_R^{\mathcal{A}})_q^2), \quad (3.112)$$

where the sum extends over the light quark flavors $q = u, d, s, c, b$ and $\sqrt{s} = 8$ TeV. The parton luminosity functions,

$$\mathcal{F}_{ij}(\tau, \mu_f) = \frac{2}{1 + \delta_{ij}} \int_{\tau}^1 \frac{dx}{x} f_{i/p}(x, \mu_f) f_{j/p}(\tau/x, \mu_f). \quad (3.113)$$

are evaluated at the parton center-of-mass energy corresponding to the resonant production of the axigluon, *i.e.*, $\tau = (m_{\mathcal{A}}^{(1)})^2/s$. They are obtained from a convolution of the particle distribution functions (PDFs) $f_{i/p}(x, \mu_f)$, which describe the probability of finding the parton i in the proton with longitudinal momentum fraction x . We will employ MSTW2008LO PDFs with the renormalization and factorization scales set to $\mu_r = \mu_f = m_{\mathcal{A}}^{(1)}$ [228].

The branching ratio for the axigluon decay into light quarks reads

$$\mathcal{B}(\mathcal{A} \rightarrow q\bar{q}) = \Gamma_q/\Gamma_{\mathcal{A}}, \quad (3.114)$$

with the total width denoted by $\Gamma_{\mathcal{A}}$. The partial decay rate can be computed to

$$\Gamma_q = \frac{\alpha_s T_F}{6} m_{\mathcal{A}}^{(1)} \sqrt{1 - \frac{4m_q^2}{(m_1^{\mathcal{A}})^2}} \times \left[((g_L^{\mathcal{A}})_q^2 + (g_R^{\mathcal{A}})_q^2) \left(1 - \frac{m_q^2}{(m_1^{\mathcal{A}})^2} \right) + 6 (g_L^{\mathcal{A}})_q (g_R^{\mathcal{A}})_q \frac{m_q^2}{(m_1^{\mathcal{A}})^2} \right], \quad (3.115)$$

¹⁵These analysis refer to the Manohar Wise model [197] of a single scalar octet electroweak doublet, which has a considerably nicer potential than the one in the extended RS model.

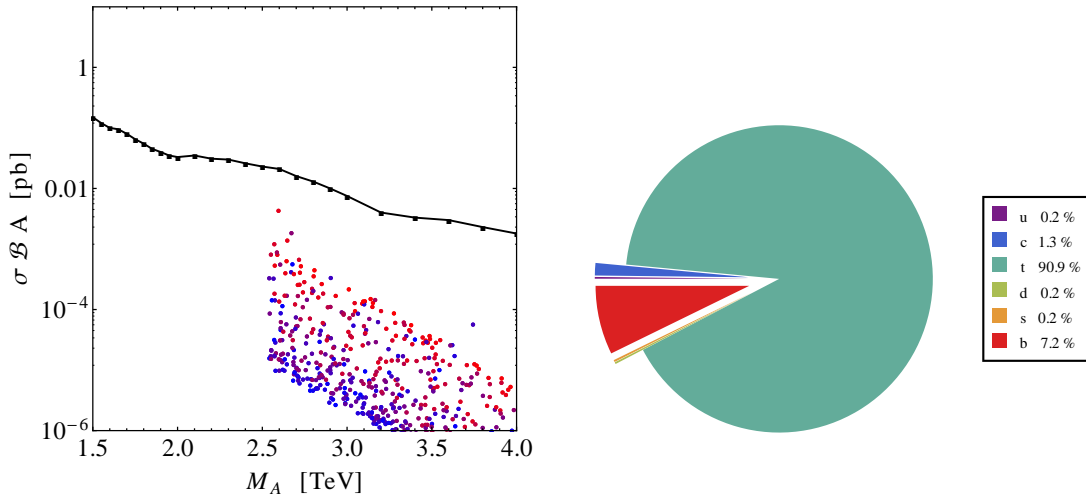


Figure 3.14: Predictions for resonant KK axigluon production as a function of $m_{\mathcal{A}}^{(1)}$. Masses below $m_{\mathcal{A}}^{(1)} \approx 2.45$ TeV are excluded by flavor bounds. The black line represents the ATLAS 95% CL upper limit on $\sigma \mathcal{B} A$ for resonances decaying to $q\bar{q}$ for $s = \sqrt{8}$ TeV, taken from [202].

which in the case of the SM quarks (especially for the light flavors) is well approximated by the limit $m_q/m_{\mathcal{A}}^{(1)}$, for which

$$\Gamma_q = \frac{\alpha_s T_q}{6} m_1^{\mathcal{A}} \left[(g_L^{\mathcal{A}})^2 + (g_R^{\mathcal{A}})^2 \right], \quad (3.116)$$

where $T_q = 1/2$.

The 95% CL upper limit on $\sigma \mathcal{B} A$ from ATLAS is also corrected for the QCD radiation, hadronization effects and acceptance of the detector, which can be incorporated in the analysis by rescaling the result by

$$\begin{aligned} R &= \frac{(\sigma \mathcal{B} A)_{\text{axigluon}}^{\text{ATLAS}}}{(\sigma \mathcal{B}(\mathcal{A} \rightarrow q\bar{q}))} \\ &= 0.54 - \frac{0.09}{2.4\text{TeV}} m_1^{\mathcal{A}} - 0.6\text{TeV} + \left[\frac{0.99}{2.4\text{TeV}} m_1^{\mathcal{A}} - 0.6\text{TeV} \right]^2, \end{aligned} \quad (3.117)$$

where the numerator is given by the axigluon prediction of ATLAS, while the denominator is calculated at the partonic level using (3.112) and (3.115), with the RS expressions for $(g_L^{\mathcal{A}})_q = +1$ and $(g_R^{\mathcal{A}})_q = -1$. The RS couplings in (3.112) and (3.115),

which are given by the overlap integrals

$$(g_L^A)_{q_i} = \frac{2\pi}{L\epsilon} \int_{\epsilon}^1 \frac{dt}{t} \chi_{\mathcal{A}}^{(1)} \quad (3.118)$$

$$\times \left(\tan \theta a_i^{(Q)\dagger} C_i^{(Q)}(t) C_i^{(Q)}(t) a_i^{(Q)} - \cot \theta a_i^{(q)\dagger} S_i^{(q)}(t) S_i^{(q)}(t) a_i^{(q)} \right),$$

$$(g_R^A)_{q_i} = \frac{2\pi}{L\epsilon} \int_{\epsilon}^1 \frac{dt}{t} \chi_{\mathcal{A}}^{(1)} \quad (3.119)$$

$$\times \left(\tan \theta a_i^{(q)\dagger} C_i^{(q)}(t) C_i^{(q)}(t) a_i^{(q)} - \cot \theta a_i^{(Q)\dagger} S_i^{(Q)}(t) S_i^{(Q)}(t) a_i^{(Q)} \right),$$

with $q, Q = \{u, d\}$ and $i = 1, 2, 3$ denoting the i th flavor. The left panel of Figure 3.14 shows the 95% CL upper bound on $\sigma \mathcal{B}A$ obtained by ATLAS (black line) to our theory predictions for resonant axigluon production for the parameter set used throughout this chapter. Scatter points above the black curve would be disfavored by the data. Points below $m_1^A \approx 2.5$ TeV are generated, because the parameter set has a lower limit on the KK scale of $M_{\text{KK}} > 1$ TeV, and the mass of the first axigluon resonance is given by (3.103). The width of the “band” quantifies the effect of a different localization of the electroweak singlet top quark, which is flatly distributed between $c_{u_3} \in [-0.5, 2]$ because we chose c_{u_3} as the free parameter in generating the parameter points, see Appendix A for details. Parameter points with an extreme IR localized t_R are colored blue and the color changes to red the more the t_R is shifted towards the UV. Since the top is not reconstructed in the analysis, a further IR localized t_R lowers the value of the branching fraction in (3.114), so that the dijet bound becomes even weaker. Note, that no relocalization has been implemented in Figure 3.14, because we can already infer, that the dijet bounds are weaker than the ones from the flavor sector for all parameter points.

In the right panel of Figure 3.14, the mean values of our dataset for the branching ratios to the different quark flavors is listed. The dominance of the top branching ratio is clearly visible. Numerically, doing the same analysis for the gluon, which corresponds to replacing the profile $\chi_{\mathcal{A}}$ by $\chi_{\mathcal{G}}$ and $\tan \theta \rightarrow 1$, $\cot \theta \rightarrow -1$ in (3.118), will change the resulting branching fractions only at the permille level.

This allows to adopt the bounds from the most recent ATLAS analysis on $t\bar{t}$ final states on the mass of a gluon KK mode for the axigluon KK modes [204]. The effect from the relocalization of the fermions will enhance the couplings to right handed tops of both gluon and axigluon resonances by a factor $p_u^2(\tan \beta = 1/2) = 15$, but the predicted rate for a resonance mass in the ballpark of $m_1^A \approx 2.5 M_{\text{KK}}$ is several orders of magnitude below the measured cross section, as shown in Figure 3.15, and can therefore not compete with the bounds from the flavor sector. However, this concerns the new physics amplitude squared, while the interference with SM amplitudes may lead to an overall enhanced cross section into top pairs. These effects will be discussed in detail in the next chapter.

One can draw the conclusion, that direct detection bounds on KK modes of gluons and axigluons are generally weaker than the strongest bounds from flavor physics, given the prejudice, that not a fine-tuned set of parameters is the reason for an unexpected agreement with experiments.

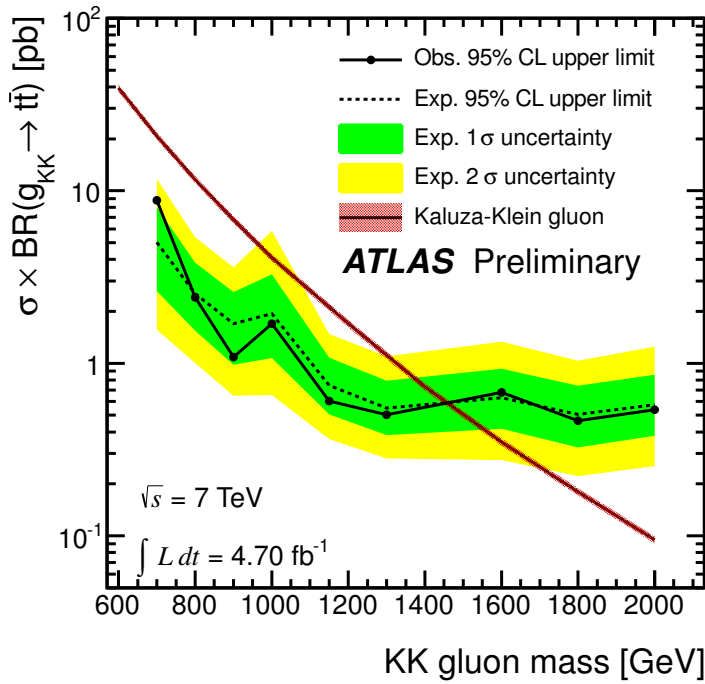


Figure 3.15: Predictions for resonant KK gluon production as a function of $m_1^{\mathcal{G}}$ taken from [204]. The red band represents the cross section times branching fraction for the decay of a KK gluon in a top antitop pair with couplings $g_L^{\mathcal{G}} = g_R = -0.2 g_s$ to the light flavors, $g_L^{\mathcal{G}} = 1 g_s^{\mathcal{G}}$, $g_R^{\mathcal{G}} = -0.2 g_s$ to bottom quarks and $g_L^{\mathcal{G}} = 1 g_s$, $g_R^{\mathcal{G}} = 4 g_s$ to the top quark. The dashed (solid) black lines show the expected (observed) limit, and the expected 1σ (2σ) uncertainty is plotted green (yellow).

4 The Asymmetry in Top Pair Production

The top quark is the heaviest particle in the SM and explaining its large mass provides a challenge for many theories which try to extend it. Especially technicolor like models of physics beyond the SM have a problem to generate the top mass, because typically the Yukawa interaction is an irrelevant operator in these theories. The RS model with fermions in the bulk avoids this problem by describing the top quark by a mainly composite particle, which gets its mass from the compositeness scale similar as the proton from Λ_{QCD} . In this way it differs from the light flavors which are bound to have small admixtures with their composite partners (provided one does not want to sabotage the RS-GIM mechanism and give up the explanation of the flavor hierarchies).

Therefore, besides the Higgs, the top quark is the messenger of the composite sector for strongly coupled theories featuring partial compositeness in the fermionic sector, even more so as discovering a composite top would reject models with only a composite Higgs, *e.g.* CTC. Therefore, observables sensitive to top couplings should receive special attention.

Interestingly, the only observable in which both CDF and DØ find a substantial deviation from the SM, and which is not completely overshadowed by LHC measurements, is the forward backward asymmetry in top pair production. In Sections 4.2 and 4.3 this observable will be introduced and the general implications for new physics which try to resolve the tension with the SM value, as well as for LHC measurements, are discussed. Based on the paper [205], in Section 4.4 the contributions from KK gluon exchange at tree-level and including next to leading order (NLO) SM diagrams will be examined and numerically evaluated in Section 4.5. Since the asymmetry is sensitive to the axial vector current, one expects large effects from an RS axigluon and Section 4.6 is dedicated to the analysis on how the effects change if the extended color gauge group is assumed.

4.1 Top-Antitop Pair Production and Observables at Tevatron and the LHC

Since the top quark was discovered in 1995 by the Tevatron experiments CDF and DØ, thousands of top-antitop pairs have been produced which allowed for a measurement of the top mass m_t with an accuracy of below 1% [206],

$$m_t^{\text{Tevatron}} = 173.2 \pm 0.9_{\text{stat+syst}} \text{ GeV} \quad (4.1)$$

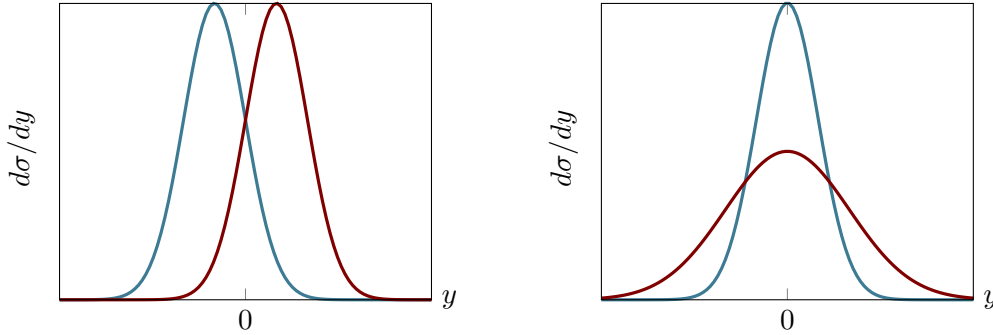


Figure 4.1: Rapidity distributions for top (red) and antitop (blue) quarks for the Tevatron in the left panel and the LHC in the right panel. The distributions are not to scale and represent only a qualitative illustration.

which more recently has been confirmed by the LHC detectors ATLAS and CMS [208],

$$m_t^{\text{LHC}} = 173.3 \pm 0.5_{\text{stat}} \pm 1.3_{\text{syst}} \text{ GeV}. \quad (4.2)$$

Using the mass as an input, the theoretical predictions for the total inclusive cross section turns out to be in very good agreement with the data from the Tevatron [212, 207],

$$\sigma_{t\bar{t}}|_{\text{D}\emptyset} = 7.56^{+0.63}_{-0.56} \text{ pb}, \quad (4.3)$$

$$\sigma_{t\bar{t}}|_{\text{NNLO}_{\text{appr}}^{1.96 \text{ TeV}}} = 7.06^{+0.27}_{-0.34} \text{ }^{+0.69}_{-0.53} \text{ pb}, \quad (4.4)$$

as well as with measurements at the LHC [209, 210],

$$\sigma_{t\bar{t}}|_{\text{CMS}} = 165.8 \pm 2.2_{\text{stat}} \pm 10.6_{\text{syst}} \pm 7.8_{\text{lumi}} \text{ pb}, \quad (4.5)$$

$$\sigma_{t\bar{t}}|_{\text{NNLO}_{\text{appr}}^{7 \text{ TeV}}} = 161^{+12.3}_{-11.9} \text{ }^{+15.2}_{-14.5} \text{ pb}. \quad (4.6)$$

Concerning the theoretical values of the cross sections in (4.4) and (4.6), consult [211, Tab. 1] and the references therein. The quoted values correspond to approximative NNLO results and the first error is the total theoretical uncertainty, the second the PDF uncertainty.

This agreement has to be contrasted with a $\sim 3\sigma$ discrepancy between SM prediction and measurements of both Tevatron detectors for the forward-backward asymmetry of top antitop pairs, which in the CM frame reads [239, Table 6],

$$(A_{\text{FB}}^t)_{\text{exp}} = (16.2 \pm 4.7_{\text{stat+syst}}) \%, \quad (4.7)$$

$$(A_{\text{FB}}^t)_{\text{SM}} = (7.3^{+1.1}_{-0.7}) \%, \quad (4.8)$$

where the experimental value corresponds to the first extraction from the full Tevatron dataset, recently done by CDF [213]. Any new physics that might explain this discrepancy should however be heavy or broad enough to have escaped detection in dijet events and in the $t\bar{t}$ invariant mass spectrum analyzed at the end of Section 3.7.

We report therefore also the mass dependent asymmetry measured by CDF, which could be interpreted as a hint at heavy new resonances, since it shows a linear slope which is significantly larger than predicted in the SM,

$$\begin{aligned} A_{\text{FB}}^t(m_{t\bar{t}} < 450\text{GeV}) &= (7.8 \pm 5.4)\%, \\ A_{\text{FB}}^t(m_{t\bar{t}} > 450\text{GeV}) &= (29.6 \pm 6.7)\%, \end{aligned} \quad (4.9)$$

although the SM prediction goes in the same direction [220]

$$\begin{aligned} A_{\text{FB}}^t(m_{t\bar{t}} < 450\text{GeV}) &= (6.2_{-0.3}^{+0.4})\%, \\ A_{\text{FB}}^t(m_{t\bar{t}} > 450\text{GeV}) &= (12.9_{-0.6}^{+0.8})\%. \end{aligned} \quad (4.10)$$

One can understand the observable (4.8) as the number of top quarks going in forward direction minus the number of top quarks going in backwards direction relative to the interaction point in the CM frame, normalized to the total number of tops,

$$A_{\text{FB}}^t = \frac{N_t(F) - N_t(B)}{N_t(F) + N_t(B)}. \quad (4.11)$$

Because of charge conjugation invariance, the antitops scattered forwards (backwards) can be counted as tops scattered backwards (forwards), so that $N_{\bar{t}}(F) = N_t(B)$. Analogous to (4.11), one can therefore define the asymmetry as the number of tops scattered in forward direction minus the number of antitops scattered in forward direction, which then corresponds to a charge asymmetry

$$A_{\text{C}}^t = \frac{N_t(F) - N_{\bar{t}}(F)}{N_t(F) + N_{\bar{t}}(F)}. \quad (4.12)$$

A charge asymmetric initial state is required in order to generate contributions to such an asymmetry. This is the case at the Tevatron, as it is a proton antiproton collider, but not at the LHC, which collides protons with each other. This is illustrated by a sketch of the rapidity distributions for the Tevatron and LHC in Figure 4.1. Clearly, counting the tops versus the antitops in forward direction ($y > 0$) will only in the case of the Tevatron lead to a non-zero number. On a more fundamental level however, the asymmetry can be traced back to the fact, that the top quark likes to go in the direction of the initial state quark and the antitop in the direction of the initial state antiquark. These directions are well defined at the Tevatron as the proton consists mainly of quarks, which results in the shifts of the rapidity distributions in the left panel of Figure 4.1. At the LHC, one can infer that the initial antiquark must be a sea quark. Sea quarks carry less momentum fraction than valence quarks and consequentially the rapidity distributions at the LHC are symmetric, but have a different width, as shown in the right panel of Figure 4.1. On average, the top carries more momentum than the antitop.

One can therefore define a charge asymmetry based on the difference in absolute rapidity, $\Delta|y| = |y_t| - |y_{\bar{t}}|$,

$$A_{\text{C}}^y = \frac{N(\Delta|y| > 0) - N(\Delta|y| < 0)}{N(\Delta|y| > 0) + N(\Delta|y| < 0)}. \quad (4.13)$$

Even though it cannot be transformed in a forward-backward asymmetry¹, the charge asymmetry at the LHC has the same physical origin and possible new physics effects showing up in A_{FB}^t will also contribute to A_C^y . It has been measured at the LHC by both ATLAS [217, 218] and CMS [216] and was found to be in good agreement with the SM [219],

$$(A_C^y)_{\text{SM}} = (1.15 \pm 0.6) \% , \quad (4.14)$$

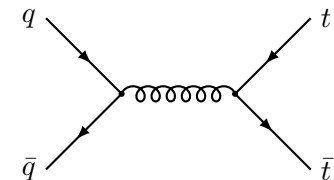
$$(A_C^y)_{\text{exp}} = (0.4 \pm 1_{\text{stat}} \pm 1.1_{\text{syst}}) \% . \quad (4.15)$$

Here, the quoted experimental value corresponds to the latest CMS result, which is based on 5fb^{-1} of data. The fact that the asymmetry at the LHC is considerably smaller than at the Tevatron is rooted in the different center of mass energies (CM) of both machines. Since the asymmetries are normalized to the total inclusive cross section, the number of top pairs produced by gluon-gluon fusion contributes to the denominator but not to the numerator as it is a charge symmetric initial state and at LHC energies gluon-gluon fusion is by far the dominating process.

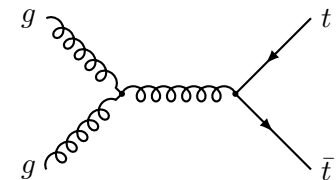
We can conclude, that whatever new physics might be responsible for the discrepancy seen at the Tevatron, its contribution to the LHC charge asymmetry should stay within the (still significant) errors. It should further not contribute to the total inclusive cross section which all experiments see in very good agreement with SM predictions, and it must be heavy or broad enough to have escaped direct detection by dijet searches or in the $t\bar{t}$ invariant mass spectrum so far.

4.2 The Forward-Backward Asymmetry in the SM

We will concentrate on the Tevatron observables at which $t\bar{t}$ pairs are produced in collisions of protons and antiprotons, $p\bar{p} \rightarrow t\bar{t}X$. At the partonic Born-level contributions from quark-antiquark annihilation and gluon fusion arise within the SM



$q(p_1) + \bar{q}(p_2) \rightarrow t(p_3) + \bar{t}(p_4) ,$



$g(p_1) + g(p_2) \rightarrow t(p_3) + \bar{t}(p_4) ,$

$$(4.16)$$

in which the four-momenta $p_{1,2}$ of the initial state partons can be expressed as the fractions $x_{1,2}$ of the four-momenta $P_{1,2}$ of the colliding hadrons, $p_{1,2} = x_{1,2}P_{1,2}$. We denote the square of the hadronic CM energy by $s = (P_1 + P_2)^2$ and introduce the

¹For more details concerning the different asymmetries and their comparability, see *e.g.* [220].

kinematic invariants

$$\hat{s} = (p_1 + p_2)^2, \quad t_1 = (p_1 - p_3)^2 - m_t^2, \quad u_1 = (p_2 - p_3)^2 - m_t^2. \quad (4.17)$$

The partonic cross section can then be described as a function of \hat{s}, t_1 and u_1 and momentum conservation at Born level implies $\hat{s} + t_1 + u_1 = 0$. Since the number of top quarks scattered in forward (backward) direction is given by integrating the differential cross section over the angle θ included by \vec{p}_1 and \vec{p}_3 in the respective ranges, we express t_1 and u_1 in terms of θ and the top-quark velocity β ,

$$\begin{aligned} t_1 &= -\frac{\hat{s}}{2}(1 - \beta \cos \theta), & u_1 &= -\frac{\hat{s}}{2}(1 + \beta \cos \theta), \\ \beta &= \sqrt{1 - \rho}, & \rho &= \frac{4m_t^2}{\hat{s}}. \end{aligned} \quad (4.18)$$

The hadronic differential cross section may then be written as

$$\frac{d\sigma^{p\bar{p} \rightarrow t\bar{t}X}}{d\cos\theta} = \frac{\alpha_s}{m_t^2} \sum_{i,j} \int_{4m_t^2}^s \frac{d\hat{s}}{s} \mathbb{f}_{ij}(\hat{s}/s, \mu_f) K_{ij} \left(\frac{4m_t^2}{\hat{s}}, \cos\theta, \mu_f \right), \quad (4.19)$$

where μ_f denotes the factorization scale and \mathbb{f}_{ij} denote the parton luminosity functions introduced in (3.113). The luminosities for $ij = q\bar{q}, \bar{q}q$ are understood to be summed over all species of light quarks, and the functions $f_{i/p}(x, \mu_f)$ ($f_{i/\bar{p}}(x, \mu_f)$) are the universal non-perturbative PDFs, which describe the probability of finding the parton i in the proton (antiproton) with longitudinal momentum fraction x . The hard-scattering kernels $K_{ij}(\rho, \cos\theta, \mu_f)$ are related to the partonic cross sections and can be expanded in α_s ,

$$K_{ij}(\rho, \cos\theta, \mu_f) = \sum_{n=0}^{\infty} \left(\frac{\alpha_s}{4\pi} \right)^n K_{ij}^{(n)}(\rho, \cos\theta, \mu_f). \quad (4.20)$$

At leading order, only the diagrams in (4.16) contribute, and one finds

$$\begin{aligned} K_{q\bar{q}}^{(0)} &= \alpha_s \frac{\pi\beta\rho}{8} \frac{C_F}{N_c} \left(\frac{t_1^2 + u_1^2}{\hat{s}^2} + \frac{2m_t^2}{\hat{s}} \right) \\ &= \alpha_s \frac{\pi\beta\rho}{16} \frac{C_F}{N_c} \left(1 + \beta^2 \cos^2\theta + \frac{4m_t^2}{\hat{s}} \right), \end{aligned} \quad (4.21)$$

$$\begin{aligned} K_{g\bar{g}}^{(0)} &= \alpha_s \frac{\pi\beta\rho}{8(N_c^2 - 1)} \left(C_F \frac{\hat{s}^2}{t_1 u_1} - N_c \right) \left[\frac{t_1^2 + u_1^2}{\hat{s}^2} + \frac{4m_t^2}{\hat{s}} - \frac{4m_t^4}{t_1 u_1} \right] \\ &= \alpha_s \frac{\pi\beta\rho}{8(N_c^2 - 1)} \left(\frac{4C_F}{1 - \beta^2 \cos^2\theta} - N_c \right) \\ &\quad \times \left[\frac{1}{2}(1 - \beta^2 \cos^2\theta) + \frac{4m_t^2}{\hat{s}} - \frac{16m_t^4}{\hat{s}^2(1 - \beta^2 \cos^2\theta)} \right]. \end{aligned} \quad (4.22)$$

The factors $N_c = 3$ and $C_F = 4/3$ are the usual color factors and $K_{q\bar{q}}^{(0)} = K_{\bar{q}q}^{(0)}$ in the SM, because they are related by replacing $\cos\theta$ with $-\cos\theta$ the coefficients.

Following [222], we introduce the charge-asymmetric (a) and -symmetric (s) averaged differential cross sections. In the former case, we define

$$\frac{d\sigma_a}{d\cos\theta} \equiv \frac{1}{2} \left[\frac{d\sigma^{p\bar{p} \rightarrow t\bar{t}X}}{d\cos\theta} - \frac{d\sigma^{p\bar{p} \rightarrow \bar{t}tX}}{d\cos\theta} \right], \quad (4.23)$$

with $d\sigma^{p\bar{p} \rightarrow t\bar{t}X}/d\cos\theta$ given in (4.19). The corresponding expression for the charge-symmetric averaged differential cross section $d\sigma_s/d\cos\theta$ is simply obtained from the above by changing the minus into a plus sign. The notation indicates that in the process labeled by the superscript $p\bar{p} \rightarrow t\bar{t}X$ ($p\bar{p} \rightarrow \bar{t}tX$) the angle θ corresponds to the scattering angle of the top (antitop) quark in the partonic CM frame. Using (4.23) one can derive various physical observables in $t\bar{t}$ production. For example, the total hadronic cross section is given by

$$\sigma_{t\bar{t}} = \int_{-1}^1 d\cos\theta \frac{d\sigma_s}{d\cos\theta}. \quad (4.24)$$

The total $t\bar{t}$ charge asymmetry can then be defined as

$$A_c^t \equiv \frac{\int_0^1 d\cos\theta \frac{d\sigma_a}{d\cos\theta}}{\int_0^1 d\cos\theta \frac{d\sigma_s}{d\cos\theta}}. \quad (4.25)$$

Since QCD is symmetric under charge conjugation, it allows to identify

$$\left. \frac{d\sigma^{p\bar{p} \rightarrow t\bar{t}X}}{d\cos\theta} \right|_{\cos\theta=c} = \left. \frac{d\sigma^{p\bar{p} \rightarrow \bar{t}tX}}{d\cos\theta} \right|_{\cos\theta=-c}, \quad (4.26)$$

for any fixed value c . As mentioned in the previous section, the charge asymmetry can then be understood as a forward-backward asymmetry

$$A_c^t = A_{\text{FB}}^t \equiv \frac{\int_0^1 d\cos\theta \frac{d\sigma^{p\bar{p} \rightarrow t\bar{t}X}}{d\cos\theta} - \int_{-1}^0 d\cos\theta \frac{d\sigma^{p\bar{p} \rightarrow t\bar{t}X}}{d\cos\theta}}{\int_0^1 d\cos\theta \frac{d\sigma^{p\bar{p} \rightarrow t\bar{t}X}}{d\cos\theta} + \int_{-1}^0 d\cos\theta \frac{d\sigma^{p\bar{p} \rightarrow t\bar{t}X}}{d\cos\theta}} = \frac{\sigma_a}{\sigma_s}. \quad (4.27)$$

It makes sense to express contributions to the symmetric and asymmetric cross section already at the level of the hard scattering kernels,

$$\sigma_s = \frac{\alpha_s}{m_t^2} \sum_{i,j} \int_{4m_t^2}^s \frac{d\hat{s}}{s} \mathbb{f}_{ij}(\hat{s}/s, \mu_f) S_{ij} \left(\frac{4m_t^2}{\hat{s}} \right). \quad (4.28)$$

$$\sigma_a = \frac{\alpha_s}{m_t^2} \sum_{i,j} \int_{4m_t^2}^s \frac{d\hat{s}}{s} \mathbb{f}_{ij}(\hat{s}/s, \mu_f) A_{ij} \left(\frac{4m_t^2}{\hat{s}} \right), \quad (4.29)$$

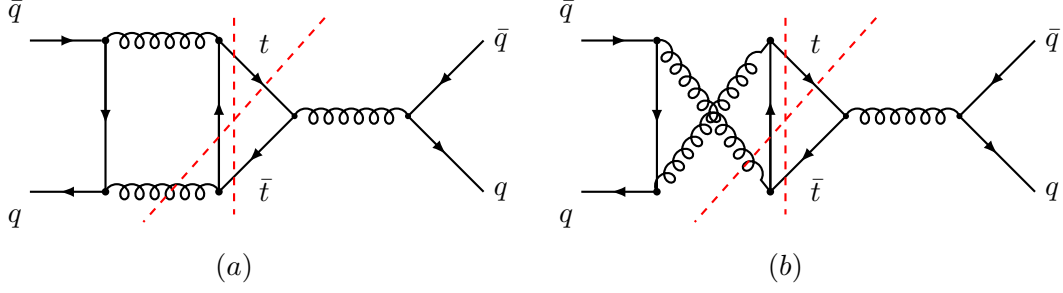


Figure 4.2: Cut diagrams which contribute to the charge asymmetry at $\mathcal{O}(\alpha_s^3)$ in QCD. The cuts refer to the initial- and final state interference and the box diagram-Born level interference respectively.

with the corresponding expansion (4.20). Since the coefficients (4.21) and (4.22) are symmetric under $\cos\theta \rightarrow -\cos\theta$, one finds for the LO SM coefficients

$$S_{q\bar{q}}^{(0)} = \alpha_s \frac{\pi\beta\rho}{27} (2 + \rho), \quad (4.30)$$

$$S_{gg}^{(0)} = \alpha_s \frac{\pi\beta\rho}{192} \left[\frac{1}{\beta} \ln\left(\frac{1+\beta}{1-\beta}\right) (16 + 16\rho + \rho^2) - 28 - 31\rho \right], \quad (4.31)$$

$$A_{q\bar{q}}^{(0)} = A_{gg}^{(0)} = 0. \quad (4.32)$$

This result is not surprising, considering that QCD couples purely vectorially and that the diagrams in (4.16) do not discriminate between the final quark and antiquark. At NLO however, there are diagrams which are odd under the exchange of the final state top with the final state antitop. In this case, a vector coupling contributes maximally.

The diagrams in question are shown in the form of cut diagrams in Figure 4.2 and refer to the interference of initial- and final-state radiation and the interference of the box with the born level diagram. In principle, there is also a small contribution from different quark-gluon scattering amplitudes, but their contribution to the asymmetry is roughly an order of magnitude smaller compared to the ones discussed here, see [215, Fig.4]. The same holds true for QCD-electroweak interference, which can be obtained from replacing the s-channel gluon or one of the gluons in the box in Figure 4.2 by Z or γ , for which $\alpha_s^3 \rightarrow \alpha_e\alpha_s^2$.

The diagrams (a) and (b) in Figure 4.2 have the color structure [215]

$$\begin{aligned} C_{(a)} &= \frac{1}{N_C^2} \text{Tr} [T^a T^b T^c] \text{Tr} [T^a T^c T^b] = \frac{1}{16N_C^2} (f_{abc}^2 + d_{abc}^2) \\ C_{(b)} &= \frac{1}{N_C^2} \text{Tr} [T^a T^b T^c] \text{Tr} [T^b T^c T^a] = \frac{1}{16N_C^2} (-f_{abc}^2 + d_{abc}^2), \end{aligned} \quad (4.33)$$

in which $T_a = \lambda^a/2$ are the $SU(3)_C$ generators with λ^a the Gellmann matrices, and f_{abc} denote the structure constants and d_{abc} the totally symmetric d symbols of $SU(3)_C$. Since the color-stripped contributions to the asymmetry from the diagrams (a) and

(b) are related by

$$d\sigma_a|_{(a)} = -d\sigma_a|_{(b)}, \quad (4.34)$$

one can infer that the overall contribution must be proportional to

$$A_{q\bar{q}}^{(1)} \sim \frac{1}{16N_c^2} \alpha_s d_{abc}^2. \quad (4.35)$$

Note, that one factor α_s is factored out in (4.28) and another one in (4.20), so that the $A_{ij}^{(n)}$ will always be linear in α_s although the overall contributions are $\sim \alpha_s^3$.

One can conclude, that the Born-Box diagram interference in Figure 4.2 gives a positive overall contribution, while the contributions from interference of initial- with final state radiation diagrams enter with the opposite sign. The exact computation reveals, that the latter are smaller, so that one ends up with a net positive asymmetry. The exact formulas are compiled in [215, App. A] and will not be repeated here. The final result can however be described by the parametrization

$$A_{q\bar{q}}^{(1)} = \frac{\alpha_s d_{abc}^2}{16N_c^2} 5.994 \beta \rho \left[1 + 17.948 \beta - 20.391 \beta^2 + 6.291 \beta^3 + 0.253 \ln(1 - \beta) \right], \quad (4.36)$$

which approximates the exact result with permille level accuracy. It has been obtained by integrating the expressions for the charge-asymmetric contributions to the differential $t\bar{t}$ production cross section over the relevant phase space.²

Employing $N_c = 3$, $d_{abc}^2 = (N_c^2 - 1)(N_c^2 - 4)/N_c = 40/3$, $m_t = 173.1$ GeV, and $\alpha_s(m_t) = 0.126$, one can plot (4.36) as a function of the square root of the CM energy \sqrt{s} . This is shown by the solid black plot in the left panel of Figure 4.3, while in the right panel $A_{q\bar{q}}^{(1)}$ is multiplied with the up-quark PDFs $\mathbb{f}_{u\bar{u}}(\hat{s}/s, \mu_f)$ and also plotted in solid black. In both cases the function peaks at $\sqrt{s} \approx 420$ GeV, *i.e.* around the $t\bar{t}$ threshold. The right panel shows also, that the integrated asymmetry (4.29) will be saturated long before the upper integration limit s is reached, which is rooted in the fact that the quark luminosities behave roughly like $1/\hat{s}^2$. These results can be compared with the plots of the exact calculation, which can be found in [215, Fig. 7].

4.3 New Physics and the Forward-Backward Asymmetry

Since it is the only observable dealt with in this thesis, which shows significant deviations from the SM and because top physics are largely unaffected by hadronic uncertainties, it makes sense to categorize what kind of new physics would be able to explain the observed deviation. Severely constrained by the requirement to achieve agreement with the SM regarding the other observables introduced in Section 4.1, the vast space of new physics models can be reduced to two different classes, new physics

²The numerical integration has been performed using the Vegas Monte Carlo algorithm implemented in the CUBA library [223]

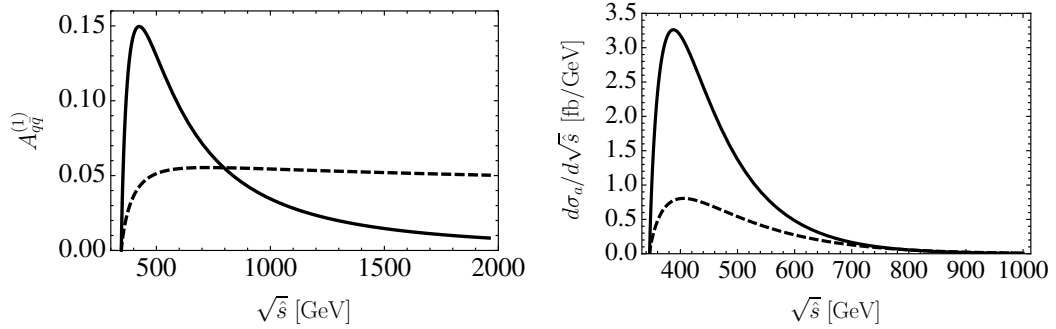


Figure 4.3: The asymmetric coefficient $A_{q\bar{q}}^{(1)}$ (left panel) and the differential hadronic asymmetry $d\sigma_a/d\sqrt{\hat{s}}$ (right panel) as functions of $\sqrt{\hat{s}}$ in the SM plotted in solid black and in the minimal RS model plotted in dashed black.

which contribute through the s channel and new physics which contribute through the t or u channel.

New Physics in the s Channel

From the SM calculation it is clear, that if the effect is due to s channel exchange of some new resonances, it will only lead to an asymmetry if these new resonances have sizable axial vector couplings to the SM quarks. In addition, the vector couplings should be under control in order not to induce a large contribution to the total inclusive cross section.

Direct searches do also prefer heavy resonances, so that the interference with the gluon s channel diagram will give the dominant contributions, while the new physics squared contribution can be neglected away from the resonance peak. Such an interference term from new physics in the s channel can only contribute to the asymmetry if the new resonance is a spin 1 boson, which is a consequence of the Dirac structure. Scalar color octets do not contribute to the asymmetry even if they have purely axial couplings, compare [224, Sec. II], and references therein, while colored spin 2 resonances exchanged in the s channel do not interfere with gluons at all [225].

Such a new resonance will thus lead to an additional term in the Lagrangian

$$\mathcal{L}_{\mathcal{A}} \ni g_s T^a \bar{q}_i (g_V^{q_i} + g_A^{q_i} \gamma_5) \gamma^\mu \mathcal{A}_\mu^a q_i, \quad (4.37)$$

and with the notation $C_{\pm} \equiv 1 + \beta^2 \cos^2 \theta \pm \frac{4m_t^2}{\hat{s}}$, one finds in addition to the SM kernel (4.21) the hard-scattering kernels

$$K_{q\bar{q}, \text{SM} \times \text{NP}}^{(0)} = \alpha_s \frac{\pi\beta\rho}{16N_C} \frac{2\hat{s}(\hat{s} - m_{\mathcal{A}}^2)}{(\hat{s} - m_{\mathcal{A}}^2)^2 + m_{\mathcal{A}}^2\Gamma_{\mathcal{A}}^2} [g_V^q g_V^t C_+ + 2g_A^q g_A^t \beta \cos \theta], \quad (4.38)$$

$$K_{q\bar{q}, \text{NP}^2}^{(0)} = \alpha_s \frac{\pi\beta\rho}{16N_C} \frac{\hat{s}^2}{(\hat{s} - m_{\mathcal{A}}^2)^2 + m_{\mathcal{A}}^2\Gamma_{\mathcal{A}}^2} \left[((g_V^q)^2 + (g_A^q)^2) ((g_V^t)^2 C_+ + (g_A^t)^2 C_-) + 8g_V^q g_A^q g_V^t g_A^t \beta \cos \theta \right], \quad (4.39)$$

from the interference between SM and new physics amplitude and from the new physics amplitude squared, respectively. Both expressions have terms linear in $\cos \theta$, which contribute to the asymmetry, but not to the cross section. For the interference kernel this term depends only on the axial couplings to top and light quarks, while in the case of the new physics squared contribution it is sensitive to all couplings in (4.37). For large masses of the resonance, the latter is suppressed by an additional $1/m_{\mathcal{A}}^2$ and for light resonances, assumed they are broad enough to be concealed in the invariant $t\bar{t}$ mass spectrum, the vector couplings need to be large for $8g_V^q g_A^q g_V^t g_A^t$ to explain the effect. Sizable vector couplings lead to an enlarged cross section, which does not only induce a tension with the total cross section measurements, but in turn also decreases the asymmetry, because the cross section appears in the denominator in (4.25). Since the main contribution to the cross section comes from the interference term, it will always dominate over the asymmetric contributions³. It is therefore justified to concentrate on the interference term in looking for a viable model which explains the asymmetry.

In order for the interference kernel to generate a large asymmetric contribution to the differential cross section, at the Born level only the axial vector couplings are relevant, while sizable vector couplings are even dangerous for the reasons explained above. Note, that at the one-loop level, the situation is reversed and the vector couplings contribute to the asymmetry, because the corresponding diagrams 4.6 are already odd under the exchange of t and \bar{t} (which is the original reason for the asymmetry being an NLO effect in the SM). However, if NP contributions to the asymmetry are generated at the one-loop level by vector couplings, one would expect that the same couplings enhance the cross section at the Born level and thus partially cancel the effect in (4.25). We will later confirm this assumption for KK gluon exchange in the minimal RS model.

Besides a large axial vector and a small vector coupling, there are further requirements on the couplings in (4.37). For large masses $m_{\mathcal{A}}^2 > \hat{s}$, the relevant term in (4.38) comes with a minus sign, which will lead to a negative asymmetry (4.27). Therefore, either the new resonance is light, $m_{\mathcal{A}}^2 < \hat{s}$, or the couplings are flavor non-universal

³If the effect is due to the new physics amplitude squared it is more likely that the new resonance is a color singlet, for which the interference term vanishes, but $K_{q\bar{q}, \text{NP}^2}^{(0)}$ is larger by a factor of 9/2 [224].

$g_A^t g_A^q < 0$.⁴ A light axigluon could generate a positive asymmetry for large invariant masses of the $t\bar{t}$ pair [226]. Such an axigluon with a mass around $m_A \approx 450$ GeV was actually encouraged by an earlier analysis by CDF [227], in which a sign change in the central values of the mass dependent asymmetry in bins with $m_{t\bar{t}} < 450$ GeV and $m_{t\bar{t}} > 450$ GeV was reported,

$$A_{\text{FB}}^t(m_{t\bar{t}} < 450 \text{ GeV}) = (-11.6 \pm 15.3)\%, \quad (4.40)$$

$$A_{\text{FB}}^t(m_{t\bar{t}} > 450 \text{ GeV}) = (47.5 \pm 11.4)\%, \quad (4.41)$$

which however was neither seen by $D\bar{O}$, nor in the results of the full CDF analysis (4.9). It requires also a very sophisticated extension of the fermionic sector for such a light resonance to have the necessary width in order to not show up as a bump in the $t\bar{t}$ invariant mass spectrum.

One can therefore conclude, that a heavy resonance with purely axial, flavor non-universal couplings is the best bet if new physics in the s channel are responsible for the forward backward asymmetry observed at the Tevatron. However, this would in general also induce a sizable charge asymmetry at the LHC, which has not been observed. In order to accommodate both measurements, such an axigluon must not only have a sign between couplings to up- and top quarks, but also between up- and down quark couplings [221]. The reason is, that quark antiquark annihilation always involves a sea quark at the LHC. Regarding the valence quarks, the PDFs for the up (anti)quarks dominate over the down (anti)quarks in the (anti)proton, while for the sea quarks the \bar{d} PDF is even slightly larger than the \bar{u} PDF for the proton as shown in Figure 4.4. Therefore, at the LHC $d\bar{d}$ annihilation contributes roughly half as much to the charge asymmetry as $u\bar{u}$ annihilation, while at the Tevatron the $u\bar{u}$ initial state contributes four times as much as the $d\bar{d}$ initial state. A sign between both contributions would therefore partially cancel the effect at the LHC but only slightly decrease the asymmetry at the Tevatron. Finally, it should be noted that a large asymmetry does also require that the resonance is not too heavy, which implies that the couplings to the light flavors should be rather small in order to escape the dijet bounds cited in (3.58).

New Physics in the t and u Channel

New physics resonances which are exchanged in the t or u channel can be provided by a much larger class of models, because the new resonances need not to be color-charged in order to interfere with the SM gluon in the s channel. This can be understood from the color structure of the gluon propagator, which by using (3.19) can be split into a $U(N_C)$ and a $U(1)$ part

$$\begin{array}{c} \diagup \quad \diagdown \\ \text{---} \text{---} \text{---} \text{---} \text{---} \text{---} \\ \diagdown \quad \diagup \end{array} = \frac{1}{2} \begin{array}{c} \diagup \quad \diagdown \\ \text{---} \text{---} \text{---} \text{---} \\ \diagdown \quad \diagup \end{array} - \frac{1}{2N_C} \left(\begin{array}{c} \diagup \quad \diagdown \\ \text{---} \text{---} \text{---} \text{---} \\ \diagdown \quad \diagup \end{array} \right), \quad (4.42)$$

⁴The FCNCs induced from such flavor non-universal couplings are discussed in [203] and found to be negligible.

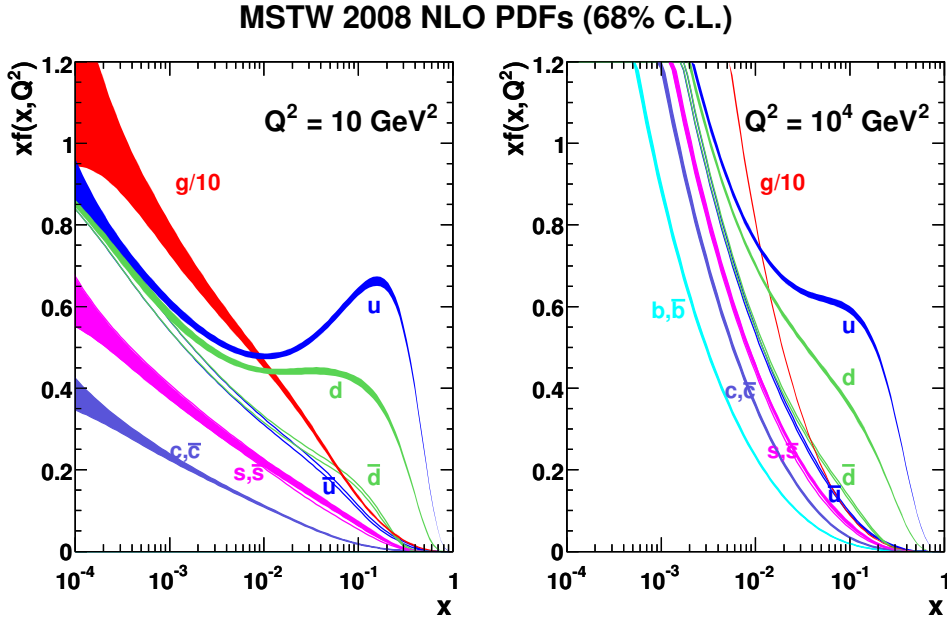


Figure 4.4: Figure shows a plot of the PDFs of the gluon and the valence and sea quarks in the proton for $Q^2 = 10 \text{ GeV}^2$ and $Q^2 = 10^4 \text{ GeV}^2$. They are taken from the homepage of the MSTW collaboration and were computed using MSTW2008NLO [228].

from which the former has the same color flow as the t channel diagram and thus leads to interference [229].

The common characteristic of models featuring large t channel currents is a sizable flavor off-diagonal coupling between the up (or down) and the top quark, while other flavor changing couplings have to be under control in order to not violate bounds from FCNCs. This can be realized by a W' or Z' gauge boson with accordingly adjusted couplings, so that the relevant interaction terms read

$$\mathcal{L}_{Z'/W'} \ni \bar{t} \left(g_V^{Z'} + g_A^{Z'} \gamma_5 \right) \gamma^\mu Z'_\mu u + \bar{t} \left(g_V^{W'} + g_A^{W'} \gamma_5 \right) \gamma^\mu W'_\mu d. \quad (4.43)$$

The corresponding expressions for the cross sections will not be explicitly repeated here and can be found for the Z' in [230, Sec VI] and for the W' in [231, Sec.II]. In the case of interference between t and s channel, both vector and axial vector couplings contribute equally to the cross section and the asymmetry and one has therefore more freedom to choose the couplings. If there is no flavor diagonal coupling however, the new gauge bosons are forced to decay into top quarks which will yield a clear signal of like sign leptons. Searches for this final state already place very strong bounds on the parameter space of these resonances, except for a Z', W' which is too light to decay into the top [232, 233]. This typically excludes models with resonances in the few 100 GeV range which is preferred in order to explain the large asymmetry assuming perturbative couplings.

Analogous considerations apply to a scalar with flavor off-diagonal couplings. The

interaction terms for different color representations in the Lagrangian read [234]

$$\mathcal{L}_\phi \ni \bar{t}(g_V^\phi + g_A^\phi \gamma_5)\phi_{1,8}^a \tilde{T}_{1,8}^a u + \bar{t}^c(g_V^\phi + g_A^\phi \gamma_5)\phi_{3,6}^a \tilde{T}_{3,6}^a u, \quad (4.44)$$

in which the subscript identifies the color representation of the scalar as singlet, triplet, sextet or octet, \tilde{T}^a denotes the corresponding $SU(3)_C$ Clebsch Gordon coefficient which connects it to the two quarks and $t^c = i\gamma^0\gamma^2 t$. The corresponding contribution to the cross section can be found in [234, Sec. III] and we content ourselves with quoting the result, that the sextet and triplet color representation can accommodate the asymmetry while the color singlet and octet runs into trouble with other observables. Taking into account the LHC measurements does require similar adaptations as in the case of s channel models and leads to a modification of the already very tuned flavor-changing couplings.

4.4 Cross Section and Asymmetry in the Minimal RS Model

In the RS model, many of the contributions described in Section 4.3 are generated. Since left- and right-handed fermions are localized at different points in the bulk, the KK gluon couplings to quarks are in general not purely vector-like, but receive non-vanishing axial-vector components. These couplings generate a charge asymmetry in top-quark pair production at the Born level, which is associated to quark-antiquark annihilation $q\bar{q} \rightarrow t\bar{t}$ and proceeds through tree-level exchange of KK gluons in the s channel. Further corrections to A_{FB}^t arise from the fact that the couplings of KK gluons and photons, the Z boson and its KK excitations, as well as the Higgs boson are flavor non-diagonal, leading to the flavor-changing $u\bar{u} \rightarrow t\bar{t}$ transition which affects the t channel.⁵ The corresponding diagrams are shown in Figure 4.5. On the other hand, the gluon-fusion channel $gg \rightarrow t\bar{t}$ does not receive a correction at Born level, since owing to the orthonormality of gauge-boson wave functions the coupling of two gluons to a KK gluon is zero.

Leading Order Contributions of the RS Model with and without Custodial Protection

The effective Lagrangian needed to account for the effects of intermediate vector and scalar states reads

$$\mathcal{L}_{\text{eff}} = \sum_{q,u} \sum_{A,B=L,R} \left[C_{q\bar{q},AB}^{(V,8)} Q_{q\bar{q},AB}^{(V,8)} + C_{t\bar{u},AB}^{(V,8)} Q_{t\bar{u},AB}^{(V,8)} + C_{t\bar{u},AB}^{(V,1)} Q_{t\bar{u},AB}^{(V,1)} + C_{t\bar{u},AB}^{(S,1)} Q_{t\bar{u},AB}^{(S,1)} \right], \quad (4.45)$$

⁵In principle, also the $d\bar{d} \rightarrow t\bar{t}$ transition receives corrections due to the t channel exchange of the W boson and its KK partners. However, these effects are negligibly small for viable values of M_{KK} and will therefore be ignored in the following.

in which the operators are

$$\begin{aligned}
 Q_{q\bar{q},AB}^{(V,8)} &= (\bar{q}\gamma_\mu T^a P_A q)(\bar{t}\gamma^\mu T^a P_B t), \\
 Q_{t\bar{u},AB}^{(V,8)} &= (\bar{u}\gamma_\mu T^a P_A t)(\bar{t}\gamma^\mu T^a P_B u), \\
 Q_{t\bar{u},AB}^{(V,1)} &= (\bar{u}\gamma_\mu P_A t)(\bar{t}\gamma^\mu P_B u), \\
 Q_{t\bar{u},AB}^{(S,1)} &= (\bar{u}P_A t)(\bar{t}P_B u),
 \end{aligned} \tag{4.46}$$

and the sum over q (u) involves all light (up-type) quark flavors. In addition, $P_{L,R} = (1 \mp \gamma_5)/2$ project onto left- and right-handed chiral quark fields, and T^a are the generators of $SU(3)_C$. The superscripts V and S (8 and 1) label vector and scalar (color-octet and -singlet) contributions, respectively.

Using the effective Lagrangian (4.45) it is straightforward to calculate the interference between the tree-level matrix element describing s channel SM gluon exchange and the s and t channel new-physics contributions arising from the Feynman graphs displayed in Figure 4.5. In terms of the following combinations of Wilson coefficients

$$C_{ij,\parallel}^{(P,a)} = \text{Re} \left[C_{ij,LL}^{(P,a)} + C_{ij,RR}^{(P,a)} \right], \quad C_{ij,\perp}^{(P,a)} = \text{Re} \left[C_{ij,LR}^{(P,a)} + C_{ij,RL}^{(P,a)} \right], \tag{4.47}$$

the resulting hard-scattering kernels take the form

$$\begin{aligned}
 K_{q\bar{q},\text{RS}}^{(0)} &= \frac{\beta\rho}{32} \frac{C_F}{N_c} \left[\frac{t_1^2}{\hat{s}} C_{q\bar{q},\perp}^{(V,8)} + \frac{u_1^2}{\hat{s}} C_{q\bar{q},\parallel}^{(V,8)} + m_t^2 \left(C_{q\bar{q},\parallel}^{(V,8)} + C_{q\bar{q},\perp}^{(V,8)} \right) \right], \\
 K_{t\bar{u},\text{RS}}^{(0)} &= \frac{\beta\rho}{32} \frac{C_F}{N_c} \left[\left(\frac{u_1^2}{\hat{s}} + m_t^2 \right) \left(\frac{1}{N_c} C_{t\bar{u},\parallel}^{(V,8)} - 2C_{t\bar{u},\parallel}^{(V,1)} \right) + \left(\frac{t_1^2}{\hat{s}} + m_t^2 \right) C_{t\bar{u},\perp}^{(S,1)} \right].
 \end{aligned} \tag{4.48}$$

Note, that per definition a factor of α_s or α_e has been absorbed in the Wilson coefficients. As in (4.22), the coefficient $K_{q\bar{q},\text{RS}}^{(0)}$ ($K_{t\bar{u},\text{RS}}^{(0)}$) is obtained from $K_{q\bar{q},\text{RS}}^{(0)}$ ($K_{t\bar{u},\text{RS}}^{(0)}$) by simply replacing $\cos\theta$ with $-\cos\theta$.

After integrating over $\cos\theta$, one obtains the LO corrections to the symmetric and asymmetric parts of the cross section defined in (4.28). In the case of the symmetric part it follows

$$S_{u\bar{u},\text{RS}}^{(0)} = \frac{\beta\rho}{216} (2 + \rho) \hat{s} \left[C_{u\bar{u},\parallel}^{(V,8)} + C_{u\bar{u},\perp}^{(V,8)} + \frac{1}{3} C_{t\bar{u},\parallel}^{(V,8)} - 2C_{t\bar{u},\parallel}^{(V,1)} \right] + f_S(z) \tilde{C}_{t\bar{u}}^S, \tag{4.50}$$

$$S_{d\bar{d},\text{RS}}^{(0)} = \frac{\beta\rho}{216} (2 + \rho) \hat{s} \left[C_{d\bar{d},\parallel}^{(V,8)} + C_{d\bar{d},\perp}^{(V,8)} \right], \tag{4.51}$$

while the asymmetric part in the partonic CM frame reads

$$A_{u\bar{u},\text{RS}}^{(0)} = \frac{\beta^2\rho}{144} \hat{s} \left[C_{u\bar{u},\parallel}^{(V,8)} - C_{u\bar{u},\perp}^{(V,8)} + \frac{1}{3} C_{t\bar{u},\parallel}^{(V,8)} - 2C_{t\bar{u},\parallel}^{(V,1)} \right] + f_A(z) \tilde{C}_{t\bar{u}}^S, \tag{4.52}$$

$$A_{d\bar{d},\text{RS}}^{(0)} = \frac{\beta^2\rho}{144} \hat{s} \left[C_{d\bar{d},\parallel}^{(V,8)} - C_{d\bar{d},\perp}^{(V,8)} \right]. \tag{4.53}$$

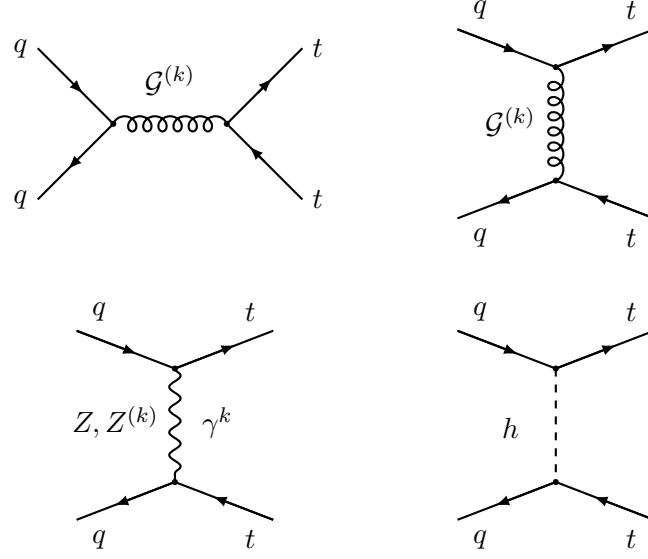


Figure 4.5: Upper row: Tree-level contributions to the $q\bar{q} \rightarrow t\bar{t}$ (left) and the $u\bar{u} \rightarrow t\bar{t}$ (right) transition arising from s and t channel exchange of KK gluons. Lower row: Tree-level contributions to the $u\bar{u} \rightarrow t\bar{t}$ transition arising from t channel exchange of the Z boson, of KK photons and Z bosons as well as of the Higgs boson. The s channel (t channel) amplitudes receive corrections from all light up- and down-type (up-type) quark flavors.

Note, that coefficients involving down-type quarks do not receive corrections from flavor-changing t channel transitions, as the exchange of the W and its KK modes is not considered. The coefficients $C_{q\bar{q},\parallel}^{(V,8)}$ and $C_{q\bar{q},\perp}^{(V,8)}$ enter in (4.50) always in the combination $C_{q\bar{q}}^V \equiv (C_{q\bar{q},\parallel}^{(V,8)} + C_{q\bar{q},\perp}^{(V,8)})$, while in (4.52) they always appear in the form $C_{q\bar{q}}^A \equiv (C_{q\bar{q},\parallel}^{(V,8)} - C_{q\bar{q},\perp}^{(V,8)})$. This feature expresses the fact that the symmetric (asymmetric) LO cross section σ_s (σ_a) measures the product $g_V^q g_V^t$ ($g_A^q g_A^t$) of the vector (axial-vector) parts of the couplings of the KK gluons to light quarks and top quarks. One can alternatively express (4.48) in the parameters given in (4.18) and compare it with the general expression (4.38) in the limit $m_A \gg \hat{s}$.

In order to be able to incorporate a light Higgs boson with $m_h \ll M_{\text{KK}}$ into our analysis, we have kept the full Higgs-boson mass dependence arising from the t channel propagator. This dependence is described by the phase-space factors

$$f_S(z) = -\frac{\beta\rho}{72} \left[1 + \frac{\rho(1-z)}{2} + \frac{\rho(4 + \rho(1-z)^2)}{8\beta} \ln \left(\frac{2(1+\beta) - \rho(1-z)}{2(1-\beta) - \rho(1-z)} \right) \right],$$

$$f_A(z) = \frac{\rho}{144} \left[1 - \rho + \frac{\rho(4 + \rho(1-z)^2)}{4} \ln \left(\frac{\rho(4z + \rho(1-z)^2)}{(2 - \rho(1-z))^2} \right) \right], \quad (4.54)$$

with $z \equiv m_h^2/m_t^2$, so that the new Wilson coefficient $\tilde{C}_{t\bar{t}}^S$ is the dimensionless counter-part of $C_{t\bar{t},\perp}^{(S,1)}$.

The expressions (4.50) and (4.52) encode in a model-independent way possible new-physics contributions to $\sigma_{s,a}$ that arise from tree-level exchange of color-octet vectors in the s and t channels, as well as from t channel corrections due to both new color-singlet vector and scalar states. Based on the general expressions compiled in Section 2.6, the Wilson coefficients appearing in $S_{ij,RS}^{(0)}$ and $A_{ij,RS}^{(0)}$ take the form

$$\begin{aligned}
 C_{q\bar{q},\parallel}^{(V,8)} &= -\frac{\alpha_s\pi}{2M_{\text{KK}}^2} \left\{ \frac{1}{L} - \sum_{a=Q,q} \left[(\Delta'_a)_{11} + (\Delta'_a)_{33} - 2L (\tilde{\Delta}_a)_{11} \otimes (\tilde{\Delta}_a)_{33} \right] \right\}, \quad (4.55) \\
 C_{q\bar{q},\perp}^{(V,8)} &= -\frac{\alpha_s\pi}{2M_{\text{KK}}^2} \left\{ \frac{1}{L} - \sum_{a=Q,q} \left[(\Delta'_a)_{11} + (\Delta'_a)_{33} \right] \right. \\
 &\quad \left. + 2L \left[(\tilde{\Delta}_Q)_{11} \otimes (\tilde{\Delta}_q)_{33} + (\tilde{\Delta}_q)_{11} \otimes (\tilde{\Delta}_Q)_{33} \right] \right\}, \\
 C_{t\bar{u},\parallel}^{(V,8)} &= -\frac{\alpha_s\pi}{M_{\text{KK}}^2} L \sum_{a=U,u} \left[(\tilde{\Delta}_a)_{13} \otimes (\tilde{\Delta}_a)_{31} \right], \\
 C_{t\bar{u},\parallel}^{(V,1)} &= -\frac{\alpha_e\pi}{M_{\text{KK}}^2} \frac{L}{s_w^2 c_w^2} \left[(T_3^u - s_w^2 Q_u)^2 (\tilde{\Delta}_U)_{13} \otimes (\tilde{\Delta}_U)_{31} + (s_w^2 Q_u)^2 (\tilde{\Delta}_u)_{13} \otimes (\tilde{\Delta}_u)_{31} \right] \\
 &\quad - \frac{\alpha_e\pi}{M_{\text{KK}}^2} L Q_u^2 \sum_{a=U,u} \left[(\tilde{\Delta}_a)_{13} \otimes (\tilde{\Delta}_a)_{31} \right],
 \end{aligned}$$

for $q = u, d$ and $Q = U, D$. Since the coefficient $C_{t\bar{u},\perp}^{(S,1)}$ is formally of $\mathcal{O}(v^4/M_{\text{KK}}^4)$, its explicit form is not presented here. Further, while the expressions for $C_{q\bar{q},\parallel}^{(V,8)}$, $C_{q\bar{q},\perp}^{(V,8)}$, and $C_{t\bar{u},\parallel}^{(V,8)}$ are exact, in the coefficient $C_{t\bar{u},\parallel}^{(V,1)}$ we have only kept terms leading in v^2/M_{KK}^2 . In the numerical analysis however, we implement the Higgs exchange and the subleading terms as well. Note, that these coefficients are subject to a symmetry factor $S_{uutt} = 1/4$ compared to the $1/2$ in the case of neutral meson mixing. This is rooted in the fact, that t and s channel exchanges are matched to different operators here, while in Section 2.6 these diagrams were indistinguishable in the full theory.

For the custodially protected RS model based on an $SU(2)_R \times SU(2)_L \times U(1)_X \times P_{LR}$ bulk gauge group, the expressions for the Wilson coefficients can simply be obtained from (4.55) by multiplying the left-handed part of the Z -boson contribution to $C_{t\bar{u},\parallel}^{(V,1)}$ by a factor of around 3, while the right-handed contribution is protected by custodial symmetry and thus smaller by a factor of roughly $1/L \approx 1/37$. Note, that this couplings are enhanced for the opposite chirality compared to the down sector, which is a consequence of the embedding of the fermions, which in return was fixed by the requirement to protect the Zbb vertex from huge corrections, see [114] for details. The custodial protection does not really play a role here, as the electroweak corrections turn out to be subleading for all realistic choices of bulk mass parameters and the KK gluon contributions, encoded in $C_{q\bar{q},\parallel}^{(V,8)}$, $C_{q\bar{q},\perp}^{(V,8)}$, and $C_{t\bar{u},\parallel}^{(V,8)}$, remain unchanged.

The Wilson coefficients (4.55) are understood to be evaluated at the KK scale. The renormalization group (RG) running down to the top-quark mass scale at leading-logarithmic accuracy, *i.e.* at one-loop order, neglecting tiny effects that arise from the

mixing with QCD penguin operators gives for $P = V, A$,

$$\tilde{C}_{q\bar{q}}^P(m_t) = \left(\frac{2}{3\eta^{4/7}} + \frac{\eta^{2/7}}{3} \right) \tilde{C}_{q\bar{q}}^P(M_{\text{KK}}), \quad (4.56)$$

where $\eta \equiv \alpha_s(M_{\text{KK}})/\alpha_s(m_t)$ is the ratio of strong coupling constants evaluated at the relevant scales M_{KK} and m_t . The impact of RG effects is however limited, as can be seen from evaluating (4.56) using $\alpha_s(M_Z) = 0.139$, $M_{\text{KK}} = 1$ TeV, and $m_t = 173.1$ GeV, so that $\eta = 0.803$ at one-loop order. We obtain

$$\tilde{C}_{q\bar{q}}^P(m_t) = 1.07 \tilde{C}_{q\bar{q}}^P(M_{\text{KK}}), \quad (4.57)$$

which makes for an effect of the order of a few percent. We anticipate, that the t channel contributions are suppressed, because they always feel the localization of the up quarks, which yields an exponential suppression due to the zero mode profiles and will therefore neglect renormalization group effects for the corresponding Wilson coefficients.

Restricting ourselves to the corrections proportional to α_s and suppressing relative $\mathcal{O}(1)$ factors as well as numerically subleading terms, one finds from the ZMA expansion of the Wilson coefficients of the results given in (4.55) that the coefficient functions $S_{ij,\text{RS}}^{(0)}$ and $A_{ij,\text{RS}}^{(0)}$ introduced in (4.50) and (4.52) scale in the case of the up quark like

$$S_{u\bar{u},\text{RS}}^{(0)} \sim \frac{\alpha_s \pi}{M_{\text{KK}}^2} \sum_{A=L,R} F^2(c_{t_A}), \quad (4.58)$$

$$A_{u\bar{u},\text{RS}}^{(0)} \sim -\frac{\alpha_s \pi}{M_{\text{KK}}^2} L \left\{ \prod_{q=t,u} \left[F^2(c_{q_R}) - F^2(c_{q_L}) \right] + \frac{1}{3} \sum_{A=L,R} F^2(c_{t_A}) F^2(c_{u_A}) \right\}, \quad (4.59)$$

where $c_{t_L} \equiv c_{Q_3}$, $c_{t_R} \equiv c_{u_3}$, $c_{u_L} \equiv c_{Q_1}$, and $c_{u_R} \equiv c_{u_1}$.

As a consequence of the composite character of the top, its bulk mass parameters are typically $c_{t_A} > -1/2$, while the up quark, being mostly elementary is located close to the UV brane. The relevant $F^2(c_{q_A})$ factors can therefore be approximated by

$$F^2(c_{t_A}) \approx 1 + 2c_{t_A}, \quad F^2(c_{u_A}) \approx (-1 - 2c_{u_A}) e^{L(2c_{u_A}+1)}, \quad (4.60)$$

with $A = L, R$, as elaborated in Section 2.4. The difference of bulk mass parameters for light quarks ($c_{u_L} - c_{u_R}$) is typically small and positive, whereas ($c_{t_L} - c_{t_R}$) can be of $\mathcal{O}(1)$ and is usually negative, because the localization parameter of the $SU(2)_L$ doublet also enters the mass formula for the bottom quark (2.158), which typically results in $c_{t_R} > c_{t_L}$. Using the above approximations and expanding in powers of

$(c_{u_L} - c_{u_R})$, we find

$$S_{u\bar{u},\text{RS}}^{(0)} \sim \frac{2\pi\alpha_s}{M_{\text{KK}}^2} (1 + c_{t_L} + c_{t_R}), \quad (4.61)$$

$$A_{u\bar{u},\text{RS}}^{(0)} \sim \frac{2\pi\alpha_s}{M_{\text{KK}}^2} L e^{L(1+c_{u_L}+c_{u_R})} (1 + c_{u_L} + c_{u_R}) \times \left\{ \left(2 + \frac{1}{3} \right) L (c_{t_L} - c_{t_R}) (c_{u_L} - c_{u_R}) + \frac{1}{3} (1 + c_{t_L} + c_{t_R}) \right\}, \quad (4.62)$$

where the symmetric function $S_{u\bar{u},\text{RS}}^{(0)}$ is entirely due to s channel KK gluon exchange, while the contributions to the asymmetric coefficient $A_{u\bar{u},\text{RS}}^{(0)}$ that arise from the s channel (t channel) correspond to the term(s) with coefficient 2 (1/3) in the curly bracket.

The relations (4.58) exhibit some interesting features. We observe that $S_{u\bar{u},\text{RS}}^{(0)}$, which enters the RS prediction for σ_s in (4.28), is in our approximation independent of the localization of the up-quark fields and strictly positive (as long as $c_{t_A} > -1/2$). This in turn implies an enhancement of the inclusive $t\bar{t}$ production cross section which gets more pronounced the stronger the right- and left-handed top-quark wave functions are localized in the IR.

In contrast to $S_{u\bar{u},\text{RS}}^{(0)}$, both terms in $A_{u\bar{u},\text{RS}}^{(0)}$ are exponentially suppressed for UV-localized up quarks, *i.e.*, $c_{u_A} < -1/2$. For typical values of the bulk mass parameters, $c_{t_L} = -0.34$, $c_{t_R} = 0.57$, $c_{u_L} = -0.63$, and $c_{u_R} = -0.68$ [150], one finds numerically that the first term in the curly bracket of (4.73), which is enhanced by a factor of L but suppressed by the small difference $(c_{u_L} - c_{u_R})$ of bulk mass parameters, is larger in magnitude than the second one by almost a factor of 10. This implies that to first order the charge asymmetry can be described by including only the effects from s channel KK gluon exchange, which can already be inferred from the fact that the coefficients $C_{t\bar{u},\parallel}^{(V,1)}$ and $C_{t\bar{u},\parallel}^{(V,8)}$ in (4.55) are only generated by the tensor structures (2.181), which include the zero mode profiles of all external fermions, compare (2.182).

Since generically $(1 + c_{u_L} + c_{u_R})(c_{u_L} - c_{u_R}) < 0$, we furthermore observe that a positive LO contribution to $A_{u\bar{u},\text{RS}}^{(0)}$ requires $(c_{t_L} - c_{t_R})$ to be negative, which can be achieved by localizing the right-handed top quark sufficiently far in the IR. To leading powers in hierarchies, one finds using the mass relation for the top quark (2.158) the condition

$$c_{t_R} \gtrsim \frac{m_t}{\sqrt{2}v |Y_t|} - \frac{1}{2}, \quad (4.63)$$

in which the top-quark mass is understood to be normalized at the KK scale. Numerically, this means that for $m_t(1 \text{ TeV}) = 144 \text{ GeV}$ and $|Y_t| = 1$ values for c_{t_R} bigger than 0 lead to $A_{u\bar{u},\text{RS}}^{(0)} > 0$ and thus to a positive shift in σ_a .

In conclusion, we can identify three independent aspects of the RS model which render the contributions to the asymmetric kernel $A_{u\bar{u},\text{RS}}^{(0)}$ tiny. First, the fact that the KK gluons only have a negligible axial vector coupling will generate a small Born level

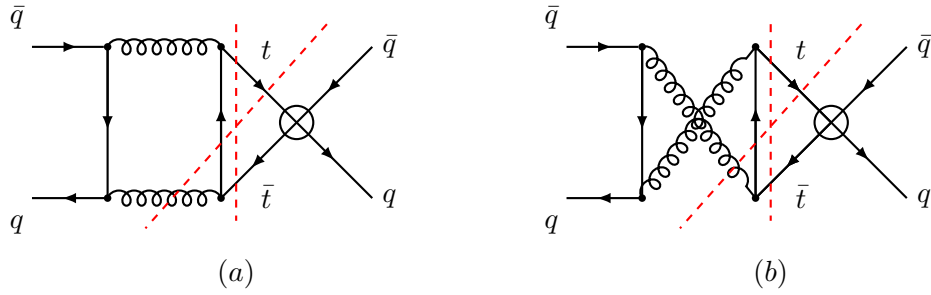


Figure 4.6: Cut diagrams which contribute to the charge asymmetry at $\mathcal{O}(\alpha_s^2)$ in the SM extended by the four quark operators (4.46). The cuts refer to the initial- and final state interference and the box diagram- Born level interference respectively.

asymmetry, as discussed in Section 4.3.⁶ Second, the localization of the up-quarks, which suppresses all contributions to $A_{u\bar{u},\text{RS}}^{(0)}$ and finally, the fact that the leading s channel contribution as well as part of the t channel contribution in (4.58) is sensitive to the difference between the localization parameters of the 5D up doublet and singlet, which is generically small. As we will see below in our numerical analysis, the inclusion of electroweak corrections arising from the Born-level exchange of the Z boson, of KK excitations of both the photon and the Z boson as well as of the Higgs boson, do not change this picture qualitatively.

The Asymmetry in the RS Model at NLO in QCD

As explained in 4.3, in models with small axial-vector couplings to light quarks and no significant FCNC effects in the t channel, the charge-asymmetric cross section σ_a is suppressed at LO. As we will show in the following, this suppression can be evaded by going to NLO, after paying the price of an additional factor of $\alpha_s/(4\pi)$. In order to understand how the LO suppression is lifted at the loop level, it is useful to recall the way in which the charge asymmetry arises in the SM. As elaborated in Section 4.2, following from the fact that QCD is a pure vector theory, the lowest-order processes $q\bar{q} \rightarrow t\bar{t}$ and $gg \rightarrow t\bar{t}$, which are of $\mathcal{O}(\alpha_s^2)$ do not contribute to A_{FB}^t . However, starting at $\mathcal{O}(\alpha_s^3)$, quark-antiquark annihilation $q\bar{q} \rightarrow t\bar{t}(g)$, as well as flavor excitation $qg \rightarrow q\bar{t}$ receive charge-asymmetric contributions, see Figure 4.2, while gluon fusion $gg \rightarrow t\bar{t}(g)$, remains symmetric to all orders in perturbation theory. Because of charge conjugation invariance the interference between the lowest-order and the QCD box graphs are the only virtual corrections to $q\bar{q} \rightarrow t\bar{t}$, which contribute to the asymmetry at NLO. Similarly, for the bremsstrahlungs (or real) contributions, only the interference between the amplitudes that are odd under the exchange of t and \bar{t} furnishes a correction. Since the axial-vector current is even under this exchange, the NLO contribution to the asymmetry arises solely from vector-current contributions.

⁶This effect concerning the mostly vector-like couplings of light quarks was emphasized in [235].

The main lesson learned from the way the charge asymmetry arises in QCD is that beyond LO vector couplings alone are sufficient to generate non-vanishing values of A_{FB}^t . In the case of the EFT (4.45) this means that cut diagrams like the ones shown in Figure 4.6, can give a sizable contribution to the charge asymmetry if the combination $C_{q\bar{q}}^V = (C_{q\bar{q},\parallel}^{(V,8)} + C_{q\bar{q},\perp}^{(V,8)})$ of Wilson coefficients is large enough. In fact, from (4.50), (4.52), and (4.73) it is not difficult to see that in the case of the RS model NLO corrections to σ_a should dominate over the LO ones, if the condition⁷

$$\frac{\alpha_s}{4\pi} (1 + c_{t_L} + c_{t_R}) \gtrsim L e^{L(1+c_{u_L}+c_{u_R})} \quad (4.64)$$

is fulfilled. For example, employing $c_{t_L} = -0.34$, $c_{u_L} = -0.63$, and $c_{u_R} = -0.68$, the above formula tells us that for $c_{t_R} = 0.57$ the NLO contributions are bigger than the LO corrections by a factor of roughly 25. This suggests that it might be possible to generate values of A_{FB}^t that can reach the percent level with typical and completely natural choices of parameters. Notice that in contrast to QCD, in the RS framework the Feynman graphs displayed in 4.6 are not the only sources of charge-asymmetric contributions. Self-energy, vertex, and counterterm diagrams as well as box diagrams involving the virtual exchange of one zero-mode and one KK gluon might also give a contribution to A_{FB}^t at NLO. As in Chapter 3, we will however not implement KK modes in loops as it is technically involved to compute the nested sums over KK modes in these diagrams. Also, those corrections are, like the Born-level contribution, all exponentially suppressed by the UV localization of the light-quark fields (and the small axial-vector coupling of the light quarks for what concerns the contributions from the operators $Q_{q\bar{q},AB}^{(V,8)}$). Compared to the tree-level corrections, these contributions are thus suppressed by an additional loop factor, so that they can be ignored for all practical purposes in this particular observable.

The relevant contributions to A_{FB}^t arising in the RS model beyond LO include the graphs depicted in Figure 4.6. After integrating over $\cos\theta$, one obtains in the partonic CM frame ($q\bar{q} = u\bar{u}, d\bar{d}$)

$$A_{q\bar{q},\text{RS}}^{(1)} = \frac{\hat{s}}{16\pi\alpha_s} C_{q\bar{q}}^V A_{q\bar{q}}^{(1)}, \quad (4.65)$$

where $A_{q\bar{q}}^{(1)}$ denotes the NLO asymmetric SM coefficient, given in (4.36), and $C_{q\bar{q}}^V$ the Wilson coefficient including the vector couplings as defined below (4.52). Employing an exemplary value of $C_V^{q\bar{q}} = 10 \text{ TeV}^{-2}$, Figure 4.3 shows $A_{q\bar{q},\text{RS}}^{(1)}$ in the left panel and $A_{q\bar{q},\text{RS}}^{(1)}$ multiplied with the up-quark PDFs in the right panel, both plotted against the CM energy \sqrt{s} in dashed black. This has to be compared with the solid black plots in Figure 4.3, which shows the same plots for the SM expressions. Clearly, the peak at the $t\bar{t}$ threshold is washed-out in the RS model, because the extra factor \hat{s} in (4.65) prevents the function from dropping off for large CM energies. This is a consequence of the fact that the new physics is considered heavy, which means that interference terms scale as \hat{s}/m_A^2 , compare (4.38), and is symbolized by the propagators being replaced by contact interactions in Figure 4.6.

⁷This inequality should be considered only as a crude approximation valid up to a factor of $\mathcal{O}(1)$.

4.5 Numerical Analysis

The Wilson coefficients appearing in the effective Lagrangian (4.45) are constrained by the measurements of the forward-backward asymmetry A_{FB}^t , the total cross section $\sigma_{t\bar{t}}$, and the $t\bar{t}$ invariant mass spectrum $d\sigma_{t\bar{t}}/dM_{t\bar{t}}$. In Section 4.1 the experimental values for the cross section (4.3) and the forward backward asymmetry in the CM frame (4.7) are quoted. In addition, we will include in the analysis the last bin of the invariant $t\bar{t}$ mass spectrum, $M_{t\bar{t}} \in [800, 1400]$ GeV, which is most sensitive to new physics [236],

$$\left(\frac{d\sigma_{t\bar{t}}}{dM_{t\bar{t}}}\right)_{\text{exp}}^{M_{t\bar{t}} \in [800, 1400] \text{ GeV}} = (0.068 \pm 0.032_{\text{stat.}} \pm 0.015_{\text{syst.}} \pm 0.004_{\text{lumi.}}) \frac{\text{fb}}{\text{GeV}}. \quad (4.66)$$

Here the quoted individual errors are of statistical and systematic origin, and due to the luminosity uncertainty, respectively.

The above results should be compared to the predictions obtained in the SM supplemented by the dimension-six operators (4.45). Ignoring tiny contributions related to the (anti)strange-, (anti)charm-, and (anti)bottom-quark content of the proton (antiproton), and using the dimensionless coefficients

$$\begin{aligned} \tilde{C}_{q\bar{q}}^V &\equiv 1 \text{ TeV}^2 C_{q\bar{q}}^V, \\ \tilde{C}_{t\bar{u}}^V &\equiv 1 \text{ TeV}^2 (1/3 C_{t\bar{u},\parallel}^{(V,8)} - 2C_{t\bar{u},\parallel}^{(V,1)}), \end{aligned} \quad (4.67)$$

one obtains for the cross section

$$(\sigma_{t\bar{t}})_{\text{RS}} = \left[1 + 0.053 (\tilde{C}_{u\bar{u}}^V + \tilde{C}_{t\bar{u}}^V) - 0.612 \tilde{C}_{t\bar{u}}^S + 0.008 \tilde{C}_{d\bar{d}}^V\right] (6.73_{-0.80}^{+0.52}) \text{ pb}, \quad (4.68)$$

and for the last bin of the invariant mass spectrum

$$\begin{aligned} \left(\frac{d\sigma_{t\bar{t}}}{dM_{t\bar{t}}}\right)_{\text{RS}}^{M_{t\bar{t}} \in [800, 1400] \text{ GeV}} &= \\ \left[1 + 0.33 (\tilde{C}_{u\bar{u}}^V + \tilde{C}_{t\bar{u}}^V) - 0.81 \tilde{C}_{t\bar{u}}^S + 0.02 \tilde{C}_{d\bar{d}}^V\right] &(0.061_{-0.006}^{+0.012}) \frac{\text{fb}}{\text{GeV}}. \end{aligned} \quad (4.69)$$

All Wilson coefficients in the above expressions are understood to be evaluated at m_t . The numerical factors multiplying $\tilde{C}_{t\bar{u}}^S$ correspond to a Higgs mass of $m_h = 115$ GeV.⁸ The RG evolution of the Wilson coefficients from M_{KK} to m_t is achieved with the formula (4.56). The dependence of $\sigma_{t\bar{t}}$ and $d\sigma_{t\bar{t}}/dM_{t\bar{t}}$ on \tilde{C}_{ij}^P has been obtained by convoluting the kernels (4.50) with the parton luminosities $\mathbb{f}_{ij}(\hat{s}/s, \mu_f)$ by means of the charge-symmetric analog of formula (4.28), using MSTW2008LO PDFs [228] with renormalization and factorization scales fixed to $\mu_r = \mu_f = m_t = 173.1$ GeV. The corresponding value of the strong coupling constant is $\alpha_s(M_Z) = 0.139$, which translates into $\alpha_s(m_t) = 0.126$ using one-loop RG running. The total cross section

⁸The conclusions will not depend on the Higgs mass, so that it is unnecessary to update the calculation with the measured value here.

c_{t_L}	c_{t_R}	$\tilde{C}_{u\bar{u}}^V/\alpha_s$	$\tilde{C}_{u\bar{u}}^A/\alpha_s$	$\tilde{C}_{d\bar{d}}^V/\alpha_s$	$\tilde{C}_{d\bar{d}}^A/\alpha_s$	$\tilde{C}_{t\bar{t}}^V/\alpha_s$
-0.46	0.11	1.00	$0.035 \cdot 10^{-2}$	1.00	$-0.070 \cdot 10^{-2}$	$-0.009 \cdot 10^{-4}$
-0.47	0.50	1.19	$0.081 \cdot 10^{-2}$	1.19	$0.004 \cdot 10^{-2}$	$-0.026 \cdot 10^{-4}$
-0.49	1.00	1.29	$0.201 \cdot 10^{-2}$	1.29	$-0.027 \cdot 10^{-2}$	$0.108 \cdot 10^{-4}$

Table 4.1: Results for the Wilson coefficients corresponding to three different parameter points. The numbers shown correspond to the RS model with $SU(2)_L \times U(1)_Y$ bulk gauge symmetry and brane-localized Higgs sector. The coefficients scale as $(1 \text{ TeV}/M_{\text{KK}})^2$. Further details are given in the text.

and $t\bar{t}$ invariant mass distribution in the SM have been computed at NLO [237] using MCFM [238], employing MSTW2008NLO PDFs along with $\alpha_s(M_Z) = 0.120$, which corresponds to $\alpha_s(m_t) = 0.109$ at two-loop accuracy. The given total SM errors represent the uncertainty due to the variation of the factorization scale $\mu_r = \mu_f \in [m_t/2, 2m_t]$ as well as PDF errors within their 90% CL limits, after combining the two sources of error in quadrature. Notice that within errors our SM prediction for $\sigma_{t\bar{t}}$ is in good agreement with recent theoretical calculations, that include effects of logarithmically enhanced NNLO terms [211, 239].

With all this at hand, we are now in a position to give the forward-backward asymmetry in the CM frame. Normalizing the result for σ_a to σ_s calculated at NLO,⁹ we find the following expression

$$(A_{\text{FB}}^t)_{\text{RS}} = \left[\frac{1 + 0.243 (\tilde{C}_{u\bar{u}}^A + \tilde{C}_{t\bar{t}}^V) - 0.26 \tilde{C}_{t\bar{t}}^S + 0.034 \tilde{C}_{d\bar{d}}^A + 0.03 \tilde{C}_{u\bar{u}}^V + 0.004 \tilde{C}_{d\bar{d}}^V}{1 + 0.053 (\tilde{C}_{u\bar{u}}^V + \tilde{C}_{t\bar{t}}^V) - 0.612 \tilde{C}_{t\bar{t}}^S + 0.008 \tilde{C}_{d\bar{d}}^V} \right] (8.75_{-1.56}^{+1.72}) \%, \quad (4.70)$$

where all coefficient functions should be evaluated at the scale m_t . The central value of our SM prediction has been obtained by integrating the formulas given in [215] over the relevant phase space using (4.25), (4.27), and (4.28), weighted with MSTW2008LO PDFs with the unphysical scales fixed to m_t . It is in agreement with (4.8) as well as the findings of [222]. Unlike [214], we have chosen not to include electroweak corrections to the forward-backward asymmetry in the central value of (4.70). Such effects have been found in [214, 240] to enhance the $t\bar{t}$ forward-backward asymmetry by around 9% to 4% depending on whether only mixed electroweak-QCD contributions or also purely electroweak corrections are included. To account for the uncertainty of our SM prediction due to electroweak effects we have added in quadrature an error of 5% to the combined scale and PDF uncertainties.

In order to investigate the importance of the different contributions entering the RS predictions (4.68), (4.69) and (4.70) for the $t\bar{t}$ observables, we have calculated the relevant Wilson coefficients at the KK scale for three benchmark points with typical

⁹Using MSTW2008 PDFs and $\mu_r = \mu_f = m_t = 173.1 \text{ GeV}$, we obtain in the SM the symmetric cross sections $(\sigma_s)_{\text{LO}} = 6.66 \text{ pb}$ and $(\sigma_s)_{\text{NLO}} = 6.73 \text{ pb}$ using MCFM. Since these results differ by only 1%, the central value of A_{FB}^t does essentially not depend on whether the LO or the NLO cross section is used to normalize (4.70).

bulk mass parameters chosen from our dataset. In Table 4.1 the numerical results for the coefficient functions are presented. To keep the presentation simple, we show in the table only the values of the left- and right-handed top-quark bulk mass parameters c_{t_L} and c_{t_R} . The numerical values for the remaining bulk mass parameters and Yukawa matrices, specifying the three parameter points completely are collected in Appendix A. It should be emphasized that the magnitudes of the shown results are generic predictions in the allowed parameter space and do not reflect a specific choice of model parameters. From the numbers given in the table, we see that the ratios of magnitudes of the Wilson coefficients are given by

$$\frac{|\tilde{C}_{q\bar{q}}^A|}{|\tilde{C}_{q\bar{q}}^V|} \approx 10^{-3}, \quad \frac{|\tilde{C}_{t\bar{u}}^V|}{|\tilde{C}_{u\bar{u}}^V|} \approx 10^{-5}. \quad (4.71)$$

For what concerns the size of the corrections due to flavor-changing currents in the t channel (encoded in $\tilde{C}_{t\bar{u}}^V$ and $\tilde{C}_{t\bar{u}}^S$), we mention that in the RS model based on an $SU(2)_L \times U(1)_Y$ bulk gauge group, the ratio of neutral electroweak gauge boson (Higgs-boson) to KK gluon effects is roughly 1/3 (on average 1/50). In the RS variant with extended $SU(2)_R$ symmetry and custodial protection of the $Zb_L\bar{b}_L$ vertex, one finds a very similar pattern. The scalar contributions are not explicitly listed but are another factor of 10^2 smaller than the $\tilde{C}_{t\bar{u}}^V$ coefficients.

Focusing on the numerical dominant corrections arising from s channel KK gluon exchange, we see from Table 4.1 that $\tilde{C}_{u\bar{u}}^V$ and $\tilde{C}_{u\bar{u}}^A$ are comparable in size to their counterparts involving down quarks. Since the latter coefficients are suppressed in the total cross section relative to the coefficients involving up quarks by the small ratio of quark luminosities $\mathcal{L}_{d\bar{d}}(0.04)/\mathcal{L}_{u\bar{u}}(0.04) \approx 1/5$, the numerical impact of $\tilde{C}_{d\bar{d}}^V$ in (4.70) is negligible. In practice, we find that the relevant ratio $(0.008\tilde{C}_{d\bar{d}}^V)/(0.053\tilde{C}_{u\bar{u}}^V)$ amounts to less than 2.3% for the considered parameter points. For the last bin of the $t\bar{t}$ invariant mass spectrum, the picture is similar. The quark luminosity ratio is $\mathcal{L}_{d\bar{d}}(0.17)/\mathcal{L}_{u\bar{u}}(0.17) \approx 1/15$, which results in a ratio $(0.02\tilde{C}_{d\bar{d}}^V)/(0.33\tilde{C}_{u\bar{u}}^V)$ which is a 1.0% effect for our benchmark points. It is therefore sensible to restrict our attention to the coefficients $\tilde{C}_{u\bar{u}}^{V,A}$ that render by far the largest contributions to the $t\bar{t}$ observables in the RS model. Note however, that this situation is significantly changed at the LHC, where the luminosities give a ratio of $\mathcal{L}_{d\bar{d}}^{pp}(0.003)/\mathcal{L}_{u\bar{u}}^{pp}(0.003) \approx 2/3$ at a corresponding CM energy of $s = \sqrt{7}$ TeV, compare Figure 4.4.

These results, which hold true for all new physics models which try to explain the forward backward asymmetry through s channel exchanges of new resonances can be illustrated by a combined fit to the latest measurements of the asymmetry A_{FB}^t , the total inclusive cross section $\sigma_{t\bar{t}}$ and the last bin of the invariant mass spectrum, as shown in Figure 4.7. In addition to the 99%, 95% and 68% CL ellipses in the $\tilde{C}_{u\bar{u}}^V - \tilde{C}_{u\bar{u}}^A$ plane, the best fit point is indicated by a black cross as well as the prediction of the SM, which is indicated by a black point. The dashed lines denote the region of parameter space in which significant changes to the cross section as well as to the forward backward asymmetry are expected. From Table 4.1, one can clearly see that the RS corrections are expected to be nowhere near the right size in order to explain the asymmetry.

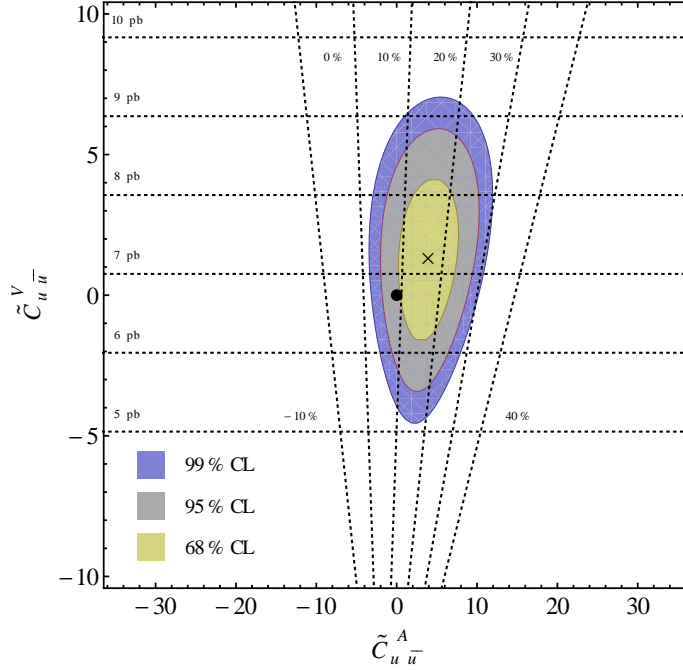


Figure 4.7: A combined fit to the latest measurements of the asymmetry A_{FB}^t , the total inclusive cross section $\sigma_{t\bar{t}}$ and the last bin of the invariant mass spectrum in the $\tilde{C}_{u\bar{u}}^V - \tilde{C}_{u\bar{u}}^A$ plane. The 99%, 95% and 68% CL ellipses are shown in blue, grayish blue and yellow respectively. The black cross (dot) represents the best fit point (SM expectation). Dashed black lines show the regions of parameter space which induce a large corrections to the total cross section and A_{FB}^t respectively.

From Table 4.1 we further observe that $\tilde{C}_{u\bar{u}}^V$ grows with increasing $(c_{t_L} + c_{t_R})$, *i.e.* if the top quark is localized more strongly in the IR, which was expected from (4.73) and (4.63). A similar trend in terms of c_{t_R} , though less pronounced, is also visible in the case of $\tilde{C}_{u\bar{u}}^A$. The numbers given in the table furthermore confirm our qualitative findings from Section 4.4 of strongly suppressed axial-vector couplings, $|\tilde{C}_{u\bar{u}}^A|/|\tilde{C}_{u\bar{u}}^V| \ll 1$. As a consequence, upon inserting the numerical values of $\tilde{C}_{u\bar{u}}^V$ and $\tilde{C}_{u\bar{u}}^A$ into the numerator of (4.70), it becomes clear, that in the RS model the NLO contributions to A_{FB}^t arising from $\tilde{C}_{u\bar{u}}^V$ dominate over the LO contributions from $\tilde{C}_{u\bar{u}}^A$. Numerically, we find that the vector-current contributions to the asymmetry are typically larger by about a factor of 100 than the corrections due to the axial-vector current. This strong enhancement reflects the fact that the KK gluons couple mainly vectorially with a small axial component. A closer inspection of (4.70) shows however, that in the ratio of the asymmetric and symmetric cross sections the effects of $\tilde{C}_{u\bar{u}}^V$ tend to cancel, as anticipated in Section 4.3. Since both σ_a and σ_s are enhanced for $\tilde{C}_{u\bar{u}}^V > 0$, but the dependence of σ_s on $\tilde{C}_{u\bar{u}}^V$ is stronger than the one of σ_a , positive values of $\tilde{C}_{u\bar{u}}^V$ will effectively lead to a reduction and not to an enhancement of the $t\bar{t}$ forward-backward

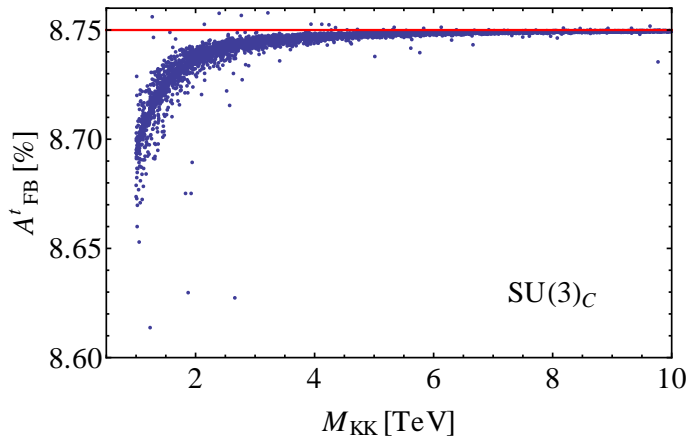


Figure 4.8: The forward backward asymmetry A_{FB}^t in the minimal RS model plotted for the complete dataset versus M_{KK} . The red line indicates the SM value.

asymmetry as envisioned. Given that $\tilde{C}_{u\bar{u}}^V > 0$ is a robust prediction of the RS framework, as long as the top quark is mainly composite, we conclude that the corrections to A_{FB}^t are necessarily negative.

This feature is illustrated in Figure 4.8, which shows the predictions for the RS corrections to the forward-backward asymmetry for our complete dataset, plotted versus the KK scale. The central value of the SM prediction is indicated by the red line. It is evident, that the maximal attainable effects amount to not even -0.05% . For all parameter points, the correction to the total inclusive cross section is larger than the contribution to the asymmetric cross section, which fixes the sign of the overall correction. Another representation of the small effects can be found in Figure 4.10, which shows that the scatter plot of the complete parameter set in the $\tilde{C}_{u\bar{u}}^V - \tilde{C}_{u\bar{u}}^A$ plane ends up in the tiny red region. These results should be contrasted with the analysis [124], which finds positive corrections to the $t\bar{t}$ forward-backward asymmetry of up to 5.6% (7%) arising from KK gluons (Z' -boson exchange) at LO. In the latter article, sizable corrections to $\tilde{C}_{q\bar{q}}^A$ arise since the 5D doublet and singlet light-quark fields are localized at different ends of the extra dimension by choosing $c_{u_L} = c_{d_L} \in [-0.4, 0.4]$ (IR-localized) and $c_{u_R} = c_{d_R} = -0.8$ (UV-localized).¹⁰ This will sabotage the generation of hierarchical masses and mixings on the basis of fundamental anarchic parameters. As a consequence, one would have to reintroduce a structure in the fundamental Yukawas in order to make such a model viable.

¹⁰Notice that the convention of the bulk mass parameters used in [124] differs from ours by an overall sign.

4.6 Axigluon Contributions to the Cross Section and the Asymmetry

The conclusions drawn in Section 4.3 and at the end of the last Section suggest that a new resonance with mainly axial vector couplings can bring the measured value of the forward backward asymmetry in agreement with the SM prediction.

The model introduced in Chapter 3, which features an extended strong interaction gauge group $SU(3)_D \times SU(3)_S$ in the bulk fulfills some of the criteria which we identified as essential for a solution of the A_{FB}^t puzzle in Section 4.3. It provides a large axial vector coupling with negligible vector coupling component for mixing angles $\theta \approx 45^\circ$ preferred by the flavor sector. Further, the couplings are large for the top, even larger than in the minimal model, because the extended scalar sector implies extremely IR localized top profiles. In addition, the extended model furnishes a hierarchy between couplings to down and to up type quarks, which is rooted in the different scalar fields which provide their masses. Such a hierarchy might explain why the measurements point to a smaller asymmetry at a machine which collides protons that contain equal shares of \bar{u} and \bar{d} quarks, compared to a proton-antiproton collider which provides 3/2 more \bar{u} than \bar{d} in the initial state.

From (3.63) and (3.108), one finds that in the model with extended color gauge group the Wilson coefficients in (4.55) take the form

$$C_{q\bar{q},\parallel}^{(V,8)} = -\frac{\pi\alpha_s}{2M_{\text{KK}}^2} \left\{ \frac{1}{L} - (\Delta'_Q)_{11} - (\Delta'_Q)_{33} - p_q^2 (\Delta'_q)_{11} - p_q^2 (\Delta'_q)_{33} \right. \\ \left. + 2L \left[\frac{1}{c_\theta^2} (\tilde{\Delta}_Q)_{11} \otimes (\tilde{\Delta}_Q)_{33} + \frac{p_q^4}{s_\theta^2} (\tilde{\Delta}_q)_{11} \otimes (\tilde{\Delta}_q)_{33} \right. \right. \\ \left. \left. - \frac{v_{\text{IR}}}{4} (t_\theta^2 (\Delta_Q)_{11} (\Delta_Q)_{33} + p_q^4 c t_\theta^2 (\Delta_q)_{11} (\Delta_q)_{33}) \right] \right\}, \quad (4.72)$$

$$C_{q\bar{q},\perp}^{(V,8)} = -\frac{\pi\alpha_s}{2M_{\text{KK}}^2} \left\{ \frac{1}{L} - (\Delta'_Q)_{11} - (\Delta'_Q)_{33} - p_q^2 (\Delta'_q)_{11} - p_q^2 (\Delta'_q)_{33} \right. \\ \left. + \frac{p_q^2 v_{\text{IR}}}{2} L ((\Delta_Q)_{11} (\Delta_q)_{33} + (\Delta_Q)_{33} (\Delta_q)_{11}) \right\},$$

$$C_{t\bar{u},\parallel}^{(V,8)} = -\frac{\pi\alpha_s}{M_{\text{KK}}^2} L \left\{ \frac{1}{c_\theta^2} (\Delta_Q)_{13} \otimes (\tilde{\Delta}_Q)_{31} + \frac{p_q^4}{s_\theta^2} (\Delta_q)_{13} \otimes (\tilde{\Delta}_q)_{31} \right. \\ \left. - \frac{v_{\text{IR}}}{4} (t_\theta^2 (\Delta_Q)_{13} (\Delta_Q)_{31} + p_q^4 c t_\theta^2 (\Delta_q)_{13} (\Delta_q)_{31}) \right\},$$

and $C_{t\bar{u},\parallel}^{(V,1)}$ is not modified by the axigluon KK modes, but only by the relocalization of the fermions and is therefore not repeated here. In the above expressions, only $\mathcal{O}(v^2/M_{\text{KK}}^2)$ contributions are kept, except for terms $\sim v_{\text{IR}}$, that become significant if the suppression from v_{IR} is balanced by powers of p_u , which parametrizes the effect

of the IR shift of the up-type quarks due to the extended Higgs sector. This factor is defined in (3.105) and is a function of $\tan\beta$, which is preferred to be small by flavor observables.

From the expressions (4.72) one can infer, that the tensor structures contributing to $C_{q\bar{q},\perp}^{(V,8)}$ in the minimal model cancel between the gluon and the axigluon contributions, which is expected, because this effect is exactly what renders the contributions to ϵ_K small. In contrast to the down sector however, the remaining contributions are $\sim v_{\text{IR}}p_u^2$ (for up quarks in the initial state), which is not small, because $p_u^2 > p_d^2$ if $\tan\beta < 1$. The definition of the relocalization factors p_u, p_d is given in (3.105), and for our reference value $\tan\beta = 1/2$, one finds $p_u^2 = 15$. It follows for the ZMA relations for the symmetric and antisymmetric hard scattering kernels introduced in (4.50) and (4.52) in the case of the extended model,

$$S_{u\bar{u},\text{RS}+\mathcal{A}}^{(0)} \sim \frac{\alpha_s\pi}{M_{\text{KK}}^2} \left\{ F^2(c_{t_L}) + F^2(c_{u_L}) + p_u^2 F^2(c_{t_R}) + p_u^2 F^2(c_{u_R}) \right\}, \quad (4.73)$$

$$A_{u\bar{u},\text{RS}+\mathcal{A}}^{(0)} \sim -\frac{\alpha_s\pi}{M_{\text{KK}}^2} L \left\{ \frac{1}{c_\theta^2} \left(\frac{4}{3} - s_\theta^2 \frac{v_{\text{IR}}}{3} \right) F^2(c_{t_L}) F^2(c_{u_L}) \right. \\ \left. + \frac{p_u^4}{s_\theta^2} \left(\frac{4}{3} - c_\theta^2 \frac{v_{\text{IR}}}{3} \right) F^2(c_{t_R}) F^2(c_{u_R}) \right. \\ \left. - \frac{p_u^2 v_{\text{IR}}}{4} \left(F^2(c_{t_L}) F^2(c_{u_R}) + F^2(c_{t_R}) F^2(c_{u_L}) \right) \right\}, \quad (4.74)$$

which has to be compared to (4.58). The cancellation of contributions to $C_{t\bar{u},\parallel}^{(V,1)}$ are the reason for the absence of a term with overall positive sign in $A_{u\bar{u},\text{RS}+\mathcal{A}}^{(0)}$, which is not formally of the order v^4/M_{KK}^4 , because $v_{\text{IR}} \sim v^2/M_{\text{KK}}^2$. Keep in mind, that the asymmetric cross section σ_a in the minimal model is positive, if the condition (4.63) is fulfilled. Naively, one might think that this leads to an even larger set of parameter points for which $\sigma_a > 0$ in the extended model, due to the IR shift of the up-type quark localization parameters. However, condition (4.63) basically ensures that the term $\sim F^2(c_{t_R}) F^2(c_{u_L})$ dominates in $A_{u\bar{u},\text{RS}}^{(0)}$ in (4.73). This would not lead to a positive asymmetric cross section in the extended model, because this term is suppressed by v_{IR}/p_u^2 compared to the leading negative contribution to $A_{u\bar{u},\text{RS}+\mathcal{A}}^{(0)}$. In this explicit example, we recover the result from Section 4.3, that an axigluon generically generates the wrong sign in the asymmetry. A two Higgs doublet model on the IR brane with $\tan\beta < 1$ would actually lead to an overall positive $\sigma_a > 0$, but the cancellations in the left-right chirality operator due to the axigluon tower spoils this effect.

In writing only the dominant terms in (4.73) and using the approximation (4.60), this becomes even more apparent,

$$S_{u\bar{u},\text{RS}+\mathcal{A}}^{(0)} \sim \frac{2\pi\alpha_s}{M_{\text{KK}}^2} \left(\frac{1}{2} + \frac{p_u^2}{2} + c_{t_L} + p_u^2 c_{t_R} \right), \quad (4.75)$$

$$A_{u\bar{u},\text{RS}+\mathcal{A}}^{(0)} \sim \frac{2\pi\alpha_s}{M_{\text{KK}}^2} L \frac{p_u^4}{s_\theta^2} \left(\frac{4}{3} - c_\theta^2 \frac{v_{\text{IR}}}{3} \right) (1 + 2c_{t_R})(1 + 2c_{u_R}) e^{L(2c_{u_R}+1)}. \quad (4.76)$$

c_{t_L}	c_{t_R}	$\tilde{C}_{u\bar{u}}^V/\alpha_s$	$\tilde{C}_{u\bar{u}}^A/\alpha_s$	$\tilde{C}_{d\bar{d}}^V/\alpha_s$	$\tilde{C}_{d\bar{d}}^A/\alpha_s$	$\tilde{C}_{t\bar{t}}^V/\alpha_s$
-0.46	0.11	14.5	$-2.66 \cdot 10^{-2}$	14.3	$-17.5 \cdot 10^{-2}$	$-12.8 \cdot 10^{-4}$
-0.47	0.50	17.6	$-5.82 \cdot 10^{-2}$	17.6	$-6.41 \cdot 10^{-2}$	$-20.2 \cdot 10^{-4}$
-0.49	1.00	19.4	$-22.2 \cdot 10^{-2}$	19.6	$-11.3 \cdot 10^{-2}$	$15.5 \cdot 10^{-4}$

Table 4.2: Results for the Wilson coefficients corresponding to three different parameter points. The numbers shown correspond to the RS model with $SU(3)_D \times SU(3)_S \times SU(2)_L \times U(1)_Y$ bulk gauge symmetry and brane-localized Higgs sector. The coefficients scale as $(1 \text{ TeV}/M_{\text{KK}})^2$. Further details are given in the text.

Since $c_{u_R} < -1/2$ for all parameter points, this would only allow for a positive contribution to $A_{u\bar{u},\text{RS}+\mathcal{A}}^{(0)}$, if either $c_{t_R} < -1/2$ as well or $c_{u_R} > -1/2$, which both are choices that will undermine the generation of flavor hierarchies with $\mathcal{O}(1)$ Yukawa couplings or the RS GIM suppression of FCNCs.

In addition, because the contributions to $S_{u\bar{u},\text{RS}+\mathcal{A}}^{(0)}$ are enhanced as well, which leads to a further suppression by the total inclusive cross section in the denominator of (4.27), the contributions to A_{FB}^t are strictly negative, and larger than in the minimal model. However, the absolute size of the corrections that can be generated in the extended model is still an order of magnitude too small for realistic values of M_{KK} , because all contributions to the asymmetric cross section feel the localization of the light up quarks.

It is interesting to note, that one can understand from the dual theory, why the new resonances although they couple almost purely axial to quarks, and the tops are extremely IR localized, do not lead to larger effects. The deeper reason for this is the fact, that unlike for the gluon, for the axigluon there is no elementary field in the dual Lagrangian. In the analysis of the bulk gauge boson propagator in Section 2.3, we found, that only for Neumann BCs in the UV, which corresponds to the existence of an elementary field in the dual theory, terms which are proportional to only one of the bulk coordinates t or t' appear in the small momentum expansion. This makes sense, because we could also show that these terms are related to diagrams which mix the composites with the elementary bosons. As a consequence, the gluon KK tower does contribute terms which are only proportional to the top localization to $C_{u\bar{u}}^V$, because there are diagrams with the gluon coupling to up quarks and then mixing into its composite partner, which couples strongly to the tops. On the other hand, the axigluon KK modes always contribute terms suppressed by the zero mode profiles of the up quark to $C_{u\bar{u}}^A$, because the only possible diagrams include the axigluon composites coupling to the composite partners of the up quarks, and the mixing between up composites and elementaries is suppressed by exactly those ZMA profiles. In contrast, an RS axigluon with only Dirichlet BCs in the IR (due to an IR brane Higgs sector) and Neumann BCs in the UV would lead to a sum over the KK tower of the type (2.87), which in turn would furnish a sizable contribution to A_{FB}^t .

In order to make these results comparable to the findings in the minimal model, we give the Wilson coefficients in the extended model in Table 4.2 for the same reference

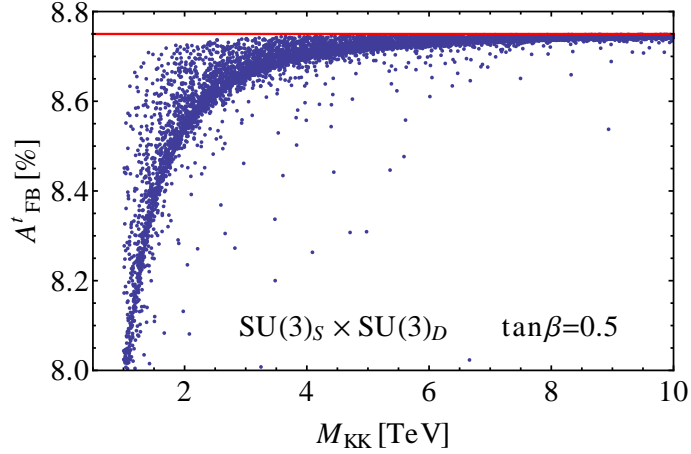


Figure 4.9: A_{FB}^t in the extended RS model with $SU(3)_D \times SU(3)_S$ strong interaction bulk gauge group, plotted for the complete dataset versus M_{KK} . The red line indicates the SM value.

points and for $\theta = 45^\circ$ and $\tan\beta = 1/2$. We refrain from giving the result for the coefficient of the scalar operator even though it may be larger by a factor of a few, depending on the different contributions from the extended Higgs sector, the generic suppression of these contributions will prevail in the extended model.¹¹ Note, that for $\tan\beta = 1/2$, the contributions to $\tilde{C}_{u\bar{u}}^V$ in Table 4.2 are already large, but still feasible, as can be seen from the green points plotted in Figure 4.10. Further, the analogue of the scatter plot in Figure 4.8 for the forward backward asymmetry versus the KK scale is shown in Figure 4.9 for the extended model and $\theta = 45^\circ$ and $\tan\beta = 1/2$. One can see, that the effects are enhanced due to the relocalization of the top quarks, but still do not exceed -0.5% even for extremely small KK scales and go invariably in the wrong direction for a possible explanation of the measured asymmetry.

We can conclude from the results found in both the minimal and the extended RS model, that without invoking additional *ad hoc* assumptions about the flavor structure of the light-quark sector, the RS model and the corresponding strongly coupled theories can not explain the asymmetry, even if a resonance with purely axial couplings is introduced. There thus seems to be a generic tension between having large effects in A_{FB}^t and achieving a natural solution to the flavor problem.

¹¹This is the case, because the couplings to quarks are still proportional to the Yukawa couplings for all new scalar fields.

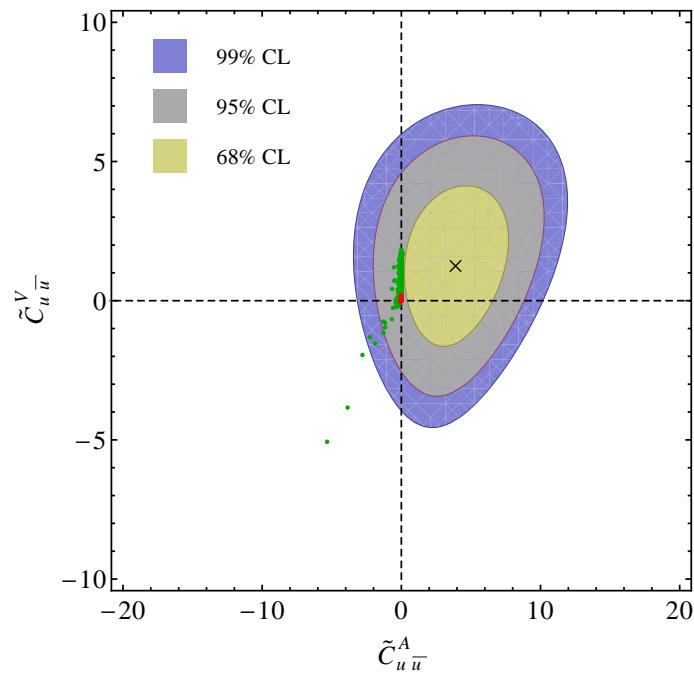


Figure 4.10: The figure shows the CL ellipses described in 4.7 and a scatterplot of the parameter set in the $\tilde{C}_{u\bar{u}}^V - \tilde{C}_{u\bar{u}}^A$ plane for the minimal model colored red and for the model with extended color gauge group for $\tan\beta = 1/2$ and $\theta = 45^\circ$ in green.

5 Conclusions

Whenever the Large Hadron Collider begins a new run, the first sign of physics beyond the Standard Model could be revealed, and this becomes more likely with the recorded luminosity growing exponentially. However, as long as the mass gap between the Higgs and new physics resonances grows, theories which naturally predict new particles with masses around the electroweak scale become more and more tuned. In the Randall Sundrum model and its dual description by a strongly coupled theory, new resonances are only expected in the multiple TeV range, and, due to the RS GIM mechanism, couple more or less exclusively to top quarks. As was shown in Chapter 3 and 4, this can explain why they have stayed below the radar of the ever increasing exclusion limits of the LHC.

In addition, the RS model arguably provides the best explanation of flavor we have today. Both the absence of FCNCs as well as the structure of the CKM matrix can be explained based on the fact that the quarks are localized differently along the extra dimension, which can be interpreted as a mixing with new composite degrees of freedom. As a result, flavor bounds are suppressed by orders of magnitude compared to general new physics without such a protection mechanism. This becomes apparent in the generically good agreement of the RS predictions for the flavor changing processes studied in Chapter 3. We find that both the contributions to $S_{\psi\phi}$ and $\Delta\Gamma/\Gamma$ in the $B_s - \bar{B}_s$ system as well as the branching ratios $\mathcal{B}(B_s \rightarrow \mu^+\mu^-)$ and $\mathcal{B}(B_d \rightarrow \mu^+\mu^-)$ do not exceed the experimental expectations and can even lead to an improved agreement, even if the contributions from the custodially protected model are taken into account.

It is thus remarkable that the RS-GIM mechanism leads to a broad agreement with measurements in the flavor sector, except for indirect CP violation in the Kaon system, which requires one percent fine-tuning despite the good suppression for the light flavors involved. It was extensively discussed how this problem arises and how it can be ameliorated following the approaches proposed in the literature. Most of these solutions modify the Yukawa couplings or constrain the localization parameters for the quarks, whose randomness is essential for the explanation of the flavor structure of the CKM matrix.

A new solution has been motivated by the observation, that the dangerous contributions to ϵ_K arise almost exclusively because of the exchange of color-charged resonances, the KK modes of the gluon. The extension of the strong interaction gauge group to a $SU(3)_D \times SU(3)_S$ surprisingly cancels these contributions independently of the imposed boundary conditions for the bulk fields and the choice of gauge couplings for the two subgroups.

Invoking the AdS/CFT duality, in a detailed analysis the part of the 5D gauge boson propagator which is responsible for the excessive contributions could be related to the purely composite contribution of the mixed elementary-composite propagator in Chapter 2. This allowed for a deeper understanding of the cancellation, that protects ϵ_K and ultimately leads to an RS model in agreement with all bounds from the quark flavor sector. In Chapter 3, the thorough implementation of this model is

described, which unfortunately implies a baroque Higgs sector in order to realize the Yukawa couplings on the IR brane, that does not lead to a predictive mass spectrum for the new scalar states due to the vast number of free parameters in the potential. The impact of the RS model with and without the extended color gauge group on flavor diagonal processes, namely electroweak precision observables, has also been studied in Chapter 3. It turns out that the recent updates on the fit to the $Z \rightarrow \bar{b}b$ pseudo observables put very severe constraints on the couplings of the Z or induces a large KK scale. Adopting a custodial protection in order to prevent this, which is also the best way to suppress large contribution to the oblique T parameter, however reintroduces a tension with the contributions from the resonances charged under the extended color gauge group to ϵ_K .

If the flavor problem of the RS model is explained by the mechanism introduced in this thesis, this tension must be addressed by either a different suppression of contributions to the electroweak precision observables, or by a more inventive realization of the scalar sector. In this context it should be mentioned that during the completion of this thesis, a paper has been published, whose authors also find only a minor improvement for the custodial model with extended color gauge group [244]. The bound derived there comes from the loop induced direct CP violation in Kaon mixing measured by ϵ'/ϵ_K and is due to the exchange of the new scalar degrees of freedom and therefore also rooted in the extended Higgs sector.

The last chapter focuses on the question of whether the question whether the observed forward-backward asymmetry at the Tevatron could be explained by new physics, with the emphasis on the RS model and its extensions. Because the KK gluons have almost pure vector couplings to quarks, one finds generically larger contributions to the total inclusive cross section than to the asymmetric cross section in the RS model. This leads to a negative correction to A_{FB}^t , that is defined as the ration of the two. The measurement however suggests an enhancement. This result could be generalized to all new physics with primarily vectorial couplings and its robustness under the inclusion of interference effects with NLO QCD diagrams has been confirmed.

The almost axial vector couplings of the other linear combination of gauge fields from the $SU(3)_D \times SU(3)_S \rightarrow SU(3)_C$ breaking in the extended model does already lead to a suppression of the asymmetric cross section and consequentially leads to an even worse fit, which is in agreement with the general expectations of resonances with axial vector couplings. In contrast to ϵ_K , A_{FB}^t is very sensitive to the boundary conditions of the color-charged 5D gauge bosons and it could be shown that the BCs imposed by direct detection bounds and the Yukawa couplings guarantee that the effects are always suppressed by the localization of the up quarks and are therefore rendered very small.

A Generating Parameter Points

In order to generate a point in the parameter space, we have to fix 38 (real) parameters. These are the 36 real parameters corresponding to the 18 complex entries of the 5D Yukawa matrices, the KK scale M_{KK} and the remaining c_{u_3} -parameter corresponding to the wave function $F(c_{u_3})$ which we chose in the Froggatt-Nielsen analysis to derive the formulas (2.163), (2.164), (2.165) and (2.165). For the implementation of the parameter scan we the program `Mathematica` was used and the functions mentioned in this chapter will refer to predefined functions within `Mathematica`, if not stated otherwise. The code conducts the following steps:

1. Random Yukawas

In the first step 18 random complex numbers are produced in the range $y_{ij} \in [0.3, 3]$. The random number generator is `MersenneTwister`, which turned out to be the fastest.

2. First χ^2 Test

From these numbers the profile-independent Wolfenstein parameters $\bar{\eta}, \bar{\rho}$ are computed. If they fail to minimise

$$\chi^2[X_i] = \sum_i \left(\frac{X_i - \mu_i}{\sigma(X_i)} \right)^2, \quad \text{with } X_i = (\bar{\eta}, \bar{\rho}), \quad (\text{A.1})$$

the respective point is rejected. The central values are experimental data $\mu_i = (\bar{\rho}_{exp}, \bar{\eta}_{exp})$ (see Appendix C for the reference) and the variance corresponds to one experimental σ . Interestingly, the code fails to produce acceptable points, if this condition is implemented as an upper bound, like $\chi^2[\bar{\eta}, \bar{\rho}] < 2$, even if the bound is lowered significantly. Therefore the points are required to yield the solution of a `FindMinimum` condition.

3. Random c_{u_3}

The ZMA profile $F(c_{u_3})$, defined in (2.150) is randomised within a range $F(c_{u_3}) \in (0, F_{max})$. With the help of experimental values for the remaining Wolfenstein parameters λ and A as well as for the quark masses, the other zero mode profiles are computed according to the formulas in the Froggatt-Nielsen analysis (2.164), (2.165) and (2.165). The distributions for the localization parameters are shown in Figure A.1.

4. Second χ^2 Test

In the last step the KK scale is randomised within $M_{\text{KK}} \in [10^3, 10^4]$ GeV and with the help of the Yukawa matrices and the parameters $F(c_{Q,q})$, already determined in the third step, the quark masses and the CKM matrix are computed, according to (2.158) and (2.159). These expressions have to pass another χ^2 test,

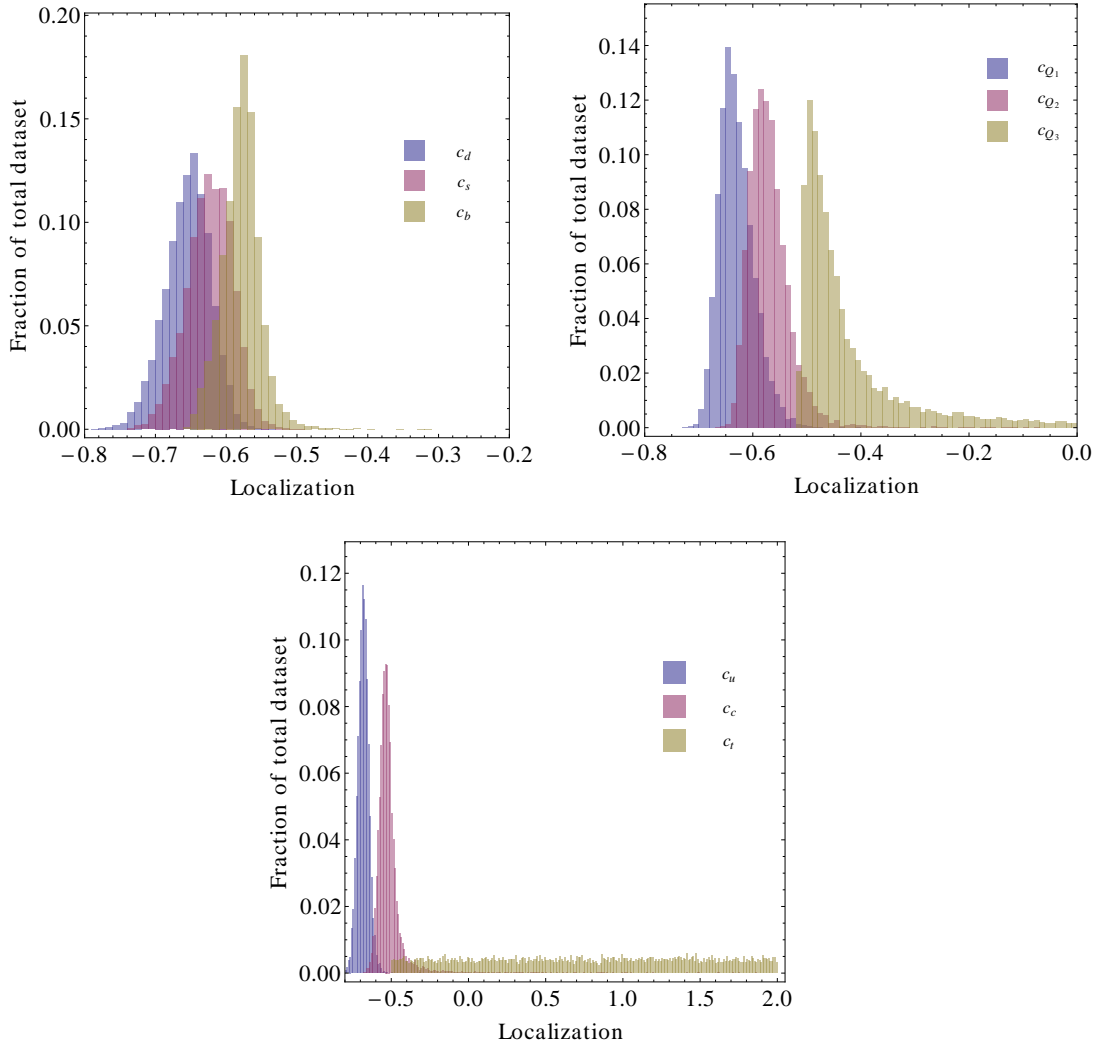


Figure A.1: Distributions of the quark localization parameters for the dataset used in throughout the thesis.

with $X_i = (m_u, m_c, m_t, m_d, m_s, m_b, A, \lambda, \rho, \eta)$, again compared to experimental values, that must fulfill $\chi^2 < 10$, which corresponds to the degrees of freedom here.

Reference Points

In the last chapter, three reference points have been chosen to illustrate the results. The localization parameters of the top singlet and third generation doublet are given in Table 4.1, and the full set of parameters, which specify these reference points completely are compiled in the following. Our first parameter point is specified by the

following bulk mass parameters¹

$$\begin{aligned} c_{Q_1} &= -0.632, & c_{Q_2} &= -0.581, & c_{Q_3} &= -0.459, \\ c_{u_1} &= -0.667, & c_{u_2} &= -0.543, & c_{u_3} &= +0.108, \\ c_{d_1} &= -0.617, & c_{d_2} &= -0.625, & c_{d_3} &= -0.581, \end{aligned}$$

and Yukawa matrices

$$\mathbf{Y}_u = \begin{pmatrix} 1.798 - 0.629i & -0.981 + 0.343i & -0.555 - 0.780i \\ 0.326 + 0.023i & -1.468 - 1.898i & -0.409 - 1.351i \\ 0.494 - 1.834i & 0.300 - 0.416i & -1.128 + 2.220i \end{pmatrix},$$

$$\mathbf{Y}_d = \begin{pmatrix} 0.330 - 0.330i & 0.273 + 2.626i & 0.669 + 0.255i \\ -0.647 + 0.124i & -0.021 - 2.913i & -0.221 - 0.045i \\ 1.223 - 1.134i & -0.019 - 0.030i & 0.318 - 2.092i \end{pmatrix}.$$

The second parameter point is given by

$$\begin{aligned} c_{Q_1} &= -0.651, & c_{Q_2} &= -0.586, & c_{Q_3} &= -0.469, \\ c_{u_1} &= -0.666, & c_{u_2} &= -0.521, & c_{u_3} &= +0.501, \\ c_{d_1} &= -0.644, & c_{d_2} &= -0.618, & c_{d_3} &= -0.563, \end{aligned}$$

and

$$\mathbf{Y}_u = \begin{pmatrix} -0.495 - 0.151i & 0.471 - 0.208i & 1.850 - 2.155i \\ 0.032 - 1.198i & -2.280 + 0.216i & 1.285 + 0.756i \\ 0.571 + 0.842i & -1.031 + 0.223i & 2.131 - 0.343i \end{pmatrix},$$

$$\mathbf{Y}_d = \begin{pmatrix} -1.003 - 0.146i & -1.677 + 1.677i & 1.249 + 1.812i \\ 0.165 - 0.762i & -2.736 - 0.514i & 0.338 - 0.039i \\ 0.971 + 1.203i & 0.454 + 0.532i & 0.202 + 1.370i \end{pmatrix}.$$

Finally, our third parameter point features

$$\begin{aligned} c_{Q_1} &= -0.652, & c_{Q_2} &= -0.563, & c_{Q_3} &= -0.486, \\ c_{u_1} &= -0.655, & c_{u_2} &= -0.497, & c_{u_3} &= +0.999, \\ c_{d_1} &= -0.639, & c_{d_2} &= -0.612, & c_{d_3} &= -0.578, \end{aligned}$$

and

$$\mathbf{Y}_u = \begin{pmatrix} 0.100 + 1.586i & -0.024 + 0.772i & 0.956 + 1.828i \\ 0.228 + 0.835i & -0.018 + 0.145i & -0.969 + 1.064i \\ -0.101 - 0.060i & -0.116 - 0.238i & -0.223 + 2.312i \end{pmatrix},$$

$$\mathbf{Y}_d = \begin{pmatrix} 0.232 + 2.313i & 0.597 - 1.654i & -0.219 + 1.182i \\ 0.661 - 2.200i & -0.765 - 0.815i & -1.270 + 1.060i \\ -1.021 + 1.220i & -0.066 + 0.097i & 2.497 + 1.067i \end{pmatrix}.$$

¹Here and below, results are given to at least three significant digits.

Here $c_{Q_1} = c_{u_L} = c_{d_L}$, $c_{u_1} = c_{u_R}$, and $c_{d_1} = c_{d_R}$ and similarly in the case of the second and third quark generation.

B Neutral Meson Mixing

Neutral mesons and antimesons are composite states of quarks with different flavor and zero electric charge,

$$\begin{aligned}
 K &\sim (\bar{s}d), & \bar{K} &\sim (s\bar{d}), \\
 B_d &\sim (\bar{b}d), & \bar{B}_d &\sim (b\bar{d}), \\
 B_s &\sim (\bar{b}s), & \bar{B}_s &\sim (b\bar{s}), \\
 D &\sim (\bar{u}c), & \bar{D} &\sim (u\bar{c}).
 \end{aligned}
 \tag{B.1}$$

Apart from different flavor and antiflavor content, they share the same quantum numbers and therefore mix. By mixing one means that the mass eigenstates are not the same as the flavor eigenstates (B.1), but linear combinations thereof,

$$\begin{aligned}
 |M_L\rangle &= p|M\rangle + q|\bar{M}\rangle, \\
 |M_H\rangle &= p|M\rangle - q|\bar{M}\rangle,
 \end{aligned}
 \tag{B.2}$$

where $|p|^2 + |q|^2 = 1$ and the indices H and L indicate the heavy and light mass eigenstate respectively. Further, an initially produced pure meson or antimeson state will always oscillate with time into a superposition of both. Because this oscillation involves time scales $\gg 1/\Lambda_{\text{QCD}}$, it can be described by an effective Hamiltonian H , and a Schrödinger equation

$$i\frac{\partial}{\partial t} \begin{pmatrix} \bar{M} \\ M \end{pmatrix} = H \begin{pmatrix} \bar{M} \\ M \end{pmatrix}.
 \tag{B.3}$$

This Hamiltonian can only be hermitian, if the Hilbert space consisting of M, \bar{M} is complete. However, these (anti)meson states do not only oscillate, but will also decay into different final states, which is consequentially described by the non-hermitian component of H . One can write

$$H = M - \frac{i}{2}\Gamma,
 \tag{B.4}$$

so that the mass matrix M and the decay matrix Γ are hermitian and one can write

$$\begin{pmatrix} H_{11} & H_{12} \\ H_{21} & H_{22} \end{pmatrix} = \begin{pmatrix} M_{11} & M_{12} \\ M_{12}^* & M_{22} \end{pmatrix} + \frac{i}{2} \begin{pmatrix} \Gamma_{11} & \Gamma_{12} \\ \Gamma_{12}^* & \Gamma_{22} \end{pmatrix}.
 \tag{B.5}$$

In this notation, mixing only means that these matrices have non-vanishing off-diagonal components, and one finds for the “mixing angles” in (B.2) the relation

$$\left(\frac{q}{p}\right)^2 = \frac{M_{12}^* - (i/2)\Gamma_{12}^*}{M_{12} - (i/2)\Gamma_{12}}
 \tag{B.6}$$

and for the eigenvalues

$$\omega_{L,H} = H_{11} \mp \sqrt{H_{12}H_{21}}. \quad (\text{B.7})$$

One can express the mass and width difference of the mass eigenstates by the real and imaginary part of the eigenvalues

$$\begin{aligned} \Delta m &\equiv m_H - m_L = \text{Re}(\omega_H - \omega_L), \\ \Delta\Gamma &\equiv \Gamma_H - \Gamma_L = -2\text{Im}(\omega_H - \omega_L), \end{aligned} \quad (\text{B.8})$$

which allows for the definition of the parameters

$$x \equiv \frac{\Delta m}{\Gamma}, \quad y \equiv \frac{\Delta\Gamma}{2\Gamma}, \quad (\text{B.9})$$

which are well suited to categorize the different meson-antimeson systems in (B.1). A large mass difference expresses itself in a large x parameter and y measures the difference in the lifetime of the two mass eigenstates. Interestingly, all of the four systems in (B.1) differ in these parameters [159, 241], which implies different oscillation behaviour, as one can see from plotting the percentage of antimesons \bar{M} and mesons M in an initially pure meson beam versus the time normalized to the average lifetime $T = t/\tau$ of the involved states,

$$\begin{aligned} \frac{N_M(t)}{N_M(0)} &= \frac{e^{-T}}{2} [\cosh(yT) + \cos(xT)], \\ \frac{N_{\bar{M}}(t)}{N_M(0)} &= \frac{e^{-T}}{2} [\cosh(yT) - \cos(xT)], \end{aligned} \quad (\text{B.10})$$

see [241, Sec.2.2.4] for details. The plots are reproduced in Figure B.1. For the Kaon system, both $x \sim 1$ and $y \sim -1$ are large, which corresponds to a large mass difference as well as a considerable difference in the lifetimes of the two mass eigenstates. The sign of y does also imply, that the heavier state lives longer, so that one usually identifies $K_L = K_H$ and $K_S = K_l$ with the subscript denoting $S = \text{short}$ and $L = \text{long}$ lifetime. The relaxation process dominates, because it takes little more than one oscillation for all of the K_S to decay, so that the beam consists entirely of K_L states after one period, as shown in the upper left panel of Figure B.1. This feature is shared by $D - \bar{D}$ mixing and $B_d - \bar{B}_d$ mixing, which both have $x \sim 0.6 - 0.8$, so that it takes only one oscillation for most of the mesons to decay. The difference in lifetimes is with $y \sim 10^{-3}$ however negligible for the $B_d - \bar{B}_d$ system, so that there are basically no particles left in the beam after one period as shown in the lower left panel of Figure B.1. For the $D - \bar{D}$ system $y \sim 0.75$, which results in a not totally depleted beam, compare the upper right panel of Figure B.1. The situation is very different for $B_s - \bar{B}_s$ system, for which $x \sim 27$ and $y \sim 10^{-2}$. The system shows the biggest mass difference of the four, but it is not possible to identify long- or short lived states with the mass eigenstates, because their lifetimes are almost equal and the oscillation frequency allows for several oscillations before the beam is depleted, as shown in the lower right panel of Figure B.1.

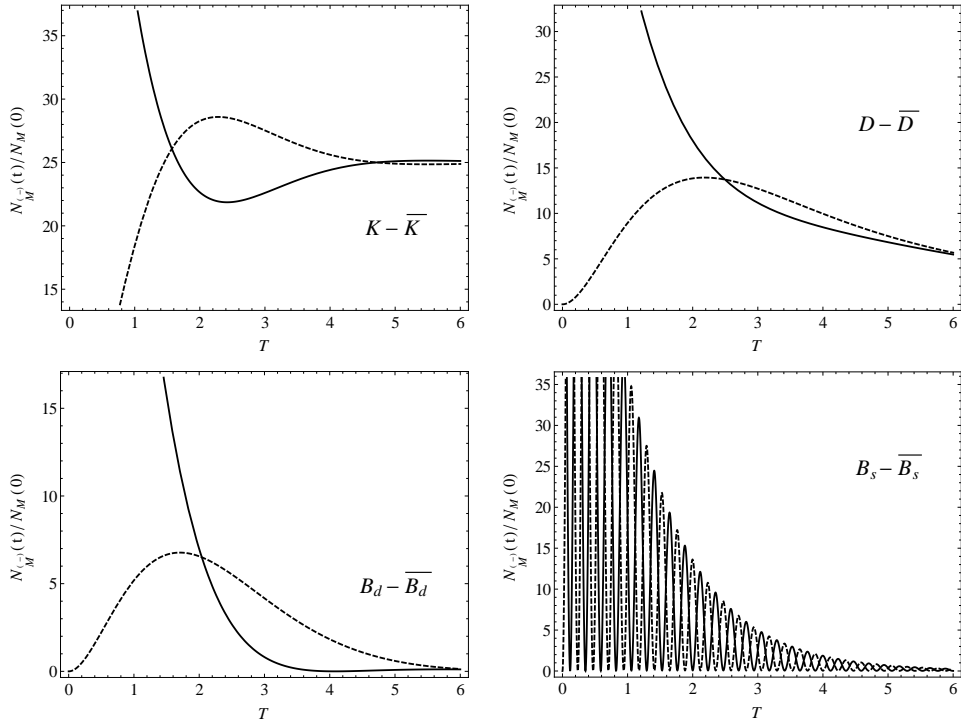


Figure B.1: The plots show the percentage of (anti-)mesons of a beam of 100% mesons at $T = 0$ evolving over time T in (dashed) solid black. In the upper left(right) panel for the $K - \bar{K}$ ($D - \bar{D}$) system and in the lower left (right) panel for the $B_d - \bar{B}_d$ ($B_s - \bar{B}_s$) system.

In the SM, the contributions to the off-diagonal elements in (B.5) can only be generated by W^\pm exchange in loops, because they correspond to $\Delta F = 2$ neutral currents. The relevant diagrams are box-diagrams as shown in Figure 1.8, which also include all up-type (down-type) quarks in the case of external K , B_d or B_s (D) mesons. Because of this virtual exchange, historically, meson mixing played an important role. The charm mass was predicted from Δm_K measurements and similarly, the large $B_d - \bar{B}_d$ oscillation rate gave a first hint on a really heavy top, for details see [242, Sec. 1.2] and references therein.

Meson-antimeson mixing played also an important role in discovering C and CP violation in the electroweak interactions. The latter represents the toughest test for New Physics models, because the measurements do agree so well the small SM expectations.

One differentiates between CP violation in mixing, decay and in the interference of mixing and decay. With the help of the weak Hamiltonian \mathcal{H}_W , one can define the amplitudes

$$A_f = \langle f | \mathcal{H}_W | M \rangle, \quad A_{\bar{f}} = \langle \bar{f} | \mathcal{H}_W | M \rangle, \quad (\text{B.11})$$

for the decay of a neutral meson into some final state f and its antistate \bar{f} , and analogous for the decay of the antimeson \bar{A}_f and $A_{\bar{f}}$. The variable

$$\lambda_f \equiv \frac{q \bar{A}_f}{p A_f} \quad (\text{B.12})$$

allows then to distinguish between the three types of CP violation,

1. CP Violation in Mixing is characterized by $|q/p| \neq 1$,
2. CP Violation in Decay occurs for $|\bar{A}_{\bar{f}}/A_f| \neq 1$, and
3. CP Violation in Interference of Mixing and Decays] is expected if $\text{Im}\lambda_f \neq 0$.

A complementary way to categorize CP violation is by defining *direct* CP violation for decays with $|A_f/A_{\bar{f}}| \neq 1$ and *indirect* CP violation if this ratio does not deviate from one.

The observables in the Kaon and $B_s - \bar{B}_s$ system discussed in Chapter 3 correspond to different measures of these types of CP violation. The ratio of the decay of long- and short-lived Kaons into pions in the strong isospin $I = 0$ eigenstates,

$$\epsilon_K \equiv \frac{\langle (\pi\pi)_{I=0} | K_L \rangle}{\langle (\pi\pi)_{I=0} | K_S \rangle} \quad (\text{B.13})$$

measures the indirect CP violation in $K - \bar{K}$ mixing. By writing $\lambda_0 \equiv \lambda_{(\pi\pi)_{I=0}}$ and inserting (B.2) in (B.13), one finds that

$$\epsilon_K = \frac{1 - \lambda_0}{1 + \lambda_0} \approx \frac{1}{2}(1 - \lambda_0) \approx \frac{1}{2} \left(1 + \left| \frac{q}{p} \right| + \text{Im}\lambda_0 \right), \quad (\text{B.14})$$

where in the second to last step it was used that the experimental value of ϵ_K implies that $|\lambda_0| \approx 1$, and in the last step the fact that direct CP violation is absent was employed. Therefore, the real part of ϵ_K is sensitive to CP violation in mixing and the imaginary part quantifies CP violation in the interference of mixing and decay.

Because of the characteristics discussed above, the decays of the B_s meson mass eigenstates cannot clearly be identified with the decays of a short or a long lived state. Consequentially, the relevant observables are different. Relevant for this thesis is the time-dependent asymmetry, which measures the difference in of the B_s and \bar{B}_s into some final state. In the case of semileptonic final states, it will only measure indirect CP violation,

$$A_{\text{SL}}^s = \frac{\Gamma(\bar{B}_s(t) \rightarrow \ell^+ X) - \Gamma(B_s(t) \rightarrow \ell^- X)}{\Gamma(\bar{B}_s(t) \rightarrow \ell^+ X) + \Gamma(B_s(t) \rightarrow \ell^- X)} = \frac{1 - |q/p|^4}{1 + |q/p|^4}, \quad (\text{B.15})$$

because the only source of CP violation is the oscillation $B_s \rightarrow \bar{B}_s \rightarrow \ell^- X$. It is therefore sensitive to the CP violating phase in the CKM element V_{ts} , which appears

in the corresponding SM box diagram or to new phases from the exchange of new physics resonances.

Further observables not discussed in this thesis are explained in [242] and references therein.

C Input Parameters

This appendix is a collection of input parameters used in the phenomenological part of the thesis

Parameter	Value \pm Error	Reference
G_F	$1.16637 \cdot 10^{-5} \text{ GeV}^{-2}$	[245]
s_w^2	0.2312	[146]
m_W	80.398 GeV	[146]
m_Z	91.1875 GeV	[146]
$\alpha(m_Z)$	1/127.9	[146]
$\alpha_s(m_Z)$	0.118 ± 0.003	[245]
m_t	$(144 \pm 5) \text{ GeV}$	[248]
m_b	$(2.3 \pm 0.1) \text{ GeV}$	[245]
m_c	$(560 \pm 40) \text{ MeV}$	[245]
m_s	$(50 \pm 15) \text{ MeV}$	[245]
m_d	$(3.0 \pm 2.0) \text{ MeV}$	[245]
m_u	$(1.5 \pm 1.0) \text{ MeV}$	[245]
λ	0.2265 ± 0.0008	[246]
A	0.807 ± 0.018	[246]
$\bar{\rho}$	$0.147^{+0.029}_{-0.017}$	[246]
$\bar{\eta}$	0.343 ± 0.016	[246]

Table C.1: Parameters used in the SM predictions and the generation of RS parameter points. The quoted values of the quark masses correspond to $\overline{\text{MS}}$ masses evaluated at a scale of 1 TeV.

Parameter	Value \pm Error	Reference
η_B	0.55 ± 0.01	[249]
m_{B_s}	5.3661 GeV	[245]
f_{B_s}	(245 ± 25) MeV	[247]
B_1^{bs}	0.80 ± 0.08	[247]
B_4^{bs}	1.15 ± 0.13	[247]
B_5^{bs}	1.74 ± 0.19	[247]
$(m_b + m_s)$	(4.30 ± 0.08) GeV	[247]
$2\beta_s^{\text{SM}}$	$(0.0363^{+0.0016}_{-0.0015})$	[160]
$(\Delta m_s / \Gamma_s)_{\text{exp}}$	26.3 ± 0.6	[250]
$\text{Re}(\Gamma_{12}^s / M_{12}^s)$	$(-4.97 \pm 0.94) \cdot 10^{-3}$	[158]
$\text{Im}(\Gamma_{12}^s / M_{12}^s)$	$(2.06 \pm 0.57) \cdot 10^{-5}$	[158]

Table C.2: Parameters used in the B_s - \bar{B}_s mixing observables. The given values for the B_i^{bs} parameters and the sums $(m_b + m_s)$ are $\overline{\text{MS}}$ quantities normalized at the scale 4.2 GeV.

Parameter	Value \pm Error	Reference
m_K	497.6 MeV	[245]
f_K	156.1 MeV	[245]
B_1^{sd}	0.51 ± 0.02	[176, Table 2]
B_4^{sd}	1.04 ± 0.07	[176, Table 2]
B_5^{sd}	0.76 ± 0.09	[176, Table 2]
$(m_s + m_d)$	(135 ± 18) MeV	[247]
ϕ_ϵ	$(43.51 \pm 0.05)^\circ$	[245]
κ_ϵ	0.92 ± 0.02	[173]
$(\Delta m_K)_{\text{exp}}$	$3.4833 \cdot 10^{-15}$ GeV	[245]
$m_t(m_t)$	(163.8 ± 1.3) GeV	[248]
$m_c(m_c)$	$(1.27^{+0.07}_{-0.11})$ GeV	[245]

Table C.3: Parameters used in the K - \bar{K} mixing observables. The given values for the B_i^{sd} parameters and the sum $(m_s + m_d)$ correspond to the RI-MOM scheme taken at the scale 2 GeV.

Parameter	Value \pm Error	Reference
m_{B_d}	5.2795 GeV	[245]
f_{B_d}	(200 ± 20) MeV	[247]
τ_{B_s}	$(1.472^{+0.024}_{-0.026})$ ps	[250]
c_A	0.96 ± 0.02	[169, 170]
m_μ	105.66 MeV	[245]
m_τ	1.777 GeV	[245]

Table C.4: Parameters entering the predictions for the $B \rightarrow \mu^+ \mu^-$ -meson decays.

The relevant magic numbers for the renormalization group running of the Wilson coefficients in neutral meson mixing read [152] for $K - \bar{K}$ mixing

$$a_i = (0.29, 0.69, 0.79, 1.1, 0.14)$$

$$b_i^{11} = (0.82, 0, 0, 0, 0),$$

$$b_i^{44} = (0, 0, 0, 4.4, 0),$$

$$b_i^{45} = (0, 0, 0, 1.5, 0.17),$$

$$b_i^{54} = (0, 0, 0, 0.18, 0),$$

$$b_i^{55} = (0, 0, 0, 0.061, 0.82),$$

$$c_i^{11} = (0.016, 0, 0, 0, 0),$$

$$c_i^{44} = (0, 0, 0, 0.68, 0.0055),$$

$$c_i^{45} = (0, 0, 0, 0.35, 0.0062),$$

$$c_i^{54} = (0, 0, 0, 0.026, 0.016),$$

$$c_i^{55} = (0, 0, 0, 0.013, 0.018) .$$

and $B_s - \bar{B}_s$ mixing

$$a_i = (0.286, 0.692, 0.787, 1.143, 0.143)$$

$$b_i^{11} = (0.865, 0, 0, 0, 0),$$

$$b_i^{44} = (0, 0, 0, 2.87, 0),$$

$$b_i^{45} = (0, 0, 0, 0.961, 0.22),$$

$$b_i^{54} = (0, 0, 0, 0.09, 0),$$

$$b_i^{55} = (0, 0, 0, 0.029, 0.863),$$

$$c_i^{11} = (0.017, 0, 0, 0, 0),$$

$$c_i^{44} = (0, 0, 0, 0.48, 0.005),$$

$$c_i^{45} = (0, 0, 0, 0.25, 0.006),$$

$$c_i^{54} = (0, 0, 0, 0.013, 0.016),$$

$$c_i^{55} = (0, 0, 0, 0.007, 0.019) .$$

D Higgs Potential for the Extended Scalar Sector

In this appendix, the full potential of the scalar sector on the IR brane of an RS model with $SU(3)_D \times SU(3)_S \times SU(2)_L \times U(1)_Y$ bulk gauge symmetry introduced in Section 3.6 is presented. It can be put into the form

$$\begin{aligned}
V(h, H_u, H_d) = & -\mu_\ell h^\dagger h + \lambda^\ell (h^\dagger h)^2 \tag{D.1} \\
& + \sum_{q=u,d} \left(-\mu_q (H_q)_A (H_q)_B^\dagger \text{Tr}[T_A T_B] \right. \\
& \quad + (H_q)_A^i (H_q^\dagger)_B^i (H_q)_C^j (H_q^\dagger)_D^j \mathbf{P}_{ABCD}^{13}(\lambda^q) \\
& \quad \left. + (H_q)_A^i (H_q^\dagger)_B^j (H_q)_C^j (H_q^\dagger)_D^i \mathbf{P}_{ABCD}^{24}(\lambda^q) \right) \\
& + (H_d)_A^i (H_d^\dagger)_B^i (H_u)_C^i (H_u^\dagger)_D^i \mathbf{Q}_{ABCD}^{1379}(f) \\
& + (H_d)_A^j (H_d^\dagger)_B^i (H_u)_C^i (H_u^\dagger)_D^j \mathbf{Q}_{ABCD}^{24810}(f) \\
& + \epsilon_{lk} \epsilon_{mn} (H_d)_A^l (H_d^\dagger)_B^m (H_u)_C^k (H_u^\dagger)_D^n \mathbf{Q}_{ABCD}^{561112}(f) \\
& + \sum_{q=u,d} \left(c_1^q h^\dagger h (H_q)_A (H_q^\dagger)_B \right. \\
& \quad + c_2^q (h^\dagger)^j h^i (H_q)_A^j (H_q^\dagger)_B^i \\
& \quad \left. + c_3^q \epsilon_{ij} \epsilon_{kl} (h^\dagger)^i h^k (H_q)_A^l (H_q^\dagger)_B^j \right) \text{Tr}[T_A T_B] \\
& + d_1 \epsilon_{mn} h^l h^j (H_u)_A^k (H_d^\dagger)_{aggger}^j \text{Tr}[T_A T_B] \\
& + \left(e_1 \epsilon_{lk} \epsilon_{mn} h^l (H_d)_A^m (H_u)_B^k (H_u)_C^n \right. \\
& \quad \left. + e_2 \epsilon_{mn} (h^\dagger)^l (H_u)_A^m (H_d)_B^l (H_u)_C^n + h.c. \right) \mathbf{R}_{ABC} \tag{D.2}
\end{aligned}$$

where the color structure is split off and implemented as follows. Each color bitriplet is written as a product $X_A T_A$, where $T_A = \{\mathbb{1}/2, \lambda_a/2\}$ and t_a , $a = 1 \dots 8$ denote the Gell-Mann matrices, small latin characters denote $SU(2)$ indices. In the quartic couplings, the color structure is repetitive and allows for at most four different color traces, which we abbreviate by \mathbf{Q} . In the cases in which the fields are indistinguishable, this reduces to two independent color traces and we use the abbreviation \mathbf{P} . The \mathbf{R}

structure only appears in the terms which mix all three fields,

$$\begin{aligned}
 \mathbf{Q}_{ABCD}^{ijkl}(x) &\equiv x_i \text{Tr}[T_A T_B] \text{Tr}[T_C T_D] + x_j \text{Tr}[T_A T_D T_C T_B] \\
 &\quad + x_k \text{Tr}[T_A T_D] \text{Tr}[T_B T_C] + x_l \text{Tr}[T_A T_B T_C T_D], \\
 \mathbf{P}_{ABCD}^{ij}(y) &\equiv y_i \text{Tr}[T_A T_B] \text{Tr}[T_C T_D] + y_j \text{Tr}[T_A T_D T_B T_C], \\
 \mathbf{R}_{ABC} &\equiv \left(\frac{N_c}{2}\right)^2 \delta_{A0} \delta_{B0} \delta_{C0} - \frac{N_c}{2} (\text{Tr}[T_A T_B] \delta_{C0} + \text{Tr}[T_A T_C] \delta_{B0} + \text{Tr}[T_C T_B] \delta_{A0}) \\
 &\quad + \text{Tr}[T_A T_B T_C] + \text{Tr}[T_B T_A T_C].
 \end{aligned} \tag{D.3}$$

The Higgs sector comprises 3 mass terms, 2×4 real parameters describing self-couplings of the bitriplets (the \mathbf{P} structures), one parameter describing the self-couplings of the color singlet, 6 real and 3 complex parameters from mixing between the color singlet and one of the bitriplets as well as 12 f -terms which describe mixing between the colored scalars (the \mathbf{Q} structures). This makes for a total of 36 real parameters.

It is straightforward to solve the extremal conditions, which are given by

$$\frac{\partial V(v_\ell, v_u, v_d)}{\partial v_u} = 0, \quad \frac{\partial V(v_\ell, v_u, v_d)}{\partial v_d} = 0, \quad \frac{\partial V(v_\ell, v_u, v_d)}{\partial v_\ell} = 0, \tag{D.4}$$

and can be used to eliminate three parameters. For a general Higgs potential, it is however not possible to analytically proof that this extremum is a minimum. The reason is, that a minmum is only obtained if the Hessian of the potential is positive definite. The potential will however give rise to $8 + 4$ Goldstone bosons, which correspond to zeros on the diagonal of the Hessian (in blockdiagonal form). As a consequence it is a numerical problem to minimize the potential. One can further constrain the parameter space by the condition that all masses are positive, and that the vacuum value of the potential signals a local minimum, $V(v_\ell, v_u, v_d) > V(0, 0, 0)$ [243].

Bibliography

- [1] V. F. Weisskopf, “On the Self-Energy and the Electromagnetic Field of the Electron,” *Phys. Rev.* **56**, 72 (1939). Cited on page 1.
- [2] M. Tegmark *et al.* [SDSS Collaboration], “Cosmological parameters from SDSS and WMAP,” *Phys. Rev. D* **69**, 103501 (2004) [[arXiv:astro-ph/0310723](#)]. Cited on page 2.
- [3] G. 't Hooft, (ed.), C. Itzykson, (ed.), A. Jaffe, (ed.), H. Lehmann, (ed.), P. K. Mittelner, (ed.), I. M. Singer, (ed.) and R. Stora, (ed.), “Recent Developments in Gauge Theories. Proceedings, Nato Advanced Study Institute, Cargese, France, August 26 - September 8, 1979,” *NATO Adv. Study Inst. Ser. B Phys.* **59**, 1 (1980). Cited on page 2.
- [4] P. F. Bedaque and U. van Kolck, “Effective field theory for few nucleon systems,” *Ann. Rev. Nucl. Part. Sci.* **52**, 339 (2002) [[arXiv:nucl-th/0203055](#)]. Cited on page 3.
- [5] S. P. Martin, “A Supersymmetry primer,” In *Kane, G.L. (ed.): Perspectives on supersymmetry II* 1-153 [[arXiv:hep-ph/9709356](#)]. Cited on page 6.
- [6] L. E. Ibanez and G. G. Ross, “ $SU(2)_L \times U(1)$ Symmetry Breaking as a Radiative Effect of Supersymmetry Breaking in Guts,” *Phys. Lett. B* **110**, 215 (1982). Cited on page 6.
- [7] R. Kitano and Y. Nomura, “Supersymmetry, naturalness, and signatures at the LHC,” *Phys. Rev. D* **73**, 095004 (2006) [[arXiv:hep-ph/0602096](#)]. Cited on page 6.
- [8] S. R. Coleman and J. Mandula, “All Possible Symmetries Of The S Matrix,” *Phys. Rev.* **159**, 1251 (1967). Cited on page 5.
- [9] B. Sakita, “Supermultiplets of elementary particles,” *Phys. Rev.* **136**, B1756 (1964). Cited on page 5.
- [10] H. Miyazawa, “Baryon Number Changing Currents,” *Progress of Theoretical Physics* **36**, 1266 (1966). Cited on page 5.
- [11] J. Wess and B. Zumino, “A Lagrangian Model Invariant Under Supergauge Transformations,” *Phys. Lett. B* **49**, 52 (1974). Cited on page 5.
- [12] R. Haag, J. T. Lopuszanski and M. Sohnius, “All Possible Generators of Supersymmetries of the S Matrix,” *Nucl. Phys. B* **88**, 257 (1975). Cited on page 5.

- [13] S. Dimopoulos and H. Georgi, “Softly Broken Supersymmetry and SU(5),” Nucl. Phys. B **193**, 150 (1981). Cited on page 5.
- [14] N. Seiberg, “Naturalness versus supersymmetric nonrenormalization theorems,” Phys. Lett. B **318**, 469 (1993) [[arXiv:hep-ph/9309335](#)]. Cited on page 6.
- [15] N. Polonsky, “Supersymmetry: Structure and phenomena. Extensions of the standard model,” Lect. Notes Phys. M **68**, 1 (2001) [[arXiv:hep-ph/0108236](#)]. Cited on page 6.
- [16] P. Fayet, “Supersymmetry and Weak, Electromagnetic and Strong Interactions,” Phys. Lett. B **64**, 159 (1976). Cited on page 7.
- [17] R. Barbier, C. Berat, M. Besancon, M. Chemtob, A. Deandrea, E. Dudas, P. Fayet and S. Lavignac *et al.*, “R-parity violating supersymmetry,” Phys. Rept. **420**, 1 (2005) [[arXiv:hep-ph/0406039](#)]. Cited on page 7.
- [18] E. Nikolidakis and C. Smith, “Minimal Flavor Violation, Seesaw, and R-parity,” Phys. Rev. D **77**, 015021 (2008) [[arXiv:0710.3129](#) [[hep-ph](#)]]. Cited on page 7.
- [19] C. Csaki, Y. Grossman and B. Heidenreich, “MFV SUSY: A Natural Theory for R-Parity Violation,” Phys. Rev. D **85**, 095009 (2012) [[arXiv:1111.1239](#) [[hep-ph](#)]]. Cited on page 7.
- [20] B. Holdom, “Raising the Sideways Scale,” Phys. Rev. D **24**, 1441 (1981). Cited on page 10.
- [21] R. Jackiw and K. Johnson, “Dynamical Model of Spontaneously Broken Gauge Symmetries,” Phys. Rev. D **8**, 2386 (1973). Cited on page 8.
- [22] C. Quigg and R. Shrock, “Gedanken Worlds without Higgs: QCD-Induced Electroweak Symmetry Breaking,” Phys. Rev. D **79**, 096002 (2009) [[arXiv:0901.3958](#) [[hep-ph](#)]]. Cited on page 8.
- [23] S. Weinberg, “Implications of Dynamical Symmetry Breaking: An Addendum,” Phys. Rev. D **19**, 1277 (1979). Cited on page 8.
- [24] L. Susskind, “Dynamics of Spontaneous Symmetry Breaking in the Weinberg-Salam Theory,” Phys. Rev. D **20**, 2619 (1979). Cited on page 8.
- [25] S. Dimopoulos and L. Susskind, “Mass Without Scalars,” Nucl. Phys. B **155**, 237 (1979). Cited on page 9.
- [26] E. Eichten and K. D. Lane, “Dynamical Breaking of Weak Interaction Symmetries,” Phys. Lett. B **90**, 125 (1980). Cited on page 9.
- [27] C. T. Hill and E. H. Simmons, “Strong dynamics and electroweak symmetry breaking,” Phys. Rept. **381**, 235 (2003) [Erratum-*ibid.* **390**, 553 (2004)] [[arXiv:hep-ph/0203079](#)]. Cited on pages 9 and 11.
- [28] F. Sannino, “Dynamical Stabilization of the Fermi Scale: Phase Diagram of Strongly Coupled Theories for (Minimal) Walking Technicolor and Unparticles,” [[arXiv:0804.0182](#) [[hep-ph](#)]]. Cited on page 13.

-
- [29] M. A. Luty and T. Okui, “Conformal technicolor,” *JHEP* **0609**, 070 (2006) [[arXiv:hep-ph/0409274](#)]. Cited on pages 13, 49, and 125.
- [30] D. Poland, D. Simmons-Duffin and A. Vichi, “Carving Out the Space of 4D CFTs,” [[arXiv:1109.5176 \[hep-th\]](#)]. Cited on pages 14, 125, and 126.
- [31] D. B. Kaplan, “Flavor at SSC energies: A New mechanism for dynamically generated fermion masses,” *Nucl. Phys. B* **365**, 259 (1991). Cited on pages 14 and 78.
- [32] A. J. Buras, J. R. Ellis, M. K. Gaillard and D. V. Nanopoulos, “Aspects of the Grand Unification of Strong, Weak and Electromagnetic Interactions,” *Nucl. Phys. B* **135**, 66 (1978). Cited on page 14.
- [33] A. Delgado, K. Lane and A. Martin, “A Light Scalar in Low-Scale Technicolor,” *Phys. Lett. B* **696**, 482 (2011) [[arXiv:1011.0745 \[hep-ph\]](#)]. Cited on page 17.
- [34] W. D. Goldberger, B. Grinstein and W. Skiba, “Distinguishing the Higgs boson from the dilaton at the Large Hadron Collider,” *Phys. Rev. Lett.* **100**, 111802 (2008) [[arXiv:0708.1463 \[hep-ph\]](#)]. Cited on page 17.
- [35] D. D. Dietrich, F. Sannino and K. Tuominen, “Light composite Higgs from higher representations versus electroweak precision measurements: Predictions for CERN LHC,” *Phys. Rev. D* **72**, 055001 (2005) [[arXiv:hep-ph/0505059](#)]. Cited on page 17.
- [36] M. J. Dugan, H. Georgi and D. B. Kaplan, “Anatomy of a Composite Higgs Model,” *Nucl. Phys. B* **254**, 299 (1985). Cited on page 17.
- [37] K. Agashe, R. Contino and A. Pomarol, “The Minimal composite Higgs model,” *Nucl. Phys. B* **719**, 165 (2005) [[arXiv:hep-ph/0412089](#)]. Cited on pages 17, 48, and 53.
- [38] N. Arkani-Hamed, A. G. Cohen, T. Gregoire and J. G. Wacker, “Phenomenology of electroweak symmetry breaking from theory space,” *JHEP* **0208**, 020 (2002) [[arXiv:hep-ph/0202089](#)]. Cited on page 18.
- [39] M. Schmaltz, “The Simplest little Higgs,” *JHEP* **0408**, 056 (2004) [[arXiv:hep-ph/0407143](#)]. Cited on page 19.
- [40] N. Arkani-Hamed, A. G. Cohen, E. Katz and A. E. Nelson, “The Littlest Higgs,” *JHEP* **0207**, 034 (2002) [[arXiv:hep-ph/0206021](#)]. Cited on page 21.
- [41] N. Arkani-Hamed and M. Schmaltz, “Hierarchies without symmetries from extra dimensions,” *Phys. Rev. D* **61**, 033005 (2000) [[arXiv:hep-ph/9903417](#)]. Cited on page 23.
- [42] T. Appelquist, H. -C. Cheng and B. A. Dobrescu, “Bounds on universal extra dimensions,” *Phys. Rev. D* **64**, 035002 (2001) [[arXiv:hep-ph/0012100](#)]. Cited on page 23.

- [43] G. Nordström, “On the possibility of unifying the electromagnetic and the gravitational fields,” *Phys. Z.* **15**, 504 (1914), translation: [[arXiv:gen-ph/0702221](#)]. Cited on page 21.
- [44] O. Klein, “Quantum Theory and Five-Dimensional Theory of Relativity. (In German and English),” *Z. Phys.* **37**, 895 (1926) [*Surveys High Energ. Phys.* **5**, 241 (1986)]. Cited on page 21.
- [45] T. Kaluza, “On the Problem of Unity in Physics,” *Sitzungsber. Preuss. Akad. Wiss. Berlin (Math. Phys.)* **1921**, 966 (1921). Cited on page 21.
- [46] D. J. Kapner, T. S. Cook, E. G. Adelberger, J. H. Gundlach, B. R. Heckel, C. D. Hoyle and H. E. Swanson, “Tests of the gravitational inverse-square law below the dark-energy length scale,” *Phys. Rev. Lett.* **98**, 021101 (2007) [[arXiv:hep-ph/0611184](#)]. Cited on page 21.
- [47] R. Sundrum, “Towards an effective particle string resolution of the cosmological constant problem,” *JHEP* **9907**, 001 (1999) [[arXiv:hep-ph/9708329](#)]. Cited on page 21.
- [48] N. Arkani-Hamed, S. Dimopoulos and G. R. Dvali, “The Hierarchy problem and new dimensions at a millimeter,” *Phys. Lett. B* **429**, 263 (1998) [[arXiv:hep-ph/9803315](#)]. Cited on page 21.
- [49] J. Scherk and J. H. Schwarz, “How to Get Masses from Extra Dimensions,” *Nucl. Phys. B* **153**, 61 (1979). Cited on page 23.
- [50] C. Csaki, C. Grojean, H. Murayama, L. Pilo and J. Terning, “Gauge theories on an interval: Unitarity without a Higgs,” *Phys. Rev. D* **69**, 055006 (2004) [[hep-ph/0305237](#)]. Cited on pages 24 and 57.
- [51] N. S. Manton, “A New Six-Dimensional Approach to the Weinberg-Salam Model,” *Nucl. Phys. B* **158**, 141 (1979). Cited on page 24.
- [52] H. Hatanaka, T. Inami and C. S. Lim, “The Gauge hierarchy problem and higher dimensional gauge theories,” *Mod. Phys. Lett. A* **13**, 2601 (1998) [[arXiv:hep-th/9805067](#)]. Cited on page 24.
- [53] M. Kubo, C. S. Lim and H. Yamashita, “The Hosotani mechanism in bulk gauge theories with an orbifold extra space $S^1/Z(2)$,” *Mod. Phys. Lett. A* **17**, 2249 (2002) [[hep-ph/0111327](#)]. Cited on page 24.
- [54] M. Serone, “The Higgs boson as a gauge field in extra dimensions,” *AIP Conf. Proc.* **794**, 139 (2005) [[arXiv:hep-ph/0508019](#)]. Cited on page 24.
- [55] L. Randall, R. Sundrum, “A large mass hierarchy from a small extra dimension,” *Phys. Rev. Lett.* **83** (1999) 3370. [[arXiv:hep-ph/9905221](#)]. Cited on pages 25, 35, and 36.
- [56] L. Randall and R. Sundrum, “An Alternative to compactification,” *Phys. Rev. Lett.* **83**, 4690 (1999) [[arXiv:hep-th/9906064](#)]. Cited on pages 26 and 46.

-
- [57] H. Davoudiasl, J. L. Hewett and T. G. Rizzo, “Bulk gauge fields in the Randall-Sundrum model,” *Phys. Lett. B* **473**, 43 (2000) [[arXiv:hep-ph/9911262](#)]. Cited on pages 26 and 57.
- [58] Y. Grossman and M. Neubert, “Neutrino masses and mixings in nonfactorizable geometry,” *Phys. Lett. B* **474**, 361 (2000) [[arXiv:hep-ph/9912408](#)]. Cited on pages 26 and 76.
- [59] T. Gherghetta and A. Pomarol, “Bulk fields and supersymmetry in a slice of AdS,” *Nucl. Phys. B* **586**, 141 (2000) [[arXiv:hep-ph/0003129](#)]. Cited on pages 26, 76, and 78.
- [60] J. Thaler and I. Yavin, “The Littlest Higgs in Anti-de Sitter space,” *JHEP* **0508**, 022 (2005) [[arXiv:hep-ph/0501036](#)]. Cited on page 26.
- [61] R. Contino, “The Higgs as a Composite Nambu-Goldstone Boson,” [[arXiv:1005.4269 \[hep-ph\]](#)]. Cited on pages 15 and 18.
- [62] R. Contino, Y. Nomura and A. Pomarol, “Higgs as a holographic pseudoGoldstone boson,” *Nucl. Phys. B* **671**, 148 (2003) [[arXiv:hep-ph/0306259](#)]. Cited on pages 26, 52, and 57.
- [63] C. Csaki, C. Grojean, L. Pilo and J. Terning, “Towards a realistic model of Higgsless electroweak symmetry breaking,” *Phys. Rev. Lett.* **92**, 101802 (2004) [[arXiv:hep-ph/0308038](#)]. Cited on pages 26 and 53.
- [64] S. Weinberg and E. Witten, “Limits on Massless Particles,” *Phys. Lett. B* **96**, 59 (1980). Cited on page 26.
- [65] F. Loebbert, “The Weinberg-Witten theorem on massless particles: An Essay,” *Annalen Phys.* **17**, 803 (2008). Cited on page 26.
- [66] A. Pomarol and D. Tommasini, “Horizontal symmetries for the supersymmetric flavor problem,” *Nucl. Phys. B* **466**, 3 (1996) [[arXiv:hep-ph/9507462](#)]. Cited on page 28.
- [67] S. L. Glashow, J. Iliopoulos and L. Maiani, “Weak Interactions with Lepton-Hadron Symmetry,” *Phys. Rev. D* **2**, 1285 (1970). Cited on page 27.
- [68] L. Wolfenstein, “Parametrization of the Kobayashi-Maskawa Matrix,” *Phys. Rev. Lett.* **51**, 1945 (1983). Cited on page 28.
- [69] N. Arkani-Hamed, L. J. Hall, D. Tucker-Smith and N. Weiner, “Flavor at the TeV scale with extra dimensions,” *Phys. Rev. D* **61**, 116003 (2000) [[arXiv:hep-ph/9909326](#)]. Cited on page 33.
- [70] C. D. Froggatt and H. B. Nielsen, “Hierarchy of Quark Masses, Cabibbo Angles and CP Violation,” *Nucl. Phys. B* **147**, 277 (1979). Cited on pages 29, 31, 78, 79, and 80.
- [71] A. E. Nelson and M. J. Strassler, “Suppressing flavor anarchy,” *JHEP* **0009**, 030 (2000) [[arXiv:hep-ph/0006251](#)]. Cited on page 31.

- [72] K. S. Babu, “TASI Lectures on Flavor Physics,” [arXiv:0910.2948 \[hep-ph\]](#). Cited on page 31.
- [73] F. Wilczek and A. Zee, “Horizontal Interaction and Weak Mixing Angles,” *Phys. Rev. Lett.* **42**, 421 (1979). Cited on page 32.
- [74] B. Grinstein, M. Redi and G. Villadoro, “Low Scale Flavor Gauge Symmetries,” *JHEP* **1011**, 067 (2010) [[arXiv:1009.2049 \[hep-ph\]](#)]. Cited on page 33.
- [75] R. Alonso, M. B. Gavela, L. Merlo and S. Rigolin, “On the scalar potential of minimal flavour violation,” *JHEP* **1107**, 012 (2011) [[arXiv:1103.2915 \[hep-ph\]](#)]. Cited on page 33.
- [76] R. S. Chivukula and H. Georgi, “Composite Technicolor Standard Model,” *Phys. Lett. B* **188**, 99 (1987). Cited on page 33.
- [77] G. D’Ambrosio, G. F. Giudice, G. Isidori and A. Strumia, “Minimal flavor violation: An Effective field theory approach,” *Nucl. Phys. B* **645**, 155 (2002) [[arXiv:hep-ph/0207036](#)]. Cited on page 33.
- [78] R. M. Wald, “General Relativity,” Chicago, Usa: Univ. Pr. (1984) 491p. Cited on page 36.
- [79] S. Weinberg and E. Witten, “Limits on Massless Particles,” *Phys. Lett. B* **96**, 59 (1980). Cited on page 26.
- [80] F. Loebbert, “The Weinberg-Witten theorem on massless particles: An Essay,” *Annalen Phys.* **17**, 803 (2008). Cited on page 26.
- [81] C. Csaki, J. Hubisz and P. Meade, “TASI lectures on electroweak symmetry breaking from extra dimensions,” [arXiv:hep-ph/0510275](#). Cited on page 58.
- [82] W. Israel, “Singular hypersurfaces and thin shells in general relativity,” *Nuovo Cim. B* **44S10**, 1 (1966) , [Erratum-ibid. **48**, 463 (1967)]. Cited on page 37.
- [83] W. D. Goldberger and M. B. Wise, “Bulk fields in the Randall-Sundrum compactification scenario,” *Phys. Rev. D* **60**, 107505 (1999) [[arXiv:hep-ph/9907218](#)]. Cited on page 37.
- [84] C. Csaki, M. L. Graesser and G. D. Kribs, “Radion dynamics and electroweak physics,” *Phys. Rev. D* **63**, 065002 (2001) [[arXiv:hep-th/0008151](#)]. Cited on pages 37 and 90.
- [85] D. Bailin and A. Love, “Kaluza-Klein Theories,” *Rept. Prog. Phys.* **50**, 1087 (1987). Cited on page 38.
- [86] S. Weinberg, “The quantum theory of fields. Vol. 3: Supersymmetry,” Cambridge, UK: Univ. Pr. (2000) 419 p Cited on page 39.
- [87] R. A. Bertlmann, “Anomalies in quantum field theory,” Oxford, UK: Clarendon (1996) 566 p. (International series of monographs on physics: 91). Cited on page 39.

-
- [88] P. Tanedo and Y. Tsai Warped Penguins: Derivations, [notes](#). Cited on page 39.
- [89] P. H. Ginsparg, “Applied Conformal Field Theory,” [\[arXiv:hep-th/9108028\]](#). Cited on page 44.
- [90] P. Breitenlohner and D. Z. Freedman, “Positive Energy in anti-De Sitter Backgrounds and Gauged Extended Supergravity,” *Phys. Lett. B* **115**, 197 (1982). Cited on page 42.
- [91] B. Batell and T. Gherghetta, “Warped phenomenology in the holographic basis,” *Phys. Rev. D* **77**, 045002 (2008) [\[arXiv:0710.1838 \[hep-ph\]\]](#). Cited on page 48.
- [92] R. Rattazzi and A. Zaffaroni, “Comments on the holographic picture of the Randall-Sundrum model,” *JHEP* **0104**, 021 (2001) [\[arXiv:hep-th/0012248\]](#). Cited on page 47.
- [93] S. Ferrara, C. Fronsdal and A. Zaffaroni, “On N=8 supergravity on AdS(5) and N=4 superconformal Yang-Mills theory,” *Nucl. Phys. B* **532**, 153 (1998) [\[arXiv:hep-th/9802203\]](#). Cited on page 46.
- [94] I. R. Klebanov and E. Witten, “AdS / CFT correspondence and symmetry breaking,” *Nucl. Phys. B* **556**, 89 (1999) [\[arXiv:hep-th/9905104\]](#). Cited on page 44.
- [95] J. M. Maldacena, “The Large N limit of superconformal field theories and supergravity,” *Adv. Theor. Math. Phys.* **2**, 231 (1998) [*Int. J. Theor. Phys.* **38**, 1113 (1999)] [\[arXiv:hep-th/9711200\]](#). Cited on page 40.
- [96] W. Mück, ”Studies on the AdS/CFT Correspondence” Ph.D. Thesis, Simon Fraser University, Burnaby, B.C., Canada, 1999. [NASA](#). Cited on page 44.
- [97] S. S. Gubser, I. R. Klebanov and A. M. Polyakov, “Gauge theory correlators from noncritical string theory,” *Phys. Lett. B* **428**, 105 (1998) [\[arXiv:hep-th/9802109\]](#). Cited on page 43.
- [98] S. S. Gubser, “AdS/CFT and gravity,” *Phys. Rev. D* **63**, 084017 (2001) [\[arXiv:hep-th/9912001\]](#). Cited on page 46.
- [99] E. Witten, “Anti-de Sitter space and holography,” *Adv. Theor. Math. Phys.* **2**, 253 (1998) [\[arXiv:hep-th/9802150\]](#). Cited on page 45.
- [100] E. Witten, “Baryons in the 1/N Expansion,” *Nucl. Phys. B* **160**, 57 (1979). [KEK scanned](#). Cited on page 47.
- [101] H. Georgi, “Unparticle physics,” *Phys. Rev. Lett.* **98**, 221601 (2007) [\[arXiv:hep-ph/0703260\]](#). Cited on page 46.
- [102] B. Batell and T. Gherghetta, “Holographic mixing quantified,” *Phys. Rev. D* **76**, 045017 (2007) [\[arXiv:0706.0890 \[hep-th\]\]](#). Cited on page 47.
- [103] A. Karch, E. Katz, D. T. Son and M. A. Stephanov, “Linear confinement and AdS/QCD,” *Phys. Rev. D* **74**, 015005 (2006) [\[arXiv:hep-ph/0602229\]](#). Cited on page 47.

- [104] R. Contino and A. Pomarol, “Holography for fermions,” JHEP **0411**, 058 (2004) [[arXiv:hep-th/0406257](#)]. Cited on pages 45, 46, and 48.
- [105] K. Agashe, A. Delgado, M. J. May and R. Sundrum, “RS1, custodial isospin and precision tests,” JHEP **0308**, 050 (2003) [[arXiv:hep-ph/0308036](#)]. Cited on page 46.
- [106] I. Low and A. V. Manohar, “Spontaneously broken space-time symmetries and Goldstone’s theorem,” Phys. Rev. Lett. **88**, 101602 (2002) [[arXiv:hep-th/0110285](#)]. Cited on page 47.
- [107] T. Gherghetta, “TASI Lectures on a Holographic View of Beyond the Standard Model Physics,” [[arXiv:1008.2570 \[hep-ph\]](#)]. Cited on pages 41 and 49.
- [108] S. El-Showk, Y. Nakayama and S. Rychkov, “What Maxwell Theory in $D \neq 4$ teaches us about scale and conformal invariance,” Nucl. Phys. B **848**, 578 (2011) [[arXiv:1101.5385 \[hep-th\]](#)]. Cited on page 41.
- [109] O. Aharony, S. S. Gubser, J. M. Maldacena, H. Ooguri and Y. Oz, “Large N field theories, string theory and gravity,” Phys. Rept. **323**, 183 (2000) [[arXiv:hep-th/9905111](#)]. Cited on page 41.
- [110] D. Green, “Beauty for beginners,” FERMILAB-FN-0599. **KEK scanned**. No cited.
- [111] A. Muck, A. Pilaftsis and R. Ruckl, “Minimal higher dimensional extensions of the standard model and electroweak observables,” Phys. Rev. D **65**, 085037 (2002) [[arXiv:hep-ph/0110391](#)]. Cited on page 54.
- [112] L. Randall and M. D. Schwartz, “Quantum field theory and unification in AdS5,” JHEP **0111**, 003 (2001) [[arXiv:hep-th/0108114](#)]. Cited on pages 55 and 56.
- [113] C. Csaki, J. Hubisz and P. Meade, “TASI lectures on electroweak symmetry breaking from extra dimensions,” [[arXiv:hep-ph/0510275](#)]. Cited on page 58.
- [114] S. Casagrande, F. Goertz, U. Haisch, M. Neubert and T. Pfoh, “The Custodial Randall-Sundrum Model: From Precision Tests to Higgs Physics,” JHEP **1009**, 014 (2010) [[arXiv:1005.4315 \[hep-ph\]](#)]. Cited on pages 73, 74, 96, 100, 102, and 160.
- [115] S. Casagrande, F. Goertz, U. Haisch, M. Neubert and T. Pfoh, “Flavor Physics in the Randall-Sundrum Model: I. Theoretical Setup and Electroweak Precision Tests,” JHEP **0810**, 094 (2008) [[arXiv:0807.4937 \[hep-ph\]](#)]. Cited on pages 69, 73, 95, 98, 104, and 111.
- [116] C. Bouchart and G. Moreau, “Higgs boson phenomenology and VEV shift in the RS scenario,” Phys. Rev. D **80**, 095022 (2009) [[arXiv:0909.4812 \[hep-ph\]](#)]. Cited on page 69.
- [117] J. Hirn and V. Sanz, “(Not) Summing over Kaluza-Kleins,” Phys. Rev. D **76**, 044022 (2007) [[arXiv:hep-ph/0702005](#)]. Cited on page 69.

-
- [118] F. Goertz, “Warped Extra Dimensions: Flavor, Precision Tests and Higgs Physics,” [[arXiv:1112.6387 \[hep-ph\]](#)]. Cited on pages 70 and 87.
- [119] K. Agashe and G. Servant, “Baryon number in warped GUTs: Model building and (dark matter related) phenomenology,” *JCAP* **0502**, 002 (2005) [[arXiv:hep-ph/0411254](#)]. Cited on page 71.
- [120] M. S. Carena, E. Ponton, J. Santiago and C. E. M. Wagner, “Light Kaluza Klein States in Randall-Sundrum Models with Custodial SU(2),” *Nucl. Phys. B* **759**, 202 (2006) [[arXiv:hep-ph/0607106](#)]. Cited on page 71.
- [121] A. Azatov, M. Toharia and L. Zhu, “Higgs Mediated FCNC’s in Warped Extra Dimensions,” *Phys. Rev. D* **80**, 035016 (2009) [[arXiv:0906.1990 \[hep-ph\]](#)]. Cited on page 74.
- [122] F. Goertz and T. Pfoh, “On the Perturbative Approach in the Randall-Sundrum Model,” *JHEP* **0810**, 035 (2008) [[arXiv:0809.1378 \[hep-ph\]](#)]. Cited on page 74.
- [123] K. Agashe, A. Delgado and R. Sundrum, “Grand unification in RS1,” *Annals Phys.* **304**, 145 (2003) [[arXiv:hep-ph/0212028](#)]. Cited on page 78.
- [124] A. Djouadi, G. Moreau, F. Richard and R. K. Singh, “The Forward-backward asymmetry of top quark production at the Tevatron in warped extra dimensional models,” *Phys. Rev. D* **82**, 071702 (2010) [[arXiv:0906.0604 \[hep-ph\]](#)]. Cited on page 169.
- [125] A. Falkowski, “About the holographic pseudo-Goldstone boson,” *Phys. Rev. D* **75**, 025017 (2007) [[arXiv:hep-ph/0610336](#)]. Cited on page 83.
- [126] S. Chatrchyan *et al.* [CMS Collaboration], “Search for quark compositeness in dijet angular distributions from pp collisions at $\sqrt{s} = 7$ TeV,” *JHEP* **1205**, 055 (2012) [[arXiv:1202.5535 \[hep-ex\]](#)]. Cited on page 83.
- [127] M. Carena, S. Casagrande, F. Goertz, U. Haisch and M. Neubert, “Higgs Production in a Warped Extra Dimension,” [[arXiv:1204.0008 \[hep-ph\]](#)]. Cited on page 87.
- [128] C. Csaki, J. Hubisz and S. J. Lee, “Radion phenomenology in realistic warped space models,” *Phys. Rev. D* **76**, 125015 (2007) [[arXiv:0705.3844 \[hep-ph\]](#)]. Cited on page 90.
- [129] K. Agashe, G. Perez and A. Soni, “Flavor structure of warped extra dimension models,” *Phys. Rev. D* **71**, 016002 (2005) [[hep-ph/0408134](#)]. Cited on page 91.
- [130] C. Csaki, Y. Grossman, P. Tanedo and Y. Tsai, “Warped penguin diagrams,” *Phys. Rev. D* **83**, 073002 (2011) [[arXiv:1004.2037 \[hep-ph\]](#)]. Cited on page 91.
- [131] C. Csaki, C. Delaunay, C. Grojean and Y. Grossman, “A Model of Lepton Masses from a Warped Extra Dimension,” *JHEP* **0810**, 055 (2008) [[arXiv:0806.0356 \[hep-ph\]](#)]. Cited on page 91.
- [132] C. Campagnari and M. Franklin, “The Discovery of the top quark,” *Rev. Mod. Phys.* **69**, 137 (1997) [[arXiv:hep-ex/9608003](#)]. Cited on page 92.

- [133] M. Baak, M. Goebel, J. Haller, A. Hoecker, D. Ludwig, K. Moenig, M. Schott and J. Stelzer, “Updated Status of the Global Electroweak Fit and Constraints on New Physics,” *Eur. Phys. J. C* **72**, 2003 (2012) [[arXiv:1107.0975 \[hep-ph\]](#)]. Cited on pages 92, 93, and 94.
- [134] S. Chatrchyan *et al.* [CMS Collaboration], “Combined results of searches for the standard model Higgs boson in pp collisions at $\sqrt{s} = 7$ TeV,” *Phys. Lett. B* **710**, 26 (2012) [[arXiv:1202.1488 \[hep-ex\]](#)]. Cited on page 93.
- [135] G. Aad *et al.* [ATLAS Collaboration], “Combined search for the Standard Model Higgs boson in pp collisions at $\sqrt{s} = 7$ TeV with the ATLAS detector,” [[arXiv:1207.0319 \[hep-ex\]](#)]. Cited on page 93.
- [136] M. E. Peskin and T. Takeuchi, “Estimation of oblique electroweak corrections,” *Phys. Rev. D* **46**, 381 (1992). Cited on page 94.
- [137] M. E. Peskin and T. Takeuchi, “A New constraint on a strongly interacting Higgs sector,” *Phys. Rev. Lett.* **65**, 964 (1990). Cited on page 94.
- [138] G. Burdman and Y. Nomura, “Holographic theories of electroweak symmetry breaking without a Higgs boson,” *Phys. Rev. D* **69**, 115013 (2004) [[arXiv:hep-ph/0312247](#)]. Cited on page 94.
- [139] M. S. Carena, A. Delgado, E. Ponton, T. M. P. Tait and C. E. M. Wagner, “Precision electroweak data and unification of couplings in warped extra dimensions,” *Phys. Rev. D* **68**, 035010 (2003) [[arXiv:hep-ph/0305188](#)]. Cited on page 95.
- [140] A. Delgado and A. Falkowski, “Electroweak observables in a general 5D background,” *JHEP* **0705**, 097 (2007) [[arXiv:hep-ph/0702234](#)]. Cited on page 95.
- [141] G. Cacciapaglia, C. Csaki, C. Grojean and J. Terning, “Oblique corrections from Higgsless models in warped space,” *Phys. Rev. D* **70**, 075014 (2004) [[arXiv:hep-ph/0401160](#)]. Cited on page 95.
- [142] C. Csaki, J. Erlich and J. Terning, “The Effective Lagrangian in the Randall-Sundrum model and electroweak physics,” *Phys. Rev. D* **66**, 064021 (2002) [[arXiv:hep-ph/0203034](#)]. Cited on page 95.
- [143] G. Cacciapaglia, C. Csaki, C. Grojean and J. Terning, “Curing the Ills of Higgsless models: The S parameter and unitarity,” *Phys. Rev. D* **71**, 035015 (2005) [[arXiv:hep-ph/0409126](#)]. Cited on page 95.
- [144] H. Davoudiasl, G. Perez and A. Soni, “The Little Randall-Sundrum Model at the Large Hadron Collider,” *Phys. Lett. B* **665**, 67 (2008) [[arXiv:0802.0203 \[hep-ph\]](#)]. Cited on page 112.
- [145] J. H. Field, “Indications for an anomalous righthanded coupling of the b-quark from a model independent analysis of LEP and SLD data on Z decays,” *Mod. Phys. Lett. A* **13**, 1937 (1998) [[arXiv:hep-ph/9801355](#)]. Cited on page 97.
- [146] S. Schael *et al.* [ALEPH Collaboration], “Precision electroweak measurements on the Z resonance,” *Phys. Rept.* **427**, 257 (2006) [[arXiv:hep-ex/0509008](#)]. Cited on pages 97, 98, and 187.

-
- [147] A. Freitas and Y. -C. Huang, “Electroweak two-loop corrections to $\sin^2 \theta_{\text{eff}}^{bb}$ and $R(b)$ using numerical Mellin-Barnes integrals,” [arXiv:1205.0299 \[hep-ph\]](#). Cited on page 97.
- [148] K. Agashe, R. Contino, L. Da Rold and A. Pomarol, “A Custodial symmetry for Zb anti-b,” *Phys. Lett. B* **641**, 62 (2006) [[arXiv:hep-ph/0605341](#)]. Cited on page 99.
- [149] M. Redi and A. Weiler, “Flavor and CP Invariant Composite Higgs Models,” *JHEP* **1111**, 108 (2011) [[arXiv:1106.6357 \[hep-ph\]](#)]. Cited on pages 99 and 113.
- [150] M. Bauer, S. Casagrande, U. Haisch and M. Neubert, “Flavor Physics in the Randall-Sundrum Model: II. Tree-Level Weak-Interaction Processes,” *JHEP* **1009**, 017 (2010) [[arXiv:0912.1625 \[hep-ph\]](#)]. Cited on pages 90, 101, 105, and 162.
- [151] J. A. Bagger, K. T. Matchev and R. -J. Zhang, “QCD corrections to flavor changing neutral currents in the supersymmetric standard model,” *Phys. Lett. B* **412**, 77 (1997) [[arXiv:hep-ph/9707225](#)]. Cited on page 101.
- [152] M. Ciuchini, V. Lubicz, L. Conti, A. Vladikas, A. Donini, E. Franco, G. Martinelli and I. Scimemi *et al.*, “Delta M(K) and epsilon(K) in SUSY at the next-to-leading order,” *JHEP* **9810**, 008 (1998) [[arXiv:hep-ph/9808328](#)]. Cited on pages 101 and 189.
- [153] A. J. Buras, M. Misiak and J. Urban, “Two loop QCD anomalous dimensions of flavor changing four quark operators within and beyond the standard model,” *Nucl. Phys. B* **586**, 397 (2000) [[arXiv:hep-ph/0005183](#)]. Cited on page 101.
- [154] M. Blanke, A. J. Buras, B. Duling, S. Gori and A. Weiler, “ $\Delta F = 2$ Observables and Fine-Tuning in a Warped Extra Dimension with Custodial Protection,” *JHEP* **0903**, 001 (2009) [[arXiv:0809.1073 \[hep-ph\]](#)]. Cited on page 102.
- [155] D. Becirevic, M. Ciuchini, E. Franco, V. Gimenez, G. Martinelli, A. Masiero, M. Papinutto and J. Reyes *et al.*, “ $B_d - \bar{B}_d$ mixing and the $B_d \rightarrow J/\psi K_s$ asymmetry in general SUSY models,” Cited on page 102.
Nucl. Phys. B **634**, 105 (2002) [[hep-ph/0112303](#)].
- [156] J. Laiho, E. Lunghi and R. S. Van de Water, “Lattice QCD inputs to the CKM unitarity triangle analysis,” *Phys. Rev. D* **81**, 034503 (2010) [[arXiv:0910.2928 \[hep-ph\]](#)], updates on [latticeaverages.org](#). Cited on page 103.
- [157] J. Beringer *et al.* [Particle Data Group Collaboration], “Review of Particle Physics (RPP),” *Phys. Rev. D* **86**, 010001 (2012). Cited on pages 28, 103, and 109.
- [158] A. Lenz and U. Nierste, “Theoretical update of $B_s - \bar{B}_s$ mixing,” *JHEP* **0706**, 072 (2007) [[arXiv:hep-ph/0612167](#)]. Cited on pages 104 and 188.
- [159] Y. Amhis *et al.* [Heavy Flavor Averaging Group Collaboration], “Averages of b-hadron, c-hadron, and tau-lepton properties as of early 2012,” [[arXiv:1207.1158 \[hep-ex\]](#)]. Cited on pages 104, 105, and 182.

- [160] J. Charles, O. Deschamps, S. Descotes-Genon, R. Itoh, H. Lacker, A. Menzel, S. Monteil and V. Niess *et al.*, “Predictions of selected flavour observables within the Standard Model,” *Phys. Rev. D* **84**, 033005 (2011) [[arXiv:1106.4041 \[hep-ph\]](#)]. Cited on pages 103, 104, 109, and 188.
- [161] M. Blanke, A. J. Buras, D. Guadagnoli and C. Tarantino, “Minimal Flavour Violation Waiting for Precise Measurements of ΔM_s , $S_{\psi\phi}$, A_{SL}^s , $|V_{ub}|$, γ and $B_{s,d}^0 \rightarrow \mu^+\mu^-$,” *JHEP* **0610**, 003 (2006) [[arXiv:hep-ph/0604057](#)]. Cited on page 104.
- [162] M. Bona *et al.* [UTfit Collaboration], “First Evidence of New Physics in $b \leftrightarrow s$ Transitions,” *PMC Phys. A* **3**, 6 (2009) [[arXiv:0803.0659 \[hep-ph\]](#)]. Cited on page 104.
- [163] T. Aaltonen *et al.* [CDF Collaboration], “Measurement of the CP-Violating Phase $\beta_s^{J/\Psi\phi}$ in $B_s^0 \rightarrow J/\Psi\phi$ Decays with the CDF II Detector,” *Phys. Rev. D* **85**, 072002 (2012) [[arXiv:1112.1726 \[hep-ex\]](#)]. Cited on page 105.
- [164] RAaij *et al.* [LHCb Collaboration], “Measurement of the CP-violating phase ϕ_s in $B_s \rightarrow J/\psi\phi + \pi^-$ decays,” *Phys. Lett. B* **713**, 378 (2012) [[arXiv:1204.5675 \[hep-ex\]](#)]. Cited on page 105.
- [165] R. Aaij *et al.* [LHCb Collaboration], “Determination of the sign of the decay width difference in the B_s system,” *Phys. Rev. Lett.* **108**, 241801 (2012) [[arXiv:1202.4717 \[hep-ex\]](#)]. Cited on page 105.
- [166] R. Aaij *et al.* [LHCb Collaboration], “Strong constraints on the rare decays $B_s \rightarrow \mu^+\mu^-$ and $B^0 \rightarrow \mu^+\mu^-$,” *Phys. Rev. Lett.* **108**, 231801 (2012) [[arXiv:1203.4493 \[hep-ex\]](#)]. Cited on page 107.
- [167] F. Goertz and T. Pfoh, “Randall-Sundrum Corrections to the Width Difference and CP-Violating Phase in B_s^0 -Meson Decays,” *Phys. Rev. D* **84**, 095016 (2011) [[arXiv:1105.1507 \[hep-ph\]](#)]. Cited on pages 102 and 107.
- [168] P. Maestro, “Rare decay searches at CDF,” *PoS HQL* **2012**, 031 (2012) [[arXiv:1207.4323 \[hep-ex\]](#)]. Cited on page 107.
- [169] M. Misiak and J. Urban, “QCD corrections to FCNC decays mediated by Z penguins and W boxes,” *Phys. Lett. B* **451**, 161 (1999) [[arXiv:hep-ph/9901278](#)]. Cited on pages 107 and 189.
- [170] G. Buchalla and A. J. Buras, “The rare decays $K \rightarrow \pi\nu\bar{\nu}$, $B \rightarrow X\nu\bar{\nu}$ and $B \rightarrow l^+l^-$: An Update,” *Nucl. Phys. B* **548**, 309 (1999) [[arXiv:hep-ph/9901288](#)]. Cited on pages 107 and 189.
- [171] E. Gamiz *et al.* [HPQCD Collaboration], “Neutral B Meson Mixing in Unquenched Lattice QCD,” *Phys. Rev. D* **80**, 014503 (2009) [[arXiv:0902.1815 \[hep-lat\]](#)]. Cited on page 107.
- [172] A. J. Buras, M. V. Carlucci, S. Gori and G. Isidori, “Higgs-mediated FCNCs: Natural Flavour Conservation vs. Minimal Flavour Violation,” *JHEP* **1010**, 009 (2010) [[arXiv:1005.5310 \[hep-ph\]](#)]. Cited on page 107.

-
- [173] A. J. Buras and D. Guadagnoli, “Correlations among new CP violating effects in $\Delta F = 2$ observables,” *Phys. Rev. D* **78**, 033005 (2008) [[arXiv:0805.3887 \[hep-ph\]](#)]. Cited on pages 109 and 188.
- [174] K. Anikeev, D. Atwood, F. Azfar, S. Bailey, C. W. Bauer, W. Bell, G. Bodwin and E. Braaten *et al.*, “ B physics at the Tevatron: Run II and beyond,” [[arXiv:hep-ph/0201071](#)]. Cited on page 109.
- [175] P. A. Boyle, N. Garron and R. J. Hudspith, “Neutral kaon mixing beyond the standard model with $n_f = 2 + 1$ chiral fermions,” [[arXiv:1206.5737 \[hep-lat\]](#)]. Cited on page 110.
- [176] V. Bertone, N. Carrasco, M. Ciuchini, P. Dimopoulos, R. Frezzotti, V. Gimenez, V. Lubicz and G. Martinelli *et al.*, “Kaon Mixing Beyond the SM from $N_f = 2$ tmQCD and model independent constraints from the UTA,” [[arXiv:1207.1287 \[hep-lat\]](#)]. Cited on pages 103, 110, and 188.
- [177] J. Brod and M. Gorbahn, “Next-to-Next-to-Leading-Order Charm-Quark Contribution to the CP Violation Parameter ϵ_K and ΔM_K ,” *Phys. Rev. Lett.* **108**, 121801 (2012) [[arXiv:1108.2036 \[hep-ph\]](#)]. Cited on page 109.
- [178] C. Csaki, A. Falkowski and A. Weiler, “The Flavor of the Composite Pseudo-Goldstone Higgs,” *JHEP* **0809**, 008 (2008) [[arXiv:0804.1954 \[hep-ph\]](#)]. Cited on page 111.
- [179] M. Bauer, S. Casagrande, L. Grunder, U. Haisch and M. Neubert, “Little Randall-Sundrum models: epsilon(K) strikes again,” *Phys. Rev. D* **79**, 076001 (2009) [[arXiv:0811.3678 \[hep-ph\]](#)]. Cited on page 112.
- [180] O. Gedalia, G. Isidori and G. Perez, “Combining Direct & Indirect Kaon CP Violation to Constrain the Warped KK Scale,” *Phys. Lett. B* **682**, 200 (2009) [[arXiv:0905.3264 \[hep-ph\]](#)]. Cited on page 112.
- [181] K. Agashe, A. Azatov and L. Zhu, “Flavor Violation Tests of Warped/-Composite SM in the Two-Site Approach,” *Phys. Rev. D* **79**, 056006 (2009) [[arXiv:0810.1016 \[hep-ph\]](#)]. Cited on pages 111 and 114.
- [182] A. L. Fitzpatrick, G. Perez and L. Randall, “Flavor anarchy in a Randall-Sundrum model with 5D minimal flavor violation and a low Kaluza-Klein scale,” *Phys. Rev. Lett.* **100**, 171604 (2008) [[arXiv:0710.1869 \[hep-ph\]](#)]. Cited on page 113.
- [183] G. Cacciapaglia, C. Csaki, J. Galloway, G. Marandella, J. Terning and A. Weiler, “A GIM Mechanism from Extra Dimensions,” *JHEP* **0804**, 006 (2008) [[arXiv:0709.1714 \[hep-ph\]](#)]. Cited on page 113.
- [184] C. Csaki, A. Falkowski and A. Weiler, “A Simple Flavor Protection for RS,” *Phys. Rev. D* **80**, 016001 (2009) [[arXiv:0806.3757 \[hep-ph\]](#)]. Cited on pages 112 and 113.

- [185] C. Csaki, G. Perez, Z. e. Surujon and A. Weiler, “Flavor Alignment via Shining in RS,” *Phys. Rev. D* **81**, 075025 (2010) [[arXiv:0907.0474 \[hep-ph\]](#)]. Cited on page 113.
- [186] J. Santiago, “Minimal Flavor Protection: A New Flavor Paradigm in Warped Models,” *JHEP* **0812**, 046 (2008) [[arXiv:0806.1230 \[hep-ph\]](#)]. Cited on page 113.
- [187] H. Davoudiasl, B. Lillie and T. G. Rizzo, “Off-the-wall Higgs in the universal Randall-Sundrum model,” *JHEP* **0608**, 042 (2006) [[arXiv:hep-ph/0508279](#)]. Cited on page 114.
- [188] P. R. Archer, S. J. Huber and S. Jager, “Flavour Physics in the Soft Wall Model,” *JHEP* **1112**, 101 (2011) [[arXiv:1108.1433 \[hep-ph\]](#)]. Cited on page 115.
- [189] B. Batell, T. Gherghetta and D. Sword, “The Soft-Wall Standard Model,” *Phys. Rev. D* **78**, 116011 (2008) [[arXiv:0808.3977 \[hep-ph\]](#)]. Cited on page 115.
- [190] J. A. Cabrer, G. von Gersdorff and M. Quiros, “Flavor Phenomenology in General 5D Warped Spaces,” *JHEP* **1201**, 033 (2012) [[arXiv:1110.3324 \[hep-ph\]](#)]. Cited on page 115.
- [191] M. Bauer, R. Malm and M. Neubert, “A Solution to the Flavor Problem of Warped Extra-Dimension Models,” *Phys. Rev. Lett.* **108**, 081603 (2012) [[arXiv:1110.0471 \[hep-ph\]](#)]. Cited on page 115.
- [192] P. H. Frampton and S. L. Glashow, “Chiral Color: An Alternative to the Standard Model,” *Phys. Lett. B* **190**, 157 (1987). Cited on page 116.
- [193] CMS-PAS-EXO-12-016, ”Search for Narrow Resonances using the Dijet Mass Spectrum in pp Collisions at \sqrt{s} of 8 TeV”, CERN Note. Cited on pages 118 and 140.
- [194] S. Rajpoot, “A Chiral Color Model With A Simple Higgs Structure,” *Phys. Rev. Lett.* **60**, 2003 (1988). Cited on page 127.
- [195] M. V. Martynov and A. D. Smirnov, “Chiral color symmetry and possible G-prime-boson effects at the Tevatron and LHC,” *Mod. Phys. Lett. A* **24**, 1897 (2009) [[arXiv:0906.4525 \[hep-ph\]](#)]. Cited on page 129.
- [196] K. Agashe, G. Perez and A. Soni, “Collider Signals of Top Quark Flavor Violation from a Warped Extra Dimension,” *Phys. Rev. D* **75**, 015002 (2007) [[arXiv:hep-ph/0606293](#)]. Cited on page 136.
- [197] A. V. Manohar and M. B. Wise, “Flavor changing neutral currents, an extended scalar sector, and the Higgs production rate at the CERN LHC,” *Phys. Rev. D* **74**, 035009 (2006) [[arXiv:hep-ph/0606172](#)]. Cited on pages 136 and 141.
- [198] C. P. Burgess, M. Trott and S. Zuberi, “Light Octet Scalars, a Heavy Higgs and Minimal Flavour Violation,” *JHEP* **0909**, 082 (2009) [[arXiv:0907.2696 \[hep-ph\]](#)]. Cited on page 137.
- [199] M. I. Gresham and M. B. Wise, “Color octet scalar production at the LHC,” *Phys. Rev. D* **76**, 075003 (2007) [[arXiv:0706.0909 \[hep-ph\]](#)]. Cited on page 141.

-
- [200] J. M. Arnold and B. Fornal, “Color octet scalars and high pT four-jet events at LHC,” *Phys. Rev. D* **85**, 055020 (2012) [[arXiv:1112.0003 \[hep-ph\]](#)]. Cited on pages 140 and 141.
- [201] M. Gerbush, T. J. Khoo, D. J. Phalen, A. Pierce and D. Tucker-Smith, “Color-octet scalars at the CERN LHC,” *Phys. Rev. D* **77**, 095003 (2008) [[arXiv:0710.3133 \[hep-ph\]](#)]. Cited on page 141.
- [202] G. Aad et al. [ATLAS Collaboration], “Search for New Phenomena in the Dijet Mass Distribution using 5.8fb^{-1} of pp Collisions at $\sqrt{s} = 8$ TeV collected by the ATLAS Detector”, ATLAS-CONF-2012-088. Cited on pages 141 and 142.
- [203] U. Haisch and S. Westhoff, “Massive Color-Octet Bosons: Bounds on Effects in Top-Quark Pair Production,” *JHEP* **1108**, 088 (2011) [[arXiv:1106.0529 \[hep-ph\]](#)]. Cited on pages 141 and 155.
- [204] G. Aad et al. [ATLAS Collaboration], “Search for resonances decaying into top quark pairs using fully hadronic decays in pp collisions with ATLAS at $\sqrt{s} = 7$ TeV”, ATLAS-CONF-2012-102. Cited on pages 143 and 144.
- [205] M. Bauer, F. Goertz, U. Haisch, T. Pfoh and S. Westhoff, “Top-Quark Forward-Backward Asymmetry in Randall-Sundrum Models Beyond the Leading Order,” *JHEP* **1011**, 039 (2010) [[arXiv:1008.0742 \[hep-ph\]](#)]. Cited on page 145.
- [206] [Tevatron Electroweak Working Group and CDF and D0 Collaborations], “Combination of CDF and D0 results on the mass of the top quark using up to 5.8fb^{-1} of data,” [arXiv:1107.5255 \[hep-ex\]](#). Cited on page 145.
- [207] V. M. Abazov et al. [D0 Collaboration], “Measurement of the $t\bar{t}$ production cross section using dilepton events in $p\bar{p}$ collisions,” *Phys. Lett. B* **704**, 403 (2011) [[arXiv:1105.5384 \[hep-ex\]](#)]. Cited on page 146.
- [208] ”LHC Combination: Top mass” [CMS Physics Analysis Summary , July 6, 2012](#). Cited on page 146.
- [209] [CMS Collaboration] ”Combination of top pair production cross section measurements”, [CMS Physics Analysis Summary 11-024, November 23, 2011](#) Cited on page 146.
- [210] ”Statistical combination of top quark pair production cross-section measurements using dilepton, single-lepton, and all-hadronic final states at $\sqrt{s} = 7$ TeV with the ATLAS detector”, [Conference Note 2012-032, March 12, 2012](#). Cited on page 146.
- [211] M. Beneke, P. Falgari, S. Klein, J. Piclum and C. Schwinn, “NNLL threshold resummation for the total top-pair production cross section,” [[arXiv:1205.0988 \[hep-ph\]](#)]. Cited on pages 146 and 166.
- [212] E. Thomson et al. [CDF Collaboration], “Combination of CDF top quark pair production cross section with up to 4.6fb^{-1} ” [Conference Note 9913, October 14, 2009](#). Cited on page 146.

- [213] E. Thomson *et al.* [CDF Collaboration], “Study of the Top Quark Production Asymmetry and Its Mass and Rapidity Dependence in the Full Run II Tevatron Dataset” *Conference Note 10807*, March 3, 2012. Cited on page 146.
- [214] O. Antunano, J. H. Kühn, and G. Rodrigo, “Top quarks, axigluons and charge asymmetries at hadron colliders,” *Phys. Rev. D* **77**, 014003 (2008), [[arXiv:0709.1652 \[hep-ph\]](#)]. Cited on page 166.
- [215] J. H. Kühn and G. Rodrigo, “Charge asymmetry of heavy quarks at hadron colliders,” *Phys. Rev. D* **59**, 054017 (1999) [[arXiv:hep-ph/9807420](#)]. Cited on pages 151, 152, and 166.
- [216] S. Chatrchyan *et al.* [CMS Collaboration], “Inclusive and differential measurements of the $t\bar{t}$ charge asymmetry in proton-proton collisions at 7 TeV,” [[arXiv:1207.0065 \[hep-ex\]](#)]. Cited on page 148.
- [217] G. Aad *et al.* [ATLAS Collaboration], “Measurement of the charge asymmetry in top quark pair production in pp collisions at $\sqrt{s} = 7$ TeV using the ATLAS detector,” *Eur. Phys. J. C* **72**, 2039 (2012) [[arXiv:1203.4211 \[hep-ex\]](#)]. Cited on page 148.
- [218] G. Aad *et al.* [ATLAS Collaboration], “Measurement of the charge asymmetry in dileptonic decays of top quark pairs in pp collisions at $\sqrt{s} = 7$ TeV using the ATLAS detector” *Conference Note 2012-057*, June 2, 2012. Cited on page 148.
- [219] J. H. Kuhn and G. Rodrigo, “Charge asymmetries of top quarks at hadron colliders revisited,” *JHEP* **1201**, 063 (2012) [[arXiv:1109.6830 \[hep-ph\]](#)]. Cited on page 148.
- [220] W. Bernreuther and Z. -G. Si, “Top quark and leptonic charge asymmetries for the Tevatron and LHC,” *Phys. Rev. D* **86**, 034026 (2012) [[arXiv:1205.6580 \[hep-ph\]](#)]. Cited on pages 147 and 148.
- [221] J. Drobnak, J. F. Kamenik and J. Zupan, “Flipping t t bar asymmetries at the Tevatron and the LHC,” [[arXiv:1205.4721 \[hep-ph\]](#)]. Cited on page 155.
- [222] L. G. Almeida, G. Sterman and W. Vogelsang, “Threshold Resummation for the Top Quark Charge Asymmetry,” *Phys. Rev. D* **78**, 014008 (2008) [[arXiv:0805.1885 \[hep-ph\]](#)]. Cited on pages 150 and 166.
- [223] T. Hahn, “CUBA: A library for multidimensional numerical integration,” *Comput. Phys. Commun.* **168**, 78 (2005) [[arXiv:hep-ph/0404043](#)]. Cited on page 152.
- [224] M. I. Gresham, I. -W. Kim and K. M. Zurek, “Tevatron Top A_{FB} Versus LHC Top Physics,” *Phys. Rev. D* **85**, 014022 (2012) [[arXiv:1107.4364 \[hep-ph\]](#)]. Cited on pages 153 and 154.
- [225] B. Grinstein, C. W. Murphy, D. Pirskhalava and P. Uttayarat, “Massive Spin-2 States as the Origin of the Top Quark Forward-Backward Asymmetry,” *JHEP* **1208**, 073 (2012) [[arXiv:1203.2183 \[hep-ph\]](#)]. Cited on page 153.

- [226] G. Marques Tavares and M. Schmaltz, “Explaining the t-tbar asymmetry with a light axigluon,” *Phys. Rev. D* **84**, 054008 (2011) [[arXiv:1107.0978 \[hep-ph\]](#)]. Cited on page 155.
- [227] T. Aaltonen *et al.* [CDF Collaboration], “Evidence for a Mass Dependent Forward-Backward Asymmetry in Top Quark Pair Production,” *Phys. Rev. D* **83**, 112003 (2011) [[arXiv:1101.0034 \[hep-ex\]](#)]. Cited on page 155.
- [228] A. D. Martin, W. J. Stirling, R. S. Thorne and G. Watt, “Parton distributions for the LHC,” *Eur. Phys. J. C* **63**, 189 (2009) [[arXiv:0901.0002 \[hep-ph\]](#)]. Cited on pages 141, 156, and 165.
- [229] F. Maltoni, K. Paul, T. Stelzer and S. Willenbrock, “Color flow decomposition of QCD amplitudes,” *Phys. Rev. D* **67**, 014026 (2003) [[arXiv:hep-ph/0209271](#)]. Cited on page 156.
- [230] Q. -H. Cao, D. McKeen, J. L. Rosner, G. Shaughnessy and C. E. M. Wagner, “Forward-Backward Asymmetry of Top Quark Pair Production,” *Phys. Rev. D* **81**, 114004 (2010) [[arXiv:1003.3461 \[hep-ph\]](#)]. Cited on page 156.
- [231] K. Cheung, W. -Y. Keung and T. -C. Yuan, “Top Quark Forward-Backward Asymmetry,” *Phys. Lett. B* **682**, 287 (2009) [[arXiv:0908.2589 \[hep-ph\]](#)]. Cited on page 156.
- [232] D. Duffy, Z. Sullivan and H. Zhang, “Top quark forward-backward asymmetry and W' bosons,” *Phys. Rev. D* **85**, 094027 (2012) [[arXiv:1203.4489 \[hep-ph\]](#)]. Cited on page 156.
- [233] E. L. Berger, Q. -H. Cao, C. -R. Chen, C. S. Li and H. Zhang, “Top Quark Forward-Backward Asymmetry and Same-Sign Top Quark Pairs,” *Phys. Rev. Lett.* **106**, 201801 (2011) [[arXiv:1101.5625 \[hep-ph\]](#)]. Cited on page 156.
- [234] J. Shu, T. M. P. Tait and K. Wang, “Explorations of the Top Quark Forward-Backward Asymmetry at the Tevatron,” *Phys. Rev. D* **81**, 034012 (2010) [[arXiv:0911.3237 \[hep-ph\]](#)]. Cited on page 157.
- [235] K. Agashe, A. Belyaev, T. Krupovnickas, G. Perez and J. Virzi, “LHC Signals from Warped Extra Dimensions,” *Phys. Rev. D* **77**, 015003 (2008) [[arXiv:hep-ph/0612015](#)]. Cited on page 163.
- [236] T. Aaltonen *et al.* [CDF Collaboration], “First Measurement of the t anti-t Differential Cross Section $d\sigma/dM_{\bar{t}t}$ in p anti-p Collisions at $\sqrt{s} = 1.96\text{TeV}$,” *Phys. Rev. Lett.* **102**, 222003 (2009) [[arXiv:0903.2850 \[hep-ex\]](#)]. Cited on page 165.
- [237] P. Nason, S. Dawson and R. K. Ellis, “The Total Cross-Section for the Production of Heavy Quarks in Hadronic Collisions,” *Nucl. Phys. B* **303**, 607 (1988). Cited on page 166.
- [238] J. Campbell and R. K. Ellis, “MCFM – A Monte Carlo for FeMtobarn processes at Hadron Colliders”, <http://mcfm.fnal.gov>. Cited on page 166.

- [239] V. Ahrens, A. Ferroglia, M. Neubert, B. D. Pecjak and L. L. Yang, “Renormalization-Group Improved Predictions for Top-Quark Pair Production at Hadron Colliders,” *JHEP* **1009**, 097 (2010) [[arXiv:1003.5827 \[hep-ph\]](#)]. Cited on pages 146 and 166.
- [240] W. Bernreuther and Z. -G. Si, “Distributions and correlations for top quark pair production and decay at the Tevatron and LHC.,” *Nucl. Phys. B* **837**, 90 (2010) [[arXiv:1003.3926 \[hep-ph\]](#)]. Cited on page 166.
- [241] R. Waldi, “Flavour oscillation and CP violation of B mesons,” *Prog. Part. Nucl. Phys.* **47**, 1 (2001). Cited on page 182.
- [242] U. Nierste, “Three Lectures on Meson Mixing and CKM phenomenology,” [[arXiv:0904.1869 \[hep-ph\]](#)]. Cited on pages 183 and 185.
- [243] P. Langacker, “The standard model and beyond,” Boca Raton, USA: CRC Pr. (2010) 663 p. Cited on page 192.
- [244] L. Da Rold, C. Delaunay, C. Grojean and G. Perez, “Up Asymmetries From Exhilarated Composite Flavor Structures,” [[arXiv:1208.1499 \[hep-ph\]](#)]. Cited on page 176.
- [245] C. Amsler and A. Masoni, “The $\eta(1405)$, $\eta(1475)$, $f_1(1420)$, and $f_1(1510)$ ”. Cited on pages 187, 188, and 189.
- [246] J. Charles *et al.* [CKMfitter Group Collaboration], “CP violation and the CKM matrix: Assessing the impact of the asymmetric B factories,” *Eur. Phys. J. C* **41**, 1 (2005) [[arXiv:hep-ph/0406184](#)]. Cited on page 187.
- [247] V. Lubicz and C. Tarantino, “Flavour physics and Lattice QCD: Averages of lattice inputs for the Unitarity Triangle Analysis,” *Nuovo Cim. B* **123**, 674 (2008) [[arXiv:0807.4605 \[hep-lat\]](#)]. Cited on pages 188 and 189.
- [248] [Tevatron Electroweak Working Group and CDF and D0 Collaboration], “A Combination of CDF and D0 Results on the Mass of the Top Quark,” [[arXiv:0803.1683 \[hep-ex\]](#)]. Cited on pages 187 and 188.
- [249] A. J. Buras, M. Jamin and P. H. Weisz, “Leading And Next-to-leading Qcd Corrections To Epsilon Parameter And B_0 - Anti- b_0 Mixing In The Presence Of A Heavy Top Quark,” *Nucl. Phys. B* **347**, 491 (1990). Cited on page 188.
- [250] E. Barberio *et al.* [Heavy Flavor Averaging Group Collaboration], “Averages of b -hadron and c -hadron Properties at the End of 2007,” [[arXiv:0808.1297 \[hep-ex\]](#)]. Cited on pages 188 and 189.